UNIVERSITY OF SOUTHAMPTON

DIVISION OF BIOCHEMISTRY AND MOLECULAR BIOLOGY
SCHOOL OF BIOLOGICAL SCIENCES

THE ROLE OF METAL IONS IN THE STRUCTURE AND FUNCTION OF GLUCOSE DEHYDROGENASE IN *ESCHERICHIA COLI*

BY
PETER LEE JAMES

A thesis submitted for the degree of Doctor of Philosophy

January 2002

UNIVERSITY OF SOUTHAMPTON

ABSTRACT

Division of Biochemistry and molecular Biology
School of Biological Sciences

Doctor of Philosophy

THE ROLE OF METAL IONS IN THE STRUCTURE AND FUNCTION OF GLUCOSE DEHYDROGENASE IN *ESCHERICHIA COLI*

by Peter Lee James

Glucose dehydrogenase (GDH) is a quinoprotein, containing the prosthetic group pyrroloquinoline quinone (PQQ), that catalyses the oxidation of D-glucose to D-gluconate in the periplasm, transferring electrons to ubiquinone in the membrane. It is a single polypeptide (87kDa) that is attached to the inner membrane of *E. coli*. It occurs as an apoenzyme because *E. coli* cannot synthesise PQQ but holoGDH can be formed by incubation with Mg^{2+} and PQQ. Analysis of the amino acid sequence predicts that it has a transmembrane domain and a periplasmic superbarrel domain. The structure of GDH has not been solved but a model of the periplasmic domain has been made, based on the X-ray coordinates of methanol dehydrogenase (MDH). My attempts to isolate and purify the periplasmic domain by genetic engineering failed. Inserting a protease cleavage site between the membrane and periplasmic domain resulted in poor expression of the protein.

The principle aim of this thesis was to study the role of divalent metal ions in the structure and function of GDH. All other quinoproteins contain Ca^{2+} at the active site where it plays a structural and catalytic role. However, it is unclear whether Mg^{2+} or Ca^{2+} forms part of the active site of GDH because Mg^{2+} (and not Ca^{2+}) is required for reconstitution of active enzyme from PQQ and apoGDH. To investigate this, the amino acids that have been predicted to bind to the active site metal ion were mutated (D354N, N355D and T424N).

Characterisation of WT-GDH, D354N-GDH, N355D-GDH, D354N/N355D-GDH and T424N-GDH suggested that the metal ion added in the reconstitution process becomes incorporated into the active site and that in WT-GDH, Mg^{2+} replaces the Ca^{2+} seen in all other quinoproteins. WT-GDH could be reconstituted with Mg^{2+} but Ca^{2+}, Sr^{2+} and Ba^{2+} inhibited this process by competing for the same binding site. Mutant GDHs had an altered specificity; usually they could only be reconstituted with Ca^{2+}, Sr^{2+} or Ba^{2+}. ApoGDH contained 3.5 molecules of Ca^{2+} and 0.82 molecules of Mg^{2+} per molecule of enzyme. This suggested that active site Ca^{2+} was already bound, but this is perhaps unlikely as eventually half the bonds to this active site metal ion are provided by PQQ, which is not present until the reconstitution process.

Mutant GDHs had a lower affinity for substrates as well in addition to the altered specificity for metal ions, suggesting that Ca^{2+}, Sr^{2+} and Ba^{2+}, but not Mg^{2+} are able to stabilise a conformation of the active site suitable for substrate binding. Affinity for substrates was higher with Sr^{2+} and Ba^{2+}-GDH than with Ca^{2+}-GDH suggesting larger metal ions are better for stabilisation than smaller metal ions.

Contents

List of Figures

Chapter 4

List of Tables

Chapter 6

Acknowledgements

I thank Chris Anthony for giving me the opportunity to work in his research group. Over the last three years he has given me valuable advice concerning work and personal matters, and has been more of a friend than a supervisor. I am also grateful to the University of Southampton for my funding.

I would like to thank all members of the CA group, past and present for all their help. Gyles Cozier was the first person in the group to work with GDH and he was responsible for setting up the expression system for WT-GDH. Without him my project wouldn't have existed. I thank Paul Williams for being a great friend and for all the detailed discussions on more or less everything. Thanks for not getting annoyed when I hogged all the equipment! Paul Afolabi (Remmi), Martin Stevens and Jeff Pilot have made life in Boldrewood more enjoyable over the last three years.

Dr Severmann and Dr Delves measured the Mg^{2+} and Ca^{2+} content of WT and mutant GDHs; thanks for your time and help. I must also thank Mike Gore for allowing me to use his group's equipment and for his helpful discussions on enzyme kinetics.

I thank all my family for their support throughout my life. Finally, a big thank you to my wife Sarah who has supported me emotionally and financially throughout my postgraduate studies. I guess its time I start paying my way!

Abbreviations

α	Alpha
ADH	Alcohol dehydrogenase
ATP	Adenosine-5'-triphosphate
β	Beta
Ba^{2+}	Barium ion
bp	Base pair
Bis-Tris	Bis[2-hydroxyethyl]imino-tris[hydroxymethyl]methane
BSA	Bovine serum albumin
Ca^{2+}	Calcium ion
dATP	2'deoxyadenosine-5'-triphoshate
DCPIP	2,6-dichlorophenolindophenol
dCTP	2'deoxycytosine-5'-triphoshate
ddATP	2', 3'-dideoxyadenosine-5'-triphosphate
ddCTP	2', 3'-dideoxycytosine-5'-triphosphate
ddGTP	2', 3'-dideoxyguanosine-5'-triphosphate
ddTTP	2', 3'-dideoxythymidine-5'-triphosphate
DEAE	Diethylaminoethyl
dGTP	2'deoxyguanosine-5'-triphoshate
DNA	Deoxyribonucleic acid
ds	Double stranded
DTT	Dithiothreitol
dTTP	2'deoxythymidine-5'-triphoshate
dUTP	2'deoxyuridine-5'-triphoshate
EDTA	Ethylenediamine-N,N,N',N'-tetraacetic acid
EGTA	Ethyleneglycol-bis(β-aminoethylether)-N,N,N',N'-tetraacetic acid
GDH	Glucose dehydrogenase
IPTG	Isopropylthio-β-D-galactose
LB	Luria-Bertani
MDH	Methanol dehydrogenase
MES	3-(N-morpholino)ethane sulphonic acid
Mg^{2+}	Magnesium ion
mGDH	Membrane glucose dehydrogenase
MOPS	3-[N-morpholino]propanesulfonic acid
PCR	Polymerase chain reaction
PeriGDH	Periplasmic domain of GDH
PES	Phenazine ethosulphate
PQQ	Pyrroloquinoline quinone
SDS-PAGE	Sodium dodecyl sulfate polyacrylamide gel electrophoresis
sGDH	Soluble glucose dehydrogenase
ss	Single stranded
Sr^{2+}	Strontium ion
TEMED	N,N,N',N'-tetramethylethylenediamine
Tris	Tris(hydroxymethyl)aminomethane

Chapter 1

Introduction

Introduction

Glucose dehydrogenase (GDH) is a quinoprotein that contains the prosthetic group pyrroloquinoline quinone (PQQ). A soluble form (sGDH) and a membrane bound form (mGDH) have been identified, but only the membrane form is going to be discussed in detail. The amino acid sequence of sGDH is completely different from that of mGDH. Membrane bound GDH has been purified from the membranes of *Escherichia coli* (Ameyama *et al.*, 1986), *Gluconobacter suboxydans* (Ameyama *et al.*, 1981) and *Acinetobacter calcoaceticus* (Matsushita *et al.*, 1989a).

The aim of this thesis is to study the metal ion that binds to the active site of the membrane GDH of *E. coli* and the effect that site-directed mutagenesis has on the enzyme's activity. In this Chapter the structure of GDH and methanol dehydrogenase (MDH) will be discussed. The structure of GDH has not been solved but it is expected to have a similar structure to MDH (Cozier and Anthony, 1995).

1.1 Pyrroloquinoline quinone (PQQ)

Pyrroloquinoline quinone or PQQ is an abbreviation for 2,7,9-tricarboxy-1H-pyrrolo(2,3-f)quinoline-4,5-dione; it is also known as methoxatin. In 1980 Duine, Frank and co-workers named proteins that contained pyrroloquinoline quinone (PQQ) as their prosthetic group quinoproteins. The discovery of quinoproteins began in 1964 when Hauge characterised glucose dehydrogenase of *Bacterium anitratum* and noticed that the co-factor was neither a pyridine nucleotide nor a flavin (Hauge, 1964). Anthony and Zatman (1967) then characterised methanol dehydrogenase (MDH), and isolated its prosthetic group. This was extracted by boiling MDH or by treating the enzyme with acid or alkali. The pure prosthetic group was red in colour and had a green fluorescence. Based on it's spectral properties Anthony and Zatman thought it was likely to be an unusual pteridine or a novel type of prosthetic group (Anthony and Zatman, 1967). It was not until 1979 that X-ray crystallography showed that this prosthetic group was PQQ (Salisbury *et al.*, 1979). The structure is shown in Figure 1.1. Electron spin resonance, nuclear magnetic resonance and mass spectroscopy also proved this prosthetic group to be PQQ (Duine *et al.*, 1980).

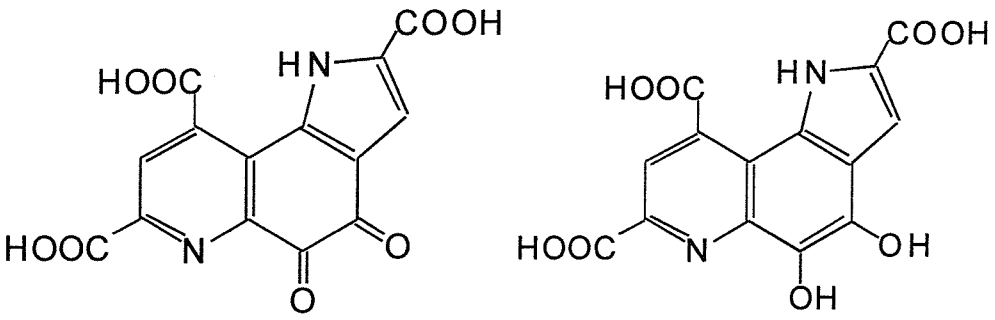

PQQ

(Quinone)

$PQQH_2$

(Quinol)

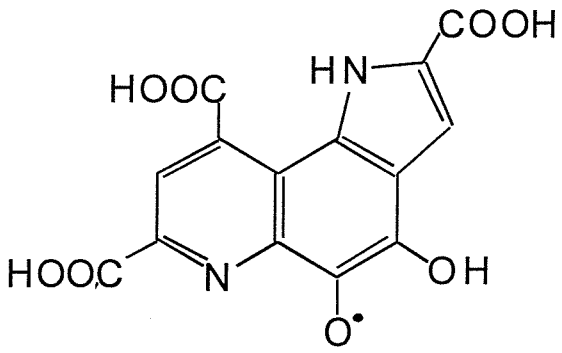

$PQQH^{\bullet}$

(Semiquinone)

Figure 1.1 The structures of the various forms of pyrroloquinoline quinone (PQQ)

The quinone is reduced by substrate in the enzyme's active site, producing quinol which is re-oxidised (by way of the semiquinone) in two single electron transfer steps back to the quinone.

PQQ acts as a prosthetic group of dehydrogenases in bacteria but in animals its role (if any) is unknown (see reviews Bishop *et al.*, 1998 and Stites *et al.*, 2000). There is debate that it is a vitamin but no animal enzyme has been characterised that requires PQQ. Mice fed on PQQ deficient diets show evidence of friable skin, reduced number of mitochondria, haemorrhage, reduction in general fitness and a hunched posture (Steinberg *et al.*, 1994). In cell culture experiments, PQQ enhanced cell growth and proliferation (Naito *et al.*, 1993).

1.1.1 Properties of PQQ

The sodium salt of PQQ crystallises from NaCl solutions to give a red compound. PQQ is a highly polar compound. The absorption spectrum at pH 7 (Figure 1.2), has maxima at 249nM, 325nM and 775nM (Dekker *et al.*, 1982). PQQ has a characteristic green fluorescence. The fluorescence excitation spectrum is different from the absorption spectrum at pH7, because PQQ in water is a mixture of PQQ and PQQ.H_2O at the C-5 carbonyl. Only PQQ.H_2O is fluorescent but both species absorb (Dekker *et al.*, 1982). The C5 carbonyl in the oxidised form is very reactive towards nucleophilic reagents such as methanol, aldehydes, ketones, KCN, ammonia and can form adducts with such compounds. PQQ is stable because it is resistant to H_2SO_4, 1M NaOH and UV light, but stability is reduced when it reacts with nucleophiles to produce adducts. It is easily reduced by hydrazine, $NaBH_4$ and β-mercaptoethanol (Itoh *et al.*, 1993). There are three forms of PQQ: PQQ (oxidised form); PQQH (semiquinone form) and $PQQH_2$ (reduced form). The structures of each form are shown in Figure 1.1. Quinoproteins have absorption bands between 300nM and 420nM due to PQQ. PQQ is not covalently bound to quinoproteins.

1.1.2 Biosynthesis of PQQ

NMR spectrometry showed that when *Hyphomicrobium X* and *Methylobacterium extorquens AM1* were grown on labelled substrates, PQQ was derived from glutamate and tyrosine (Houck *et al.*, 1988, 1989; van Kleef and Duine,1998; Unkefer *et al.*, 1995). Both amino acids are incorporated completely; the tyrosyl side chain provides the orthoquinone ring of PQQ and the pyrrole-2- carboxylic acid moiety is derived from cyclization of the amino acid backbone (Figure 1.3). Glutamate makes up the remaining portion of the compound. It is expected that a small polypeptide is involved as a precursor for the production of PQQ in a number of bacteria. These polypeptides vary in length from 23-39 amino acids and have a high identity; they contain a conserved motif with glutamate and tyrosine residues (Goosen *et al.*, 1989; Morris *et al.*, 1994). Mutating the conserved glutamate

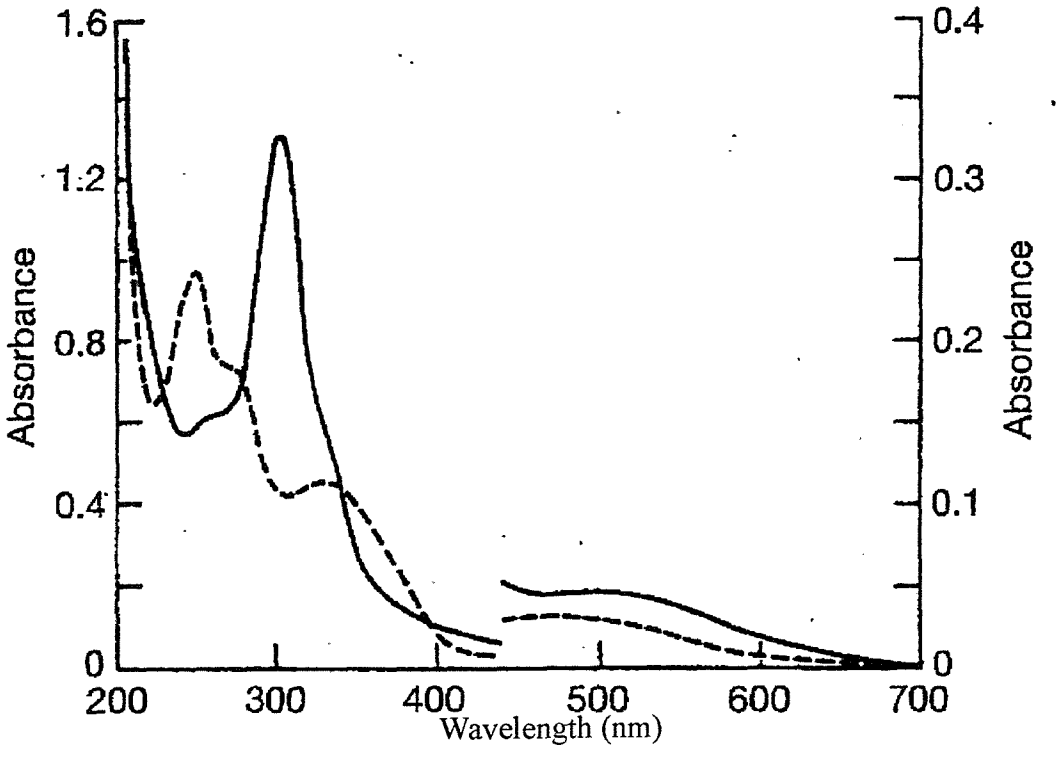

Figure 1.2 Absorption spectra of PQQ

Spectra of 40μM PQQ measured at pH 7.0 in phosphate buffer. (—) reduced PQQ; (---) oxidised PQQ (Dekker *et al.*, 1982).

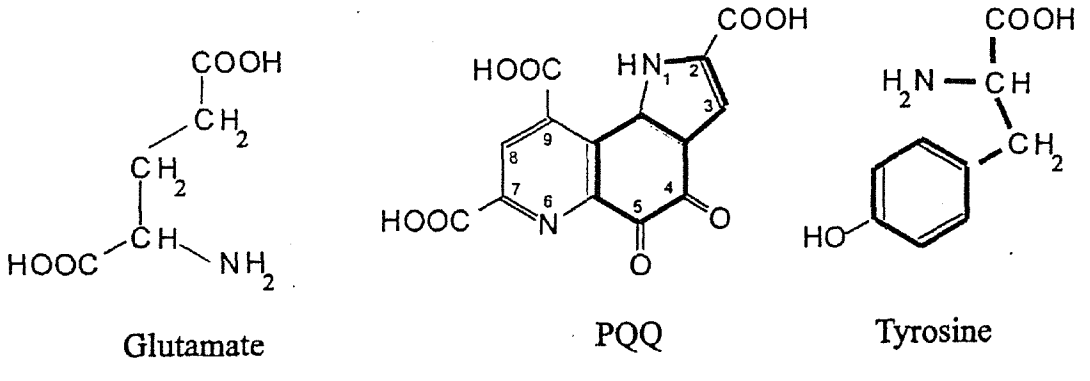

Figure 1.3 Biosynthesis of PQQ

PQQ is derived from glutamate and tyrosine (taken from Goodwin and Anthony, 1998).

or tyrosine abolished PQQ synthesis. The precursor is expected to be cleaved by specific proteases to form PQQ. The genes involved in PQQ synthesis have been identified in a number of bacteria. *Klebsiella pneumoniae* contains a cluster of six *pqq* genes named *pqqA, B, C, D, E* and *F* (Meulenberg *et al.*,1992) and *Gluconobacter oxydans* requires 5 genes (Felder *et al.*, 2000). *Methylobacterium extorquens* also has six *pqq* genes but they are found in two separate clusters (Goodwin and Anthony, 1998). The polypeptide precursor is encoded by *pqqA* and the remaining genes could code for proteins that cleave the precursor to form PQQ.

E. coli cannot synthesise PQQ as it does not contain the *pqq* genes. Transforming DNA containing all six *pqq* genes from *Klebsiella pneumoniae* into *E. coli* led to the production of PQQ in *E. coli* (Meulenberg *et al.*, 1990). [^{14}C]PQQ has been produced in *E. coli* using genes from *K pneumoniae*, 100-200nmol/L was purified from the growth medium (Stites *et al.*, 2000). The introduction of the four genes from *A. calcoaceticus* (*pqq I, II, III, IV*) also led to production of the prosthetic group (Goosen *et al.*, 1989).

1.2 The function of glucose dehydrogenase (GDH)

The function of quinoprotein dehydrogenases is to transfer reducing equivalents from substrates to a bacterial aerobic electron transport chain. GDH catalyses the oxidation of D-glucose to D-gluconate in the periplasm; and transfers electrons to cytochrome oxidase through ubiquinone in the respiratory chain (Figures 1.4 and 1.5).

In *E. coli* GDH is located in the inner membrane and occurs as an apoenzyme- the prosthetic group PQQ is not present. Hommes and his co-workers (1984) showed that several strains of *E. coli* synthesise a glucose dehydrogenase apoenzyme that has no function in growing cells as it cannot synthesise PQQ. Active GDH was produced when PQQ was added to the growth medium. Purified GDH is made active by reconstituting the enzyme with Mg^{2+} and PQQ (Ameyama *et al.*, 1985).

E. coli does not produce PQQ so the role of GDH is unclear. Two physiological functions for GDH have been proposed in *E. coli* (Goodwin and Anthony, 1998). GDH can produce ATP by way of oxidative phosphorylation; this may give the bacterium a bioenergetic advantage over competitors if PQQ is present. PQQ acts as a chemoattractant for *E. coli.* Secondly, an electron transport chain involving GDH may remove oxygen very rapidly during transition to anaerobic conditions, as newly synthesised fermentation enzymes are extremely oxygen sensitive. GDH may therefore have a protective role.

GDH transfers electrons to the bacterial respiratory chain. In *E. coli*, the oxidation of

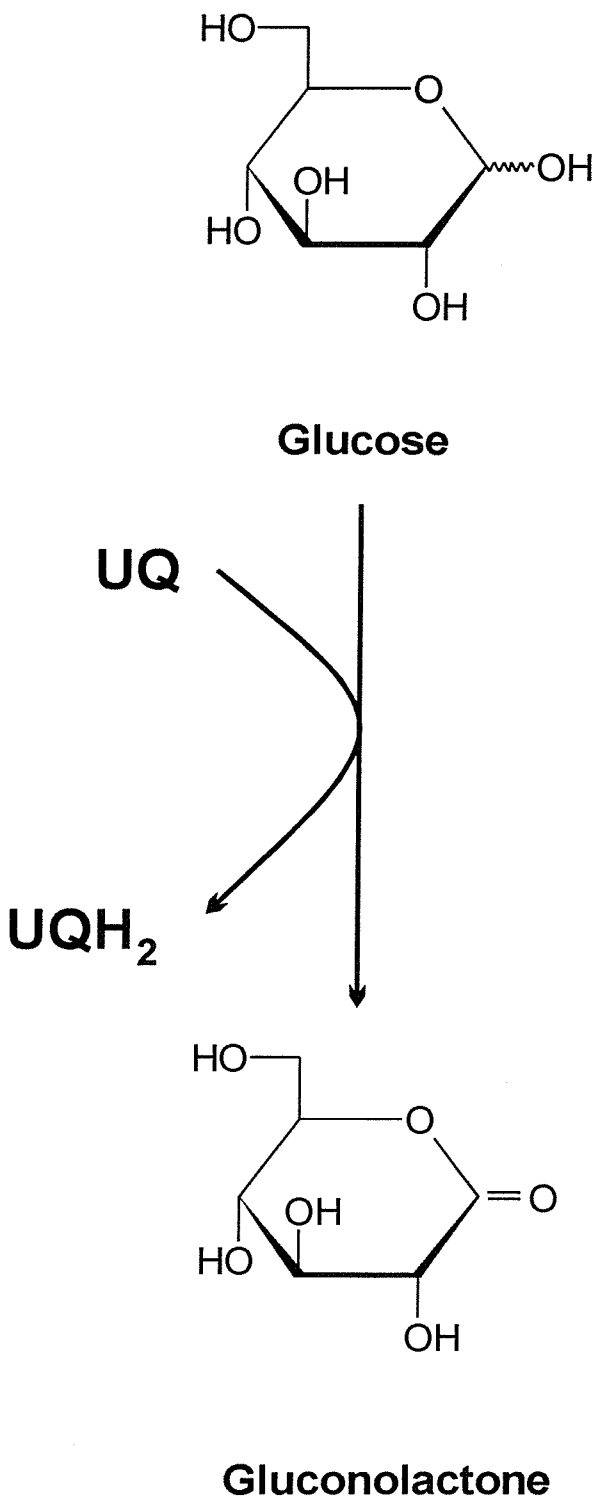

Figure 1.4 The reaction catalysed by GDH

Glucose is converted to gluconolactone by GDH. Two electrons are transferred to ubiquinone that is located in the inner membrane.

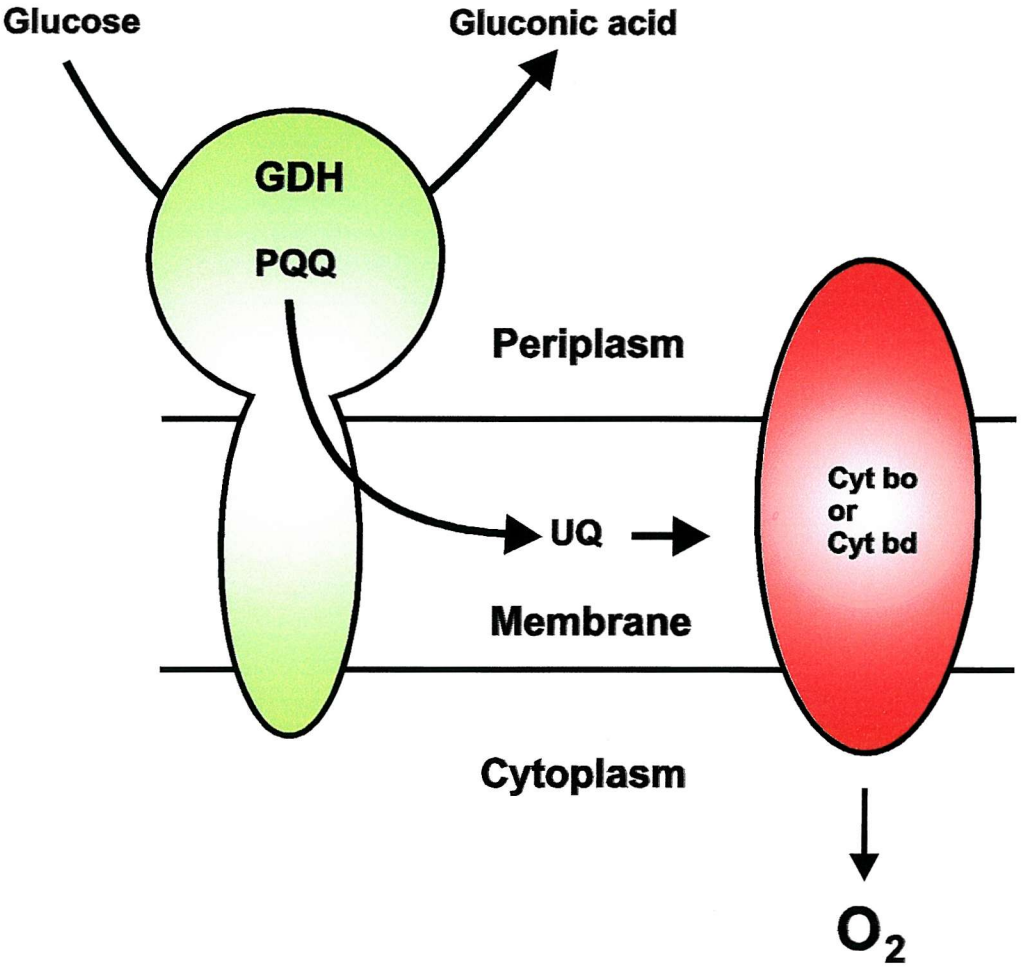

Figure 1.5 The electron transport chain for oxidation of glucose in *E. coli*

Electrons are transferred from glucose to ubiquinone by GDH. Two electrons are passed to ubiqinone in a single step. Then electrons are passed via cytochrome *bo* or *bd* to oxygen.

glucose by GDH generates an electrochemical proton gradient that is responsible for producing ATP via ATP synthase. This was shown using purified GDH (containing PQQ), cytochrome *o* oxidase and *E. coli* phospholipids containing ubiquinone 8, by reconstitution into proteoliposomes (Matsushita *et al.*, 1987). During glucose oxidation electron transfer rates and membrane potential were the same as those measured in membrane vesicles isolated from whole cells. This showed that ubiquinone 8, the native ubiquinone in *E. coli's* respiratory chain is the electron acceptor from GDH. The respiratory chain in *E. coli* is simple as it consists of three components:- GDH, ubiquinone and a cytochrome oxidase. The chain is branched as cytochrome *bd* and cytochrome *bo* act as terminal oxidases (Figure 1.5). Further work has suggested that proton pumping occurs due to the terminal oxidase and not by GDH and ubiquinone (Yamada *et al.*, 1993).

GDH is also present in other types of bacteria such as *Acinetobacter, Pseudomonads* and other enteric bacteria. *Pseudomonads* are aerobic but can grow in the absence of oxygen as they can use nitrate as a terminal electron acceptor. Most lack a complete glycolytic pathway so the role of GDH is to oxidise glucose to gluconic acid, which can then be further oxidised to 2-ketogluconic acid. These products can be metabolised by the Entner Doudoroff pathway. GDH in *P. aeruginosa* has a lower affinity for glucose than the glucose uptake system. Therefore under excess glucose GDH may provide extra energy for growth.

Some species of *Acinetobacter* can grow on glucose by metabolising it by GDH and the Entner Doudoroff pathway; however some species cannot. Even those species that cannot grow on glucose can use GDH to oxidise glucose to produce a protonmotive force and ATP. It could function as an auxiliary energy-generating system (van Schie *et al.*, 1987)

It has been suggested that GDH in *Klebsiella pneumoniae* provides an additional contribution to the protonmotive force and ATP synthesis (Hommes *et al.*, 1985). A second role of GDH could be to replace glycolysis and the TCA cycle when glyceraldehyde 3-phosphate is limited (Buurman *et al.*, 1994). A third role could be to protect nitrogenase enzymes because *K. pneumoniae* is a facultative anaerobe capable of nitrogen fixation (Goodwin and Anthony, 1998). GDH may protect nitrogenase in conditions supporting nitrogen fixation as the enzyme is induced before complete anaerobic conditions occur. GDH may reduce the remaining oxygen so the nitrogenase is not affected. *Gluconobacter* strains oxidise glucose to gluconate via GDH. This product can be oxidised by the pentose phosphate pathway as they do not have a TCA cycle.

1.3 The structure of glucose

The structure and uptake of glucose by *E. coli* is going to be discussed because it is the substrate for GDH. Glucose is the main fuel used for the generation of energy in *E. coli*; it is a monosaccharide that consists of six carbon atoms. This sugar is an aldose as the carbonyl group is an aldehyde. Four chiral centres are present (C2, C3, C4, and C5), so D-glucose is one of sixteen stereoisomers. In water D-glucose predominantly occurs in a ring form. For this ring form to be produced from the linear form, the C-1 aldehyde reacts with the alcohol at C-5 to form a hemiacetal. The resulting six member ring is called a pyranose (Figure 1.6).

The ring form of glucose makes C-1 asymmetric; this means two diastereomers can occur. In solution 36.4% is the α anomer and 63.6% is in the form of the β anomer. The pyranose ring occurs in a chair or boat conformation because the geometry of the saturated carbon atoms forbids the molecule from being planar (this is illustrated in Figure 1.10).

1.3.1 Glucose uptake and metabolism in *E. coli*

For cells to use glucose as the primary fuel source for the generation of ATP, it must be able to enter the cell. Translocation of carbon sources is catalysed by a variety of specific transport systems. The phosphoenolpyruvate-dependent phosphotransferase system (PTS) is responsible for the uptake of glucose in some bacteria (e.g. *E. coli*) (Kundig *et al.*,1964). It couples glucose translocation and phosphorylation. PTS transports and phosphorylates glucose from the periplasm to the cytoplasm but also acts as a sensing system as it is involved in chemotaxis. The PTS transport system is shown in Figure 1.7. Enzyme I (EI) and histidine protein (HPr) are soluble enzymes. These enzymes are the general enzymes of the PTS system as they participate in the phosphorylation of all PTS carbohydrates. The first step in the pathway in the transfer of the phosho group of PEP to EI. Phosphorylation occurs at the N-3 position of His-189 to form a phoshohistidine adduct. Phosphorylation by PEP occurs when EI is in a dimeric form and a divalent metal such as Mg^{2+} or Mn^{2+} is present. The dimer then dissociates to phosphorylate HPr. The phosphoryl group is transferred to N1 of His-15 on HPr. The phosphoryl group is transferred from HPr to soluble EIIAglc. This protein is specific for glucose uptake, it is phosphorylated by HPr at the N-3 position of His-90. EIIAglc then phosphorylates the EIIBglc protein that is found bound in the membrane in the complex EIICBglc protein. Glucose is then phosphorylated by this complex and translocated into the cytoplasm (Robillard and Bros, 1999).

There are several pathways in *E. coli* that metabolise glucose to produce ATP; these include glycolysis (Embden-Meyerhof-Pathway), the Entner-Doudoroff pathway and the TCA

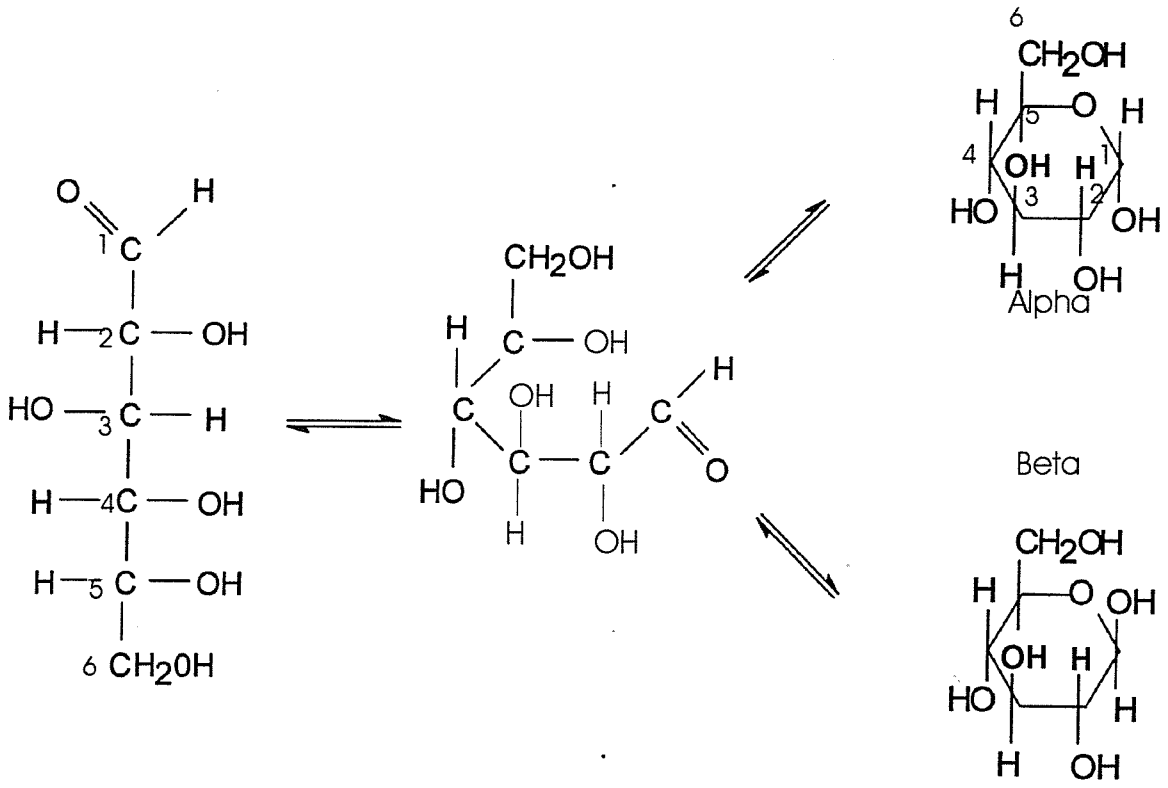

Figure 1.6 The structure of glucose

This is the linear and ring structure of D-glucose. The ring form is made when the C-1 aldehyde reacts with the alcohol at C-5. Then the C-1 in the ring structure becomes asymmetric and two diastereomers can occur. In solution 36.4% is the alpha anomer and 63.6% is in the form of the beta anomer.

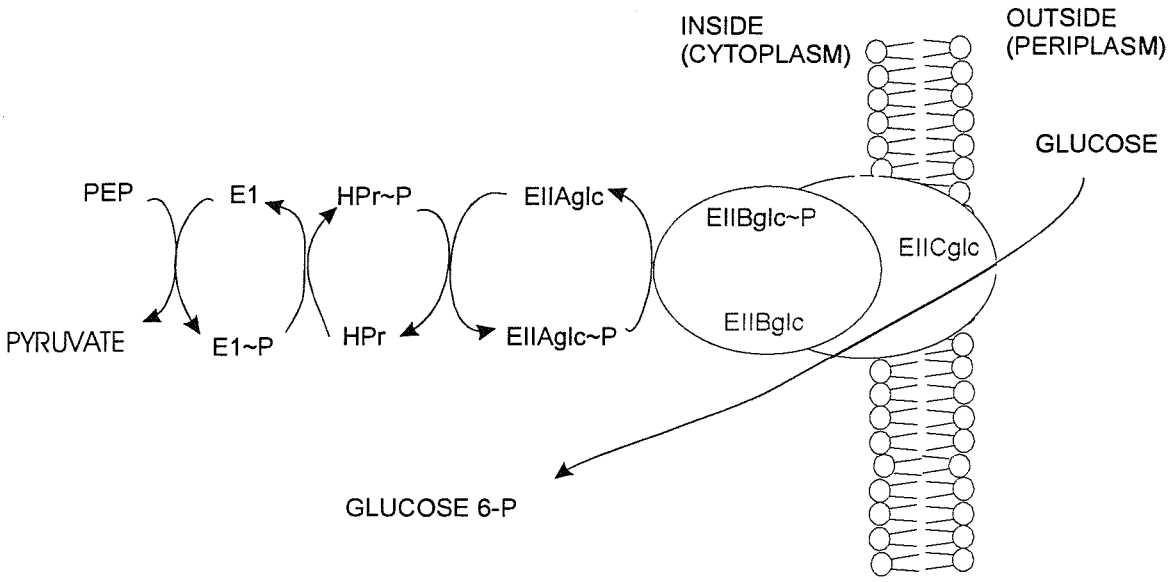

Figure 1.7 The phosphoenolpyruvate -dependent phosphotransferase system

The phosphoenolpyruvate-dependent phosphotransferase system (PTS) translocates D-glucose from the periplasm to the cytoplasm. Phosphorylation is coupled with this translocation so glucose becomes glucose-6-phosphate. The diagram shows that phosphate is transfered from phosphoenolpyruvate to glucose by E1, HPr, EIIAglc, EIIBglc and EIICglc.

cycle. The pentose phosphate pathway is an additional metabolic pathway for glucose that generates NADPH and ribose-5-phosphate from glucose-6-phosphate. NADPH is required for biosynthetic purposes, not ATP production. All pathways occur in the cytoplasm and each will be discussed below. Figure 1.8 shows an overview of the metabolism of glucose.

Glycolysis converts glucose-6-phosphate to pyruvate with a small production of ATP and NADH. In aerobic conditions pyruvate is decarboxylated to form acetyl coenzyme A, carbon dioxide and NADH and then the acetyl coenzyme A is oxidised by the TCA cycle. NADH and $FADH_2$ from glycolysis and the TCA cycle provide most of the cell's energy via the electron transport chain. The net reaction for the transformation of glucose to pyruvate is;

$$\text{Glucose} + 2\text{Pi} + 2\text{ADP} + 2\text{NAD}^+ \rightarrow 2 \text{ pyruvate} + 2\text{ATP} + 2\text{NADH} + 2\text{H}^+ + 2\text{H}_2\text{O}$$

The TCA cycle also provides intermediates for biosynthesis. The net reaction of the TCA cycle is:-

$$\text{Acetyl CoA} + 3\ \text{NAD}^+ + \text{FAD}^+ + \text{Pi} + 2\text{H}_2\text{O} \rightarrow 2\text{CO}_2 + 3\ \text{NADH} + \text{FADH}_2 + \text{GTP} + 2\text{H}^+ + \text{CoA}$$

In anaerobic conditions glycolysis is the first part of the fermentation pathway. The resulting pyruvate is cleaved by pyruvate:formate lyase to formate and acetyl CoA. Then acetaldehyde dehydrogenase catalyses the reduction of acetyl CoA to ethanol ($CH_3CHO\text{-}SCoA + NADH + H^+ \rightarrow$ Ethanol + NAD + CoASH). Formate is split into carbon dioxide and hydrogen by formate lyase.

The Entner-Duodoroff pathway (ED) is an alternative route to convert glucose to pyruvate in *E. coli* (Esienberg and Dobrogosz, 1967). The ED pathway is shown in Figure 1.9. The resulting pyruvate can then be oxidised by the TCA cycle and glyeraldehyde3-phosphate can be metabolised by glycolysis (Peekhans and Conway, 1998).

All the above pathways involve the phosphorylative route of glucose metabolism but a non-phosphorylative route can occur in the periplasm via GDH (previously described in Section1.2). Gluconate produced by GDH can then enter the cytoplasm and be metabolised by the Entner-Duodoroff Pathway or it may be oxidised to 2-keto-gluconate by gluconate dehydrogenase. All of these enzymes are membrane bound. This pathway has been shown to be adequate for *E. coli* growth; an *E. coli* mutant lacking E1 of the phosphotransferase system could only grow on glucose if PQQ was added to the growth medium (Fliege *et al.*, 1992).

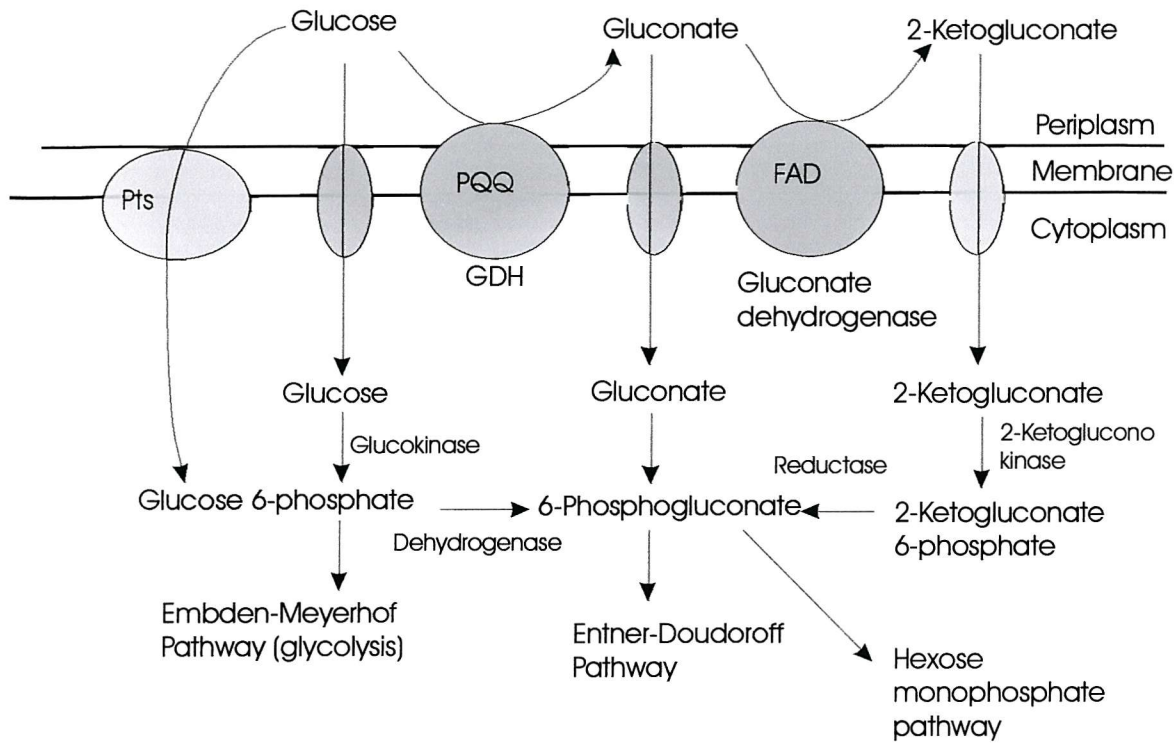

Figure 1.8 Metabolism in *E. coli* (Goodwin and Anthony, 1998)

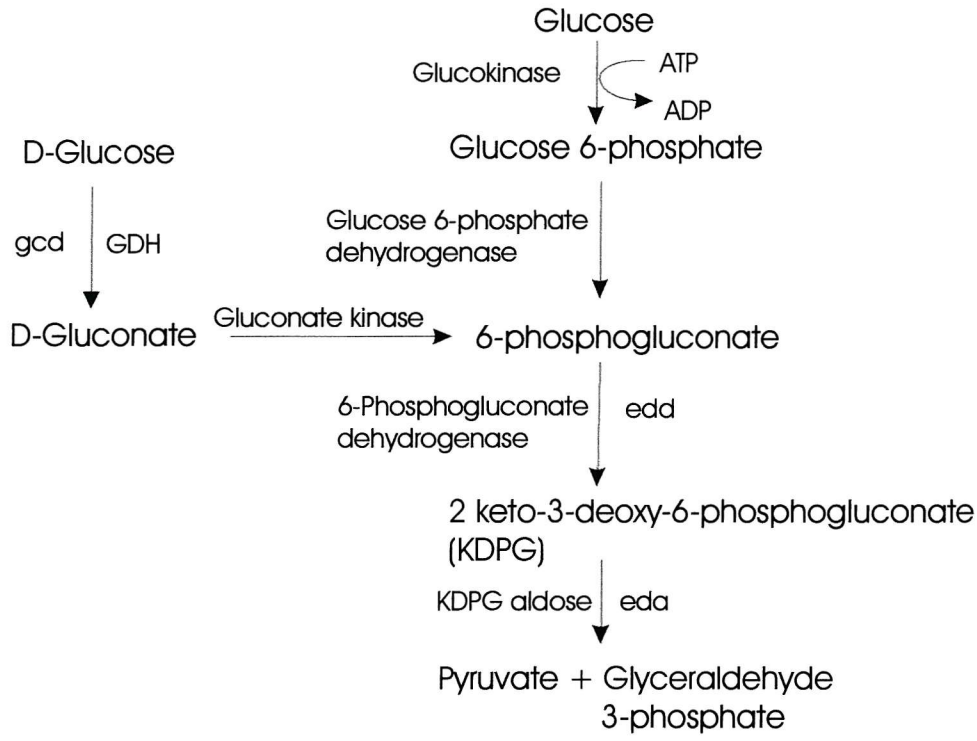

Figure 1.9 The Entner-Doudoroff pathway in *E. coli*

1.4 The substrate specificity of GDH in *E. coli*

The best substrates for GDH are 6-deoxy-D-glucose (catalytic efficiency 456 $M^{-1}sec^{-1}x10^3$) and D-glucose (catalytic efficiency 279 $M^{-1}sec^{-1}x10^3$). GDH can also oxidise D-mannose, D-galactose, D-fucose and D-xylose at more that 25% of the rate with D-glucose (Table 1.1). Figure 1.10 shows the structures of the sugars. The disaccharides maltose, lactose and sucrose are not oxidised by this enzyme (Cozier *et al.*, 1999).

No L-hexoses are oxidised by GDH and it has been found that L-hexoses do not act as inhibitors. This suggests that these compounds cannot bind to the active site. Table 1.1 shows substrate specificity and helps to identify structural features that affect binding of glucose and other hexoses at the active site. Replacing the C6-hydroxymethyl group of glucose with a methyl group (6-deoxy-D-glucose) only slightly decreased the K_m for the substrate. Therefore, the C6 hydroxymethyl group is not essential for substrate binding. The C4 hydroxyl group is also not critical for binding because GDH can oxidise galactose, which differs from glucose only at the C4 position.

The C3 and C2 hydroxyl groups are both not critical for substrate binding because GDH has a relatively high affinity for 3-deoxy-D-glucose and allose. Unlike glucose, allose has its C3-hydroxyl below the plane of the ring. The replacement of the C3 hydroxyl group by methyl in 3-O-methyl-D-glucose increases the K_m by 40 fold. This could be due to steric hindrance. The C2 is not critical for binding because 2-deoxy-D-glucose has a K_m of 1.6mM.

Therefore, for hexose binding, the C2, C3, and C4 groups of the hexose ring can be in either orientation but affinity is highest when C2 and C4 hydroxyls are below the ring and C3 hydroxyl is above the ring. The group bound to C5 (usually the C6 hydroxymethyl group) must be above the ring for substrates to bind.

All pentose sugars tested can bind to GDH because they lack the hydroxymethyl group substituent at C5. This means that some pentoses act as inhibitors. It has been suggested that pentoses can bind because in solution the pyranose form predominates (Cozier *et al.*, 1999). GDH can only oxidise one stereoisomer of each pentose, and substrates must have the C2-hydroxyl below the plane of the ring.

His-775 is expected to contribute to substrate specificity. Cleton-Jansen *et al.*, (1991) found a naturally occurring mutation in *G. oxydans* in which His-787 is substituted by Asn-787. (His-787 corresponds to His-775 in GDH). This mutation allowed GDH to oxidise the disaccharide maltose. This may occur as asparagine is a smaller amino acid than histidine, and makes the active site more accessible. Therefore, His-775 may obstruct the entrance to

Table 1.1 Substrate specificity of GDH

Data taken from Cozier *et al.* (1999). All substrates had a V_{max} value between 60-100% of that with D-glucose. Sugars that were not be oxidised by GDH are represented by X.

Substrate	Class of Sugar	K_m Value (mM)
D-glucose	Hexose	2.1
L-glucose	Hexose	X
6-deoxy-D-glucose	Hexose	1.3
2-deoxy-D-glucose	Hexose	1.6
D-allose	Hexose	2.5
D-fucose	Hexose	8.3
2-amino-D-glucose	Hexose	9.5
3-deoxy-D-glucose	Hexose	10.8
D-melibiose	Disaccharide	17.7
D-galactose	Hexose	39
D-mannose	Hexose	78
3-O-methyl-D-glucose	Hexose	79
D-xylose	Pentose	22
L-xylose	Pentose	X
D-arabinose	Pentose	X
L-arabinose	Pentose	46
D-lyxose	Pentose	X
L-lyxose	Pentose	100
D-ribose	Pentose	110
L-ribose	Pentose	X

Hexoses

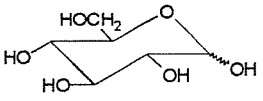

D-glucose

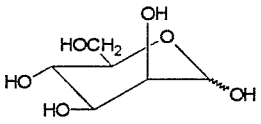

D-mannose

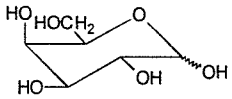

D-galactose

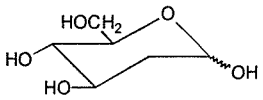

2-deoxy-D-glucose

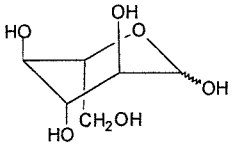

L-glucose

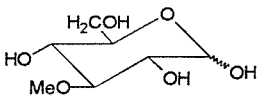

3-O-methyl D-glucose

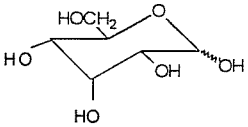

D-allose

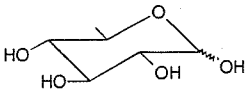

6-deoxy-D-glucose

Pentoses

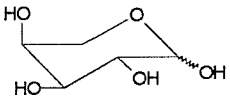

L-arabinose

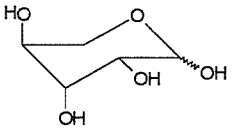

L-lyxose

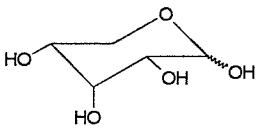

D-ribose

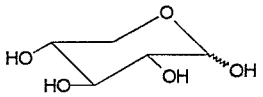

D-xylose

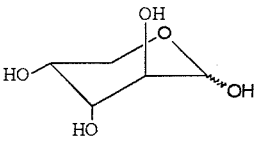

D-arabinose

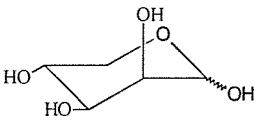

D-lyxose

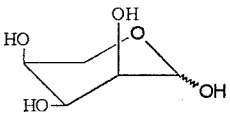

L-ribose

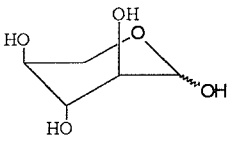

L-xylose

Disaccharide

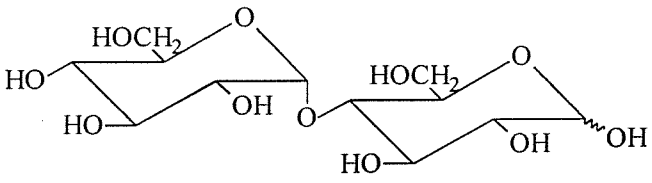

Maltose (4-O-α-D-glucopyranosyl-D-glucose)

Figure 1.10 The structure of sugars

the active site in *E. coli*, allowing glucose to be oxidised but not maltose (Cozier and Anthony, 1995).

Various groups have conducted site directed mutagenesis on His-775 in *E. coli*. Yamada *et al.* (1998) substituted His-775 with arginine and alanine. The arginine mutation had activity that was 3% compared with that of wild type GDH and the K_m for glucose was unaltered. The alanine mutation had no effect on substrate binding or activity. Therefore the arginine mutation may have changed the conformation of the active site.

Sode and Kojima (1997) converted His-775 to asparagine and aspartate. Compared with WT-GDH, the H755D mutation had a decreased affinity for glucose by 25 fold and the K_m for other substrates increased. The H775N mutation had no effect on the K_m for glucose, but increased the K_m for other substrates. Sode suggested that His-775 is hydrogen bonded to glucose at its C6 hydroxyl group; this does not agree with the results of Cozier *et al.* (1999) who concluded that the C6 group is not essential for binding glucose.

1.5 The structure and mechanism of GDH

The mGDHs from *E. coli* and other bacterial strains have a closely related structure indicated by similar amino acid sequences. GDH is a single polypeptide with a molecular mass of 87 kDa and probably occurs as a monomer (Ameyama *et al.*, 1986). The *gcd* gene sequence of *E. coli* (coding for GDH) was determined and then the amino acid sequence deduced; hydropathy indices predicted that GDH contains five hydrophobic domains at the N-terminal region. GDH has 796 amino acids (Cleton-Jansen *et al.*, 1990).

Gene fusion experiments enabled the topology to be determined (Yamada *et al.*, 1993). Constructed fusion proteins with β-galactosidase and alkaline phosphatase proved that GDH has five membrane spanning regions and that the N-terminal and C-terminal regions are found at the cytoplasmic and periplasmic side of the membrane respectively (Figure 1.11). Out of the five hydrophobic segments, four consist of more than 18 amino acids and probably form alpha helices in the membrane. Hydrophobic region 4 may have a beta sheet structure as it only consists of 15 amino acids. Amino acids 1 – 154 form this transmembrane anchor. These results agree with the hydropathy index predicted from the protein's primary structure (Yamada *et al.*, 1993). The catalytic domain of GDH is found in the periplasm. It is expected that a ubiquinone-binding site is located on the membrane portion of the protein.

The periplasmic domain of mGDH has about 30% sequence identity with alcohol dehydrogenase (ADH) and methanol dehydrogenase (MDH) (Anthony, 1996). These conserved sequences provide a general stable structure that is common in all the proteins.

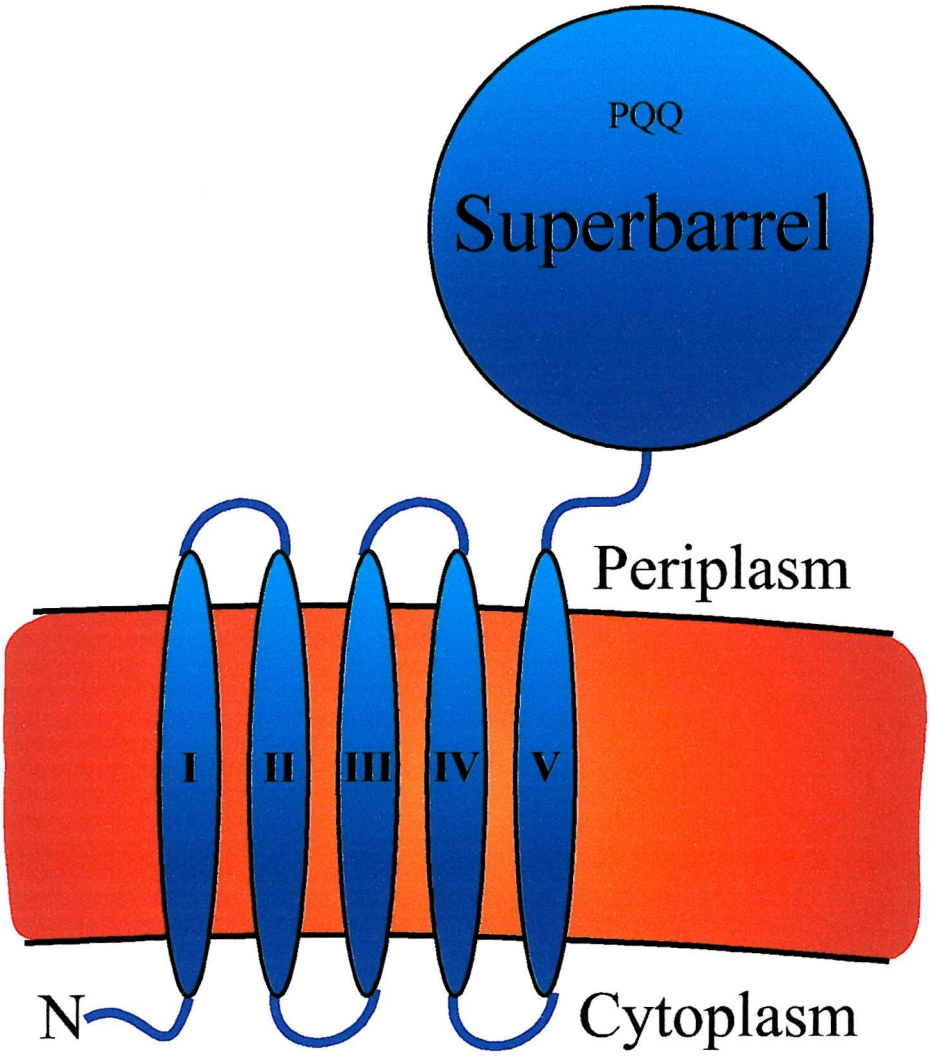

Figure 1.11 Topology of quinoprotein glucose dehydrogenase

(Yamada *et al.*, 1993)

However, PQQ only binds weakly to GDH (K_d 282nM) and tightly to MDH and ADH. This may occur because GDH could have fewer residues that form interactions with PQQ.

The X-ray structure for GDH has not been determined but it has been solved for MDH at 1.94 Å from *Methylobacterium extorquens* (Ghosh *et al.*, 1995). The periplasmic region of GDH (residues 155-796) is 26% identical to the amino acid sequence of the alpha subunit of MDH. Therefore the structure of GDH in *E. coli* has been modelled on the structure of MDH from *Methylobacterium extorquens* (Cozier and Anthony, 1995) (see Section 1.5.2). GDH is expected to have a similar mechanism as MDH.

1.5.1 The structure of methanol dehydrogenase on which a model of GDH structure is based

MDH is a soluble protein located in the periplasm of methylotrophic bacteria. Its function is to oxidise methanol to formaldehyde (Anthony, 1986). Electrons from PQQ in MDH are passed to cytochrome c_L in two separate steps (Dijkstra *et al.*, 1989) and are then transferred to a terminal oxidase via cytochrome c_H (Figure 1.12) (Anthony, 1992).

MDH has a tetrameric structure with a subunit composition of $\alpha_2\beta_2$ (Ghosh *et al.*, 1995). Each α subunit has a molecular mass of 66kDa and the β subunit 8.5kDa. The subunits cannot be reversibly dissociated and the function of the β subunit is unknown. The genes for the subunits are together but not adjacent on a single operon, together with the gene for cytochrome c_L. The α subunit is the catalytic domain and each contains a molecule of PQQ and a Ca^{2+} ion. The two β subunits fold around the surface of the α subunit but do not interact with each other. The β subunit is bonded to the α subunit by hydrogen bonds and by hydrophobic and ionic interactions.

a) The superbarrel structure of the α subunit of MDH

"The α-subunit is a superbarrel made up of eight topologically identical four-stranded antiparallel β sheets (W shaped) arranged with radial symmetry like the blades of a propeller" (Ghosh *et al.*, 1995). PQQ is located at the middle of the superbarrel with Ca^{2+} (Figure 1.13). The superbarrel structure has a pseudo eight-fold symmetry axis running through the center of the subunit. Each blade is labelled W1-W8 and each strand labelled A, B, C or D with strand D on the outer surface of the subunit (Ghosh *et al.*, 1995). The A strands are more hydrophobic and the sequence of the β strands are in the same order as the amino acid sequence (apart from D8 which is derived from the N-terminus). A-B and C-D corners are short in the motif but the B-C corners form large extensions that contain 24-30 amino acids.

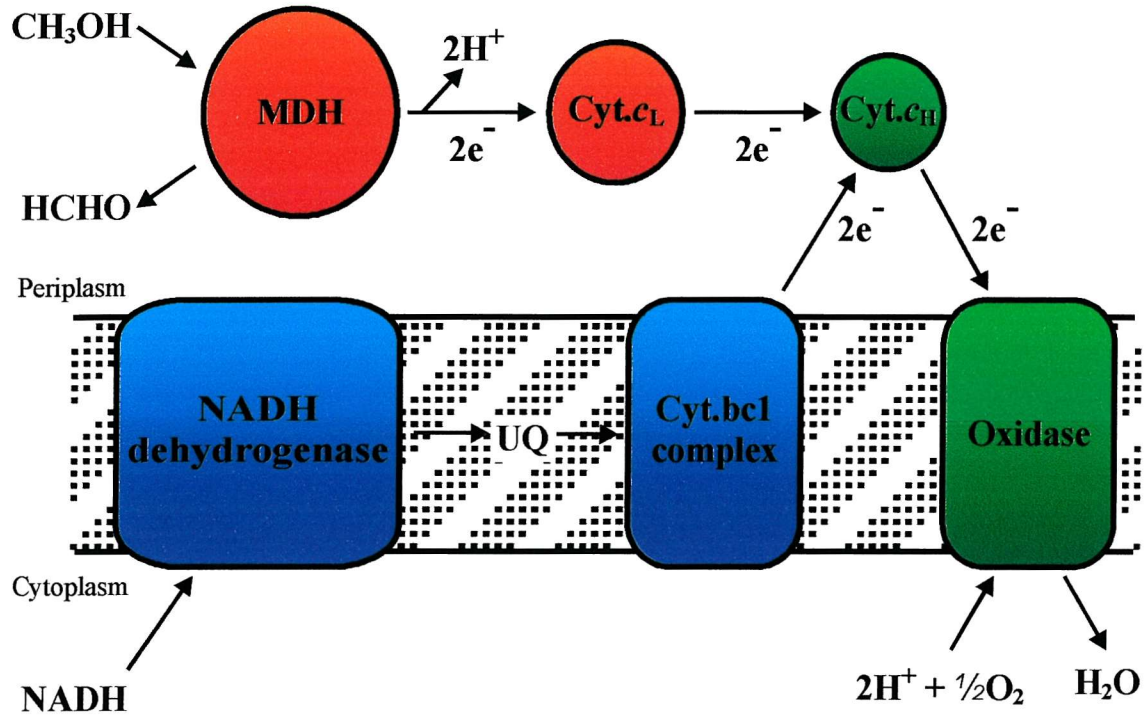

Figure 1.12 Electron transport chain involving MDH

Two electrons are transferred from methanol to cytochrome c_L by MDH in two separate steps. Electrons are then transferred via cytochrome c_H to the terminal oxidase.

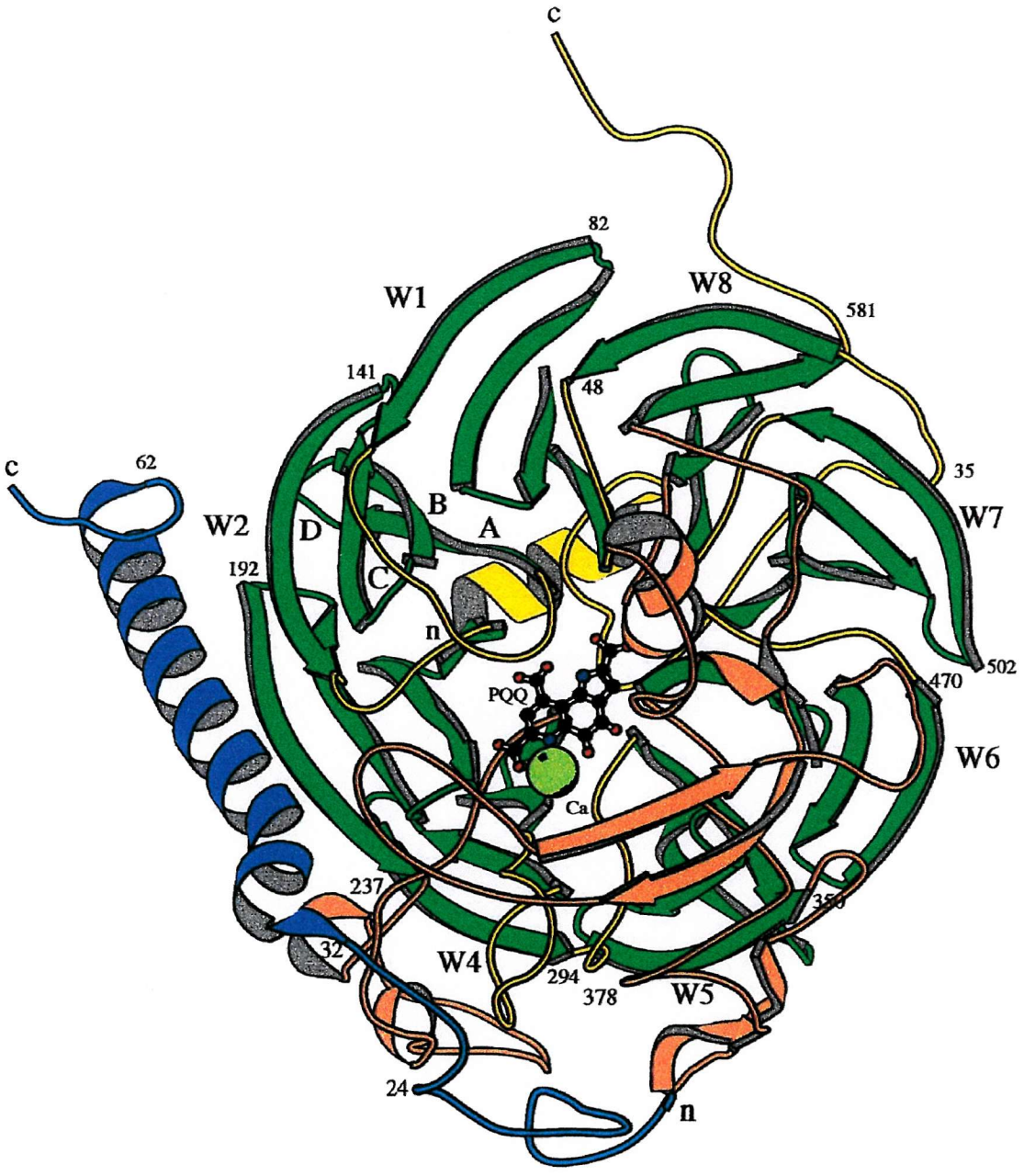

Figure 1.13 The structure of the alpha and beta subunits of methanol dehydrogenase

"The alpha subunit in MDH is a superbarrel made up of eight topologically identical four-stranded antiparallel beta sheets (W shaped) arranged like the blades of a propeller." Each blade is labelled W1-W8 and each strand labelled A, B, C or D. Strand D is on the outer surface of the subunit. PQQ and a Ca^{2+} are located in the middle of the superbarrel (Ghosh *et al.*, 1995).

This is a very compact structure as the outer D-strands overlap with each other: glycine on each D-strand interacts with tryptophan on the subsequent D-strand.

b) The tryptophan docking motif of MDH

The α subunit is stabilised by a tryptophan-docking motif made up of an 11 residue sequence in the C/D corner of all W motifs. This forms a stabilising girdle of interactions around the periphery of the subunit (Ghosh *et al.*,1995). Tryptophan in position 11 of the motif forms a stacking interaction between alanine (position 1) on the same motif and the peptide bond between position 6 and 7 on the next motif. The tryptophan is also hydrogen bonded between its indole NH and the carbonyl of the main chain residue 4 in the next motif (Figure 1.14).

c) The active site of the α subunit of MDH

A shallow hydrophobic funnel shaped depression leads to the active site of MDH. The loops between the B and C strands of motifs W6 and W8 fold over the end of the superbarrel to enclose the active site. The active site contains the non-covalently bound PQQ and a Ca^{2+} ion. The floor of the chamber is formed by a tryptophan residue (Trp-243) and the ceiling by a novel disulphide ring structure formed from two adjacent cysteine residues (Cys-103 and Cys-104). The two cysteine residues are bonded by an unusual trans-peptide bond. PQQ is sandwiched between this tryptophan and the ring structure (Anthony *et al.*, 1994). The Ca^{2+} ion may hold PQQ in the correct conformation. PQQ makes a number of polar and ionic equatorial interactions with amino acid side chains. The calcium ion is coordinated to the N-6, C-5 quinone oxygen and the C-7 carboxyl group of PQQ as well as Glu-177 and Asn-261 (Figure 1.15). Most of the amino acid side chains that interact with PQQ are from the A strand of the eight β sheets. The two carboxylates of PQQ are bonded to Ser-174, Thr-159, Arg-109, Glu-55 and Trp-476. The C4 and C5 oxygen atoms of PQQ are hydrogen bonded to Arg-331, C4 is also hydrogen bonded to Asn-394 as well. PQQ is in the semiquinone state as the C5 oxygen is in the plane of PQQ ring system and C4 oxygen is out of the plane by about 40°. The two sulphur atoms in the disulphide bridge are within 4Å of the plane of PQQ. The disulphide bridge is readily reduced and causes a loss of activity with cytochrome c_L but not with phenazine ethosulphate. Therefore the disulphide ring was expected to be important in electron transfer from $PQQH_2$ to cytochrome c_L. However, Avezoux *et al.* (1995) dismissed this theory by showing that the addition of phenazine ethosulphate re-oxidises the adjacent thiols back to the disulphide ring. Also, no free thiols were detected in the catalytic cycle

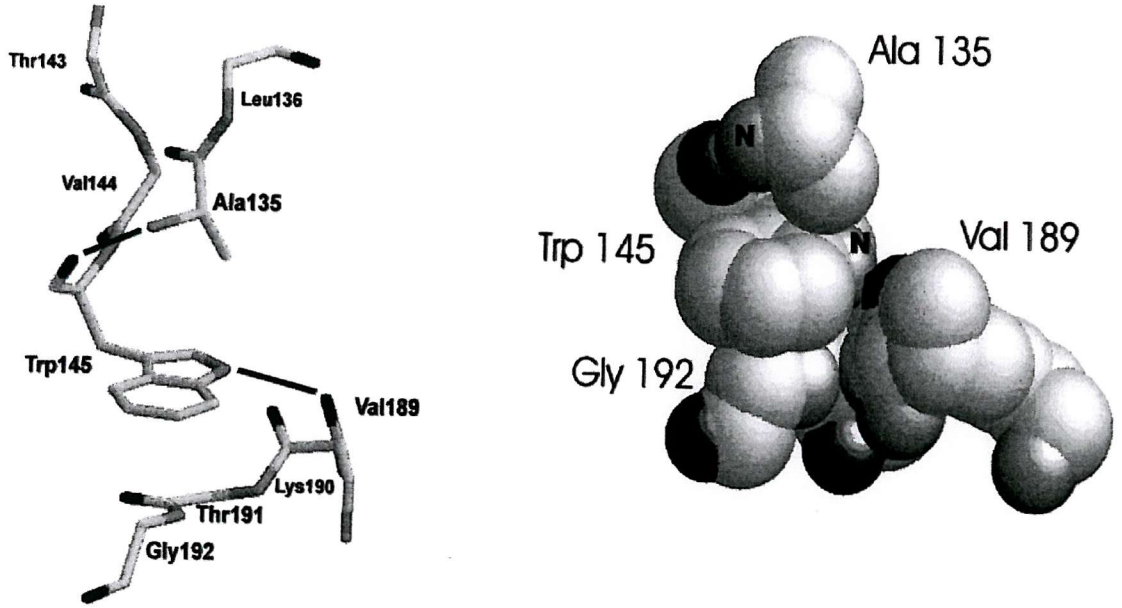

Figure 1.14 A tryptophan-docking motif

This tryptophan-docking motif is from MDH. Trp-145 from W2 and Ala-135 (W2) interact with each other. Trp-145 also interacts with the plane of the peptide bond between Thr-191 and Gly-192 in W3. Eight tryptophan-docking motifs are responsible for stabilising the structure (taken from Goodwin and Anthony, 1998).

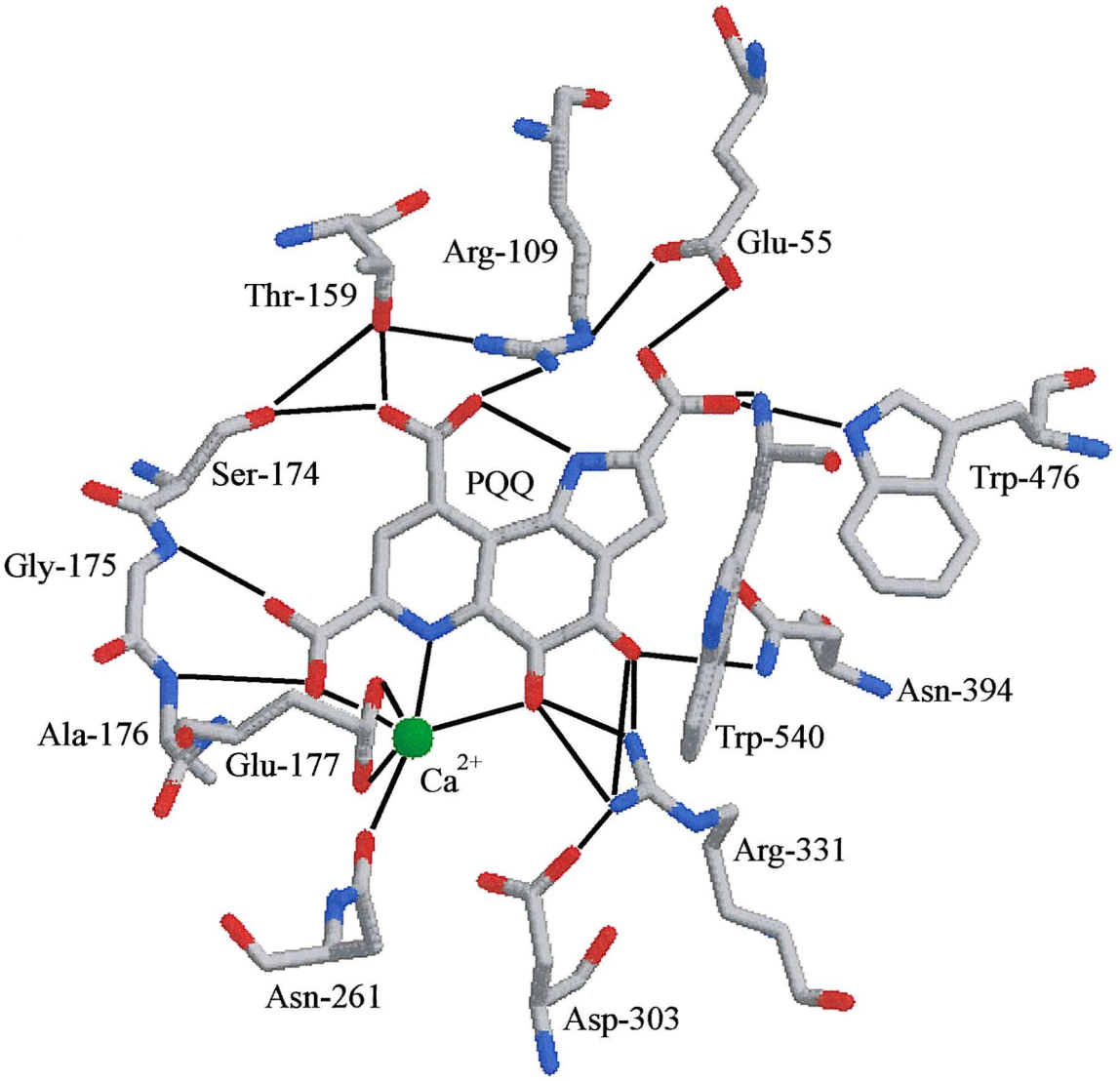

Figure 1.15 PQQ and calcium binding at the active site of MDH

This ball and stick diagram shows the residues in the active site of MDH. Two residues (Glu-177 and Asn-261) bind to the calcium ion and form three bonds (Ghosh *et al.*, 1995).

confirming that the novel structure has no role in electron transfer. The active site contains Asp-303 which is expected to act as a base in the enzyme's mechanism (Afolabi *et al.*, 2001). The base is involved in proton extraction from the substrate.

1.5.2 The model structure of GDH

GDH has been modelled on MDH (Cozier and Anthony, 1995). The model of GDH suggests that the eight β-sheet region that look like propeller blades are present (Figure 1.16); this region has the greatest sequence similarity between the two enzymes. PQQ is located at the interior of the superbarrel and a funnel (entrance wider than funnel in MDH and not hydrophobic) leading to the active site is present. The W-motifs are held together by an 11-residue consensus sequence that forms a tryptophan docking motif. The only difference between this consensus sequence compared to MDH is that GDH has a lysine/glutamate at position 8 instead of asparagine/glutamate.

The three cis prolines in MDH are not conserved in GDH. His-233 in GDH replaces Pro-72 of MDH; this is on a turn which is smaller in GDH. Pro-264 of MDH is replaced by Ile-427 in GDH, therefore altering the loop between B4 and C4. Pro-378 of MDH is replaced by Asn-600 in GDH, this is located on the external loop b.

In the GDH model six cysteines are present that could possibly form three disulphide bridges. Two disulphide bridges have been modelled satisfactorily, Cys-203/Cys-265 join strand B1 to the small loop between strands D1 and A2, and the second disulphide bridge joins strands B2 and D2. A third bridge could involve Cys-664 at the end of loop c, which is in a position that would allow the disulphide bond, but its partner is expected to be Cys-559 which occurs in a large unmodelled loop of GDH (residues 497-579). One of the major differences between GDH and MDH is that GDH lacks a disulphide bridge at the active site. Instead, His-262 is expected to hold PQQ in place (Figure 1.17). MDH has two disulphide bridges – Cys-103/Cys-104 at the active site and Cys-386/Cys-415. GDH only has one of these cysteines (Cys-265 in GDH and Cys-103 in MDH). Therefore there is no disulphide bridge at the active site of GDH as the equivalent sequence is five residues shorter and Cys-265 lies well away from PQQ. Also Cys-265 forms a disulphide bride with Cys-230.

GDH has seven loops a, b, c, d, e, f, and g. Loop a is formed between resides 382-404, loop b 597-599, loop c 628-668, loop e 690-711, loop f 320- 332 and loop g 281- 284. MDH does not have loops corresponding to e, f and g. Loop a shows little sequence homology between GDH and MDH. Also, loop a is 20 amino acids shorter in GDH but it still

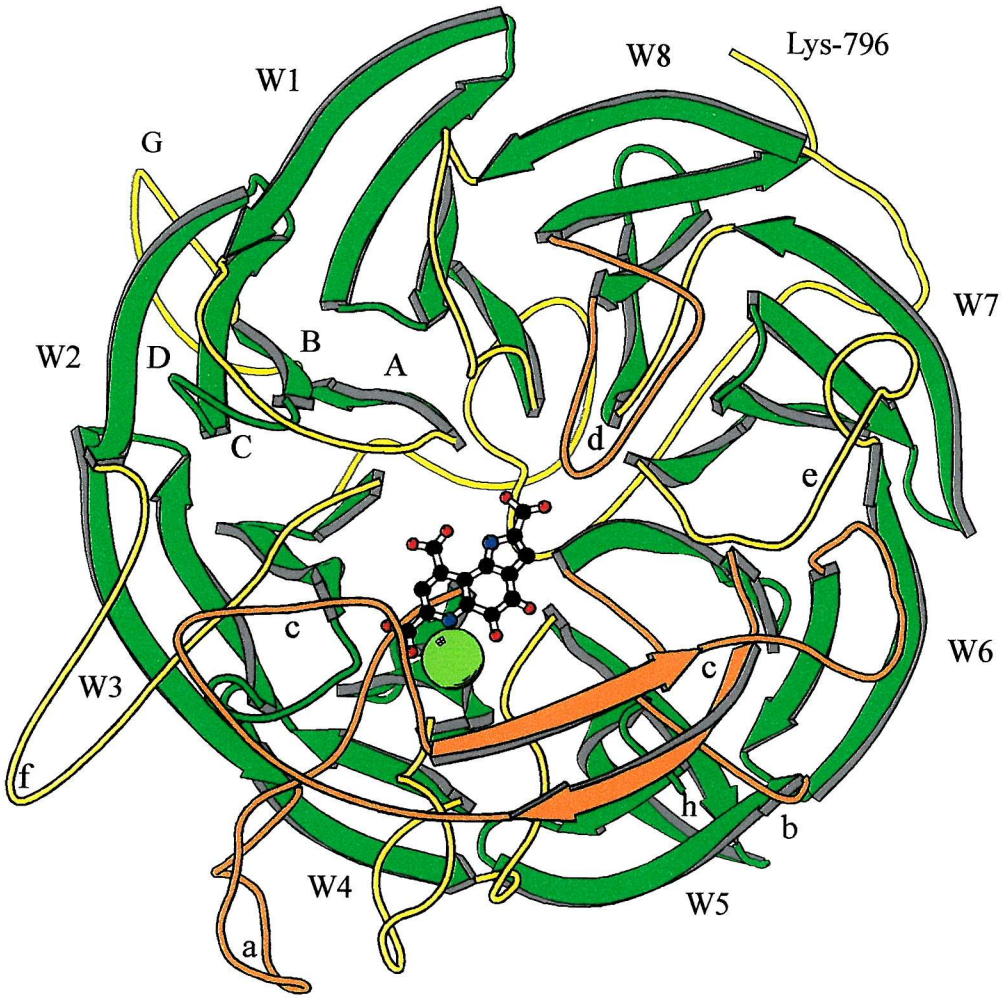

Figure 1.16 The modelled structure of GDH

This structure was produced by Cozier & Anthony (1995), based on the X-ray coordinates of methanol dehydrogenase (Ghosh *et al.*, 1995).

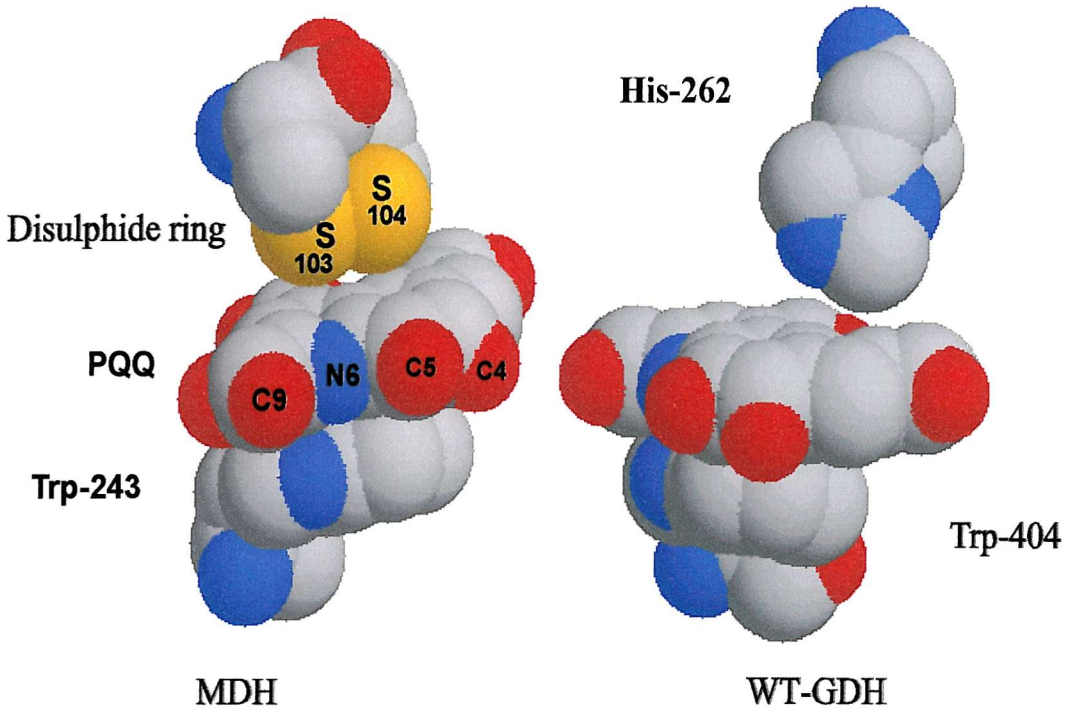

Figure 1.17 PQQ stacking in MDH and GDH

PQQ in stacked between Trp-243 and a disulphide ring in MDH. The disulphide ring is made from two cysteine residues (Cys-103 and Cys-104). His-262 replaces the disulphide ring in GDH (Goodwin and Anthony, 1998).

has a tryptophan residue that is found at the active site of MDH. There are 83 amino acids in GDH that are not present in MDH. These residues in GDH join together strands B5 and C5.

The model shows why GDH occurs as a monomer. The α subunits in MDH interact with each other due to hydrophobic and hydrophilic side chain interactions of the D strands of W7 and W8. Also the last ten C-terminal residues (590-599) form hydrophobic stacking interactions between two α subunits in MDH. In GDH the residues that interact withW7 and W8 are not that well conserved and the ten C-terminal residues are not present.

In MDH, the loops of the protein form a hydrophobic funnel leading to the active site. There are three sequences that form the funnel in MDH but these are poorly conserved in GDH. The sequence between D1 and A2 (residues 93-109 in MDH) is smaller in GDH and loop C shows little sequence homology. Loop d (774-783 in GDH) is smaller and lacks the helical structure seen in MDH. GDH has a slightly wider funnel at the entrance of the active site. In GDH, His-775 may determine specificity for monosaccharide as it partly obscures access to the active site. The surface funnel region of GDH lacks a prominent helical structure seen in MDH and this may interact with cytochrome c_L.

The active site of GDH differs from that in MDH. The two sulphur atoms of the novel disulphide ring structure that hold PQQ in MDH are not present in GDH, but the indole ring of a tryptophan that is bound to PQQ in MDH is present in GDH (Trp-243 in MDH and Trp-404 in GDH). Instead of the disulphide ring GDH has a histidine residue (His-264) that is conserved in all GDHs (Figure 1.17). It is thought that this histidine holds the PQQ in position at the active site. There are also many equatorial interactions between PQQ and amino acids in GDH. Residues of GDH that interact with PQQ include Glu-217, Arg-266, Thr-336, Val-352, Thr-353, Asp-354, Asn-402, Lys-493, Asn-607, Leu-712 and Ser-777 (Figure 1.18).

For convenience in the description, the metal ion in GDH will be referred to as Ca^{2+} (as in the model structure by Cozier and Anthony, 1995). At the active site of GDH the assumed Ca^{2+} ion is coordinated to PQQ and amino acids of the protein. PQQ ligation to Ca^{2+} is the same as MDH; the C-5 carbonyl oxygen, N-6 ring atom and one oxygen of the C-7 carboxylate of PQQ are coordinated to the Ca^{2+} ion. There are only three residues from the protein that form interactions with calcium ion; they are Asp-354, Asn-355 and Thr-424. It seems that in GDH the metal ion has a structural role and a catalytic role, it holds the PQQ in position and may act as a Lewis acid in the reaction mechanism. Asp-303 in MDH is conserved in GDH as Asp-466. This amino acid may be important in the mechanism of the

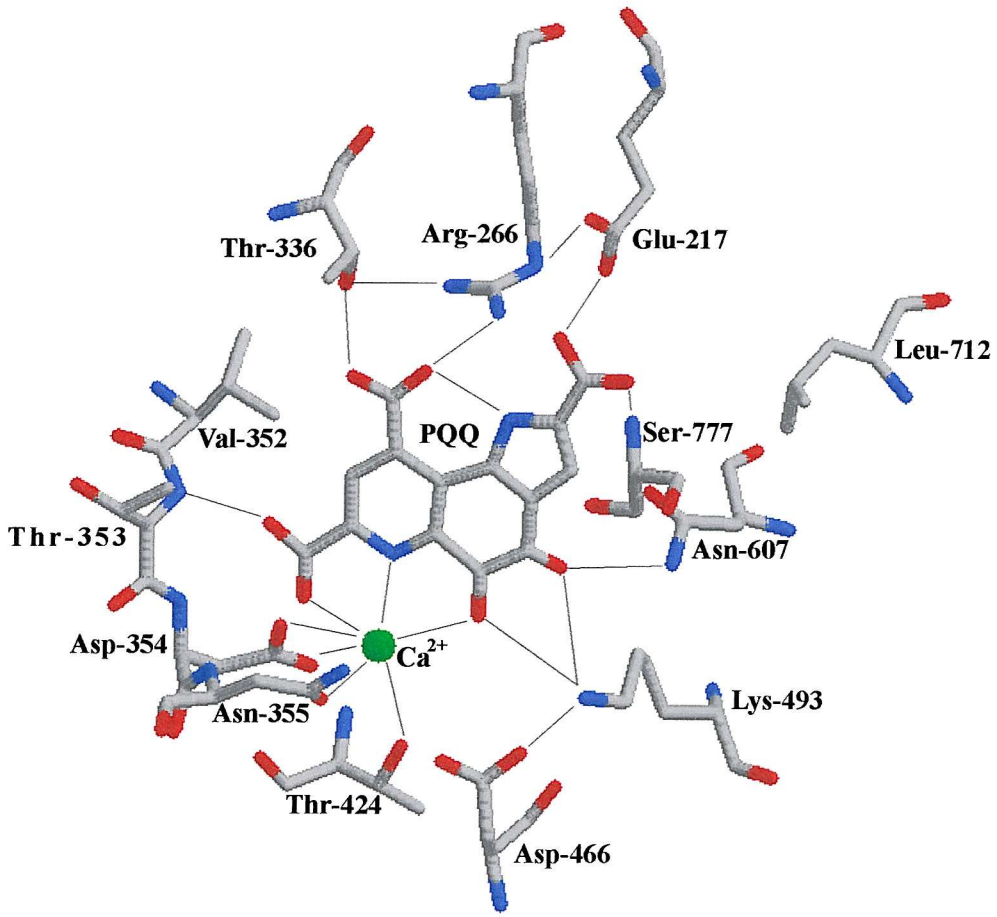

Figure 1.18 The equatorial interactions of PQQ in the active site of the model glucose dehydrogenase (Cozier and Anthony, 1995)

enzymes as the aspartate could act as an active-site base. This will be seen later in the mechanism for GDH (Section 1.5.4).

There are fewer equatorial interactions between the protein and PQQ, this may explain why it is possible to reverse the dissociation of PQQ from GDH but not MDH. PQQ can be removed by treatment with EDTA, heat, low pH or high salt concentrations. GDH from various bacteria have different stability properties. *E. coli* GDH is easily denatured and is known as a type 1 GDH (Dokter *et al.*, 1986).

Type II GDHs are usually having a greater affinity for PQQ and are resistant to inactivation by EDTA. Examples of these types of GDHs are found in *Gluconobacter suboxydans* and *Acinetobacter calcoaceticus*.

Tryptic digestion of GDH has been used to separate the catalytic domain from the membrane domain (Witarto *et al.*, 1999a) and far UV circular dichroism (CD) spectroscopy has been used to study the secondary structure. Results agreed with the model of GDH. The C-terminal consists of 35% β sheet compared to 35% in the model.

1.5.3 The ubiquinone binding site on GDH

The ubiquinone binding site on GDH is expected to be located in the membrane domain of the protein so that electrons can be transferred from PQQ to membrane ubiquinone. Friedrich *et al.* (1990) proposed that the membrane spanning domain of GDH in *Acinetobactor calcoaceticus* was similar to that of one of the subunits of mitochondrial NADH-ubiquinone-reductase (complex 1). They predicted that its interaction with ubiquinone resides at the cytoplasmic side, and makes a proton gradient. *E. coli* GDH is 70% homologous with GDH of *A. calcoaceticus*, but Yamada *et al.* (1993) predicted that the ubiquinone reduction site is on the periplasmic side of the membrane and electron transfer does not generate a proton electrochemical gradient. It was also shown that the proton gradient depends only on the terminal oxidase.

Sakamoto *et al.* (1996) used a set of ubiquinone analogues to characterise the ubiquinone reduction site of GDH, and compared it to complex 1 in mitochondria (Figure 1.19). They deduced that only half of the benzoquinone ring is recognised by the ubiquinone reduction site in GDH. Replacing methoxy groups at position 2, 3 or both to ethoxy groups in the ubiquinone analogues decreased their electron accepting efficiency. Only an ethoxy group at position 2 produced an active compound whilst ethoxy groups at position 3 or at both positions 2 and 3 produced an inactive compound. Therefore, methoxy groups at position 2 and 3 are important for ubiquinone binding. Changing the 6-alkyl side chain produced a

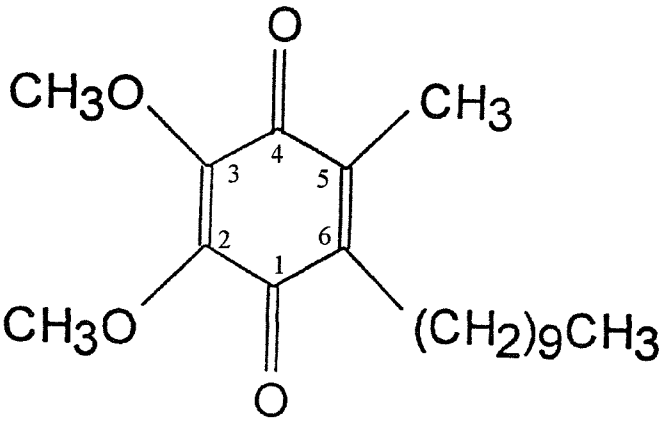

Ubiqinone analogue

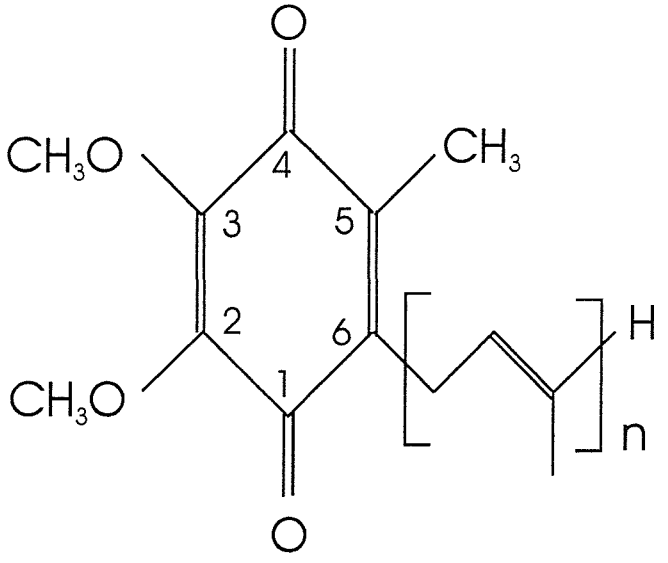

Ubiquinone

Figure 1.19 Structure of ubiquinone and a ubiquinone analogue

These are the structures of ubiquinone and a ubiquinone analogue used to investigate the ubiquinone reduction site in GDH. In *E. Coli* ubiquinone n = 8.

number of compounds that had similar K_m and V_{max} values for electron transfer. This demonstrates that the conformation of the 6-alkyl side chain does not contribute to activity and is not involved in electron transfer. Changing the methyl group at position 5 had no effect on electron transport.

Experiments with the complex 1 ubiquinone binding site indicated that the ubiquinone binding site is less restricted, as the 2- and 3-position groups are loosely recognised. Also, the ubiquinone site might have a larger pocket in which bulky ubiquinone analogues can serve as electron acceptors, as potent inhibitors of the complex 1 reduction site had different structures. This work showed that the ubiquinone binding sites are different in GDH and complex 1 in mitochondria.

Miyoshi *et al.* (1999) investigated the depth of the ubiquinone binding site using two fluorenyl fatty acids which had the GDH inhibitor capsaicin close to the fluorene. Capsaicin inhibits ubiquinone reduction. Capsaicin was located at different positions in the alkyl tail chain; one close to the polar carboxyl head group (α-DFA) and the other in the middle of the chain (θ-DFA). Purified GDH was reconstituted into phosphatidylcholine (PC) vesicles with α-DFA or θ-DFA at various molar ratios. Ubiquinone reduction activity (Q1 and Q2) of GDH in α-DFA containing vesicles was significantly lower compared with vesicles containing θ-DFA. This suggests that the ubiquinone binding site is located close to the membrane surface (Miyoshi *et al.*, 1999).

1.5.4 The mechanism of GDH

The reaction mechanism of GDH is unknown, but due to its structural similarities to MDH, it is expected to follow a similar mechanism. Therefore the proposed mechanisms for MDH are going to be discussed (Anthony, 1996).

Elucidating the mechanism for MDH has been difficult due to the lack of intermediates that can be identified spectroscopically. The enzyme has a ping-pong reaction as the binding of substrate causes the reduction of PQQ and the release of products, followed by two single electron transfer steps to cytochrome c_L. A stable semiquinone intermediate forms during the transfer of electrons (Frank *et al.*, 1988). Two mechanisms have been proposed.

In the addition/elimination mechanism (Figure 1.20), the C5 carbonyl of PQQ is expected to form a covalent PQQ-substrate complex as it has been proved that the C5 carbonyl is very reactive towards nucleophiles (Section 1.1.1). Adducts have been formed with methanol, cyclopropanol, ammonia, cyanide, aldehydes and ketones (Duine *et al.*, 1987;

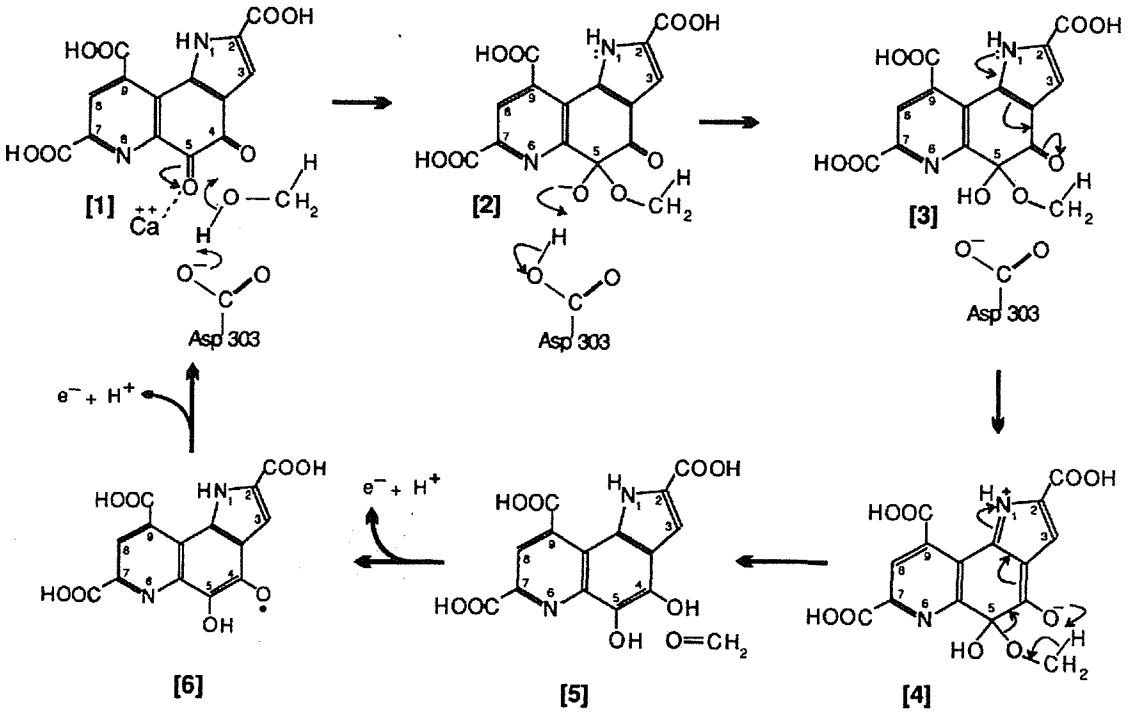

Figure 1.20 The mechanism of MDH involving a hemiketal intermediate

MDH has a ping-pong mechanism because substrate binding leads to the reduction of PQQ and the release of products; this is followed by two single electron transfer steps to cytochrome oxidase. A proton abstraction from the substrate occurs by Asp-303 (1). The oxyanion of the substrate then attacks the electrophilic C5 to form a hemiketal intermediate (2). The nitrogen of the pyrrole ring ionises the hemiketal intermediate (3) so a second proton abstraction from the substrate leads to the formation of products (4).Two electrons are then transferred separately to cytochrome c_L (5 and 6) (Anthony, 1996).

Frank *et al.*, 1989). The first step of methanol oxidation in this mechanism involves a proton abstraction from the substrate by Asp-303 (Anthony, 1996). The oxyanion of the substrate then attacks the electrophilic C5 to form a hemiketal intermediate. The nitrogen of the pyrrole ring may ionise the hemiketal intermediate so another proton abstraction from the substrate adducts leads to the formation of products. In this mechanism, the Ca^{2+} ion is expected to act as a Lewis acid, making the C5 on PQQ more electrophilic. The role of the Ca^{2+} in the mechanism is supported by preparations of methanol dehydrogenases containing Ba^{2+} and Sr^{2+} (Goodwin and Anthony, 1996; Harris and Davidson, 1994). The Ba^{2+} enzyme has a lower affinity for MDH but a lower activation energy leading to a doubling in V_{max}. This mechanism is supported by a number of experimental observations: the absorption and fluorescence spectra of PQQ covalent adducts are identical to the spectra of MDH-methanol complex and sGDH-glucose complex (Frank *et al.*, 1998); PQQ can form adducts with various compounds (Dekker *et al.*, 1982) and isolated PQQ in organic solvents can oxidise methanol to formaldehyde via this mechanism (Itoh *et al.*, 1998).

However a second mechanism has been proposed; the acid/base-catalysed hydride transfer system (Figure 1.21). Asp-303 again acts as a base and participates in proton abstraction in concert with hydride transfer from methanol to the PQQ C5 atom. The refined structure of MDH from *Methylophilus methylotrophus* W3A1 showed a tetrahedral configuration of the C5 of the reduced PQQ and no hemiketal adduct was seen (Zheng *et al.*, 2001).

Although the overall structure of sGDH is different from GDH and MDH, the active site is similar with respect to Ca^{2+} binding and the presence of a catalytic base (His-144). An X-ray crystal structure of sGDH containing PQQ and glucose also shows that the hydride transfer mechanism occurs in sGDH and overall opinion is shifting from the hemiketal intermediate mechanism towards this mechanism in all PQQ dehydrogenases (Oubrie *et al.*, 1999a). Glucose binds to sGDH in a wide solvent accessible crevice directly above PQQ and the C1 hydrogen atom points directly down towards the C5 atom of PQQ. This is ideal for hydride transfer as the distance between the two atoms is only 3.2Å and the hydride only has to be transferred a distance of 1.2Å for covalent addition to PQQ. The hemiketal intermediate mechanism is not favourable because the O1 atom of glucose would have to be reoriented before it can form a bond with C5 atom of PQQ. This rearrangement of glucose would break several hydrogen bonds and salt bridges; this would be energetically unfavourable. Other evidence supporting this mechanism includes the argument that the reduced C5 form of PQQ

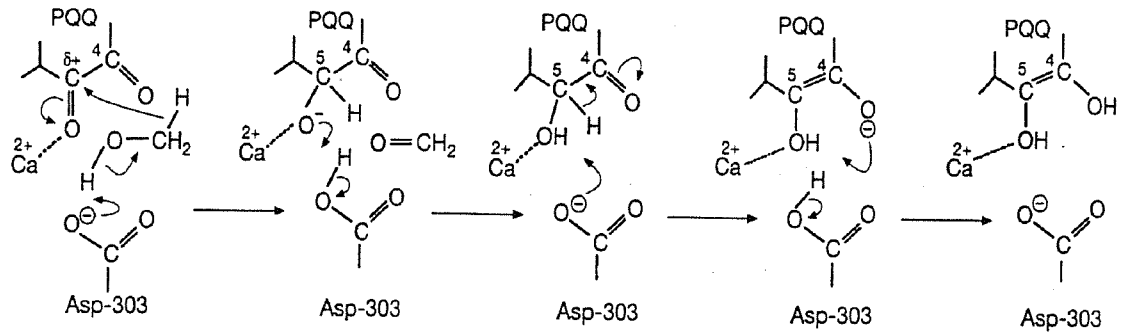

Figure 1.21 Acid/base catalysed hydride transfer mechanism proposed for MDH

Asp-303 abstracts a proton in concert with hydride transfer from methanol to the PQQ C5 atom. The reduced PQQ is then rearranged to form the quinol (Anthony, 1996).

after direct hydride transfer may also have similar spectra to the hemiketal intermediate (Dekker *et al.*, 1982).

Spectral and kinetic studies on sGDH from *Acinetobacter calcoaceticus* indicates that its mechanism involves Ca^{2+} assisted, direct hydride transfer (Dewanti and Duine, 2000). Three forms of sGDH were studied, HoloX that contained no Ca^{2+} at the active site, Ba-E that contained Ba^{2+} at the active site and E-NPQ (sGDH that contained nitroPQQ). The activity of Ba-E was two orders of magnitude lower than Ca-GDH, stopped-flow experiments showed that addition of deuteriated glucose produced a fluorescing intermediate with an increased deuterium kinetic isotope effect. This showed that the hydride transfer mechanism occurs due to the breaking of C-H bonds. E-NPQ could not form adducts with glucose or hydrazine (which binds to the C5 of PQQ) but could still oxide glucose. No intermediates were formed because once the hydride ion binds to nitroPQQ (NPQQ), it is rapidly tautomerized to $NPQQH_2$. Therefore, the inability of E-NPQ to form adducts with glucose does not prevent catalytic activity.

Finally, work in our laboratory by Afolabi and co-workers (2001) showed that mutating Asp-303 to Glu-303 gave an enzyme that retained activity. The affinity for methanol decreased more than 80,000 fold (K_m increased from 3μM to 250mM) but kinetic and deuterium isotope studies showed that the enzyme's mechanism was unchanged. The absorption spectum of D303E-MDH showed that PQQ was in its reduced or semiquinone state. However, unlike WT-MDH, a stable oxidised form could be produced by treatment with Wurster's blue, because the affinity for endogenous substrate was lower. The reduced form had a spectrum with lower absorption at 354nm and higher absorption at 400nm. Addition of ammonium and methanol to the oxidised form produced the reduced form but the rate was too fast to measure. However, when methanol or ammonium was added to oxidised D303-MDH separately, the rates could be measured but no spectral intermediated were detected. This indicated that only oxidised and reduced forms of MDH were present during the reaction and that a hemiketal intermediate was absent. The X-ray crystal structure at 3Å showed that Glu-303 was coordinated to Ca^{2+} and hydrogen bonded to the O5 atom of PQQ. This would only be possible if the C5 carries a hyroxyl group. This intermediate only occurs in the hydride transfer mechanism (see figure 1.21).

1.5.5 Investigation of the role of specific amino acid residues in GDH

The role of various amino acids has been examined by site-directed mutagenesis. A large number of mutants have been made and are listed in Table 1.2. Only important mutants

Table 1.2 Characterisation of GDH mutants previously purified
(The "conclusions" are those of the original authors)

MUTANT	LOCATION OF MUTANT	CHARACTERISTICS OF MUTANT COMPARED TO WILD TYPE GDH	CONCLUSIONS
WT-GDH	Non applicable	Non applicable	K_m for D-glucose, 0.9mM K_d for PQQ, 115nM K_d for Mg^{2+}, 0.32mM
K765- (Lysine To Stop Codon) (Yamada *et al.*, 1998)	Last 31 amino acids absent, no loop d	Immature GDH - cannot be purified.	Immature GDH susceptible to intracellular proteolytic degration.
-796K (Stop Codon To Lysine) (Yamada *et al.*, 1998)	Extra 18 amino acids after original stop codon	Reduced PMS reductase activity (50%), reduced Q-1 reductase activity, no effect on K_d/K_m values for PQQ , Mg^{2+} or glucose. Substrate specificity unchanged.	Normal electron transport from GDH to Q8 to cytoxidase. Additional amino acids may hamper access of artifical Q-1 or Q-1 site but not Q-8 site.
H775R (Histidine To Arginine) (Yamada *et al.*, 1998)	His-775 occurs at the end of the conserved c-terminal and approaches PQQ at the active site	Reduced PMS reductase activity (4%), Q-1 reductase activity and glucose oxidase activity. K_d for PQQ is 230-fold higher (21μM) and a low V_{max}. Slightly increasd maltose activity (k_M 150nM).K_M for Mg^{2+} doubled (50μM).	Mutation causes conformation of the active site to be disturbed - enzymes turnover decreased. Ser-777 moved to weaken it's H-bond with PQQ or His-775 may bind directly to the C-2 carboxyl group of PQQ. His-775 maybe exposed to funnel leading to active site.

H775N (Histidine to Asparagine) (Sode and Kojima, 1997)	See above	Affinity for substrates altered. k_M for 2-deoxy-D-glucose increased by 230-fold, k_M for D-mannose, D- xylose, D-galactose and D-allose also increased. k_M for glucose unchanged.	Increase in affinity for substrates. Role of His-775 different from that in *G.oxydans*. His-775 may bind to the C6-hydroxyl group of glucose.
H775D (Histidine to Aspartic acid) (Sode and Kojima, 1997)	See above	Increase in K_m values for D-glucose (23mM), 2-deoxy-D-glucose (60mM), D-allose, D-galactose and D-mannose (>100mM). No effect on maltose.	Increase in the K_m for D-glucose. Can be used to monitor blood glucose levels (diabetes subjects have 10-33mM D-Glucose concentrations in blood). Asp-775 may interfere the binding with C-6 hydroxyl group of the saccharide.
H775A (histidine To Alanine) (Yamada *et al.*, 1998)	See above	Low affinity for PQQ (not as low as H775R, 2.9μM), PMS reductase activity unchanged. Slightly increased maltose activity (K_m 53mM).	Conformation of active site unaltered - PMS activity same as WT-GDH. His-775 may bind directly to PQQ.
S357L (Serine To Leucine) (Yamada *et al.*, 1998)	Active site	Only purified if PQQ is present. Decreased PMS acitivty (8%), Q-1 reductase activity, glucose oxidase and affinity for PQQ. K_m for glucose and Mg^{2+} unaltered.	Ser-357 located near PQQ binding site. Local conformational change may affect Thr-357 which binds to PQQ in the model. PQQ access affected.
G689D (Glycine To Aspartic Acid) (Yamada *et al.*, 1998)	Glycine 689 is located beside D-strand of W6 and at the end of loop e, most of which is conserved in GDH but absent in MDH	Decreased PMS reductase activity (5%) and affinity for PQQ (12-fold, 640nM).Only purified in presence of PQQ. No effect on K_m values for Mg^{2+} and glucose.	Gly-689 may affect binding of amino acids to PQQ. Gly -689 gives flexibility of the local structure while asparatic acid causes a conformational change.

G689A (Glycine To Alanine) (Yamada *et al.*, 1998)	See above	Decreased PMS reductase activity (higher than G689D). No affect on K_d for PQQ.	Gly-689 probably doesn't bind to PQQ but amino acids around Gly-689 may bind to PQQ. Made R687A and D693A.
D693A (Aspartic acid To Alanine) (Yamada *et al.*, 1998)	See above	No effect on affinity for PQQ or on PMS reductase. Low amounts of GDH in membranes.	Specific residues around Gly-689 may interact with PQQ.
R687A (Arginine To Alanine) (Yamada *et al.*, 1998)	Arg-687 occurs on the outer D-strand of W6	Unstable in membrane - very low activity. K_d for PQQ not determined.	Arg-687 may interact with residue(s) which stabilizes W6 and then the entire structure.
R687D (Arginine To Aspartic Acid) (Yamada *et al.*, 1998)	See above	Unstable in membrane - very low activity.	R687 mutants are different than G689 mutants. Loop e may be important in PQQ binding.
P326L (Proline To Leucine) (Yamada *et al.*, 1998)	Pro-326 occurs in the loop f of the model, which is absent from MDH	Low PMS reductase activity (2%). Low affinity for PQQ (K_d 290nM) and Mg^{2+} (K_d 140μM).	Loop f may be near Mg^{2+} binding site.
G741S (Glycine To Serine) (Yamada *et al.*, 1998)	Located at the C-terminal region on the D-strand of W7	PMS reductase activity 42% compared with WT-GDH. Lower affinty for PQQ (K_d 220nM) and Mg^{2+} (K_d 100μM). Low amounts of GDH in Membranes.	W8 structure may be disturbed. This amino acid may be essential for stability.
E742GP757L (Glutamic acid To Glycine And Proline to Leucine) (Yamada *et al.*, 1998)	Gly-742 occurs in the D-strand of W7	Low PMS reductase activity (1%). High K_d for PQQ (280nM) and Mg^{2+} (110μM). Low amounts present.	Reduced amounts of GDH suggest W8 structure is disturbed. Reduced stability of GDH.

D730N (Aspartic Acid To Asparagine) (Yamada *et al.*, 1998)	Asp-730 occurs between B-sheet structures in W7.	Significantly decreased activities of PMS reductase (3%) and glucose oxidase. No effect on affinity for Mg^{2+}, PQQ and glucose.	No conformational change (shown by fluorescence spectrum). Made mutants D70A and D730R).
D730A (Aspartic Acid To Alanine) (Yamada *et al.*, 1998)	See above	Low PMS reductase activity,same as D730N. K_d for PQQ increased by a factor of 2.	Asp-730 may be located close to the PQQ binding site. Asp-730 may be involved in proton extraction.
D730R (Aspartic Acid To Arginine) (Yamada *et al.*, 1998)	See Above	Low PMS reductase activity, same as D730N. Higher K_d value for PQQ (37μM) than D730N and D730A.	D730R may affect structure around PQQ binding site
H787N in G. Oxydans (Histidine To Tyrosine) (His-775 in E.coli) (Cleton-Jansen *et al.*, 1991)	Mutation occurs in the isogenic strain P2 of G.oxydans. His-787 located 20 residues from C-terminal.	Mutant can oxidase maltose and glucose.	Mutation makes active site more accessible for maltose to bind. Indicates substrate binding domain located at C-terminal.
H262A (Histidine to Alanine) (Elias *et al.*, 2000)	His-262 replaces disulphide ring in MDH. Located at the active site.	Reduced PMS reductase activity (36%) and glucose oxidase activity (42%). Decrease in affinity for PQQ (K_d 880nM). K_m for glucose increased to 10mM.	His-262 is not an electron acceptor.
W404A (Tryptophan to Alanine) (Elias *et al.*, 2000)	Active site. Involved in PQQ stacking.	Very low PMS reductase activity (0.03%) and low glucose oxidase activity (3.6%). Affinity for glucose unaltered and affinity of PQQ decreased (K_d 6μM).	Low activity because alanine can't hold PQQ at the active site. Made W404F.
W404F (Tryptophan to Phenylalanine) (Elias *et al.*, 2000)	See above	Low PMS reductase activity (1.3%) and glucose activity (27%). Affinity for PQQ very low (K_d 20μM).	Phenylalanine may be able to support PQQ better than alanine.

N607A (Asparagine to Alanine) (Elias *et al.*, 2000)	Active site. Proposed to interact equatorially with C-4 of PQQ.	Slightly reduced PMS reductase activity (33%) and glucose oxidase activity (37%). Affinity of PQQ slightly decreased (K_d 220nM and K_M for glucose unaltered.	Asn-607 is not crucial for catalytic activity or stabilization of PQQ at the active site.
K493A (Lysine to Alanine) (Elias *et al.*, 2000)	Active site. Lys-493 is proposed to interact with C-4 and C-5 of PQQ.	Reduced PMS reductase activity (3.3%) and glucose oxidase activity (0.4%). Affinity for PQQ slightly increased (k_d 50nM). K_M for glucose 1.4mM. Q-2 reductase activity very low (0.075%).	No affect on the affinity of PQQ but the mutant may affect electron transport in the mutant. Made K493R.
K493R (Lysine to Arginine) (Elias *et al.*, 2000)	See above	Low PMS reductase (1%) and glucose oxidase activity (0.07). K_d for PQQ 16μM and K_M for glucose 1.5mM.	Reduced affinity for PQQ. Positive charge of the lysine is crucial for activity. Mutation may cause a local conformation change reducing activity of GDH. Arginine occurs in MDH at this position.
D466N (Aspartic acid to Asparagine) (Elias *et al.*, 2000)	Active site. Asp-466 is expected to abstract a proton from glucose.	Low PMS reductase activity (1.7%) and glucose oxidase activity (1.2%). K_d for PQQ 140nM and K_m for glucose 12mM.	Decreased affinity of D-glucose, therefore located close to glucose binding site.
D466E (Aspartic acid to glutamic acid) (Elias *et al.*, 2000)	See above.	Low PMS reductase activity (0.3%) and glucose oxidase activity (1.4%). K_d for PQQ 140nM and K_m for glucose 3mM.	Asp-466 is important for the catalytic reaction. Distance between Asp-466 and C-1 hydoxyl group is vital.

T424N (Threonine to Asparagine) (Yoshida and Sode, 1996)	Active site. Binds to the metal ion.	K_d for Mg^{2+} increased from 0.32mM to 0.78mM. K_d for Ca^{2+} increased from 0.25mM to 5.6mM. Highest activity with Ca^{2+}. Activity with Ba^{2+} and Sr^{2+} not affected. Less tolerant to EDTA treatment.	WT-GDH shows highest activity with Mg^{2+}, therefore T424N-GDH may have a bigger cavity at the metal binding site. The distance between PQQ and the metal binding site has increased.
E742K (Glutamic acid to Lysine) (Sode and Sano, 1994)	Glu-742 is Lys in *A. calcoaceticus*. This may be responsible for EDTA tolerance. D-strand of W7.	15% active after treatment with 5mM EDTA (WT-GDH 3% active).	Increase in EDTA tolerance.
H262Y (Histidine To Tyrosine) (Cozier *et al.*, 1999)	His-262 replaces disulphide ring in MDH. Located at the active site.	K_d for Mg^{2+} was 3.6mM. K_d for PQQ was 105nM. Disaccharides not oxidised. Poor substrate binding, K_m for glucose and 2-deoxy-D-glucose 460mM and 32mM respectively (2.1mM and 1.6mM for WT-GDH).	Altered configuration of the active site. This causes some steric hindrance near the hyroxyl group at the C2 position in glucose. His-262 not involved in electron transfer.

are going to be discussed. In such studies the GDH must be reconstituted with PQQ and a divalent ion. Mutations affected reconstitution and the activity of the enzyme. His-262 is expected to hold PQQ in place at the active site. Mutating this residue to tyrosine caused a decrease in catalytic efficiency for all substrates but did not affect the rate of electron transfer to oxygen (Cozier *et al.*, 1999). The major difference was poor substrate binding. All D-hexoses tested were oxidised; compared with WT-GDH the K_m for D-glucose with H262Y-GDH increased from 1mM to 460mM. L-hexoses were not oxidised and did not act as inhibitors so presumably they could not bind to the enzyme (the C-6 hydoxymethyl group is below the plane of the ring in the L anomers). C-2, C-3 and C-4 hydroxyl groups were not essential for binding. The affinity for PQQ during reconstitution was slightly higher (105nM compared with 249nM for WT-GDH) but the K_d for Mg^{2+} was unaffected. The H262Y mutation did not affect the rate of reconstitution; completion was after 5 minutes. Tyrosine may be able to hold PQQ at the active site but the tyrosine probably caused steric hindrance near the hydroxyl group at the C2 position of glucose. Experiments with the H262A mutation also showed the residue is not involved in electron transfer; PMS reductase and glucose oxidase activities were 36% and 42% respectively compared with WT-GDH values (Elias *et al.*, 2000). These results would differ from one another if His-262 had a role in electron transfer to ubiquinone.

Trp-404 is also expected to hold PQQ at the active site (Figure 1.17). Mutating this residue to alanine gave an enzyme with very low PMS reductase and glucose oxidase activities (0.03% and 3.6% respectively). This mutant could only be purified in the presence of PQQ and this indicates that it was less stable than WT-GDH. Replacing this residue with alanine caused the K_d for PQQ to increase from 115nM to 6μM because it is too small to hold PQQ. This mutation may alter the confirmation of the active site and effects PQQ accessibility or positioning of the co-factor. The K_m for D-glucose was not altered (1.9mM).

Asp-466 is expected to correspond to Asp-303 in MDH (Figure 1.18). This residue is expected to have a role in the catalytic mechanism (Section 1.5.4). D466N-GDH and D466E-GDH both had low PMS reductase activities, 0.3% and 1.7% respectively (Elias *et al.*, 2000). These mutations did not affect the affinity for PQQ but did decrease the affinity for D-glucose. For D466N and D466E-GDH the K_m for D-glucose increased from 0.9mM to 12mM and 3mM respectively. This indicates that Asp-466 has an important role in the enzymes mechanism and it could also be located close to the glucose binding site.

Lys-493 in GDH corresponds to arginine in MDH. Mutating lysine for alanine at position 493 had no effect on the affinity for PQQ but PMS reductase and glucose oxidase

activities were only 3.3% and 0.4% respectively compared to WT-values. K493R-GDH also had low PMS reductase activity (1%) and the affinity for PQQ had decreased (K_d value increased from 110nM to 16μM). Changing arginine for lysine may have caused a change in the local structure and Lys-493 may be required for activity (Elias *et al.*, 2000). The distance between C4 or C5 carbonyl groups to Lys-493 may be important.

Asn-607 is a second residue that is expected to bind to the C-4 carbonyl of PQQ (Figure 1.18). N607A-GDH had slightly reduced PMS reductase and glucose oxidase activities (33% and 37% compared with WT-GDH activities) and the K_d for PQQ slightly increased from 110nM to 220nM (Elias *et al.*, 2000). There was no effect of the affinity for D-glucose. Therefore this residue is not crucial for catalytic activity or stabilisation of PQQ.

Only one of the proposed metal binding residues (Thr-424) has been mutated (Yoshida and Sode, 1996). T424N-GDH was less tolerant to EDTA treatment and reconstitution with calcium, strontium and barium gave higher activity than with magnesium. This differed from WT-GDH that showed highest activity with Mg^{2+}. The affinity for metals decreased, the K_d for magnesium increasing from 0.32mM to 0.78mM. T424N-GDH may have a larger cavity so that smaller ions such as magnesium gave lower activity. The authors proposed that the distance between PQQ and the metal binding site had increased. The effect of this mutation on the affinity for PQQ and D-glucose was not reported.

1.6 The development of GDH as a biosensor

Sode has been studying EDTA tolerance, thermal stability and substrate specificity of GDH from *E. coli* and *A. calcoaceticus* because the enzyme could be used to monitor blood glucose concentrations. Glucose oxidase sensors are presently used but these are affected by the dissolved oxygen concentration in blood. This would not affect GDH as the enzyme passes electrons to phenazine ethosulphate. Also GDH is 20 times more active than pure glucose oxidase. Attempts have been made to construct chimeric proteins of *E. coli* and *A. calcoaceticus* GDH to produce a protein with perfect characteristics of a glucose biosensor. The section below will discuss improving EDTA tolerance, substrate specificity and thermal stability of GDH.

1.6.1 Improvement of EDTA tolerance of *E. coli* GDH

Two types of GDH have been proposed (Dokter *et al.*, 1986). Type I includes GDH found in *E. coli* and *Pseudomonas*; PQQ can be easily removed and they have a low affinity for PQQ. These enzymes have low tolerance to EDTA treatment. Type II GDH include the

membrane bound enzymes from *A. calcoaceticus* and *Gluconobacter* that have a high affinity for PQQ and higher EDTA tolerance. EDTA presumably inactivates GDH by chelating the bivalent cation from the active site that is essential for holoenzyme formation. Treating *A. calcoaceticus* GDH and *E. coli* GDH with 10mM EDTA produced enzymes that were 80% active and 0% active respectively (Sode and Yoshida, 1997). Therefore Sode made mutant GDHs and chimeric GDHs from *E. coli* GDH and *A. calcoaceticus* GDH to improve *E. coli* EDTA tolerance. For GDH to be used as a biosensor a stable protein is required that cannot easily loose its active site metal ion and its prosthetic group.

The C-terminal region of GDH is conserved in *E. coli* and *A.calcoaceticus* but amino acid 742 in *E. coli* is glutamate and in *A. calcoaceticus* it is lysine. This amino acid was thought to play a role in the tolerance of *A.calcoaceticus* GDH to EDTA so Glu-742 was mutated to Lys-747 in *E. coli* GDH (Sode and Sano, 1994). This produced an enzyme with higher EDTA tolerance because the mutant was 15% active after treatment with 10mM EDTA. Therefore this region is not the only site responsible for EDTA tolerance in *A. calcoaceticus* GDH because that enzyme was 80% active with 10mM EDTA.

To determine the site responsible for EDTA tolerance, a variety of chimeric GDHs were made by homologous recombination of the structural genes of *A. calcoaceticus* and *E. coli* GDH (Sode *et al.*, 1995a). 12 chimeric GDHs were made containing the N-terminal region of *E. coli* and the C-terminal region of *A. calcoaceticus* GDH (See Figure 1.22 for structures). E32A68-GDH was EDTA tolerant but A45E55-GDH and E56A44-GDH were EDTA sensitive. This meant that a region of 90 amino acids, between 45%-56% of the distance from the N-terminal region of *A.calcoaceticus* GDH was responsible for EDTA tolerance. This was confirmed by the EDTA sensitivity of E10A35E55-GDH and the EDTA-tolerance of proteins E10A87E3-GDH, E10A74E16-GDH and E10A49E41-GDH.

E45A14E41-GDH chimeric protein was then made to confirm that the 90 residue sequence was responsible for EDTA tolerance (Sode and Yoshida, 1997). The chimeric GDH retained 50% activity after 30 minutes incubation with 10mM EDTA but was not as tolerant *as A. calcoaceticus* GDH. The metal specificity had changed as Ca^{2+} ions gave higher activity than Mg^{2+} ions. The mutant was 1% active compared with *E. coli* GDH but the K_m values for D-glucose was similar with *E. coli* and *A. calcoaceticus* (0.5mM). The three proposed metal ion binding residues in *E. coli* GDH (Asp-354, Asn-355 and Thr-424) were conserved in *A. calcoaceticus* (Asp-359, Asn-360 and Thr-429) so the difference in EDTA tolerance is not due to the amino acids that binds to the metal ion. The substituted region in E45A14E41-GDH included W3 and W4 motifs; this region was proposed to have a different inter-motif

Schematic drawing of chimeric enzymes	EDTA tolerance*	Schematic drawing of chimeric enzymes	EDTA tolerance*	Schematic drawing of chimeric enzymes	EDTA tolerance*
E.coli DH5α (EcII,EcIII)	0 %	*A.calcoaceticus* (AcI)	84 %	E10A90	71%
E99A1	0 %	A98E2	95 %	E10A87E3	94 %
E97A3	0 %	A87E13	92 %	E10A74E16	90 %
E95A5	0 %	A45E55	0 %	E10A49E41	79 %
E87A13	0 %	A21E79	0 %	E10A35E55	0 %
E64A36	0 %				
E56A44	0 %				
E32A68	72 %				
E10A90	71 %				

Figure 1.22 Chimeric proteins made from *E. coli* and *A. calcoaceticus* GDH

Chimeric proteins were made by combining regions of the genes coding for GDH in *E. coli* and *A. calcoaceticus*. The letter in the name denotes the origin of the gene and the number shows the percentage of the gene present. 12 proteins have *E. coli* GDH at the N-terminal. EDTA tolerance is shown (activity after 30 minutes of incubation in the presence of 10mM EDTA (taken from Sode *et al.*, 1995a).

structural flexibility in *A. calcoaceticus GDH* and *E. coli* GDH. An increase in rigidity may cause *A.calcoaceticus* to be more EDTA tolerant. Cross-linking chemical modification of *E. coli* GDH supports this conclusion. EDTA tolerance was produced by cross-linking GDH with glutaraldehyde (Sode *et al.*, 1996). Cross-linked GDH was 60% active after 15 minutes incubation with 10mM EDTA instead of 0% active. Cross-linking increased the rigidity of the enzyme.

Because E45A14E41-GDH did not show the same EDTA tolerance as *A. calcoaceticus* GDH, E32A27E41-GDH was made that contained 27% of *A. calcoaceticus* GDH (known as the A27 region). This chimeric protein was completely tolerant to EDTA treatment and indicated that the A27 region is responsible for EDTA tolerance in *A. calcoaceticus* (Yoshida *et al.*, 1999). The A27 region is located in the middle of the enzyme and consists of W2, W3 and W4; it includes the putative divalent metal binding site. The insertion of the A27 region caused an increase in random structure measured by the far UV CD spectrum.

1.6.2 Improvement of the thermal stability of GDH

Chimeric proteins were used to investigate the thermal stability of GDH. GDH composed of 95% of the N-terminal region of *E. coli* GDH and 5% from the C-terminal of *A. calcoaceticus* GDH (E95A5-GDH) had a higher thermal stability than *E. coli* GDH. The same was true for E97A3 (Sode *et al.*, 1995b). E97A3-GDH was 12 times more stable than *E. coli* GDH and 3 times more stable than *A. calcoaceticus* GDH. Comparing the C-terminal region of *E. coli* GDH to E97A3-GDH showed three substitutions (S771M, I786L, D794N) and one deletion (V795). Chimeric protein E99A1-GDH was less stable than *E. coli* GDH but the only difference between E99A1-GDH and E97A3-GDH was that substitution S771M was absent. Therefore the S771M substitution possibly caused an increase in thermal stability by increasing the hydrophobicity of the enzyme. Further experiments used site-directed mutagenesis to change Ser-771 of *E. coli* GDH with Met-771 (Witarto *et al.*,1999b). *E. coli* mutant S771M-GDH showed the same thermal stability as wild-type *E. coli* GDH. However, E99A1S771M-GDH had a higher thermal stability than E99A1. Looking at the denaturation of *E.coli* GDH and E97A3-GDH by far-UV circular dichroism showed that E97A3-GDH is more stable at the first step of denaturation. There is no change in the secondary structure at this step and the results suggest that interactions between the N- and C-terminal regions of the protein maintains the overall structure of the superbarrel.

For GDH to be used as a biosensor it would be ideal if the enzyme could be stored at room temperature. The addition of trehalose to prepare lyophilized WT-GDH allowed 80% of activity to be retained after one hour at 80°C. The enzyme could be stored at 28°C for a month without loss of activity (Sode and Yasutake, 1997).

1.6.3 Improvement of the substrate specificity of *E. coli* GDH

In order to use GDH in an assay system for the measurement to D-glucose it needs to be modified so it cannot oxidise other sugars. An enzyme that is specific for only D-glucose and that can measure D-glucose between the range of 5 and 40mM would be ideal to monitor blood glucose concentrations in diabetic patients. The substrate specificity of *E. coli* GDH was made more specific for glucose by making mutants H775N-GDH and H775D-GDH (Sode and Kojima, 1997; Yoshida *et al.*,1999). His-775 was substituted as it is conserved in all GDHs and a natural mutant in *G. oxydans* (His-787 to Asn-787) had altered substrate specificity (Cleton-Jansen *et al.*, 1991). This natural mutant could oxidise maltose and glucose. Both *E. coli* GDH mutants showed increased specificity for D-glucose. H775D-GDH had increased K_m values towards all monosaccharides and increased the K_m value for glucose by 25-fold (0.9mM to 23mM). This could cover the blood glucose concentration of diabetic subjects (10-35mM). These mutant enzymes are ideal for diagnostic use because very high concentrations of monosaccharides (apart from D-glucose) are required to produce activity. The K_m value of H775N-GDH for D-glucose had increased from 0.9mM to 1.5mM and the K_m values for other sugars showed a significant increase. Experiments on thermal stability proved that the H775N-GDH had a lower thermal stability compared to WT-GDH. However the A3 region was able to complement this decrease and E97A3H775N had a higher thermal stability than wild-type GDH.

Expanding the concentration range for D-glucose of a GDH biosensor has been successful by constructing a composite colorimetric analytical system that was made from a mixture of WT-GDH and H775D-GDH (Yamazaki *et al.*, 2000a). This system could measure glucose concentrations from 0.5 to 30mM with less that 5% error. Even though this system had a wider range than a system using only one enzyme, the specificity for glucose was improved by constructing a second system with H775D-GDH plus H775N-GDH. This could measure glucose from 3mM to 70mM. The response of the system to galactose, xylose and mannose was less that 10% compared to WT-GDH.

1.6.4 The construction of a glucose biosensor

The previous section examined chimeric proteins with an improvement in EDTA tolerance, thermal stability and substrate specificity. To construct a glucose biosensor, E32A27E38A3His782Asp-GDH was made (Yoshida *et al.*, 2000). This protein retained 70% activity after treatment with 10mM EDTA, showed thermal stability higher than *E. coli* GDH and had a K_m for D-glucose of 9.7mM. D-maltose, D-xylose, D-galactose could not be oxidised. A biosensor was made by mixing the chimeric protein with a carbon paste and then it was lyophilised overnight. The resulting protein was filled into an electrode that could then measure glucose concentration 5mM-40mM. An electrode with *E. coli* WT-GDH was also produced but this electrode lost activity over time if magnesium and PQQ were not present in the electrode buffer. PQQ binding was more stable in E32A27E38A3His782Asp-GDH.

Commercially, these chimeric proteins cannot be expressed in *E. coli* because PQQ is not synthesised by the bacterium. It would be too expensive to add PQQ on a large scale. Therefore they could be expressed in *Klebsiella pneumoniae*. Soluble GDH has successfully been expressed in this bacterium but the amount of PQQ produced was insufficient to make all protein into the holo-form (Kojima *et al.*, 2000).

A novel immobilisation method has been developed that could allow membrane GDH to be used in a disposable glucose biosensor (Yamazaki *et al.*, 2000b). The surface deposition method involves absorbing GDH onto diethylaminoethyl (DEAE) filter paper because GDH has a negative charge. Then the surfactant Triton X-100 is removed from the filter paper by washing with buffer. This causes the hydrophobic region of GDH to be deposited on the surface of the paper allowing the soluble domain to remain active.

1.7 Soluble glucose dehydrogenase

Acinetobacter calcoaceticus has two types of GDH; a soluble enzyme (sGDH) and a membrane enzyme (mGDH) (Matsushita *et al.*, 1989a; Duine, 1991). Although all other PQQ-containing dehydrogenases have high sequence identity, sGDH is completely different (Cleton-Jansen *et al.*, 1988). sGDH is a dimer made up of two identical 50kDa subunits. Each subunit has 454 amino acids. One PQQ molecule is found in each subunit and can be reversibly dissociated. Apo-soluble GDH can be reconstituted with PQQ and calcium. Cadmium and manganese can replace calcium in the reconstitution process but not magnesium (Dokter *et al.*, 1986). Each dimer has six calcium ions and calcium is required for dimerization as well as for functionalization of PQQ (Olsthoorn and Duine, 1996). sGDH can oxidise a wide range of

pentoses, hexoses, monosaccharides and disaccharides (Matsushita *et al.*, 1989a), but the physiological electron acceptor is unknown.

Oubrie *et al.* (1999a) solved the X-ray crystal structure of apo-sGDH at 1.72Å resolution. It showed that the enzyme is a dimer with a water mediated interface. The structure is a "β-propeller fold consisting of six four-stranded anti-parallel β-sheets aligned around a pseudo 6-fold symmetry axis." Each monomer contains three calcium ions; two are located at the dimer interface and one calcium ion is found at the active site where it is expected to functionalize PQQ. The dimer has dimensions of 100Å x 50Å x 50Å and the monomers interact across a large planar interface (900Å^2). At this interface most of the hydrophobic protein-protein interactions occur with residues in the 4C and 4D β-strand. Hydrogen bonds are also present that are mediated by H_2O. The dimer interface is covered with polar and negatively charged residues. The structure contains a conserved repeat that gives rise to two distinct motifs; the first motif occurs at the corner of a β-turn found between the inner strands of the β-sheet. An aspartate side chain points back into the β-sheet to hydrogen bond with a tyrosine or tryptophan side chain. The second motif is formed by a bidentate salt bridge between an arginine or lysine side chain in the CB-strand of one β-sheet with a aspartate or glutamate in the CD loop of the next β-sheet. These motifs are expected to stabilise the β-propeller fold. PQQ was not present in the crystal.

The structure of sGDH with D-glucose and PQQ bond to the active site has also been solved (Oubrie *et al.*, 1999b and1999c). PQQ is located in a positively charged, deep cleft near the pseudo-symmetry axis. PQQ binding is similar to binding in MDH; the N6, O7A and O5 atoms of PQQ bind to the active site calcium. The C2, C7 and C9 carboxyl groups form salt bridges with Arg-408, Lys-377 and Arg-406 respectively. The O4 and O5 atoms are bound to Asn-229 and Arg-228 respectively. PQQ stacks onto a flat surface area made up from side chains of Ala-350, Gln-246, Leu-376 and Gln-23 but above the plane of the molecule no side chains are present, leaving space for substrate binding. The active site calcium has seven ligands: two main chain carbonyl oxygen atoms from Gly-247 and Pro-248; three ligands from PQQ and two water molecules. The structure with D-glucose bound to the active site indicates that the enzyme's mechanism involves hydride transfer due to the position of the substrate. D-Glucose binds to the deep cleft, directly above PQQ. Hydrophobic interactions occur between Leu-169 and the C1 atom of the substrate. Side chains of Gln-76 and Asp-143 form hydrogen bonds with glucose O2 atom whilst His-144, Gln-168 and Arg-228 form hydrogen bonds with O1 atom. His-144 could act as a base to initiate the first step of the mechanism. The distance between C1 atom of glucose and C5 atom of PQQ is only

3.2Å and is ideally placed for the hydride transfer mechanism because the C1 hydrogen points down towards the PQQ C5 atom. This work has provided the best evidence for a hydride transfer mechanism in PQQ containing enzymes (see Section 1.5.4).

1.7.1 Development of soluble GDH as a glucose biosensor

Soluble GDH could be used as a glucose biosensor because it has a number of advantages over mGDH. The structure of the enzyme has been determined and the protein is easier to work with because it is soluble. The major disadvantage is that it has a broad substrate specificity and can oxidise disaccharides.

Constructing various Ser-231 variants has increased the thermal stability of the enzyme (Sode *et al.*, 2000). Ser231Lys showed the highest level of thermal stability and has a similar activity to that of WT-GDH. The mutant was 66% active after incubation at 55C for 30 minute and WT-GDH activity was only 30%.

Glucose biosensors have been made by attaching sGDH to an electrode. Electrodes containing WT-sGDH, WT-sGDH cross-linked to glutaraldehyde and Ser231Lys-sGDH were tested after heating the electrodes at 60°C for 2 hours, 80% of the initial activity was observed with S231K-sGDH and cross-linked sGDH (only 30% with WT-GDH) (Takahashi *et al.*, 2000). The ranges of the sensors for D-glucose were from 10μM to 3mM.

1.8 The role of metal ions in quinoproteins

The importance of metal ions in the structure and function of quinoproteins was first indicated by reconstituting apoenzyme with PQQ and a divalent metal (see Tables 1.3 and 1.4 for references). PQQ has been removed from MDH, ADH and GDH by treatment with EDTA, heat, low pH or high salt concentrations (Goodwin and Anthony, 1998). PQQ could not be removed from MDH without denaturing the enzyme. This showed that the metal ion in quinoproteins is important in structure or function.

Adachi *et al.* (1990) were the first to demonstrate that MDH contained Ca^{2+}. This was confirmed by Richardson and Anthony (1992) by measuring the Ca^{2+} content in MDH. An apoenzyme was isolated from *Methylophaga marina* that can grow in high concentrations of salt (Chan and Anthony, 1992). Active enzyme could be formed after incubation with Ca^{2+}.

MDH from mutants of *M. extorquens* (*mxaA*$^-$, *mxaK*$^-$ and *mxaL*$^-$) indicated that Ca^{2+} had structural and functional roles in MDH. MDH from these mutants were inactive, contained PQQ but had an abnormal absorption spectrum (Richardson and Anthony, 1992). Activity and a normal absorption spectrum could be restored by incubation with Ca^{2+}. The

Table 1.3 Divalent metal ions in PQQ-containing quinoproteins that oxidize alcohols

Enzyme	Organism	Metal determined	Metal for reconstitution	References
Methanol dehydrogenase	*Methylobacillus*	Ca	Ca Sr (during growth)	Adachi *et al.* (1990)
	Methylobacterium	Ca	-	Richardson and Anthony (1992)
	Methylobacterium (*mxaA* mutant)	None	Ca=Sr=Ba (not Mg)	Goodwin *et al.* (1996); Goodwin and Anthony (1996)
	Methylophilus	Ca	-	Richardson and Anthony (1992)
	Paracoccus	Ca (Sr)	Ca Sr (during growth)	Harris and Davidson (1994); Richardson and Anthony (1992)
	Hyphomicrobium	Ca	-	Richardson and Anthony (1992)
	Methylophaga marina	Ca	Ca	Chan and Anthony (1992)
Alcohol dehydrogenase (type I); quinoprotein	*Pseudomonas aeruginosa*	Ca	Ca Sr (not Mg Mn Cd)	Mutzel and Gorisch (1991); Schrover *et al.* (1993)
Alcohol dehydrogenase (type II); soluble quinohaemoprotein	*Comamonas testosteroni*		Ca (not Mg)	Groen *et al.* (1986); de Jong *et al.* (1995)
Alcohol dehydrogenase (type III); membrane quinohaemoprotein	*Gluconobacter suboxydans*		Ca (not Mg)	Shinagawa *et al.* (1989)

(Table taken from Goodwin and Anthony, 1996)

Table 1.4 Divalent metal ions in relation to glucose dehydrogenase

Enzyme	Organism	Metal active in reconstitution	References
Glucose dehydrogenase (soluble)	*Acinetobacter calcoaceticus*	Ca(100) Mn(67) Cd(60) (not Mg)	Geiger and Gorisch (1989); Olsthoorn and Duine (1996) Oubrie *et al.* (1999a, b and c)
	Acinetobacter calcoaceticus (mutant)	Cd(127) Ca(100) Sr (68) Mn (63) Co(10) Ba(7) (not Mg)	Matsushita *et al.* (1995)
Glucose dehydrogenase (membrane)	*Acinetobacter calcoaceticus*	Mg>Ca	(Duine *et al.* (1983); Ameyama *et al.* (1985)
	Acinetobacter calcoaceticus (mutant)	Mg(115) Ca(100) Zn(100) Sr(70) Co(33) Cd(27) Ba(10)	Matsushita *et al.* (1995)
	Escherichia coli	Mg>Ca>Co	Ameyama *et al.* (1985, 1986); Shinagawa *et al.* (1986)
	Klebsiella pneumoniae	Mg, Ca	Buurman *et al.* (1990); Neijssel *et al.* (1983)
	Pseudomonas fluorescens	Mg>Ca	van Schie *et al* (1984); Ameyama *et al.* (1985); Imanaga (1989)

The presence of a metal ion (Ca^{2+}) has only been demonstrated in the soluble enzyme from *Acinetobacter calcoaceticus.*

(Table taken from Goodwin and Anthony, 1996)

reconstitution of MDH from *mxaA*⁻ was shown to have a pH optimum at pH 10 and two Ca^{2+} were irreversible incorporated into the $\alpha_2\beta_2$ dimer (Goodwin *et al.*, 1996). Also, Sr^{2+} or Ba^{2+} could replace Ca^{2+} in the reconstitution process to form active enzyme but Mg^{2+} did not support reconstitution. This is the first enzyme reported in which Ba^{2+} functions at the active site. Ba^{2+}-MDH showed a reduced affinity for methanol (K_m increased from 3μM to 3.5mM) and ammonia activator (K_A increased from 2mM to 52mM) (Goodwin and Anthony, 1996). The activation energy for the oxidation of methanol had decreased by half and the V_{max} was 2-fold higher. This indicated that Ba^{2+} had changed the conformation of the active site and decreased the free energy of substrate binding. The *mxaA*, *mxaK* and *mxaL* genes may code proteins that are responsible for Ca^{2+} insertion.

It has been shown that PQQ can form complexes with Ca^{2+} in solution (Geiger and Gorisch, 1989). The absorption maxima of this complex was 343nm and with free PQQ the absorption maxima was only 330mn. Because the absorption maxima of the Ca^{2+}/PQQ complex was similar to that of PQQ in alcohol dehydrogenases, it was suggested that PQQ was anchored to the protein with Ca^{2+}. This was confirmed in methanol dehydrogenase by studying its X-ray structure. In MDH the α subunit contains one Ca^{2+} coordinated to the N-6, C-5 quinone oxygen and the C-7 carboxyl group of PQQ (Figure 1.15) (Ghosh *et al.*, 1995; Xia *et al.*, 1996). This led to the proposal that Ca^{2+} holds PQQ in the correct configuration at the active site and also acts as a Lewis acid in the enzyme's mechanism (Section 1.5.4).

The presence of Ca^{2+} has been demonstrated in ethanol dehydrogenase of *P. aeruginosa* (type I alcohol dehydrogenase). Ca^{2+} was removed from the enzyme by CDTA treatment and active enzyme could be produced after reconstitution with PQQ and Ca^{2+} (Mutzel and Gorisch, 1991). The X-ray structure for this homodimeric enzyme was solved at 2.6Å and showed that it's overall structure was very similar to the α subunit of MDH (Keitel *et al.*, 2000). The coordination of Ca^{2+} to PQQ was identical to the coordination in MDH, and the remainder of the metal binding site was composed of the side chains of Glu-179, Asn-266 and Asp-316. Unlike MDH, a second Ca^{2+} binding site was found at the N-terminus made up from Asp-11, Thr-14 and Asp-17. Modelling studies indicated that the structures of type II and type III ADHs are similar to MDH, suggesting that Ca^{2+} is coordinated to PQQ in the same manner as MDH (Stoorvogel *et al.*, 1996; Cozier *et al.*, 1995).

The presence of a metal in sGDH was first demonstrated by reconstituting apoenzyme (produced by treatment with high salt concentrations or low pH) with Ca^{2+}, Mn^{2+} or Cd^{2+} to produce active enzyme. The expression of sGDH from *A. calcoaceticus* in *E. coli* suggested that Ca^{2+} was required for dimerisation and incorporation of PQQ (Olsthoorn and Duine,

1996). The X-ray structure showed there were three Ca^{2+} ions per monomer; two at the dimerisation site and one coordinated to PQQ (with similar binding to PQQ as in MDH) (Oubrie *et al.*, 1999a and b).

The metal ion present in membrane GDH of *E. coli*, *K. pneumoniae* or *A. calcoaceticus* has never been determined. The metal ion is assumed to be lost during the dialysis required to remove the excess metal ion that must be added to reconstitute the enzyme. Mg^{2+} is better than Ca^{2+} for reconstitution of apoenzyme with PQQ (Matsushita *et al.*, 1995; Ameyama *et al.*, 1985 and 1986). Determining the metal ion at the active site of GDH is not possible by analysing the metal ion binding ligands because generally, Ca^{2+} can accommodate up to twelve oxygen ligands but studies have shown that coordination numbers of six, seven and eight are the most common (Brown, 1988). Mg^{2+} can accommodate four to ten ligands but four, five and six are the most common. Yoshida and Sode (1996) reported that *E. coli* GDH could be reconstituted with Mg^{2+}, Ca^{2+}, Sr^{2+} or Ba^{2+} to form active enzyme. The K_d values were 0.32mM, 0.25mM, 0.39mM and 1.20mM respectively.

Itoh *et al.* (1998) studied Ca^{2+} binding to a PQQ analogue in an organic solvent. The absorption band at 354nm shifted to 368nm and the shoulder around 280nm decreased. ^{1}H and ^{13}C NMR showed Ca^{2+} binding was the same as the binding to PQQ in MDH. Similar results were seen with Sr^{2+} and Ba^{2+} but the experiment with Mg^{2+} showed weaker binding. Molecular orbital calculations suggested that Mg^{2+} binds to the C4 and C5 carbonyl groups. Mg^{2+} could not bind to PQQ in the same manor as Ca^{2+} because the distance between Mg^{2+} and O-5, N-6 and O-7 were calculated to be 2.43Å which is longer than the normal Mg^{2+}-O=C bond (2.1 Å) and Mg^{2+}-N bond (2.2 Å). Ca^{2+} binding was calculated to be stronger than Sr^{2+} or Ba^{2+} because it fits into the molecular cleft of PQQ. Ba^{2+} and Sr^{2+} may distort the PQQ molecule. It has also been shown that bound to Ca^{2+}, PQQ can oxidise methanol to formaldehyde in organic solvents (Itoh *et al.*, 2000).

1.9 Aims of the project described in this thesis

The aim of this project was to investigate the role of metal ions at the active site of membrane GDH from *E. coli*. The model structure of GDH suggests that Ca^{2+} could be located at the active site, bound to PQQ as in MDH. However, the reconstitution of active GDH from apoGDH plus PQQ prefers Mg^{2+} than Ca^{2+} (Ameyama *et al.*, 1985 and 1986). Cozier *et al.* (1999) showed that Mg^{2+} was required for the reconstitution of GDH and that Ca^{2+} could not support reconstitution. It would be surprising if Mg^{2+} occurs at the active site because all the other quinoproteins contain Ca^{2+}. One possibility is that Ca^{2+} is already bound

to the active site in apoGDH and that Mg^{2+} has a role in PQQ insertion during reconstitution to produce holoGDH.

The metal content of GDH has never been measured and this may indicate which metal is present at the active site. Site-directed mutagenesis was used to change the residues that are expected to bind to the active site metal ion.

Isolating and purifying the periplasmic domain was attempted because this will make the protein soluble. The soluble domain could be used to grow crystals that may allow the X-ray structure to be determined.

Chapter 2

Material and methods

2.1 Chemicals

All chemicals were obtained from BDH Ltd (Poole, Dorset) and Sigma Ltd (Poole, Dorset) except those listed below:-

Amersham International plc, Aytesbury, UK

α ^{35}S dATP

Hyperfilm MP

Sequenase version 2.0 DNA sequencing kit

Anachem

6.00 % (w/v) acrylamide/bis (19:1) 7M Urea 1xTBE gel

Bio-rad Laboratories Ltd, Hempsted, Hertfordshire, UK

SDS-PAGE molecular weight protein standards

Multi-Gene T7 enzyme Refill Pack, version 2

Difco Laboratories, Detroit, Michigan, USA

Bacto-Agar

Tryptone

Yeast extract

Pharmacia , Keynes, UK

Agarose

DEAE sepharase fast flow

Promega Ltd, Southampton,UK

Supercoiled DNA ladder

Restriction enzymes

Wizard plus SV miniprep purification system

Wizard M13 DNA purification system

Oswel, Southampton, UK

DNA primers

2.2 Standard buffers and growth media

Pipes buffer (Piperazine-N,N'-bis[2-ethansulfonic acid] 10 mM, pH 7.0)	30.24g per litre makes 0.1 M. Dilute to 10mM with H_20
Potassium phosphate buffer (10mM, pH 7.0)	1.5M K_2HPO_4 adjusted to pH 7.0 by adding 1.5M KH_2PO_4. 1.5M stock diluted to 0.1M and 10mM by H_2O
LB Broth	5g Yeast extract, 5g NaCl and 10g tryptone in 1 litre H_2O
H-top agar	1g NaCl, 1.3g agar, 3g tryptone and 200 ml H_2O
TBE Buffer (pH 8.8)	138mM Tris, 45mM boric acid, 2.5mM EDTA. Adjust to pH 8.8 with HCl
TE buffer (pH 8.0)	10mM Tris-HCl pH 8.0 and 1mM EDTA in 1 litre H_2O
TAE buffer (pH 8.8)	40mM Tris, 5mM acetic acid, 1mM EDTA, adjusted to pH 8.8 with HCl
DNA Loading Buffer x10	30% w/v glyercol, 0.3%w/v bromophenol blue and TE buffer
Destain	1250ml methanol, 375ml glacial acetic acid made up to 5 litres

	with H_2O
SDS Running Buffer x5	30g Tris, 144g glycine, 10g SDS and 2 litres of H_2O
SDS Loading buffer x5	1ml 0.5M Tris-HCl pH 6.8, 4ml analar H_2O, 6.6 ml 10% w/v SDS, 0.8ml Glycerol, 0.4 ml β-metcapthanol, 0.2ml 0.04% w/v bromophenol blue
Coomassie Blue Stain	2.5g Coomassie Brilliant blue R, 454ml methanol, 96ml glacial acetic acid and 450ml H_2O

2.3 Bacterial and bacteriophage strains

Table 2.1 shows the bacterial and bacteriophage strains used in this study. PPGEC1 and M13GEC1 were provided by Dr Gyles Cozier. Glycerol stocks of each bacterial strain were made by adding 500µl glycerol to 500µl of overnight cultures. Stocks were stored at -20 °C and -80 °C for long periods of time. Phage stocks were made by picking a well-isolated plaque from infected *E. coli* colonies and adding it to 1ml of LB. The mixture was then heated at 55°C for 15 minutes to kill any *E. coli* cells. These stocks were stored at 4°C. Bacterial strains were plated out on agar plates containing the appropriate antibiotic and stored at 4 °C for short periods of time. To produce plasmid pGEC1, plasmid pGP478 was cut with *Sal*I and *Eco*R1 to cut out the *gcd* gene (Cozier *et al.*, 1999). This gene was then cloned into Bluescript KS^+ which had been cut with the same restriction enzymes. Introducing pGEC1 into strain PP2418 that was provided by Dr N. Goosen and had chloroamphenicol resistant gene inserted in the gcd gene made strain PPGEC1.

Bacterial strains used in this project are shown in Table 2.1. They were grown in Luria Bertani broth (LB broth) with shaking at 37°C. Growth media were autoclaved prior to use. The appropriate antibiotic (100µl ml^{-1} ampicillin and 15µl ml^{-1} chloroamphenicol) was added to the growth medium after the heat-liable components had been sterilised using a 0.2µm filter. Bacteria were typically grown in 10ml of medium before being transferred to 1 litre flasks.

Table 2.1 Bacterial strains used in this project

STRAIN	GENOTYPE	SOURCE	NOTES
E. coli			
MV1190	Δ(*lac-pro*AB), *thi*, *sup*E, Δ(*srl-rec*A) 306:: Tn10 (tet^r) [F' : *tra* D36, *pro*AB$^+$, *lac*I^{q}Z ΔM15]	Biorad	M13 Host
CJ236	*dut*$^{-1}$, *ung*$^{-1}$, *thi*$^{-1}$, *rel* A1; pCJ105 (Cm^{r}F')	Biorad	Produces uracil containing DNA
PP2418	*pts*I, *thi*, *gal*P, *cat* insertion in the *gcd* gene.	Dr N. Goosen	Strain contains an inactivated *gcd* gene. Chl^r.
PPGEC1	*pts*I, *thi*, *gal*P, *cat* insertion in *gcd* gene, contains pGEC1.	Dr G. Cozier	PP2418 strain containing plasmid pGEC1. pGEC1 is a plasmid containing *Sal*I - *Eco*RI *gcd* fragment from pGP478 cloned into pBluescript KS$^+$.
PPGEC6	*pts*I, *thi*, *gal*P, *cat* insertion in *gcd* gene, contains pGEC6.	This work	pGEC6 contains D354N mutation in *gcd* gene.
PPGEC7	*pts*I, *thi*, *gal*P, *cat* insertion in *gcd* gene, contains pGEC7.	This work	pGEC7 contains N355D mutation in the *gcd* gene.
PPGEC8	*pts*I, *thi*, *gal*P, *cat* insertion in *gcd* gene, contains pGEC8.	This work	pGEC8 contains D354N/N355D mutation in the *gcd* gene.
PPGEC9	*pts*I, *thi*, *gal*P, *cat* insertion in *gcd* gene, contains pGEC9.	This work	pGEC9 contains W198A mutation in the *gcd* gene.
PPGEC10	*pts*I, *thi*, *gal*P, *cat* insertion in *gcd* gene, contains pGEC10.	This work	pGEC10 contains N147E/H149A mutation in the *gcd* gene.
PGEc1T424N	*pts*I, *thi*, *gal*P, *cat* insertion in *gcd* gene	Dr K. Sode	Contains T424N mutation
PPSOL2	*pts*I, *thi*, *gal*P, *cat* insertion in *gcd* gene, contains pTrcgcd2.	Dr G. Cozier	pTrcgcd2 contains a fragment of *gcd* coding for the periplasmic domain.
PPSOLO2	*trx b*$^{-1}$, *gor*$^{-1}$	This work	Origani strain of *E. coli* containing pTrcgcd2
PPSAL2	*trx b*$^{-1}$,	This work	AD494 strain of *E. coli* containing pTrcgcd2
Bacteriophage			
M13GEC1	*Sal*I-*Xma*I fragment of *gcd* gene from pGEC1 cloned into M13mp18 against *lac*Z gene	Dr G. Cozier	Vector used for site-directed mutagenesis as M13 can infect *E. coli* cells.

2.4 The purification of GDH

The protocol used to purify WT and mutant glucose dehydrogenases was adapted from the methods described previously by Matsushita *et al.* (1989b) and Yamada *et al.* (1993). Pipes buffer or potassium phosphate buffer was used. Cells were grown until late log phase, harvested by centrifugation at 5000 rpm for 15 minutes and washed twice with 0.85% NaCl. Then the cells were resuspended in 10mM buffer, pH 7, 0.5 mM $MgCl_2$ and sonicated for 2x6 cycles of 30 seconds on/off. The cell extracts were centrifuged at low speed for 10 minutes to remove the cell debris. The supernatant was then centrifuged at high speed (40,000 rpm) for one hour and the pellet collected and resuspended in 10mM buffer, pH 7, 0.5% Triton X-100, 0.2 M KCl; Triton X-100 was used because it is a detergent that solubilizes the enzyme well. The homogenised pellet was incubated on ice for 30 minutes and centrifuged at high speed (40,000 rpm) for one hour. The supernatant was then dialysed against 10mM buffer, pH 7, 0.1% Triton X-100 to obtain solublised GDH and other soluble proteins.

The solubilised protein solution was applied to a 50ml DEAE sepharose column equilibrated with 10 mM buffer, pH 7, 0.5% Triton X-100. This separated GDH from other solubilised proteins because GDH is negatively charged and binds to the positively charged column. The column was then washed with 10 bed volumes of 10mM buffer, pH7, 0.5% Triton X-100 followed by 10 bed volumes of 10mM buffer 0.1% Triton X-100. GDH was eluted by a linear gradient of 0-100mM KCl in 10mM buffer, 0.1% Triton X-100 (eluted between 30mM and 60mM KCl). Samples obtained from the column were reconstituted with PQQ and Mg^{2+} to determine the active fractions. These active fractions were pooled and dialysed overnight in 10mM buffer pH 7 , 0.1% Triton X-100.

2.4.1 Gel filtration

Gel filtration was used to purify GDH in some experiments. This also facilitated buffer exchange. Econo-Pac columns (Bio-rad) were used and these were packed with Bio-gel P-6DG gel that is a polyacrylamide gel. The matrix of the column excluded solutes greater than 6000 daltons, allowing them to elute in the void volume. 20ml of the appropriate buffer was added to the column and allowed to run through. 500µl of GDH was added to the column and allowed to enter. Then 2.5ml of buffer was added and the effluent discarded. To collect GDH, 750µl of buffer was added and the fraction collected. This technique was also used to remove EDTA or EGTA from GDH and replace it with an appropriate buffer.

2.4.2 Reconstitution of apoGDH

GDH was purified as the apoenzyme. Holoenzyme could be formed by using the protocol of Ameyama *et al.* (1985). A mixture of 25μM PQQ, 5mM Mg^{2+}, 50mM buffer (pH 6.5) and 100μl of apoGDH was incubated at 25°C for 20 minutes. The amount of enzyme added to the reconstitution mixture varied because WT-GDH showed higher activity than mutant GDH; WT-GDH 11μg, D35N-GDH 92μg, N355D-GDH 48μg, D354N/N355D-GDH 97μg and T424N-GDH 50μg was used.

In the remaining chapters it will be stated that GDH was reconstituted under standard conditions. Standard conditions were incubation at 25°C for 20 minutes with 50mM buffer pH 6.5 (depending on the buffer used to purify the enzyme unless otherwise stated).

2.4.3 Measurement of GDH Activity

10μl of reconstituted GDH (0.55μg WT-GDH) was added to a standard assay and activity was determined spectrophotometrically using a dye linked assay involving phenazine ethosulphate (PES) and 2.6 – dichlorophenolindophenol (DCPIP). PES accepts electrons from PQQ in GDH and then passes them onto DCPIP. When DCPIP is reduced the absorbance at 600nm decreases.

A 1ml assay contained 20mM Tris-HCl (pH 8.75), 40mM D-glucose, 10μl reconstituted GDH, 100μM DCPIP and 660μM PES. The change in absorbance at 600nm was recorded for the first 60 seconds and activity calculated between 20 and 50 seconds. Specific activity for GDH was then calculated by using 15100 M^{-1} as the molar extinction coefficient for DCPIP. One unit of activity corresponds to 1μmole of DCPIP reduced per minute.

2.4.4 Measurement of oxygen uptake using an oxygen electrode

An oxygen electrode was used to measure the oxygen consumption of membrane fractions containing GDH. The oxygen electrode was supplied by Rank Brothers, Cambridge, UK. The electrode was cleaned thoroughly with distilled H_2O. A few drops of 1M KCl were placed on the electrode and covered by a small square piece of tissue paper. A small squared piece of Teflon was placed over the top taking care not to trap any air bubbles. Then the electrode was connected to the sample chamber which in turn was connected to a water bath (25°C). The sample chamber was filled with water and a small magnetic stirrer was added. The voltage was set at 0.65 volts and the electrode and Servoscibe recorder calibrated. A few grains of soduim dithionite were added to measure the decrease in O_2 from 100% to 0%.

Samples to be tested were placed in the sample chamber; typically 100µl of membranes were added to 10mM potassium-phosphate buffer, pH 7 and 1.5M D-glucose. The oxygen consumption over a three minute period was measured. It was presumed that in 3ml of buffer there was 15µl of dissolved oxygen. Therefore a decrease in 1% on the chart recorder corresponded to 0.15µl of oxygen. Activity of GDH was calculated in the oxygen consumed per hour per mg of protein.

2.4.5 Measurement of protein concentration

The Bradford assay was used to measure the protein concentration of purified GDH (Bradford, 1976). Adding 100mg coomassie blue, 50ml ethanol and 100ml 85% Orthophosphoric acid to 850 ml water made one litre of Bradford reagent. 980µl of Bradford reagent was added to 20µl of protein or BSA standards. Then the mixture was incubated at room temperature for 5 minutes before the absorbance at 595nM was measured. BSA standards were used to make a calibration curve ranging from 0 to 1mg/ml. The Bicinchoninic acid assay was a second method used to confirm reliable results (Smith *et al.* 1985; Redinbaugh and Turley, 1986).

2.4.6 SDS-Polyacrylamide gel electrophoresis

Purity of GDH was determined using SDS-Polyacrylamide gel electrophoresis (SDS-PAGE) in a Bio-rad electrophoresis cell. A polyacrylamide gel was made with a 12% separating gel and a 4.5% stacking gel. The separating gel was made first and poured into the assembled kit. A layer of butanol water was used to cover the gel. After the gel had set the butanol water was carefully removed and the stacking gel was poured on top of the separating gel. A comb was inserted into the top of the stacking gel. Once the gel had set, the comb was removed and the gel placed inside the Bio-rad cell. Running buffer was used to cover the gel and then the protein samples were added. The protein samples had been mixed with 0.2 volumes of loading buffer (containing SDS) and heated at 80°C for 5 minutes. Low range molecular standards were also run with the samples so proteins could be identified by their size. The samples were run at 40mA for about 40 minutes. Once the solvent front had reached the bottom of the gel, it was removed from the apparatus and soaked in Coomassie brilliant blue for 1 hour. The gel was then soaked overnight in destain so proteins could be seen.

2.5 Measurement of the metal ion content in GDH

The Mg^{2+} and Ca^{2+} content of purified GDH was measured by atomic absorption spectrophotometery by Dr Trevor Delves and Dr Silke Severnmann. Magnesium and calcium standards (0-200μM) were made and then 500μl of enzyme or standard was added to 500μl diluent (diluted HCl). A Perkin-Elmer 2380 atomic absorption spectrophotometer was used to measure the absorbance of the sample at a set wavelength. The wavelength was set at 285nm for Mg^{2+} and 422nm for Ca^{2+}.

2.6 Site-directed mutagenesis

Two methods were used to produce mutants of the *gcd* gene that codes for GDH; the method described by Kunkel (1995) and the Stratagene quickchange method.

2.6.1 The Kunkel method

The Kunkel method (1985) involves inserting the gene to be mutated into M13mp18. This allows a single-stranded template DNA to be produced that contains uracil if M13 is grown up in *E. coli* host carrying the *dut*$^-$ and *ung*$^-$ mutations (Konrad, 1975). The primer containing the mutation is added to the M13 uracil template under standard mutagenesis procedures to produce a heteroduplex molecule. The wild-type template (containing uracil) of this heteroduplex is destroyed by transforming the DNA into an *ung*$^+$ strain such as MV1190. A large proportion of the progeny bacteriophage should be mutants.

2.6.2 Production of mutagenic primers

All primers used in mutagenesis were made by Oswel, Southampton, UK. Primers were designed to mutate a single amino acid; this meant at least one base in the primer was different from the wild-type DNA sequence. Primers were 20 to 25 bases in length with the mismatch base located in the middle of the sequence. It was important for the annealing temperature of the primer not to be too high and that the primer should not form any secondary structures. The codon in the primer was changed to a codon that was frequently seen in other regions of the *gcd* gene.

2.6.3 Production of the M13 uracil-containing template

Cozier cloned part of pGEC1 into M13mp18 (Cozier *et al.*, 1999). pGEC1 was cut with *Sal*I and *Xma*1 to produce a fragment that contained 1817 bases of the *gcd* gene. *Sal*I was located in the pBR322 backbone of the plasmid and *Xma*I at position 1817 of the *gcd*

gene. M13 was also cut with these restriction enzymes and the *gcd* gene fragment inserted to form M13GEC1.

M13GEC1 was grown in *E. coli* strain CJ236 which is a *dut*$^-$ *ung*$^-$ double mutant. The *ung* gene codes for N-glycosylase which removes uracil from DNA and *dut* gene codes for dUTPase. The dut$^-$ mutants therefore incorporated random uracils into DNA instead of thymine. 300µl of overnight culture of CJ236 was added to 40µl of phage stocks (M13GEC1) and 10ml of LB; these cells were then grown for 6 hours at 37°C. Growing these cultures for longer than 6 hours could result in random mutations. Uracil-containing M13 ssDNA was then isolated using a Wizard M13 DNA Purification Systems (Promega, Southampton, UK). 2ml of culture was centrifuged at 10000x g for 5 minutes, then 1.5 ml of supernatant was removed to a 2 ml tube and 600µl of cold phage precipitant was added. This was incubated on ice for 20 minutes before being centrifuged at 10000x g for 10 minutes and then the phage pellet was resuspended in 500µl of phage buffer. 1ml of Wizard M13 DNA Purification Resin was added to the resuspended phage and added to a minicolumn connected into a vacuum manifold. The solution was drawn through the minicolum and the vacuum broken. 2ml of 80% v/v isopropanol was added and the vacuum reapplied to draw the solution through the minicolumn. The vacuum was left on for 30 seconds after the solution had passed through the column to dry the resin. The minicolumn was then centrifuged at 10000x g for 2 minutes to remove any isopropanol and then 100µl of H_2O preheated to 80°C was added to the column to remove the ssDNA. Centrifugation at 10000x g for 20 seconds eluted the ssDNA. M13GEC1 ssDNA containing uracil was stored at -20°C. Typical yields of M13 were 1-5µg of ssDNA.

The composition of buffers used in ssDNA purification were:-

Phage buffer	150mM NaCl
	40mM Tris-HCl
	10mM $MgSO_4$
Phage precipitant	33% polyethylene glycol (PEG 8000)
	3.3M NaCl
Wizard M13 DNA purification resin	Guanidine thiocyanate

2.6.4 Production of mutagenic DNA

The DNA primer containing the mis-match base(s) was phosphorylated to increase the efficiency of the synthesis reaction. 200pmol primer was added to 13µl 1mM ATP, 0.5µl T4 polynucleotide kinase, 3µl 10x T4 polynucleotide kinase buffer and 13µl AnalaR H_2O. The mixture was incubated for 45 minutes at 37°C to phosphorylate the 5' prime end of the DNA primer. The reaction was stopped by heating at 65°C for 10 minutes.

The next step involved annealing the primer to the uracil-containing single stranded DNA template (M13GEC1). 2-3pmoles of primer was added to 200ng uracil-containing DNA template, 1µl 10x annealing buffer and made up to 10µl with AnalaR H_20. The mixture was heated at 70°C for 2 minutes and then allowed to cool to below 30 °C over 1 hour. The primer-template complex was then stored on ice until the synthesis reaction.

The synthesis reaction involved adding 1µl 10x synthesis buffer, 1µl T4 DNA ligase and 1µl T7 DNA polymerase (1:2 dilution) to the primer-template complex. The mixture was left on ice for 5 minutes, incubated at room temperature for 5 minutes and finally incubated at 37°C for 30 minutes. This allowed the mutant strand to be synthesised without any uracil being incorporated into the sequence. The reaction was stopped by freezing the DNA at -20°C.

The DNA solution containing wild-type DNA and mutant DNA was then transformed into *E. coli* strain MV1190; this strain will not replicate uracil-containing DNA so only the uracil-free mutant DNA is replicated by the host. Transformed MV1190 cells were then added to 3ml of H-top agar and 300µl of untransformed MV1190 cells. This was poured over an agar plate and allowed to dry. Incubation at 37°C for 16 hours produced M13 plaques that were then isolated and stored.

The contents of the reagents used above were:-

10x annealing buffer	20mM Tris-HCl (pH7.4), 2mM $MgCl_2$, 50mM NaCl
10x T4 polynucleotide kinase buffer	700mM Tris-HCl (pH 7.6), 50mM DTT, 100mM $MgCl_2$
10x synthesis buffer	0.4mM of 4 DNTP's, 17.5mM Tris-HCl

	(pH 7.4), 0.75mM ATP, 3.75mM $MgCl_2$, 21.5mM DTT
T7 DNA Polymerase	13U/µl
T4 DNA Ligase	2.5U/µl

2.6.5 The Stratagene QuickChange method

This was a second method used to produce site-directed mutants. The advantage of this method was that M13 uracil-containing ssDNA is not required because this mutagenesis protocol allows site-directed mutagenesis on a double stranded plasmid. Therefore your mutant does not have to be cloned back into your plasmid from M13.

2.6.6 Production of primers

All primers were made by Oswel (Southampton, UK). This method of mutagenesis required two primers, and both must anneal to the same sequence on opposite strands of the plasmid. Primers were designed to be 25-40 bases in length with a melting temperature (T_m) of 78°C or greater. The formula used to estimate T_m was:-

$$T_m = 81.5 + 0.41\ (\%GC) - 675/N - \%\ \text{mismatch}$$

where N is the primer length in bases.

Primers had to have a minimum GC content of 40% and terminated at one or more C or G bases. The primers did not need to be 5'phosphorylated.

2.6.7 Production of double stranded DNA template

Supercoiled pGEC1 double stranded DNA was used as the DNA template. pGEC1 was purified using a Wizard Plus SVminipreps DNA Purification Systems (Promega, UK). A well isolated colony of PPGEC1 was grown in Luria-Bertani medium at 37°C overnight. Next day the cells were harvested (centrifugated for 5 minutes at 10,000x g). The pellet was resuspended in 250µl of cell resuspension solution and 250µl of cell lysis solution was added. After 1-5 minutes, 10µl of Alkaline Protease solution was added to inactivate endonucleases. Then 350µl of Wizard Plus SV Neutralization solution was added before the bacterial lysate was centrifuged at 14,000x g for 10 minutes. The cleared lysate was transferred to a prepared

spincolumn and centrifuged at 14,000x g for 1 minute. 750µl of column wash was added to the spin column and centrifuged again at 14,000x g for 1 minute. The wash procedure was repeated using 250µl of column wash and centrifuged at 14,000x g for 2 minutes. The plasmid DNA was eluted by adding 100µl of Nuclease-free water to the spin column and centrifuged at 14000x g for 1 minute. The eluted DNA was stored at -20°C. Analysing the samples on a 0.6% agarose gel checked the purity of the template.

Buffers used in the procedure were:-

Wizard plus SV neutralization solution	4.09M guanidine hydrochloride, 0.76M potassium acetate, 2.12M glacial acetic acid
Wizard plus SV column wash solution	60mM potassium acetate, 10mM Tris-HCl (pH7.5), 60% v/v ethanol
Wizard plus SV cell lysis solution	0.2M NaOH, 1% w/v SDS
Wizard plus SV cell resuspension solution	50mM Tris-HCl (pH7.7), 10mM EDTA, 100µg/ml RNase A

2.6.8 Production of mutagenic DNA by PCR

Two primers (containing at least one base mismatch) and template DNA were added to Pfu Turbo™ DNA polymerase II; and then the polymerase chain reaction was used to make mutant DNA. To produce mutant DNA by PCR the following were added:-

5µl of 10x reaction buffer
5-50ng of dsDNA template
125ng oligonucleotide primer #1
125ng oligonucleotide primer #2
1µl of dNTP mix
H_2O to a final volume of 50µl
1µl of Pfu Turbo™ DNA polymerase (2.5U/µl)

The cycling parameters used for site-directed mutagenesis were:-

Segment	Cycle	Temperature	Time
1	1	95°C	30 seconds
2	16	95°C 55°C 68°C	30 seconds 1 minute 2 minutes/Kb of plasmid
3	1	37°C	10 minutes

The amounts of template and primer used were varied to optimise conditions. 10µl of the amplified product was separated on a 0.6% agarose gel to check for sufficient amplification. Then 1µl of *Dpn*I restriction enzyme (10U/µl) was directly added to the amplified product to digest methylated DNA (template DNA). Parental DNA was digested leaving only mutant DNA. Mutant DNA was then transformed into PP2418 or JM109.

Reagents used in Quickchange mutagenesis were:-

10x Reaction buffer	200mM Tris-HCl (pH8.8), 20mM $MgSO_4$, 100mM KCl, 100mM $(NH4)_2SO_4$, 1% Triton X-100, 1mg/ml nuclease free BSA
Pfu Turbo™ DNA polymerase	2.5U/µl
PCR nucleotide mix	10mM dATP, 10mM dCTP, 10mM dGTP, 10mM dTTP (pH7.5)
*Dpn*1 restriction enzyme	10U/µl

2.7 Identification of mutant DNA produced by the Kunkel and Stratagene Quickchange methods

M13 DNA produced by the Kunkel method and dsDNA produced by the Stratagene Quickchange method can only be identified as mutant DNA by sequencing the DNA. The desired mutations did not introduce unique restriction sites into the DNA sequence. DNA was sequenced by Sanger's dideoxy chain termination method.

2.7.1 Sanger's dideoxy chain termination method for DNA sequencing

DNA sequencing was done using a T7 Sequenase kit from Amersham. This method is based on the Sanger method (Sanger *et al.*, 1977). Kunkel site-directed mutagenesis produced ssDNA that could be directly sequenced but the Stratagene Quickchange method produced dsDNA that had to be denatured before sequencing.

2.7.2 Denaturing dsDNA prior to sequencing

4-6μg of purified double stranded DNA was present in 32μl with H_2O. 8μl of 1M NaOH /1mM EDTA was added to the DNA and left at room temperature for 5 minutes. Tubes were then moved to ice before adding 4μl of 2M ammonium acetate and 120μl of ice-cold ethanol. The solution was centrifuged (12,000x g) for 20 minutes at 4°C and the pellet washed with 80% v/v ethanol. The solution was centrifuged again for 5 minutes and the resulting supernatant discarded. The pellet was vacuum desiccated for 3 minutes to remove any ethanol and then the pellet was resuspended in 7μl H_2O. This produced single stranded DNA which was left on ice until it was required.

2.7.3 Annealing template ssDNA to sequencing primer

For each DNA sample to be sequenced one annealing reaction was required. The sequencing primer was annealed to the ssDNA template by adding 1μl primer (0.5pmol) and 7 μl DNA template (0.5-1pmol) to 2μl of T7 reaction buffer. The mixture was heated at 65°C for 2 minutes and then allowed to cool to room temperature. Once the samples were below 30 °C they were stored on ice until the labelling and termination reactions.

2.7.4 Labelling and termination reactions

To each annealing reaction the following was added:-

1μl DTT 0.1M

1μl Diluted labelling mix (1:8 dilution)

1μl [α^{35}S] dATP

1μl Mn

1μl diluted sequenase

This labelling reaction was incubated at room temperature for 2-5 minutes. For the termination reaction 4 tubes were labelled A, C, G, T and filled with 2.5μl of the appropriate

dideoxy termination mix. The tubes were incubated at 37°C for at least 2 minutes before 3.5µl of the labelling reaction was added to each. After 2-5 minutes incubation at 37°C , 4µl of stop solution was added to each termination reaction. Then the samples were stored at -20°C before the DNA bases were separated by electrophoresis.

Reagents used in T7 Sequenase 2.0 kit:-

T7 Sequenase™ version 2.0 DNA polymerase	20mM potassium phosphate buffer pH 7.4, 1mM DTT, 0.1mM EDTA, 50% v/v glycerol, 13U/µl
T7 Sequenase reaction buffer x5	200mM Tris-HCl ph 7.5, 100mM $MgCl_2$, 250mM NaCl
Enzyme dilution buffer	10mM Tris-HCl pH7.5, 5mM DTT
DDT	0.1M
Labelling mix(dGTP)x5	7.5µM dGTP, 7.5µM dCTP, 7.5µM dATP, 7.5µM dTTP
Termination nucleotide mix (one for each dideoxynucleotide)	80µM dATP, 80µM dCTP, 80µM dGTP, 80µM dTTP, 50mM NaCl and 8µM of ddNTP (one for each mix)
Stop solution	95% v/v formamide, 20mM EDTA, 0.05% v/v bromophenol blue, 0.05% v/v xylene cyanol FF
Mn buffer	10mM $MnCl_2$, 150mM sodium isocitrate

2.7.5 DNA sequencing gel

Each reaction had four sequencing reactions labelled A, G, C and T. Each sample was run down a sequencing gel by electrophoresis. The gel was made by assembling the Squi-Gengel nucleic acid sequencing cell (Bio-rad). Two glass plates were attached together and separated by thin spacers. A plugging gel was made by mixing 15ml of GenePage 6% gel with 0.6ml of 10% w/v APS and 75µl of TEMED. This gel was poured on the base of the gel holder before the two glass plates were put in place. This formed a seal between the two plates. The sequencing gel was then made by adding 60ml GenePage 6% gel to 0.48ml of 10% APS and 20µl TEMED. The gel was pored in between the two glass plates. The glass plate with the attached buffer tank was coated with Sigmacoat before assembly so the gel would not stick to this glass plate later on. An upside down comb was inserted into the top of the gel with its teeth not immersed into the gel.

Once the gel had set, the reservoir on one of the glass plates and the base of the apparatus was filled with TBE buffer. The comb was inserted with the teeth touching the gel and then the gel was heated to 40°C by setting the power pack at 50W and 200V. Once the gel had reached the optimum temperature the four sequencing reactions were heated to 100°C for 2 minutes and then loaded onto the gel in the order A, C, G and T. Once the bromophenol blue dye front had travelled the required length, the apparatus was disassembled and the glass plates pulled apart. The gel only stuck to one glass plate due to the Sigmacote. The glass plate containing the gel was placed in fixing buffer for 15 minutes before a piece of filter paper was laid over the gel and then the gel was peeled off the plate. The gel was covered in clingfilm and dried on a bio-rad gel dryer at 80°C for 2 hours. Hyperfilm was then placed over the dried gel and the X-ray film was left for 1-5 days.

2.8 Transformation of DNA into host *E. coli*

Transformation is based on the observation by Mandel and Higa (1970) that bacteria treated with ice cold solutions of $CaCl_2$ and then briefly heated take up bacteriophage λ DNA. Three methods of transformation were used; the heat shock method, the high efficiency 5 minute method and electroporation.

2.8.1 The heat shock method

This method used to produce fresh competent cells with $CaCl_2$ was a variation of that of Cohen *et al.* (1972). A single colony was grown for 16-20 hours at 37°C. 0.5ml was subcultured into 5mls of LB and grown for 2-3 hours at 37°C; until the OD600 was about 0.8.

The cells were recovered (centrifuged for 3 minutes at 5000rpm) and resuspended in 2ml of ice-cold 50mM $CaCl_2$. Then the cells were recovered again and resuspended in 0.5ml $CaCl_2$ and stored on ice for 1hour. 0.5μg of plasmid DNA was then added to 200μl of $CaCl_2$-treated cells, mixed gently and stored on ice for a further 45 minutes. The tubes were transferred to a circulating water bath (42°C) and left in there for exactly 90 seconds. Cells were then placed on ice for 2 minutes. 1ml of LB was added to the mixture and incubated at 37°C for 1 hour before being plated out on selective media. Plates were incubated at 37°C for 12-16 hours for colonies to grow.

2.8.2 The high efficiency 5 minute transformation method

This method is similar to the heat shock method (Pope and Kent, 1996). Competent cells were resuspended in 0.5ml $CaCl_2$ as previously described in Section 2.8.1. 0.5μg DNA was added to 200μl cells and left on ice for 5 minutes. Then the cells were poured out onto pre-warmed (37°) selective media and incubated at 37°C for 12-16 hours.

2.8.3 The electroporation method

This method was used to transform *E. coli* cells with very low amounts of DNA (less than 1ng/μl). JM109 cells were used as the host. Firstly, competent cells were prepared; 3ml of an overnight culture were added to 1litre of LB and grown to 0.6- 0.8 OD600 at 37°C. Cells were centrifuged at 4000x g at 4°C and the pellet resuspended in 1000ml of sterile cold H_2O. The pellet was collected again (centrifuged at 4000x g) and cells resupended in 500ml of sterile cold H_2O. The cells were pelleted and washed again in 500ml of sterile water before the cells were pelleted and resuspended in 20mls of sterile water and 10% glycerol. Then aliquots of 50μl were frozen at -80°C.

To insert the DNA into the competent cells, 1μl of DNA was added to 50μl of competent cells (previously thawed). The mixture was flicked and stored on ice for 5 minutes. The DNA/cell mixture was then transferred to a chilled electroporation cuvette and placed on ice. A bio-rad Gene-pulser was used to subject the cells to a 4.5ms electrical pulse at 12.5 KV.cm field strength. The machine settings were:- resistance 200 Ohms, capacitance 25 uFD and voltage 1.25volts. The time constant was checked to ensure it was in the range of 4-5 (this was the time constant for the decay of the pulse). Immediately after the pulse 1ml of LB (supplemented with 20mM glucose, 10mM magnesium sulphate, 10mM magnesium chloride and 2.5mM potassium chloride) was added to the DNA/cell mixture. This mixture was then

transferred to a new tube and incubated with shaking at 37°C for 45 minutes. Cells were then plated onto selective media and grown overnight at 37°C.

2.9 DNA electrophoresis

The purity of DNA was determined by separating DNA on a 0.6% agarose gel by electrophoresis. The gel was made by adding 0.6g of agarose to 100ml of TAE buffer containing 0.6μg/ml of ethidium bromide. The mixture was heated in a microwave at full power for 2-3 minutes until all the agarose had dissolved. The gel was poured into a mould and a comb inserted to make wells. Once set, the gel was placed in a tank and immersed in TAE buffer containing 0.6μg/ml of ethidium bromide. Typically 10μl of DNA sample was mixed with 3μl DNA loading buffer before being injected into a well on the gel. Electrophoresis was carried out at 80V for 1-2 hours. DNA was visualised by using UV light.

2.10 Concentration of DNA samples

DNA samples were concentrated by ethanol precipitation. Ammonium acetate was added to DNA to give a final concentration of 2-2.5M. Two volumes of ice-cold ethanol were added to the mixture and placed on ice for 30 minutes to allow the DNA to precipitate. The DNA was recovered (centrifuged for 10 minutes at 12,000x g at 4°C). The supernatant was removed and the pellet of nucleic acid resuspended in 70% v/v ethanol. The sample was centrifuged at 12,000x g for 2 minutes and the supernatant discarded. The tube with the DNA pellet was then stored at room temperature to let any last remaining traces of ethanol to evaporate. The DNA pellet was resuspended in the desired volume of water (typically 20μl) and stored at -20°C.

2.11 Computer packages used to study GDH activity

Kinetic analysis was performed using a program called Graphpad PRIZM™. Two equations were used to draw a line of best fit on typical saturation curves to determine V_{max} and K_m values. The first equation was $V=(V_{max}[S])/(K_m+[S])$.The equation $V=V_{max}[S]/K_m+[S]\{1+S/K_i\})$ was used when substrate inhibited GDH activity at high concentrations.

Chapter 3

Characterisation of the glucose dehydrogenase of *E. coli*

Introduction

This Chapter describes the general character of the mGDH used in this work. This was necessary preliminary work before more specific investigation aimed at determining whether Ca^{2+} or Mg^{2+} is the metal ion at the active site of GDH, or if the Mg^{2+} used in reconstitution has a different role such as PQQ insertion. Most work on GDH assumes that Mg^{2+} is the metal ion at the active site because it is required for reconstitution but there is no evidence for this. All quinoproteins that have been shown to contain a metal ion contain Ca^{2+} at the active site.

3.1 Characterisation of WT-GDH

As described in the Section 2.4.3, GDH activity is measured using a dye-linked assay. However, before activity can be measured apoGDH must be reconstituted with Mg^{2+} and PQQ to form holoGDH. In order to investigate the role of metal ions in GDH and the mutants prepared in this work, it was first necessary to fully characterise WT-GDH and the requirements for reconstitution of holoenzyme from apoenzyme and PQQ. This chapter describes the characterisation together with some observations on stability and substrate specificity.

3.1.1 Purification of WT-GDH from *E. coli*

The protocol used to purify GDH was adapted from the method used by Yamada *et al.* (1993). This is described in Section 2.4. GDH was purified from an *E. coli* strain that lacked chromosomal *gcd*, GDH being encoded on a plasmid (pGEC1). Two buffers were used to purify GDH; Piperazine-N,N-bis[2-ethanesulfonic acid] (Pipes buffer) and potassium phosphate buffer. Mops buffer was unsuitable because all activity was lost during column chromatography. Potassium phosphate buffer was initially used but this could not be used to investigate the effects of Ca^{2+}, Sr^{2+} and Ba^{2+} on reconstitution as it caused these to precipitate. Table 3.1 shows that both Pipes and potassium phosphate buffers could be used to successfully purify GDH. SDS-PAGE showed that GDH was about 80% pure (Figure 3.1). A 87kDa protein was not expressed in the *E. coli* strain that lacked pGEC1.

There were advantages and disadvantages between Pipes buffer and potassium phosphate buffer. The use of potassium phosphate buffer produced an enzyme that had an absolute requirement for Mg^{2+} for reconstitution, but the use of Pipes buffer gave an enzyme that

Table 3.1 Preparations of WT-GDH in various buffers

Pipes buffer preparation (pH adjusted with HCl)

Sample	Volume (ml)	Total protein (mg)	Specific activity (μmoles/min/mg)	Yield (%)	Purification (fold)
Crude extract	55	1292	7	100	1.0
Membranes	50	287	14 (1.4)	77.6	2.0
Soluble GDH	45	62	21 (2)	14.4	3.0
DEAE-GDH	35.5	20	116 (47)	25.7	16.5

Pipes buffer preparation (pH adjusted with NaOH)

Sample	Volume (ml)	Total protein (mg)	Specific activity (μmoles/min/mg)	Yield (%)	Purification (fold)
Crude extract	38	847	12	100	1
Membranes	29	190	25	46.5	2.1
Soluble GDH	26	66	58	37.7	4.8
DEAE-GDH	25.5	20	84 (7)	16.5	7

Potassium phosphate buffer preparation

Sample	Volume (ml)	Total protein (mg)	Specific activity (μmoles/min/mg)	Yield (%)	Purification (fold)
Crude extract	40	1399	4	100	1
Membranes	26	270	21	90.8	5.2
Soluble GDH	26	86	52 (0)	71.7	13.0
DEAE-GDH	29.5	23	95 (0)	35.0	23.8

Values in brackets indicate activity of GDH after reconstitution in the absence of added Mg^{2+}

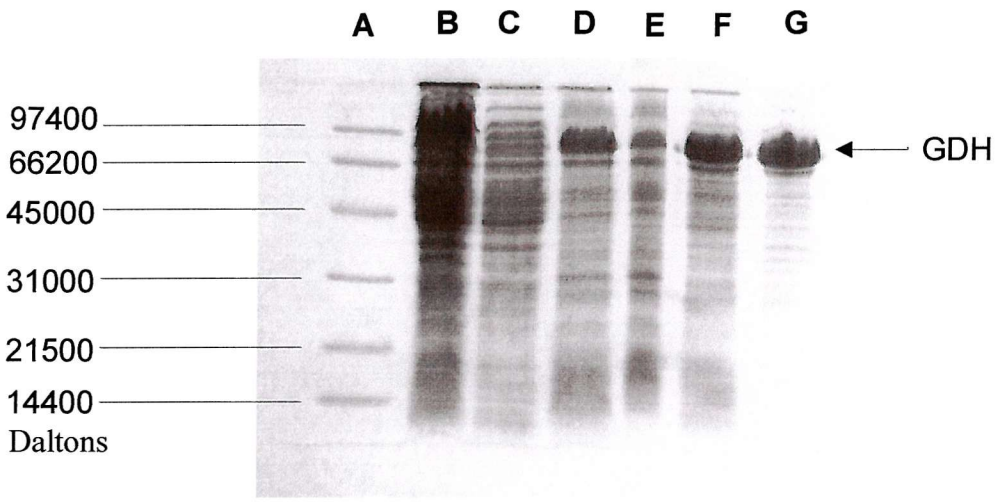

Pipes preparation

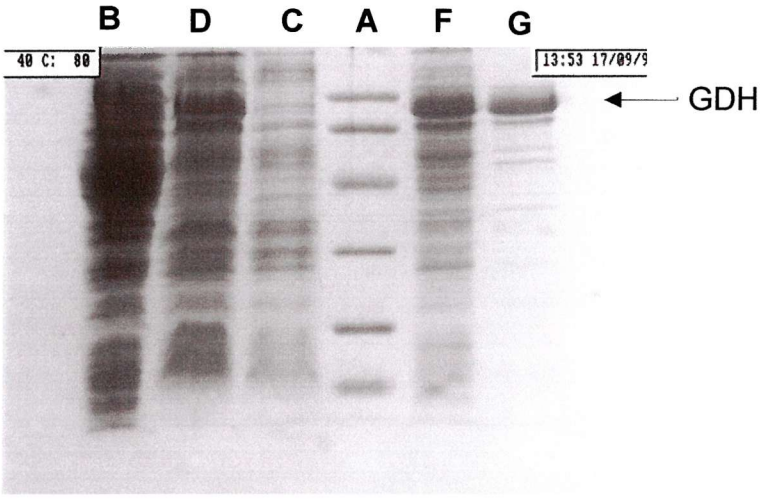

Potassium phosphate preparation

Figure 3.1 SDS-PAGE showing the purity of WT-GDH

A) Protein standards

B) Crude extract

C) Supernatant from membrane isolation

D) Membrane fraction

E) Membrane fraction after GDH solubilization

F) Solubilized GDH

G) DEAE-sepharose purified GDH

was active after reconstitution without added Mg^{2+}. Addition of Mg^{2+} increased activity. Although GDH purified in potassium phosphate buffer was preferable because it required Mg^{2+} for holo-enzyme formation, this buffer could not be used in experiments that involved Ca^{2+} because it precipitated in this buffer.

Two types of Pipes buffer were commercially available; Pipes that needed the addition of NaOH to get the correct pH, and disodium salt Pipes that required the addition of HCl. The disodium salt buffer gave GDH that was 41% active when incubated with only PQQ, but the second Pipes buffer gave GDH that was only 8% active under the same conditions. This activity may be caused by Mg^{2+} or Ca^{2+} ions remaining bound to the protein during the purification process and later work investigated this activity and how it could be removed (Section 3.7). To study the role of metal ions, a preparation of GDH was required that had no activity after reconstitution with PQQ in the absence of added metal ions. Therefore, the initial characterisation was studied with GDH purified in potassium phosphate buffer.

3.1.2 The effect of PQQ on reconstitution

Figure 3.2 shows the effect of pH on PQQ binding over time; full reconstitution was achieved within 10 minutes and usually 80% within 5 minutes. This meant that the rate of reconstitution could not be measured accurately and so the kinetics reported in this thesis refer to activity achieved after final reconstitution (after 20 minutes). When the activities achieved after completion of reconstitution were plotted against the PQQ concentration, typical reversible Michaelis-Menten kinetics were obtained (Figure 3.3). The dissociation constant (K_d) was calculated using the equation $A = A_{max}\,[PQQ]/(K_d + [PQQ])$ where A is GDH activity and A_{max} is the highest activity achieved. The binding of PQQ to GDH at pH 6.5 had a K_d of 282nM and the A_{max} was 101μmoles/min/mg. However, these results may be inaccurate as PQQ was not in excess at lower concentrations of PQQ (505nM GDH was reconstituted with PQQ).

At the lower pH range (pH 5.5) reconstitution was completed within 2-5 minutes, but at a higher pH (pH 8.0) the reconstitution times increased to 5 - 10 minutes. The K_d values over the pH range 5.5 - 8.0 increased but not in a linear fashion (Figure 3.4AP) (Figures or Tables labelled with AP are found in the appendix). Between pH 7.0 and 8.0 there were large changes in the K_d values as shown previously by Cozier *et al.* (1999) who proposed that this large decrease in affinity for PQQ is due to deprotonation of three or four groups in the apo-enzyme or PQQ molecule. These are expected to have pK values between 7.0 and 8.0, and are positively charged below pH 7.0. These could include the pyrrole nitrogen of PQQ (that could bind to a carboxylate residue of apoGDH) His-775, Arg-266 and Lys-493. Arg-266 is expected to bind to the 9-

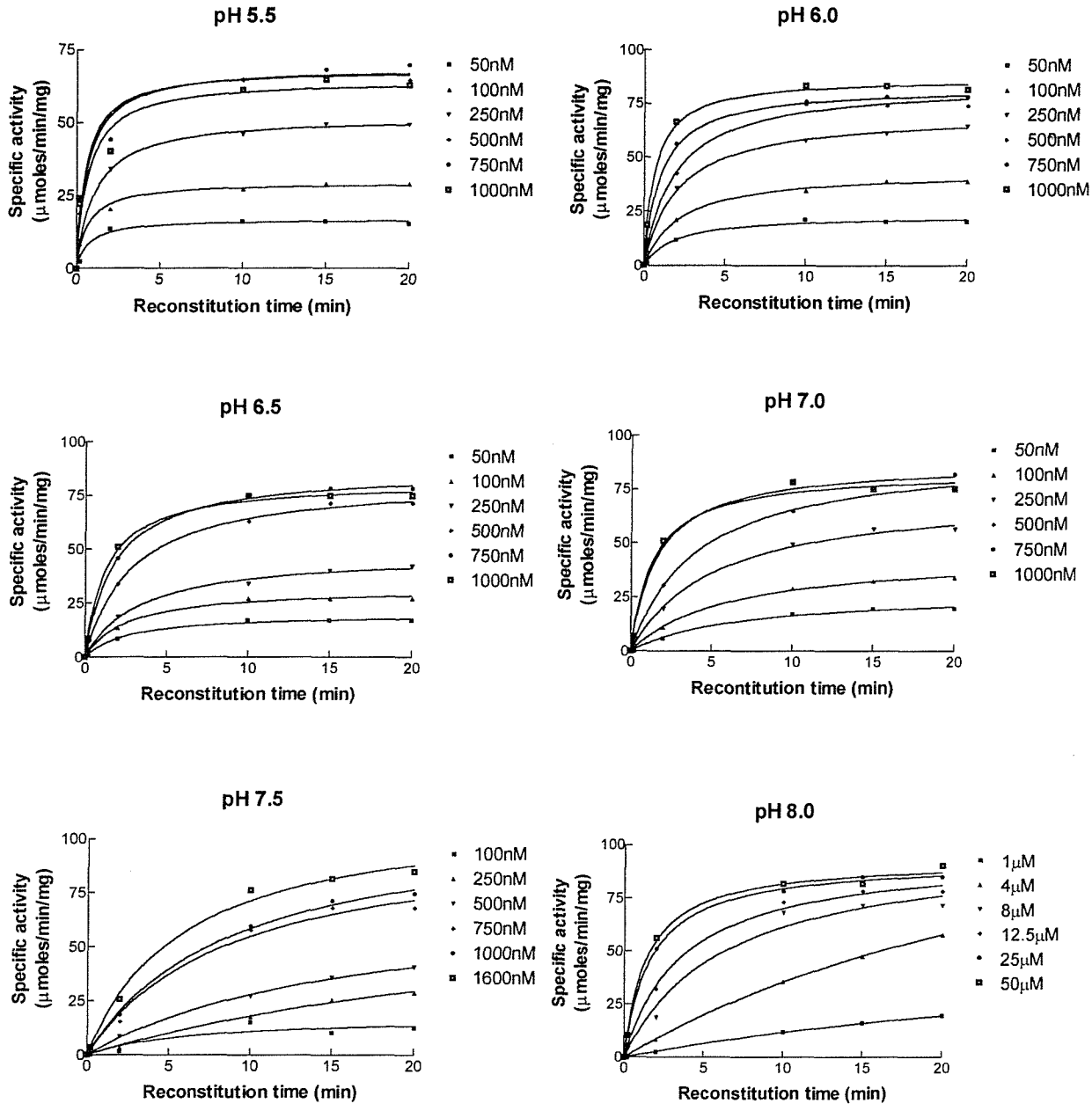

Figure 3.2 The effect of pH on PQQ binding

WT-GDH purified in Potassium phosphate buffer was reconstituted at various pH values under standard conditions (at 25°C) with 5mM Mg^{2+} . The following buffers were used:Bis-Tris (pH 5.5), MES (pH 6.0), Potassium phosphate buffer (pH 6.5 - 7.5) and Tris (pH 8.0). The affinity for PQQ may be higher because the enzyme concentration used was 632nM. Therefore PQQ is not in excess at lower concentrations.

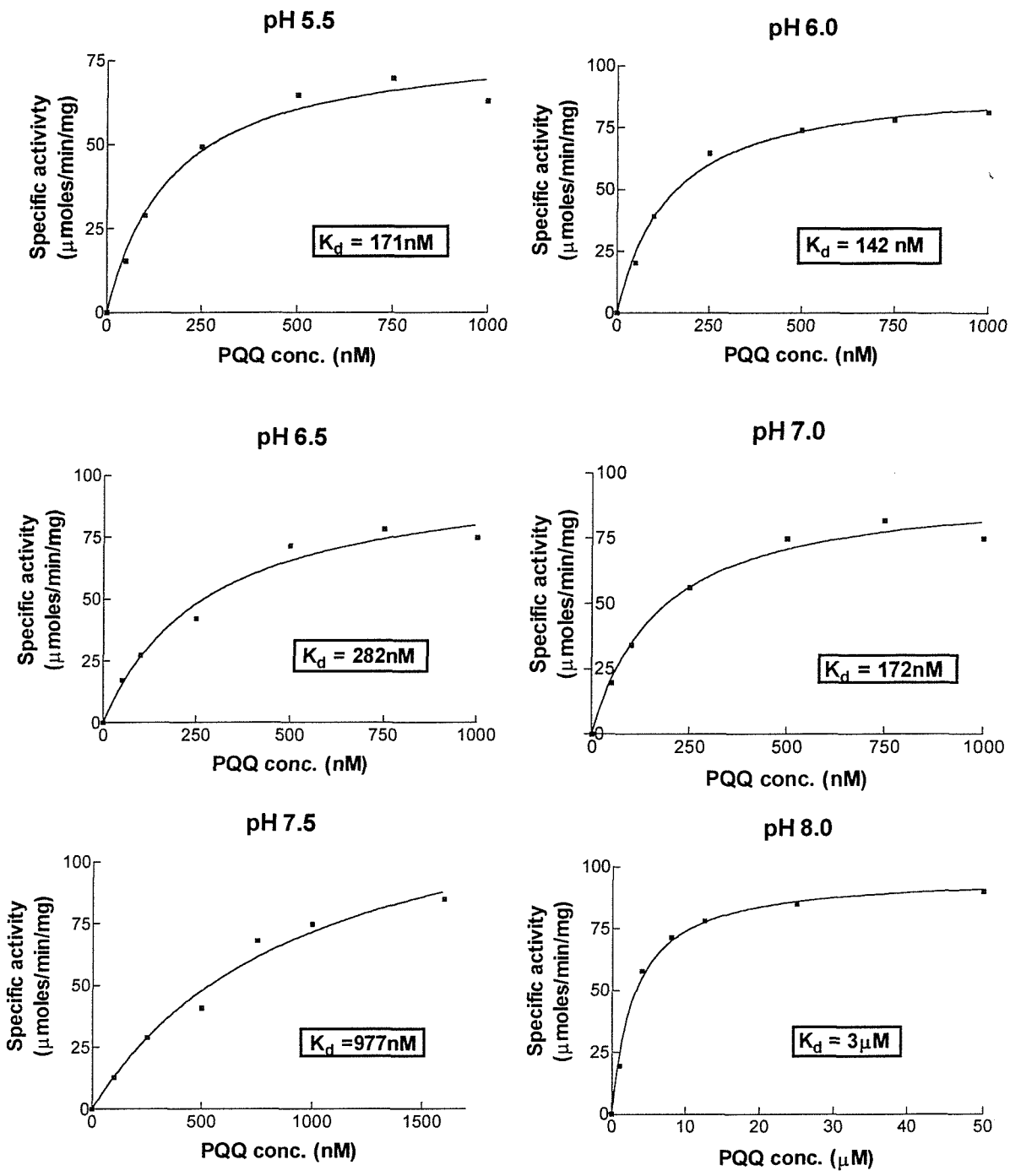

Figure 3.3 K_d values for PQQ binding between pH 5.5 and 8.0

Activity of WT-GDH after 20 minutes reconstitution with 5mM Mg^{2+} between pH 5.5 and 8.0. The following buffers (50mM) were used: Bis-tris (pH 5.5), MES (pH 6.0), Potassium phosphate buffer (pH 6.5-7.5) and Tris (pH 8.0). The lines of best fit were based on the equation $A=A_{max}[PQQ]/(K_d+[PQQ])$ where A is activity of GDH after reconstitution. The affinity for PQQ may be higher because the enzyme concentration used was 632nM. Therefore PQQ is not in excess at lower concentrations.

carboxylate of PQQ and Lys-493 to the C4 and C5 carbonyl groups (Figure 1.18). Histidine could be one of these groups because its pK value is 6.5. The pK values for lysine and arginine are 10 and 12 but these values may be reduced in the environment of the protein. However, the groups that are deprotonated may not bind directly to PQQ; they may change the folded state of the protein when they become deprotonated. It is unlikely that His-262 is one of these groups because the effect of pH on the affinity for PQQ of H262Y-GDH was identical to WT-GDH (Cozier *et al.*, 1999).

3.1.3 Determination of the substrate specificity of WT-GDH

The substrate specificity characteristic of WT-GDH will be important in later Chapters when mutant GDH is compared with WT-GDH. Figure 3.5 shows that GDH can oxidise D-glucose, 2-deoxy-D-glucose, D-xylose, D-ribose, D- galactose, D- mannose and L-arabinose. GDH had the highest affinity for D-glucose. No activity was recorded with maltose, L-glucose, L-xylose, D-lyxose and D-arabinose. This confirmed the results of Cozier *et al.* (1999) that are shown in Section 1.4.

3.2 The effect of Mg^{2+} on reconstitution of WT-GDH in potassium phosphate buffer

Ameyama *et al.* (1985) reported that holoGDH is formed by reconstituting apoGDH with Mg^{2+} and PQQ. Figures 3.6 and 3.7 shows that Mg^{2+} was an absolute requirement for reconstitution, which was a very rapid process; 80-100 % activity was achieved within the first 2 minutes and full activity within 5 minutes (Figure 3.7). As shown for PQQ (Figures 3.2 and 3.3), when the activities achieved after completion of reconstitution were plotted against the Mg^{2+} concentration, typical reversible Michaelis-Menten kinetics were obtained (Figure 3.7). Over the pH range 5.5 to 8.0, there was no significant change in K_d values (all between 1.0mM and 1.9mM. This was expected because carboxylates that bind to the metal ion (in the GDH model) are already deprotonated at pH 5.0.

However, K_d values for Mg^{2+} measured by other groups working on this enzyme differ from the value described in this thesis and those measured by Cozier *et al.* (1999). Yoshida and Sode (1996) reported that the K_d value was 320μM and Yamada *et al.* (1998) reported that the K_d value was even lower (22μM). Discussions with Yamada and Sode were unable to resolve the discrepancy. The values described in this thesis and those measured by Cozier *et al.* (1999) are the same. Similar K_m and K_d values for D-glucose and PQQ were measured by all groups.

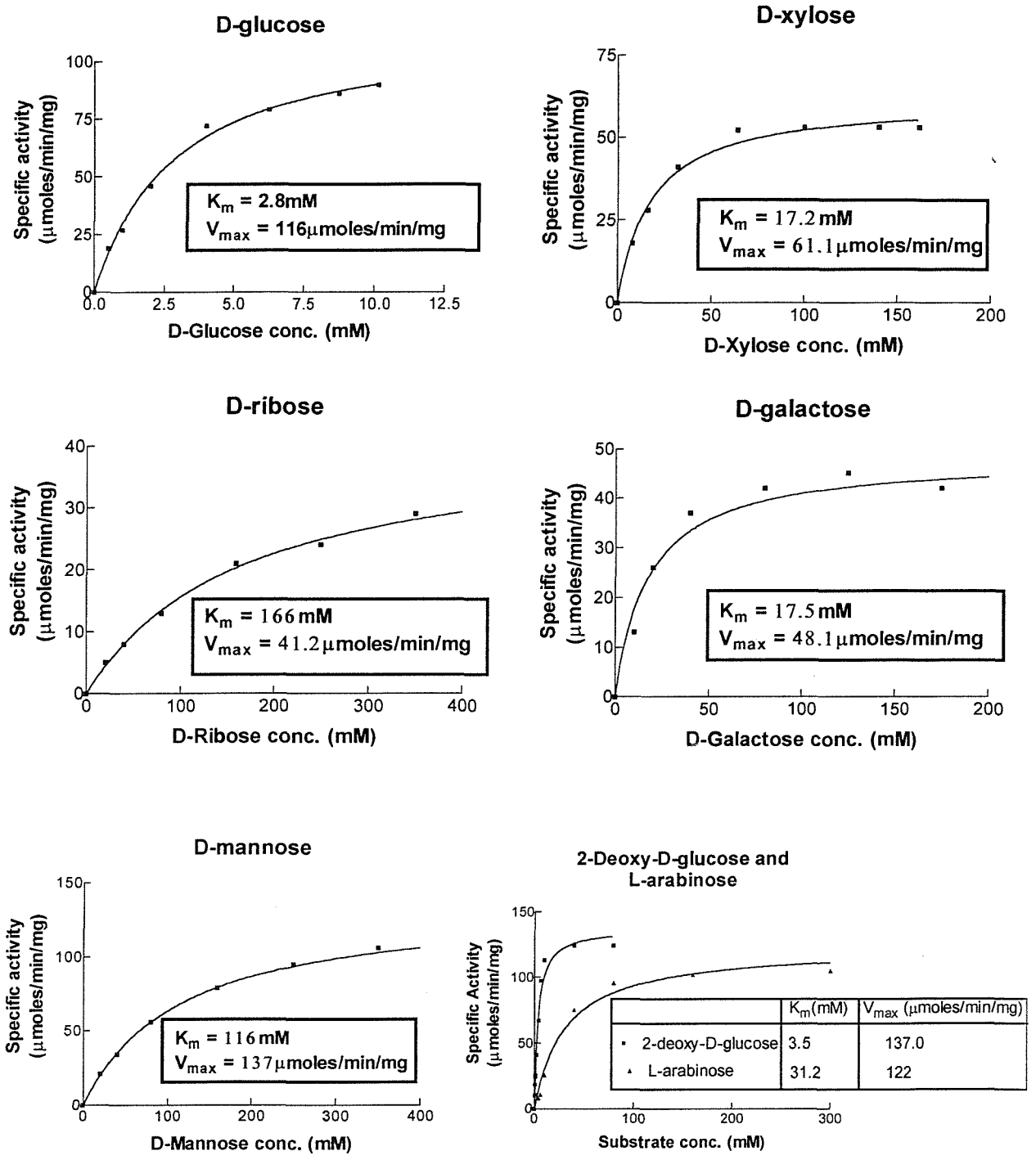

Figure 3.5 The activity of GDH with various substrates

Potassium phosphate purified WT-GDH was reconstituted under standard conditions with 5mM Mg^{2+} and 25μM PQQ. Samples were then removed and activiy measured by the dye-linked assay containing various concentrations of substrates. The best fit lines were based on the equation $v=V_{max}[S]/(K_m + [S])$ where S is substrate concentration.

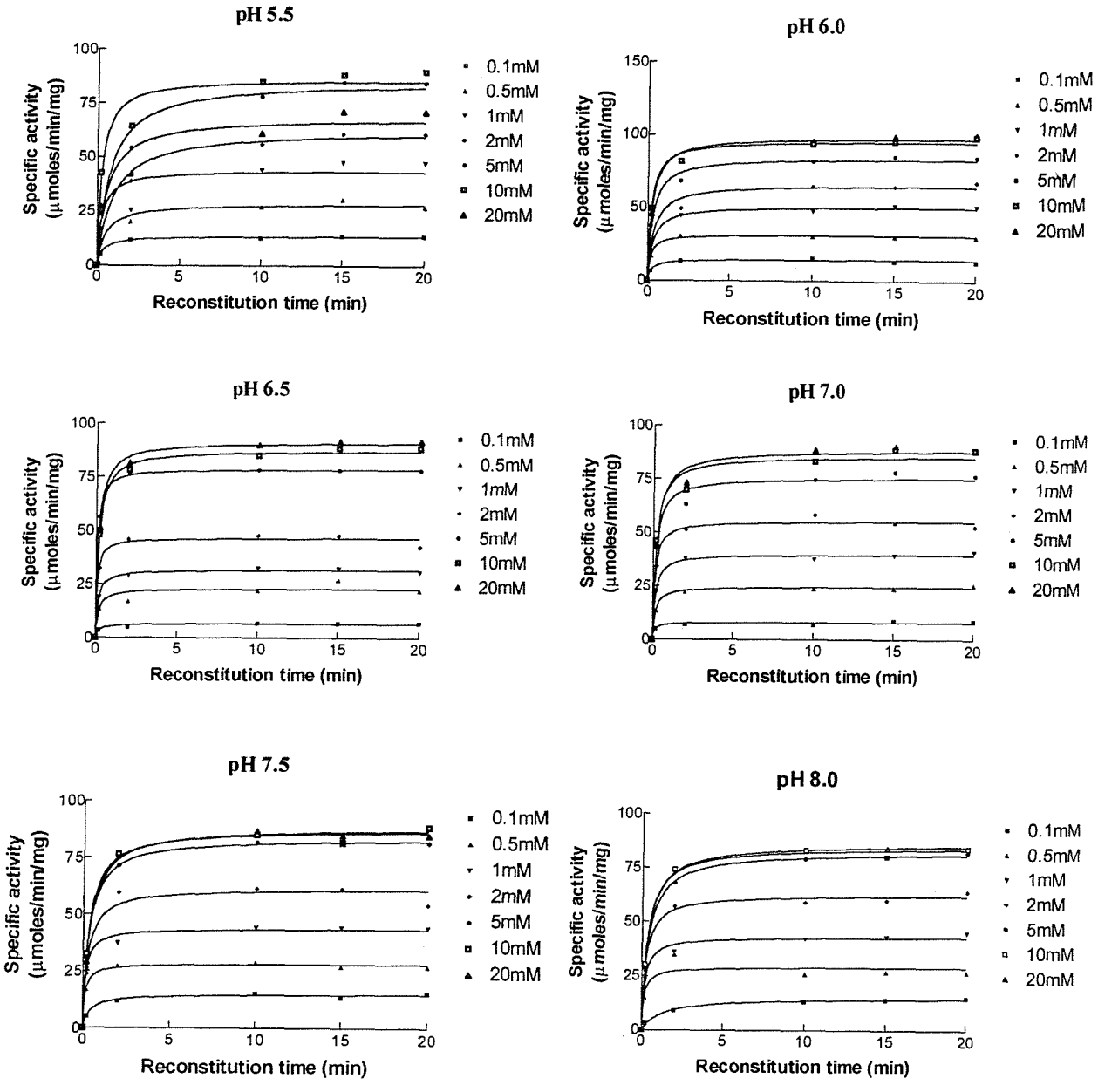

Figure 3.6 WT-GDH activity with various concentrations of Mg^{2+} between pH 5.5 and 7.5

WT-GDH was reconstituted under standard conditions with 25μM PQQ and various concentrations of Mg^{2+} between pH5.5 and 7.5. The following buffers (50mM) were used:Bis-Tris (pH 5.5), MES (pH 6.0), Potassium phosphate buffer (pH 6.5 - 7.5), and Tris (pH 8.0).

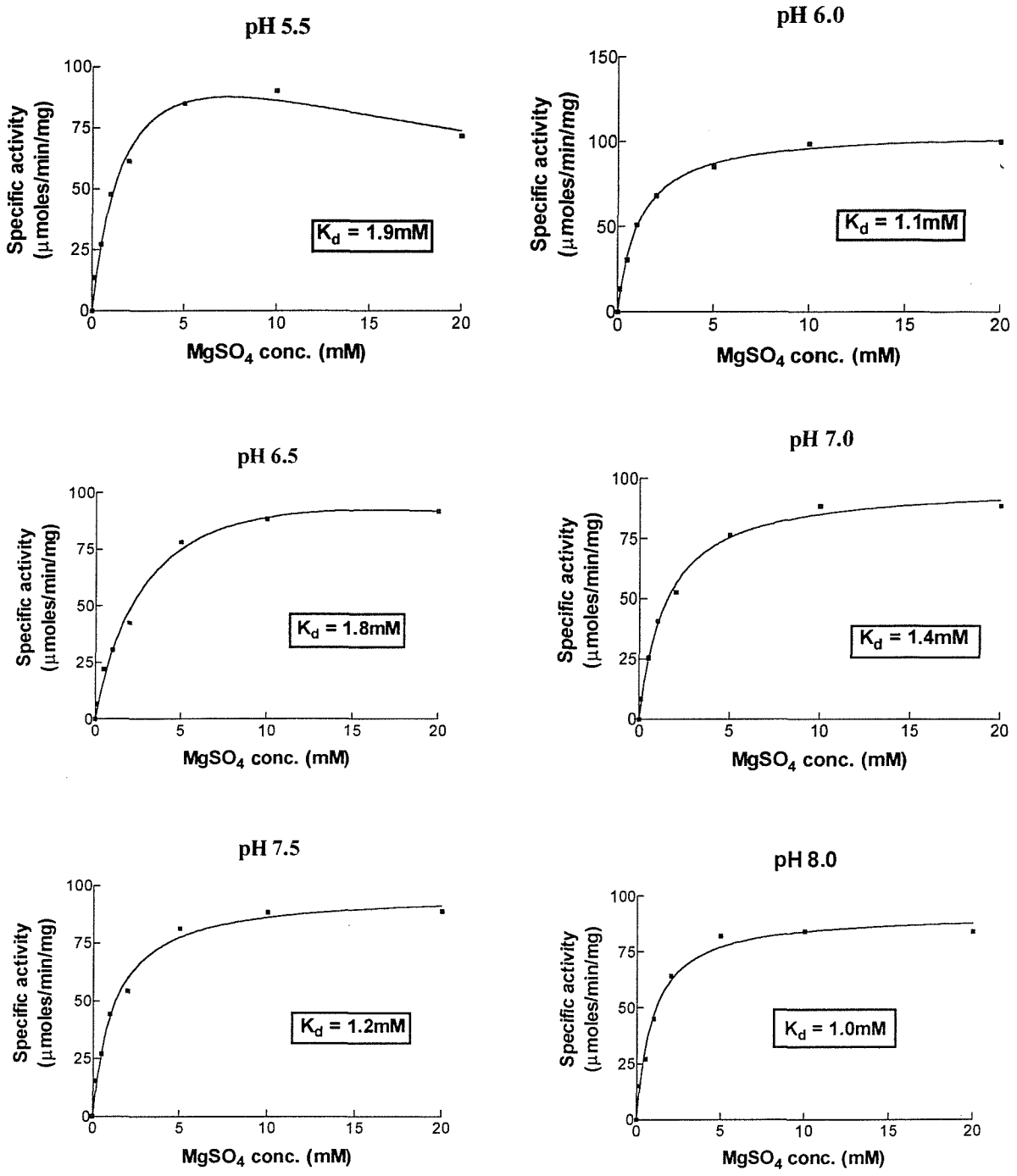

Figure 3.7 K_d values for Mg^{2+} between pH 5.5 and 7.5

Activity of WT-GDH after 20 minutes reconstitution with 25μM PQQ . The following buffers (50mM) were used: Bis-tris (pH 5.5), MES (pH 6.0) and Potassium phosphate buffer (pH 6.5-7.5). The lines of best fit were calculated by the equation $A=A_{max}[Mg^{2+}]/(K_d + [Mg^{2+}])$ where A is activity of GDH after reconstitution. The line of best fit at pH 5.5 was calculated by the equation $A=A_{max}[Mg^{2+}]/(k_d + [Mg^{2+}]\{1+Mg^{2+}/k_i\}$.

3.2.1 Mg^{2+} and PQQ binding to WT-GDH was reversed by gel filtration and dialysis

To confirm that binding of Mg^{2+} and PQQ during reconstitution is reversible, dialysis and gel filtration were used. Reconstituted GDH was dialysed at 4°C overnight in 10mM potassium phosphate buffer pH 7.0, 0.1% Triton X-100. This led to the complete loss of activity and activity was fully restored after reconstitution with Mg^{2+} and PQQ. Gel filtration also removed all activity; addition of 5mM Mg^{2+} (without PQQ) only restored activity to 46% and the addition of 25μM PQQ alone had no affect.

E. coli GDH is known to be an example of a type I GDH; it is not tolerant to EDTA treatment, which is assumed to remove the metal ion from the active site (Dokter *et al.*, 1986). As expected 10mM EDTA inhibited GDH that had been previously reconstituted. Remarkably, a low concentration gave a 35% increase in activity (Figure 3.8); this could be caused by the removal of metal ions from a second metal binding site that inhibits GDH when occupied.

3.2.2 Absorption spectra of apo and holoGDH

The absorption spectra of apo and reconstituted GDH are shown in Figure 3.9. The peak due to PQQ at 325nm (Figure 3.10) was seen in holoGDH but the spectrum could not be distinguished from that of apoGDH plus PQQ (in the absence of metal ions). It should be noted that the excess PQQ couldn't be removed before recording the spectrum of holoGDH because the necessary gel filtration would have led to dissociation of bound PQQ. Therefore, this method could not be used to study the role of metal ions in reconstitution.

3.3 The effect of Ca^{2+} on reconstitution of WT-GDH

The effect of Ca^{2+} on reconstitution could not be investigated with GDH purified in potassium phosphate buffer because calcium precipitated in this buffer. Therefore, disodium salt Pipes buffer (pH adjusted with HCl) was used. GDH was partially active (41%) after reconstitution in absence of added metal ions, suggesting that Mg^{2+} may be present in the sample. Ca^{2+} inhibited this reconstituted GDH, giving 50% inhibition with 10mM Ca^{2+} (Figure 3.11).

Figures 3.12 and 3.13 show that Ca^{2+} inhibited reconstitution with Mg^{2+} whether GDH was incubated first with Mg^{2+} or first with Ca^{2+}. These results show that Ca^{2+} does not irreversibly inactivate the enzyme and that it may be in direct competition with Mg^{2+} for a binding site on apoGDH. 30mM Ca^{2+} inhibited 5mM Mg^{2+}-reconstituted GDH by 50%.

Competition between Mg^{2+} and Ca^{2+} was confirmed by incubating GDH with PQQ and a lower concentration of Mg^{2+}(1mM)(Figure 3.14). When both metal ions were

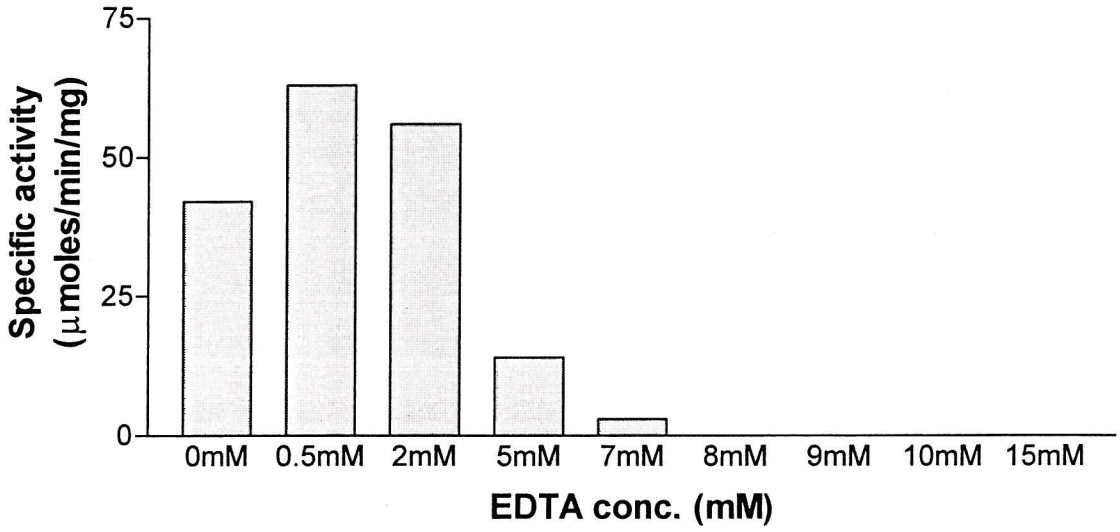

Figure 3.8 The effect of various concentrations of EDTA on Mg^{2+} reconstituted WT-GDH

WT-GDH purified in potassium phosphate buffer was reconstituted under standard conditions with 5mM Mg^{2+} and 25μM PQQ. Then various concentrations of EDTA were added to the enzyme and incubated at 25°C for a further 20 minutes and activity measured.

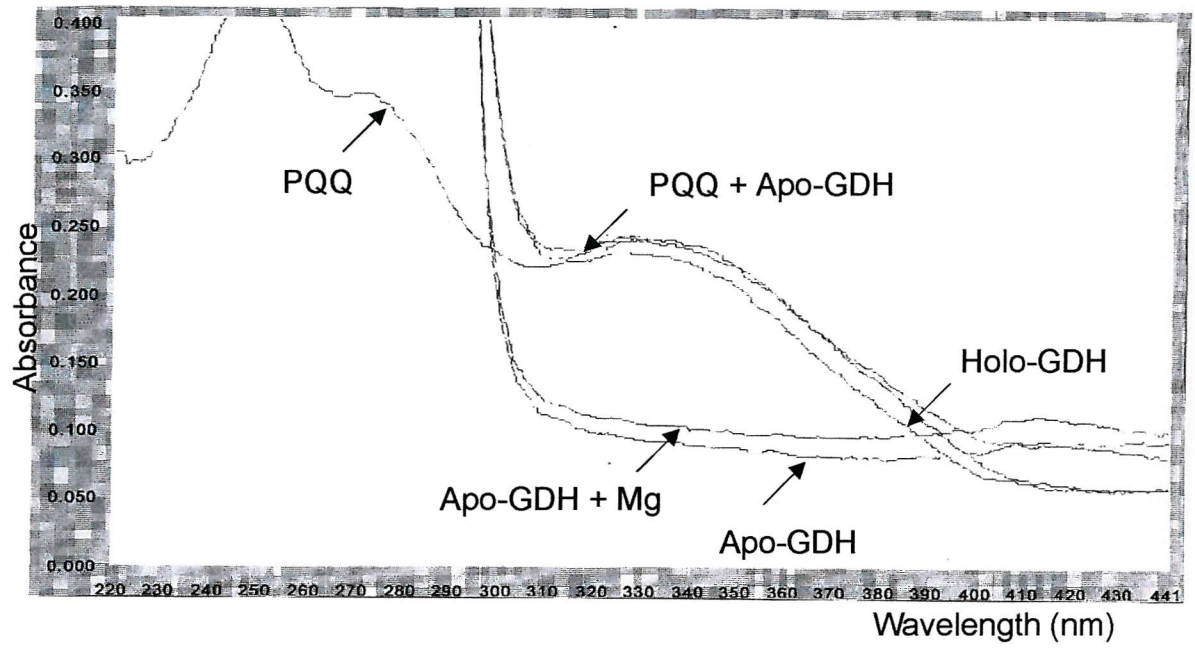

Figure 3.9 Absorption spectra of apo and holoGDH

Spectra of GDH (4μM) were measured in phosphate buffer at pH 7.0. HoloGDH had a peak at 330nm due to PQQ. There was no significant difference between apoGDH and apoGDH with Mg^{2+}. 1μM PQQ and 200μM Mg^{2+} were used in the assay.

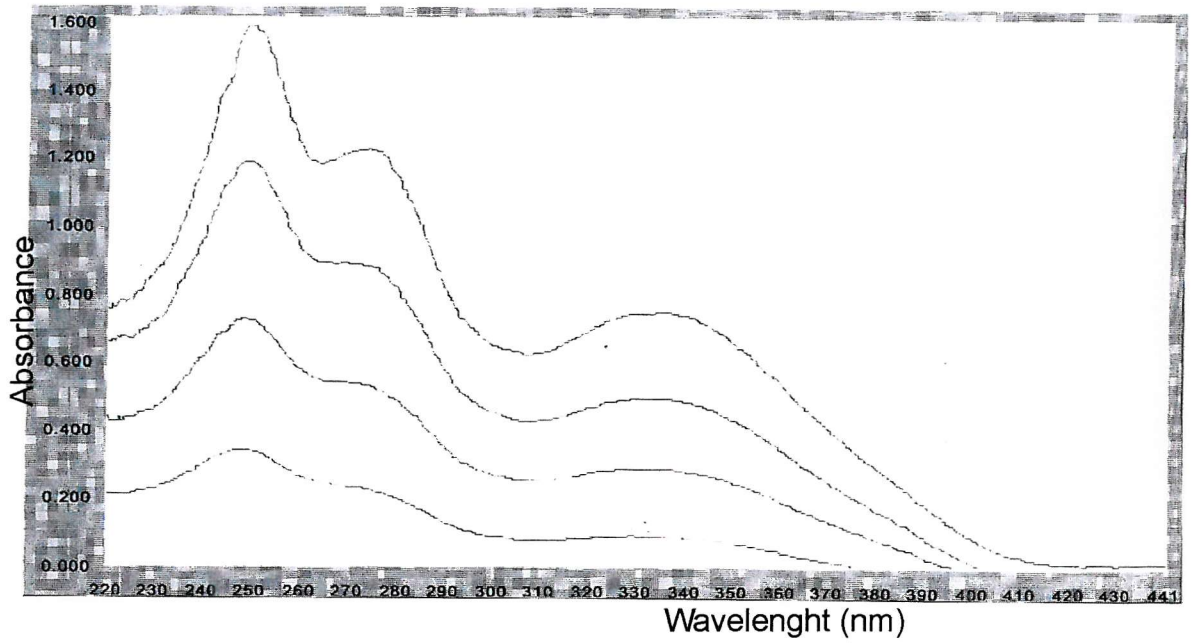

Figure 3.10 Absorption spectra of PQQ

The absorption spectra of PQQ had maximum at 249nM and 325nM. Various concentrations of PQQ were used (20μM, 40μM, 60μM and 80μM).

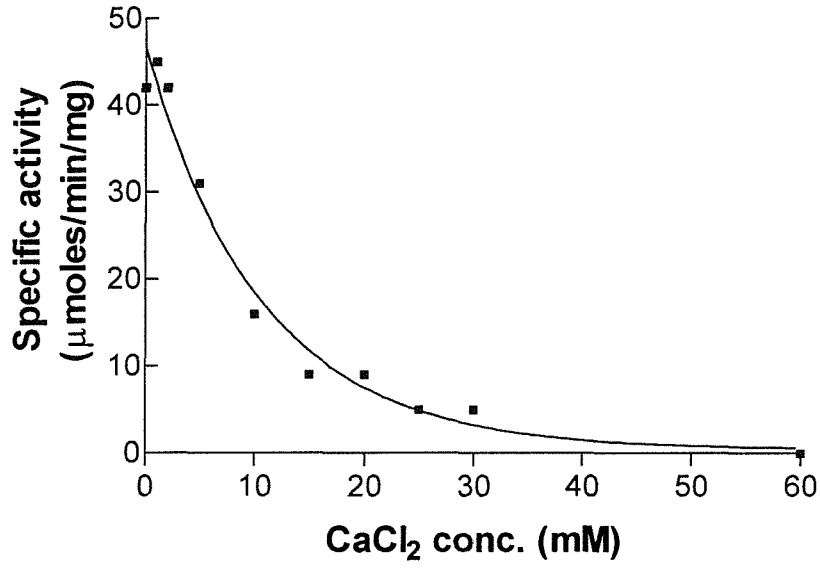

Figure 3.11 Activity of WT-GDH after incubation with Ca^{2+}

WT-GDH purified in Pipes buffer was incubated at 25°C for 20 minutes with 25μM PQQ, 50mM Pipes buffer (pH 6,5) and various concentrations of Ca^{2+} (1-60mM).

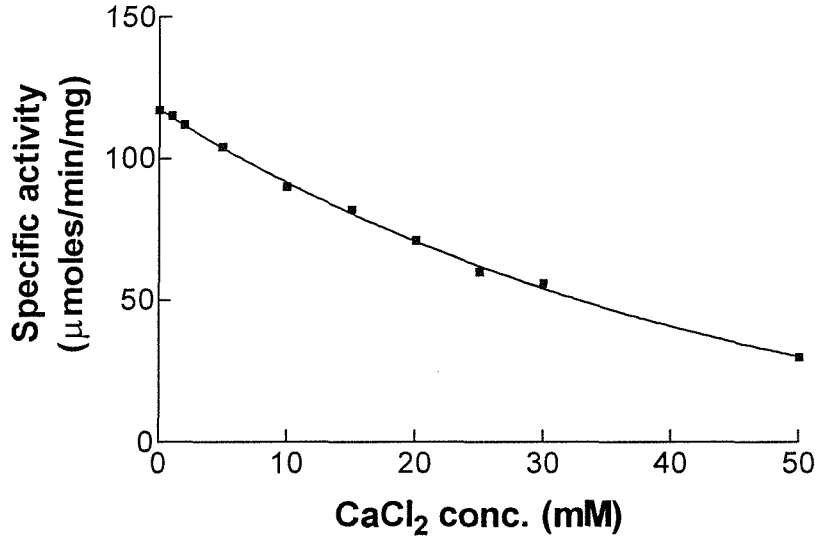

Figure 3.12 Inhibition of Mg^{2+} reconstituted GDH by Ca^{2+}

WT-GDH purified in Pipes buffer was reconstituted under standard conditions with 5mM Mg^{2+} and 25μM PQQ, and then incubated with various concentrations (1-50mM) of Ca^{2+} for a further 20 minutes at 25°C.

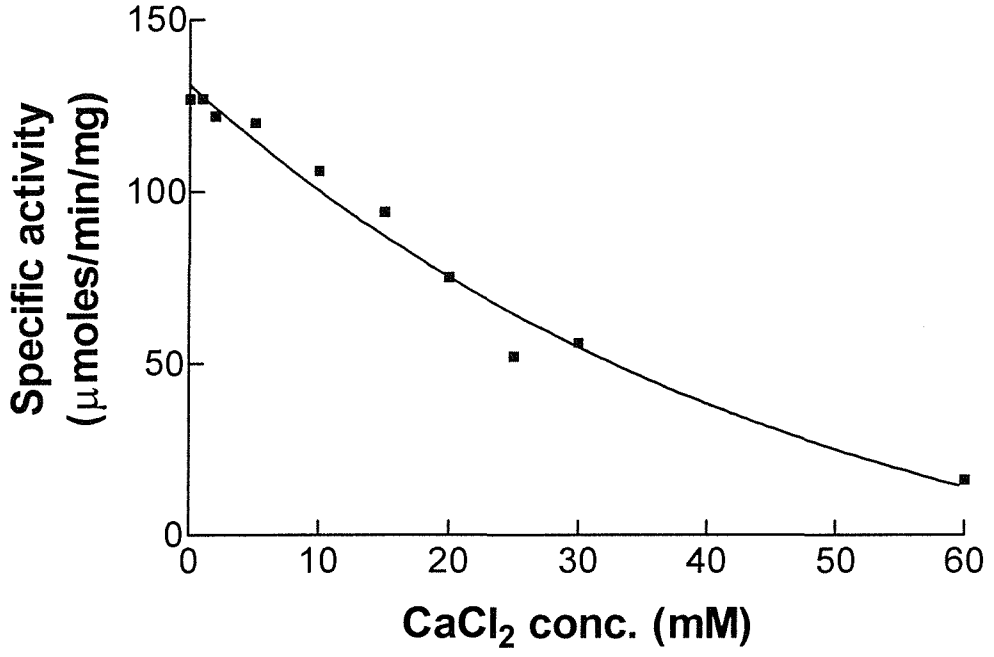

Figure 3.13 Reconstitution of GDH previously incubated with Ca^{2+}

WT-GDH purified in Pipes buffer was incubated with 25μM PQQ, 50mM Pipes buffer pH 6.5 and various concentrations of Ca^{2+} (1-60mM) for 20 minutes at 25°C. Then 5mM Mg^{2+} was added to the enzyme and incubated at 25°C for a further 20 minutes before measuring activity.

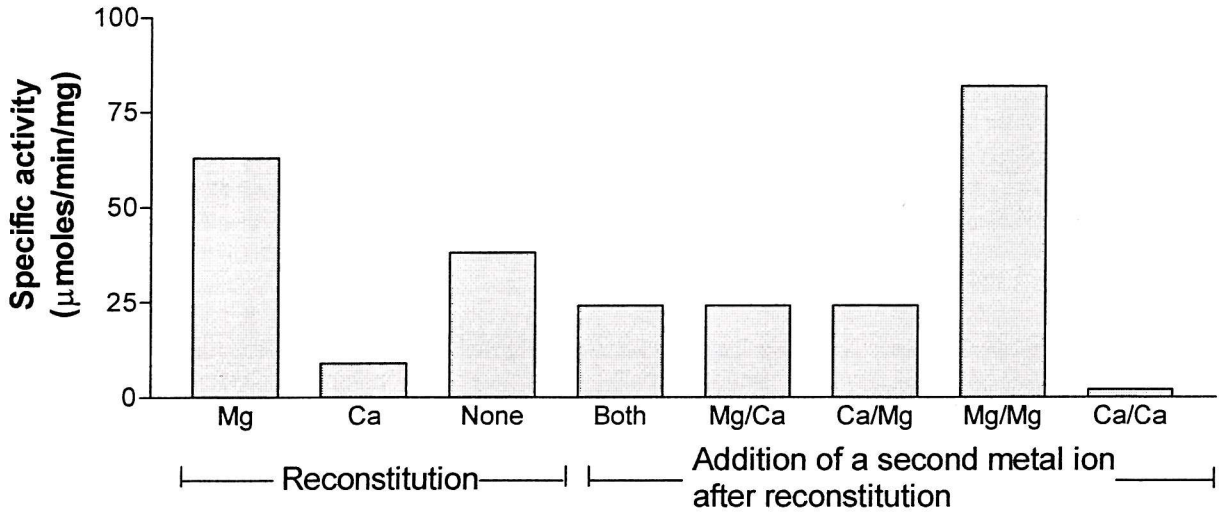

Figure 3.14 Competition between Mg^{2+} and Ca^{2+} during reconstitution of WT-GDH

WT-GDH purified in Pipes buffer was reconstituted under standard conditions with 25μM PQQ plus 1mM Mg^{2+} or 20mM Ca^{2+}. After reconstitution, Mg^{2+} or Ca^{2+} were added and activity measured after a further 20 minutes incubation. In the chart above Mg^{2+}/Ca^{2+} indicates that Mg^{2+} was used during inital reconstitution and Ca^{2+} was added subsequently.

present, it did not matter in which order they were added; the activity was identical. A high concentration of Ca^{2+} was required to significantly inhibit the enzyme indicating that GDH may have a higher affinity for Mg^{2+} than Ca^{2+}.

3.4 The effect of a variety of metals ions on the reconstitution of WT-GDH

GDH purified in Pipes disodium-salt buffer was incubated with PQQ plus various metal ions. Cu^{2+}, Fe^{2+}, Ni^{2+} and Mn^{2+} inhibited reconstitution of GDH that occurred because of the "residual" Mg^{2+} ions and the addition of Mg^{2+} did not restore activity indicating that these irreversibly inactivated the enzyme. Sr^{2+} and Ba^{2+} had a similar effect but subsequent addition of Mg^{2+} produced active GDH (Figure 3.15). This suggested that (like Ca^{2+}) Sr^{2+} and Ba^{2+} may compete for the same binding site (at the active site) as Mg^{2+} but were unable to reconstitute active GDH. However, it was not possible to distinguish whether these larger ions are incorporated with PQQ into the active site to give inactive enzyme, or if they bind to a secondary site to inhibit the protein. These larger metals may prevent PQQ incorporation.

3.5 Determination of the metal content of WT-GDH

Although GDH purified in potassium phosphate buffer was inactive in the absence of added Mg^{2+}, GDH purified in disodium salt pipes buffer was about 40-50% active, suggesting that a metal ion may have been present at the active site. Therefore, the concentration of Mg^{2+} and Ca^{2+} in purified GDH was determined by atomic absorption spectroscopy. Table 3.2 shows that GDH prepared in potassium phosphate buffer had 9.1 molecules of Ca^{2+} per molecule of enzyme and GDH prepared in Pipes buffer had 20 molecules of Ca^{2+} per molecule of enzyme. The number of molecules of Mg^{2+} per molecule of enzyme ranged from 0.38 to 0.48 and there was no significant difference between GDH purified in pipes or potassium phosphate buffer. This result was surprising because they had similar amounts of Mg^{2+} yet GDH purified in potassium phosphate buffer was not active after reconstitution with PQQ (in the absence of added Mg^{2+}). It is difficult to predict if one of these metals is bound to the active site because a 1:1 ratio between metal and enzyme would have been favourable. The high concentration of Ca^{2+} was not caused by buffer contamination, so it must have remained bound to the enzyme during the purification process. The possibility that Ca^{2+} is already bound to the active site and that the Mg^{2+} required for reconstitution is not incorporated into the active site cannot be ruled out.

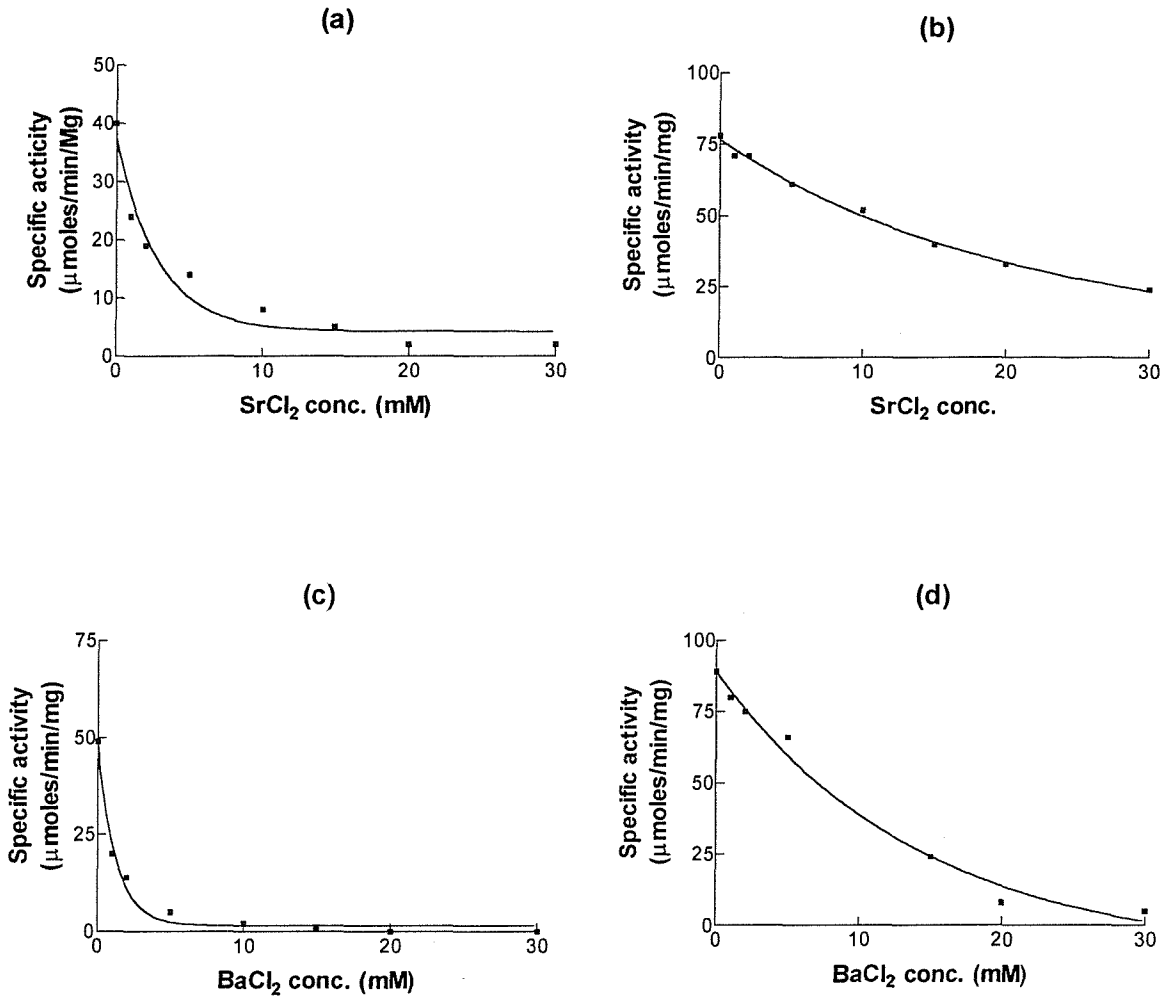

Figure 3.15 The effect of Sr^{2+} and Ba^{2+} on reconstitution of WT-GDH

a) WT-GDH incubated for 20 minutes at 25°C with various concentrations of Sr^{2+}

b) WT-GDH reconstituted with 5mM Mg^{2+} after incubation with various concentrations of Sr^{2+}

c) WT-GDH incubated for 20 minutes at 25°C with various concentrations of Ba^{2+}

d) WT-GDH reconstituted with 5mM Mg^{2+} after incubation with various concentrations of Ba^{2+}

Table 3.2 Determination of the metal ion content of WT-GDH

The Ca^{2+} and Mg^{2+} content of WT- GDH purified with potassium phosphate buffer or Pipes buffer was measured by using a Perkin-Elmer 2380 atomic absorption spectrophotometer. Mg^{2+} and Ca^{2+} content were measured at 285nm and 422nm respectively. Ca^{2+} standards ranged from 0-200μM and Mg^{2+} 0-10μM.

Sample	Protein (μM)	Ca^{2+} (μM)	Mg^{2+} (μM)	Ca^{2+} : GDH ratio	Mg^{2+} : GDH ratio
Pipes GDH	6.4	135	3	20 : 1	0.4 : 1
Phosphate GDH (1)	9.2	92	4.5	9.1 : 1	0.48 : 1
Phosphate GDH (2)	11.7	117	4.5	9.1 : 1	0.38 : 1
Phosphate buffer	N/A	7.5	0.3	N/A	N/A
Phosphate buffer (2)	N/A	8	<2	N/A	N/A
Pipes buffer	N/A	10	<2	N/A	N/A

3.6 Investigation by fluorescence of the role of Mg^{2+} in the reconstitution of WT-GDH

The role of Mg^{2+} and Ca^{2+} in the reconstitution of GDH was investigated using fluorescence spectroscopy. Fluorescence of PQQ can be measured by monitoring the emission at 469nM and the excitation at 365nm.

3.6.1 Fluorescence spectra of PQQ in the presence of apo and holoGDH

The fluorescence emission spectra were measured for PQQ, apoGDH plus PQQ, holoGDH, apoGDH, and GDH plus Mg^{2+} (Figure 3.16). PQQ alone had the highest fluorescence. The addition of GDH to PQQ quenched the fluorescence slightly but not as much as the addition of Mg^{2+} plus GDH, suggesting that Mg^{2+} may have a role in PQQ binding. ApoGDH was not fluorescent because it did not contain PQQ. Ca^{2+} plus GDH had the same effect on PQQ fluorescence as Mg^{2+} and GDH. This suggests that Mg^{2+} and Ca^{2+} supports PQQ insertion into the active site. Figures 3.17 and 3.18 also show that the quenching of PQQ fluorescence by GDH is time dependent and not instant. The addition of Mg^{2+} to apoGDH plus PQQ caused a further decrease in fluorescence but its lowest intensity was observed after 10 minutes. However, addition of Ca^{2+} produced the lowest fluorescence intensity after 5 minutes indicating that PQQ binding is more rapid with Ca^{2+} than Mg^{2+}. Ca^{2+} may bind better to PQQ than Mg^{2+} but GDH containing Ca^{2+} is inactive. The excitation and emission spectra of PQQ are shown in Figure 3.19AP. Dewanti and Duine (1998) reported that the fluorescence emission spectrum of holoGDH (from *A. calcoaceticus*) was similar to the spectrum of PQQ itself but the intensity was 20% less; this suggested that PQQ binding to GDH quenches the fluorescence.

3.6.2 The fluorescence of apo and holoGDH

HoloGDH and apoGDH were excited at 280nm and the emission spectra measured (57nM GDH, 124nM PQQ and 25μM Mg^{2+}). Figure 3.20 shows that the binding of PQQ to GDH quenched its fluorescence; this is probably caused by PQQ quenching the fluorescence of a tyrosine residue. However, no tyrosine residue is present in the active site model.

3.6.3 The use of fluorescence to measure rates of binding of PQQ to apoGDH

The binding of PQQ to GDH caused a decrease in the PQQ fluorescence with time (excited at 365nm and emission measured at 490nm). The initial rate in the absence of Mg^{2+} was 8.8 fluorescence intensity units/min and 17 fluorescence intensity units/min in the presence of Mg^{2+}. Doubling the concentration of Mg^{2+} or PQQ had no affect on the rate. When the

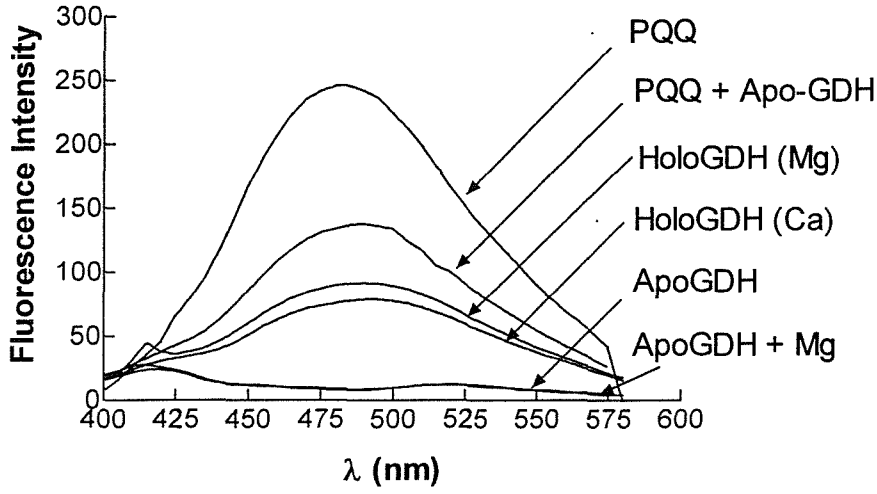

Figure 3.16 Fluorescence spectra of apo and holoGDH

HoloGDH was prepared by reconstituting Pipes purified WT-GDH with 5mM metal ions and 25μM PQQ. The emission spectra (excited at 365nm) of apo and holoGDH was measured. The assay consisted of 10mM Pipes buffer, 2.5μM GDH, 1mM Mg^{2+} or Ca^{2+} and 5μM PQQ. Ca^{2+} or Mg^{2+} had no effect on the fluorescence spectra of PQQ.

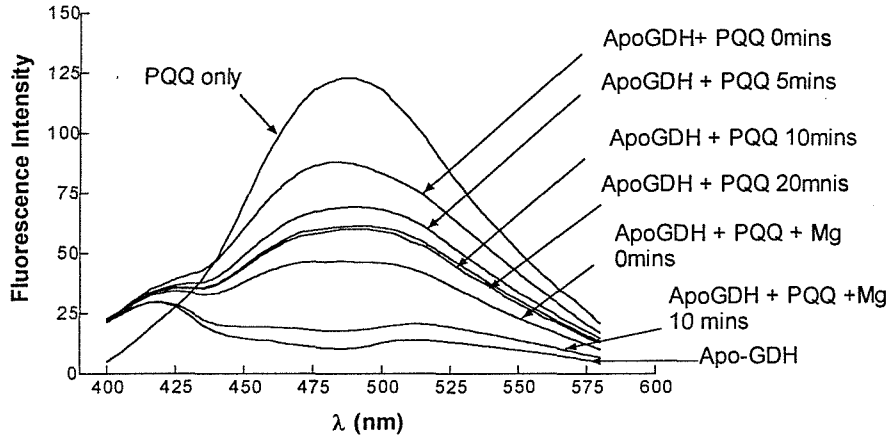

Figure 3.17 Fluorescence spectra of PQQ with Mg^{2+} and WT-GDH

The effect of WT- GDH and Mg^{2+} on the fluorescence of PQQ was determined by measuring the emission spectra of PQQ (excitation 365nm). 2.5μM WT-GDH was added to 5μM PQQ and the emission spectra measured at 0, 5, 10 and 20 minutes. Then 1mM Mg^{2+} was added to the mixture and the emission spectra measured at 0 and 10 minutes. All measurements taken at 25°C.

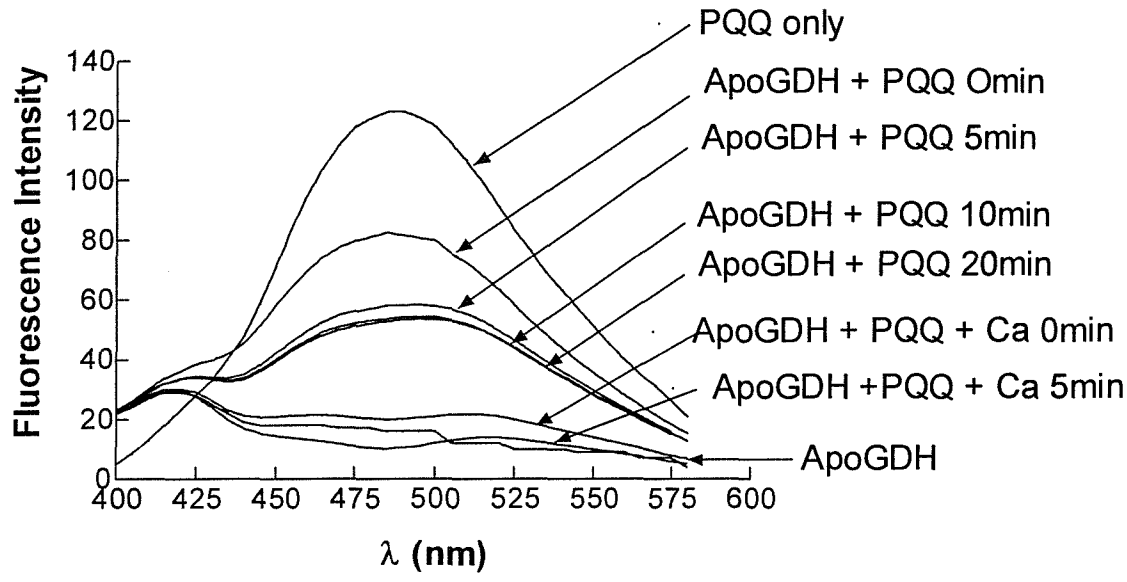

Figure 3.18 Fluorescence spectra of PQQ with Ca^{2+} and WT-GDH

The effect of WT- GDH and Ca^{2+} on the fluorescence of PQQ was determined by measuring the emission spectra of PQQ (excitation 365nm). 2.5μM WT-GDH was added to 5μM PQQ and the emission spectra measured at 0, 5, 10 and 20 minutes. Then 1mM Ca^{2+} was added to the mixture and the emission spectra measured at 0 and 5 minutes. All measurements taken at 25°C.

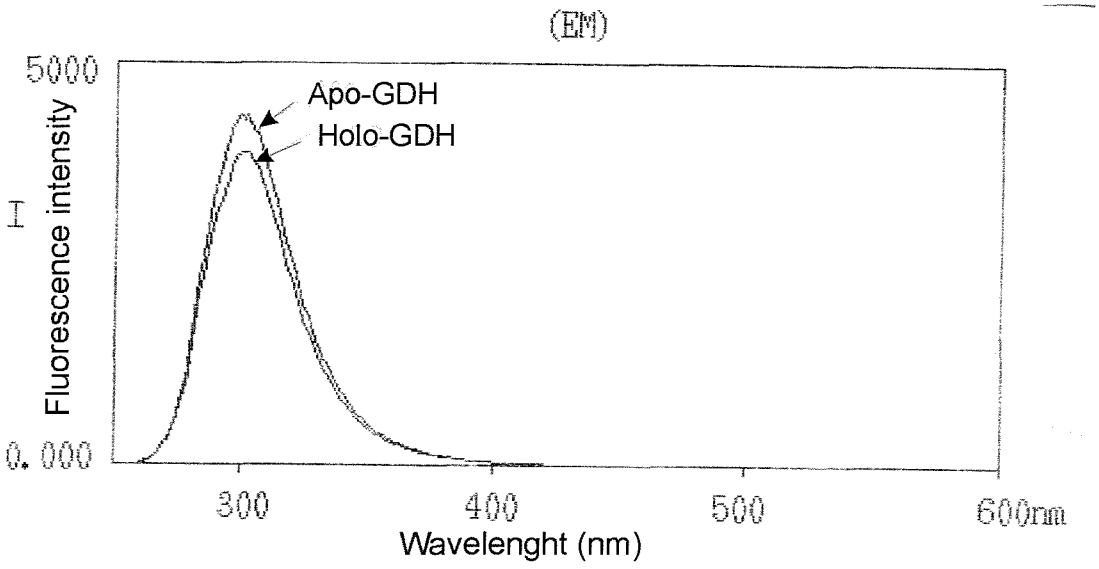

Figure 3.20 Fluorescence of apo and holoGDH (excited at 280nm)

HoloGDH had a lower fluorescence because PQQ is bound to the active site. This may quench the fluorescence of a tyrosine residue but in the model of GDH no tyrosine is present at the active site. The assay contained 10mM Pipes buffer, 57nM GDH, 124nm PQQ and 25μM Mg^{2+}.

concentration of PQQ was halved to 1μM PQQ, the initial rate was 5.2 and 10.5 fluorescence intensity units/min in the absence and presence of Mg^{2+} respectively.

Table 3.3 shows the effect of pH on PQQ binding. An increase in pH from 6-8 caused the initial rate to decrease from 27 fluorescence intensity/min to 3 fluorescence intensity/min. This is presumably due to an increase in K_d for PQQ binding as shown in Section 3.1.2. However, the large increase in initial rate between pH 5.5 and 6.0 cannot be explained.

In the presence of 10mM EDTA the fluorescence remained constant after adding GDH and Mg^{2+} to PQQ, suggesting that EDTA stopped reconstitution. Once EDTA was removed by gel filtration, the addition of PQQ and Mg^{2+} to GDH permitted reconstitution and the fluorescence intensity decreased at a rate of 8 fluorescence intensity units/ min. EDTA prevented PQQ from binding to GDH.

The decrease in the fluorescence of PQQ due to binding of GDH could not be measured in the presence of Ca^{2+} because minimal fluorescence was produced instantly (Figure 3.18).

This work described above suggests that both Mg^{2+} and Ca^{2+} aid PQQ binding to GDH. Ca^{2+} seems to be better that Mg^{2+} because minimal fluorescence was produced instantly. However, if Ca^{2+} does assist PQQ binding then it would be expected to reconstitute GDH (which it can't). Ca^{2+} may bind to GDH but cannot fulfil Mg^{2+} role in the enzyme's mechanism. Analysis of the absorption spectrum of PQQ in the presence of Mg^{2+} and Ca^{2+} showed that these metals form complexes with the prosthetic group (Geiger and Gorisch, 1989; Itoh *et al.*, 1989). However, Ca^{2+} or Mg^{2+} had no effect on PQQ fluorescence in solution, indicating GDH quenches the prosthetic groups fluorescence.

In summary, this has shown that fluorescence cannot be used to determine which metal ion binds to the active site of GDH.

3.7 Production in Pipes buffer of WT-GDH that required Mg^{2+} for activity

GDH purified in Pipes buffer was 41% or 8% active after reconstitution in the absence of metal ions, depending on the type of Pipes (Table 3.1). Metal ions present in the purified enzyme may have caused this activity and earlier work has shown that the samples contained Mg^{2+} and Ca^{2+} (Section 3.5). After reconstitution in the absence of added metal ions GDH purified in Pipes had 20% of the activity of GDH purified in disodium salt Pipes buffer. Pipes buffer (pH adjusted with NaOH) that gave the lowest activity was used in the following experiments aimed at producing enzyme that had no activity in the absence of added metal ion.

Gel filtration had no effect on this GDH (Table 3.4). Prior treatment with 10mM EDTA did not remove all the metal ions because the enzyme was 6% active compared with 10% before

Table 3.3 The effect of pH on PQQ fluorescence quenching by GDH

The rate of binding of PQQ to GDH between the pH range 5.5 – 8.0 was investigated by measuring the decrease in fluorescence (excitation 365nm: emission 490nm). The assay mixture contained 2μM WT-GDH, 2μM PQQ, 500μM Mg^{2+} and 10mM potassium phosphate buffer.

pH	Initial rate (fluorescence intensity /min)
5.5	7
6.0	27
6.5	16
7.0	17
7.5	14.5
8.0	3

Table 3.4 Gel filtration of WT-GDH purified in Pipes buffer

Gel filtration was used to remove any metal ions from apo WT-GDH to determine if a sample could be produced that required Mg^{2+} for reconstitution. WT-GDH was reconstituted before and after gel filtration with 5mM Mg^{2+}, 25μM PQQ or 5mM Mg^{2+} plus 25μM PQQ. Activity was measured by the standard dye-linked assay.

Sample	Total activity (μmoles/min)	Specific activity (μmoles/min/mg)
Reconstituted GDH before gel filtration	1568	75
GDH before gel filtration + Mg^{2+}	Zero	Zero
GDH before gel filtration + PQQ	127	6
GDH after gel filtration	Zero	Zero
GDH after gel filtration + Mg^{2+}	Zero	Zero
GDH after gel filtration + PQQ	114	7
Reconstituted GDH after gel filtration	1144	77

Table 3.5 – Treatment of WT-GDH purified in Pipes buffer with 10mM EDTA

WT-GDH was incubated with 10mM EDTA for 15 minutes. Gel filtration was used to remove EDTA. WT-GDH was reconstituted before and after gel filtration with 5mM Mg^{2+}, 25μM PQQ or 5mM Mg^{2+} plus 25μM PQQ. Activity was measured by the standard dye-linked assay.

Sample	Total activity (μmoles/min)	Specific activity (μmoles/min/mg)
Reconstituted GDH before gel filtration	1689	84
GDH before gel filtration + Mg^{2+}	Zero	Zero
GDH before gel filtration + PQQ	169	8
EDTA treated GDH after gel filtration	Zero	Zero
EDTA treated GDH after gel filtration + PQQ	55	5
EDTA treated GDH after gel filtration + Mg^{2+}	Zero	Zero
Reconstituted EDTA treated GDH after gel filtration	1034	84

treatment (Table 3.5). However, GDH treated with 100mM EDTA was appropriate for future studies because it required Mg^{2+} for activity (Figure 3.21); EGTA was less effective than EDTA. Both these chelating agents reduced the concentration of Ca^{2+} and Mg^{2+} to 0.19μmoles and 0.09μmoles per μmole of GDH respectively (Table 3.6).

3.8 The inhibition of reconstitution by Ca^{2+}, Sr^{2+} and Ba^{2+}

After the preliminary work on GDH reconstitution was done (Section 3.1-3.6) it was shown that if the Pipes buffer used during purification was based on Pipes that required the addition of NaOH to pH the buffer, then the activity produced by reconstitution in the absence of Mg^{2+} was 80% lower than when the disodium salt was used. This indicated that Na^{2+} could reconstitute apoGDH. However, incubation of Na^{2+} with apoGDH plus PQQ did not form active GDH.

GDH (purified in Pipes buffer) previously treated with 100mM EDTA was reconstituted with PQQ and various metal ions. Figure 3.22 shows that the K_d for Mg^{2+} was 1.5mM with an A_{max} of 141μmoles/min/mg, as was previously measured with GDH purified in potassium phosphate buffer (Section 3.2). Fe^{2+}, Co^{2+}, Mn^{2+} and Ni^{2+} inactivated the enzyme. Figures 3.23 – 3.25 show the inhibitory effect on reconstitution of pre-incubation with Ca^{2+}, Sr^{2+} and Ba^{2+}. Ca^{2+} had no significant affect on A_{max} but increased the k_d for Mg^{2+} suggesting that Ca^{2+} was a competitive inhibitor (Table 3.7). That is, Ca^{2+} instead of Mg^{2+} can bind at the active site but it cannot bind to GDH in which Mg^{2+} is already bound (Figure 3.26). By contrast, Sr^{2+} or Ba^{2+} caused the A_{max} to decrease and the K_d for Mg^{2+} to increase (Table 3.7), indicating that mixed (non-competitive) inhibition had occurred. That is, Sr^{2+} and Ba^{2+} can bind to the active site (the Mg^{2+} binding site) and to a second inhibitory site (Figure 3.26).

Lineweaver-Burk plots confirmed these types of inhibition caused by Ca^{2+}, Ba^{2+} and Sr^{2+} (Figures 3.27- 3.29). K_i and K_{ii} values were calculated from the data on the Lineweaver-Burk plots by plotting the slope against inhibitor concentration and the Y-intercept against inhibitor concentration respectively. Table 3.8 shows that Ba^{2+} was the strongest inhibitor because its K_i value was only 0.45mM. The K_i value for Ca^{2+} and Sr^{2+} were similar (3.41mM and 3.47mM respectively).

Reconstituting GDH with concentrations higher than 20mM Mg^{2+} indicated that there is a second metal ion binding site (Figure 3.30). At low concentrations Mg^{2+} binds to the active site to reconstitute the apoenzyme but at higher concentrations it binds to the second inhibitory site that can also bind to Sr^{2+} and Ba^{2+}.

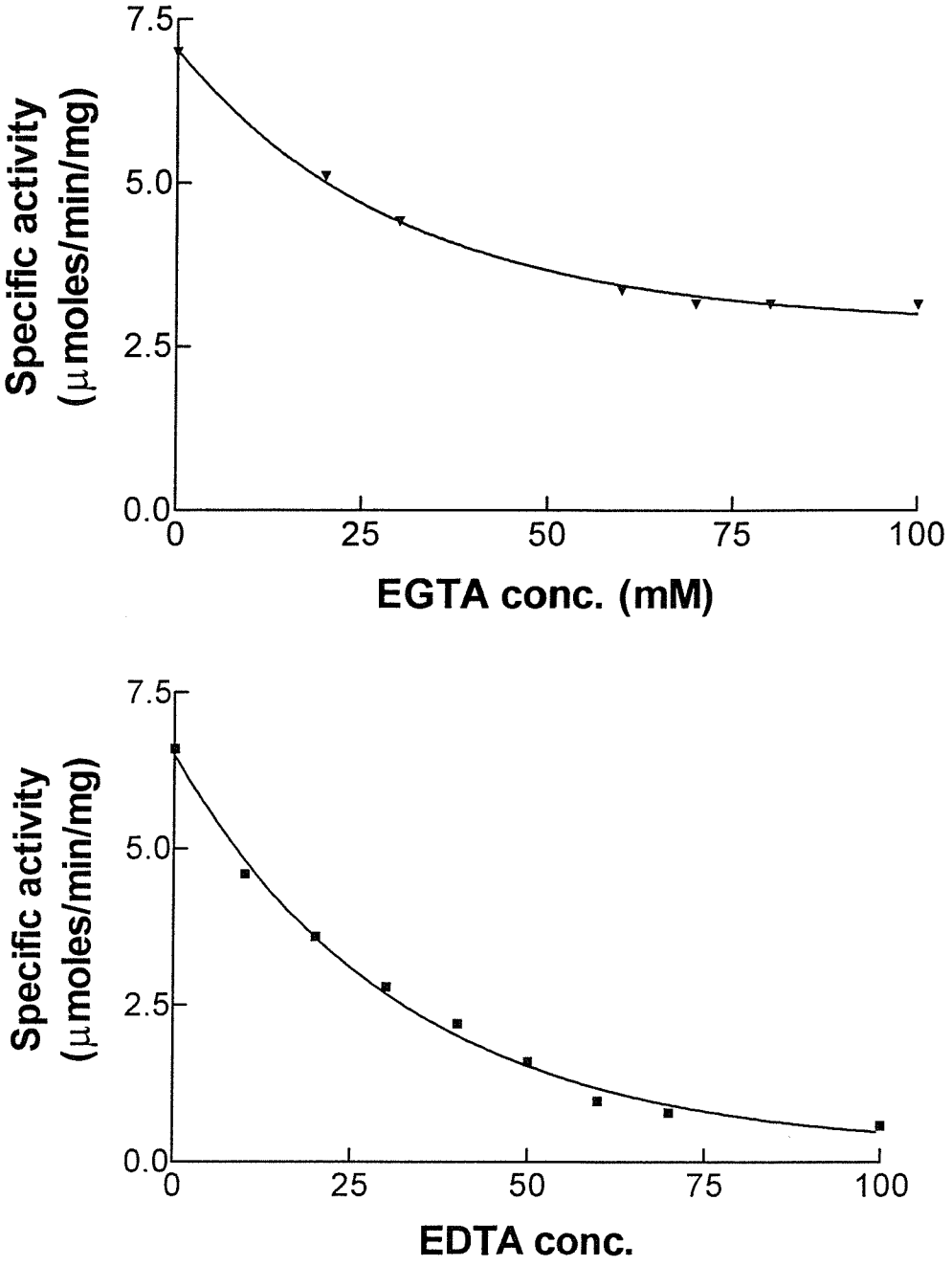

Figure 3.21 The effect of EDTA and EGTA on apoGDH prior to reconstitution

WT-GDH was incubated with various concentrations of EGTA or EDTA for 15minutes at 25°C. Then the chelating agent was removed by gel filtration and the sample incubated for 20 minutes with 25μM PQQ and 50mM Pipes buffer. Activity was then measured by the standard dye-linked assay.

Table 3.6 Determination of the metal ion content of WT-GDH treated with EDTA and EGTA

Ca^{2+} and Mg^{2+} content of WT- GDH purified with Pipes buffer (NaOH used to make buffer) was measured using a Perkin-Elmer 2380 atomic absorption spectrophotometer. Mg^{2+} and Ca^{2+} content were measured at 285nm and 422nm respectively. Ca^{2+} standards ranged from 0-200μM and Mg^{2+} 0-10μM. EDTA and EGTA samples were prepared by incubating WT-GDH for 15 minutes with 100mM chelating agent which was later removed by gel filtration.

Sample	Protein (μM)	Mg^{2+} (μM)	Ca^{2+} con (μM)	Mg^{2+}/GDH ratio	Ca^{2+}/GDH ratio
Pipes GDH	19.4	16	74	0.82 : 1	3.5 : 1
EDTA-treated GDH	5.4	0.5	8	0.09 : 1	0.19 : 1
EGTA-treated GDH	5.4	0.5	8	0.09 : 1	0.19 : 1
Pipes buffer	N/A	<0.2	7	N/A	N/A

Table 3.7 A_{max} and K_d values for Mg^{2+} during reconstitution in the presence of Ca^{2+}, Sr^{2+} and Ba^{2+}

EDTA-treated GDH was incubated for 20 minutes with 25μM PQQ and various concentrations of Ca^{2+}, Sr^{2+} or Ba^{2+}. Then Mg^{2+} (1-60mM) was added and activity measured after incubation at 25°C for a further 20 minutes. The A_{max} and K_d values shown are for Mg^{2+} binding. These values were calculated using the data from Figures 3.23-3.25.

	Ca^{2+}		Ba^{2+}		Sr^{2+}	
Inhibitor conc.	A_{max}	K_d	A_{max}	K_d	A_{max}	K_d
0mM	104.6	1.6	104.6	1.6	104.6	1.6
2.5mM	-	-	90.1	10.9	100.6	3.9
5mM	94.2	3.0	88.8	20.0	89.3	5.7
10mM	94.8	6.8	55.1	30.9	62.6	6.4
20mM	99.2	12.5	14.5	36.6	57.3	12.0

A_{max} = μmoles/min/mg
K_d = mM

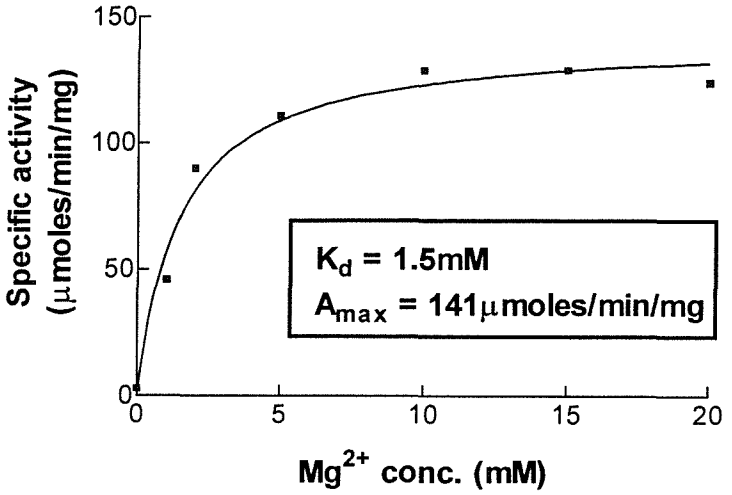

Figure 3.22 The effect of Mg^{2+} on reconstitution of EDTA-treated GDH

100mM EDTA-treated GDH (purified in Pipes buffer) was reconstituted under standard conditions with 25μM PQQ and Mg^{2+}. The line of best fit was calculated by the equation $A=A_{max}[Mg^{2+}]/(K_d + [Mg^{2+}])$ where A is enzyme activity.

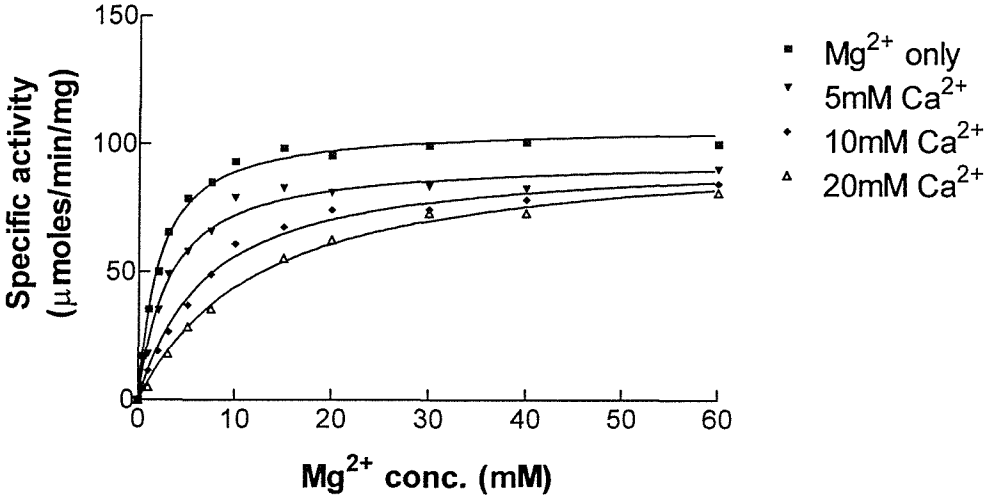

Figure 3.23 The reconstitution of GDH previously incubated with Ca^{2+}

WT-GDH was incubated for 20 minutes at 25°C with 25μM PQQ and various concentrations of Ca^{2+}. Then Mg^{2+} (1-60mM) was added and activity measured after incubation at 25°C for a further 20 minutes. The lines of best fit were calculated by the equation $A=A_{max}[Mg^{2+}]/(K_d + [Mg^{2+}])$ where A is enzyme activity.

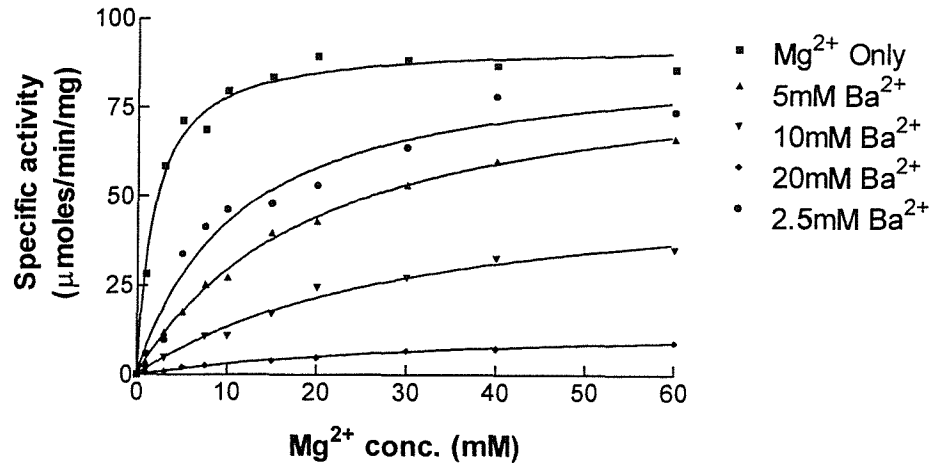

Figure 3.24 The reconstitution of GDH previously incubated with Ba^{2+}

WT-GDH was incubated at 25°C for 20 minutes with 25μM PQQ and various concentrations of Ba^{2+}. Then Mg^{2+} (1-60mM) was added and activity measured after incubation at 25°C for a further 20 minutes. The lines of best fit were calculated by the equation $A=A_{max}[Mg^{2+}]/(K_d + [Mg^{2+}])$ where A is enzyme activity.

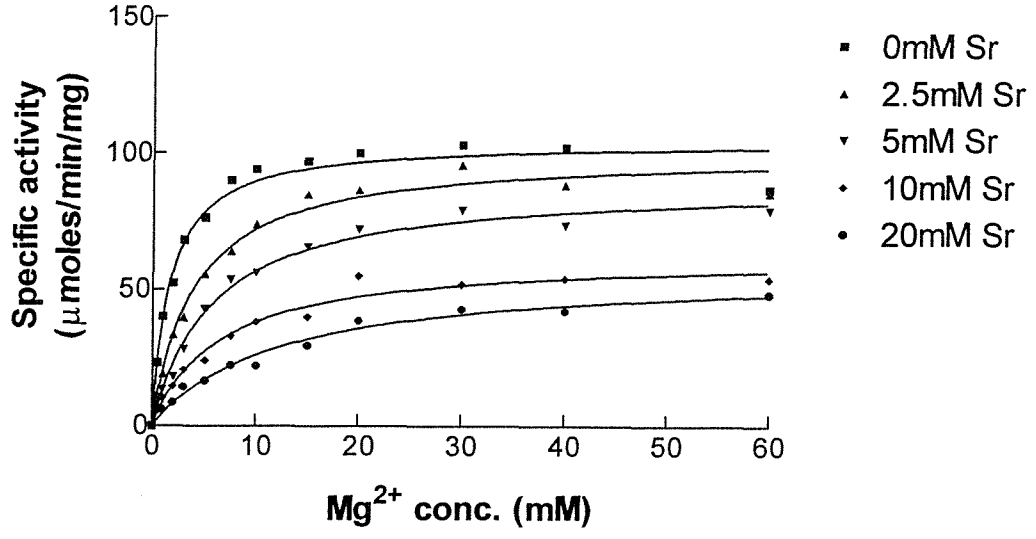

Figure 3.25 The reconstitution of GDH previously incubated with Sr^{2+}

WT-GDH was incubated at 25°C for 20 minutes with 25μM PQQ and various concentrations of Sr^{2+}. Then Mg^{2+} (1-60mM) was added and activity measured after incubation at 25°C for a further 20 minutes. The lines of best fit were calculated by the equation $A=A_{max}[Mg^{2+}]/(K_d + [Mg^{2+}])$ where A is enzyme activity.

Calcium is a competitive inhibitor

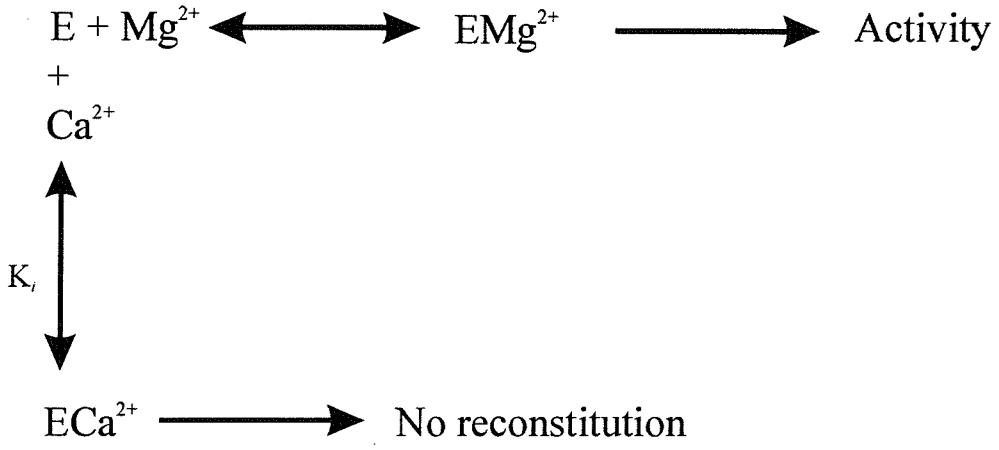

Barium and strontium are mixed (non-competitive) inhibitors

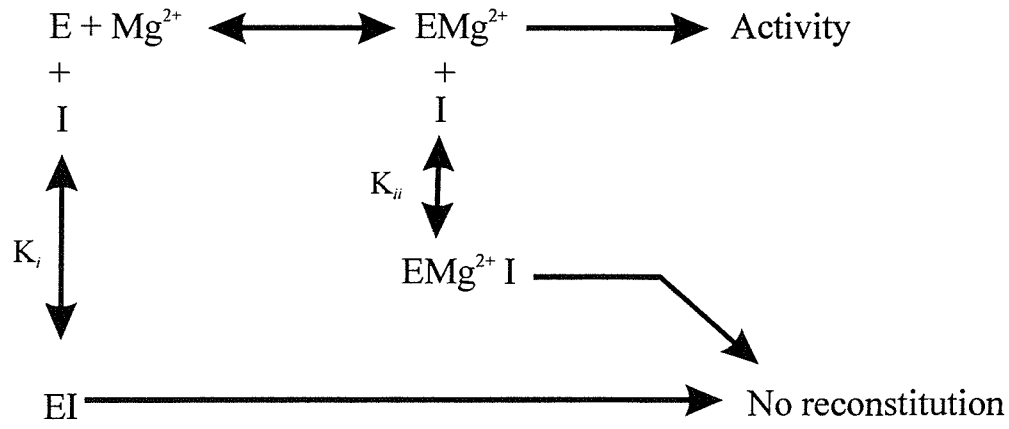

Figure 3.26 Inhibition of reconstitution of GDH by Ca^{2+}, Sr^{2+} and Ba^{2+}

Ca^{2+} binds to GDH when Mg^{2+} is not bound, but Ba^{2+} and Sr^{2+} (represented by I) are able to bind when Mg^{2+} is already bound. Binding of inhibitor to the active site is measured as K_i and binding to a secondary site is measured as K_{ii}.

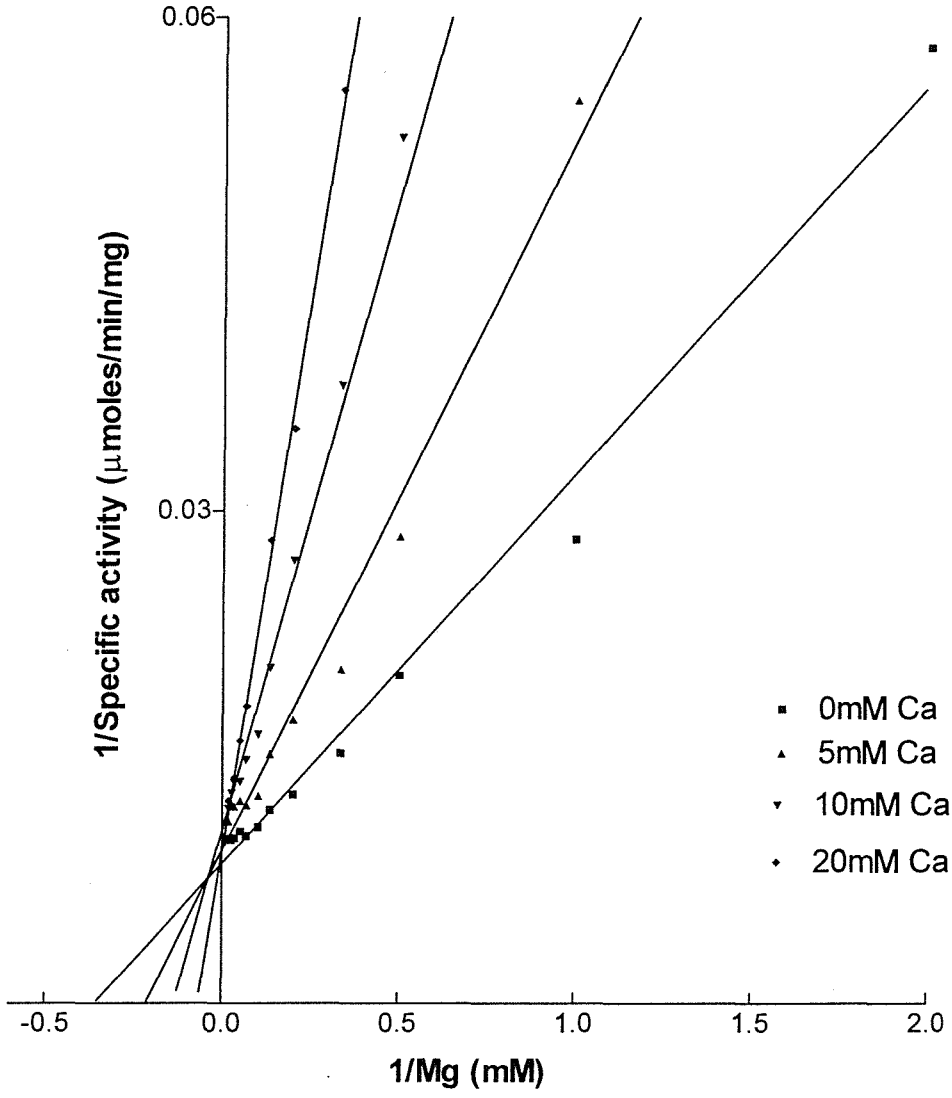

Figure 3.27 The effect of Mg^{2+} on reconstitution of GDH previously incubated with Ca^{2+} and PQQ

A Lineweaver-Burk plot based on the data from Figure 3.23. 1/V has been plotted against 1/S. S represents Mg^{2+} concentration and V represents specific activity of WT-GDH achieved after reconstitution with Mg^{2+}.

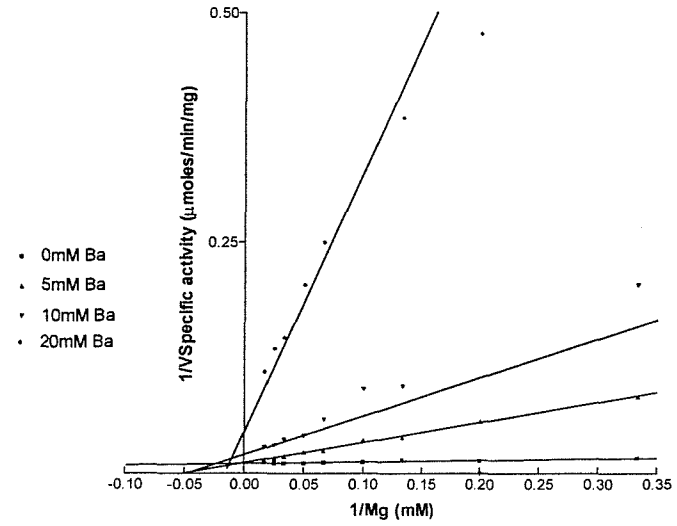

Figure 3.28 The effect of Mg^{2+} on reconstitution of GDH previously incubated with Ba^{2+} and PQQ

A Lineweaver-Burk plot based on the data from Figure 3.24. 1/V has been plotted against 1/S. S represents Mg^{2+}concentration and V represents specific activity achieved after reconstitution with Mg^{2+}.

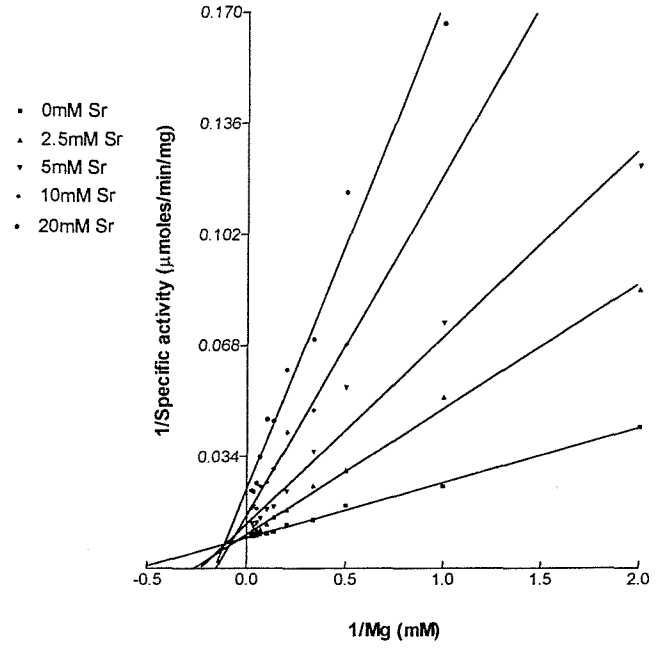

Figure 3.29 The effect of Mg^{2+} on reconstitution of GDH previously incubated with Sr^{2+} and PQQ

A Lineweaver-Burk plot based on the data from Figure 3.25. 1/V has been plotted against 1/S. S represents Mg^{2+} concentration and V represents specific activity achieved after reconstitution with Mg^{2+}.

Table 3.8 The K_i and K_{ii} values for inhibition of the reconstitution of WT-GDH by metal ions

These values were calculated from the data in Figures 3.27-3.29 (except the K_i value for Mg^{2+}). K_i value was calculated by plotting the slope of each line on the Lineweaver-Burk plot against inhibitor concentration. K_i value was determined by dividing the Y-intercept (c) by the gradient of the slope (m). K_{ii} value was calculated by plotting the Y-intercept of each line on the Lineweaver-Burk plot against inhibitor concentration. k_{ii} value was determined by dividing the intercept by the gradient of the slope. The k_I value for Mg^{2+} is 190mM and was calculated from the data in Figure 3.30.

	Ca^{2+}	Sr^{2+}	Ba^{2+}
K_i	3.41mM	3.47mM	0.45mM
K_{ii}	N/A	11.96mM	3.53mM

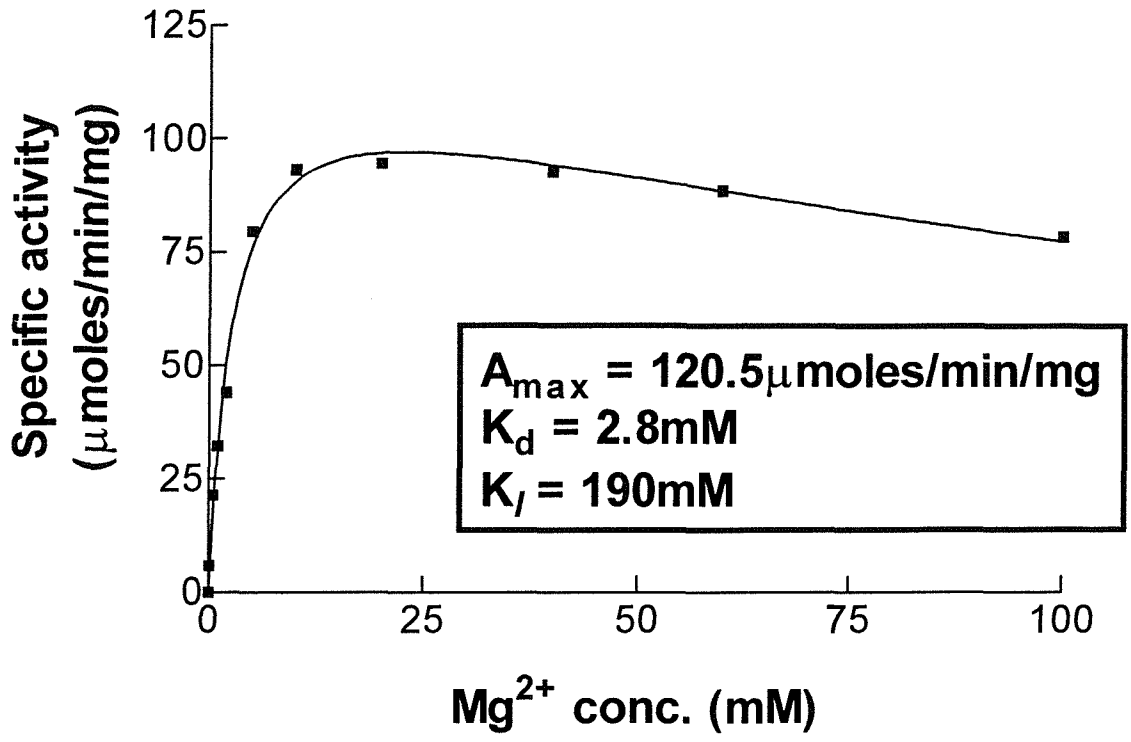

Figure 3.30 The effect of high concentrations of Mg^{2+} on reconstitution of WT-GDH

ApoGDH previously treated with 100mM EDTA was reconstituted under standard conditions with 25μM PQQ and Mg^{2+}. The line of best fit was calculated by the equation $A=A_{max}[Mg^{2+}]/k_d+[Mg^{2+}]\{1+Mg^{2+}/k_I\}$.

3.9 The thermal stability of WT-GDH

Heating reconstituted GDH at 40°C for 40 minutes did not denature the enzyme. However, apoGDH was not as stable because reconstituting apoGDH after heating at 40°C for 40 minutes gave an enzyme that was only 14% active; apoGDH was 50% denatured after 14.3 minutes (Figure 3.31a).

Incubating WT-GDH at various temperatures for 10 minutes before measuring activity confirmed that reconstituted GDH was more stable than the apo form (Figure 3.31b). Apo and holoGDH were 50% denatured at 40.8 ° and 51 °C respectively.

3.10 Activation energy for the oxidation of D-glucose

This was determined by measuring the activity of Mg^{2+} reconstituted WT-GDH between 5°C and 40°C (Figure 3.32). The activation energy was 41kJ mol^{-1}. This value is identical to previous values determined by Cozier *et al.* (1999).

3.11 Summary and discussion

This chapter has investigated the reconstitution of apoGDH with PQQ and metal ions. GDH was purified from whole cells in potassium phosphate buffer or Pipes buffer. The enzyme purified in potassium phosphate buffer (which required the addition of Mg^{2+} and PQQ for activity) could not be used to investigate the role of Ca^{2+} in the reconstitution process because it precipitated in this buffer. Pipes buffer and disodium salt Pipes buffer gave enzymes that were 8% and 41% active respectively, in the absence of added metal to the reconstitution mixture. Preliminary results showed that only Mg^{2+} could reconstitute apoGDH in the presence of PQQ whilst larger metal ions (Ca^{2+}, Sr^{2+} and Ba^{2+}) inhibited reconstitution. Ca^{2+} inhibited Mg^{2+}-reconstituted GDH suggesting that these metals compete for the same binding site.

Preparation of apoGDH purified in Pipes buffer that required added Mg^{2+} for formation of active holoGDH, involved treatment with 100mM EDTA that was subsequently removed by gel filtration. Reconstituting this apoGDH with high concentration of Mg^{2+} suggested that there is a second metal ion binding site to which Mg^{2+} binds, causing inhibition. Kinetic data obtained from the incubation of apoGDH with Ca^{2+}, Sr^{2+} or Ba^{2+} before reconstitution with Mg^{2+} showed that Ca^{2+} acted as a competitive inhibitor and, Sr^{2+} and Ba^{2+} acted as mixed inhibitors. With respect to Sr^{2+} and Ba^{2+}, these results suggest there are two metal ion binding sites; one at the active site and a second (with lower affinity for metal ions) that can inhibit the enzyme when occupied with metal ions. It might be expected that Ca^{2+} would inhibit GDH in the same manner as Sr^{2+} and Ba^{2+}. A likely possibility is that the affinity for Ca^{2+} at the second metal binding site

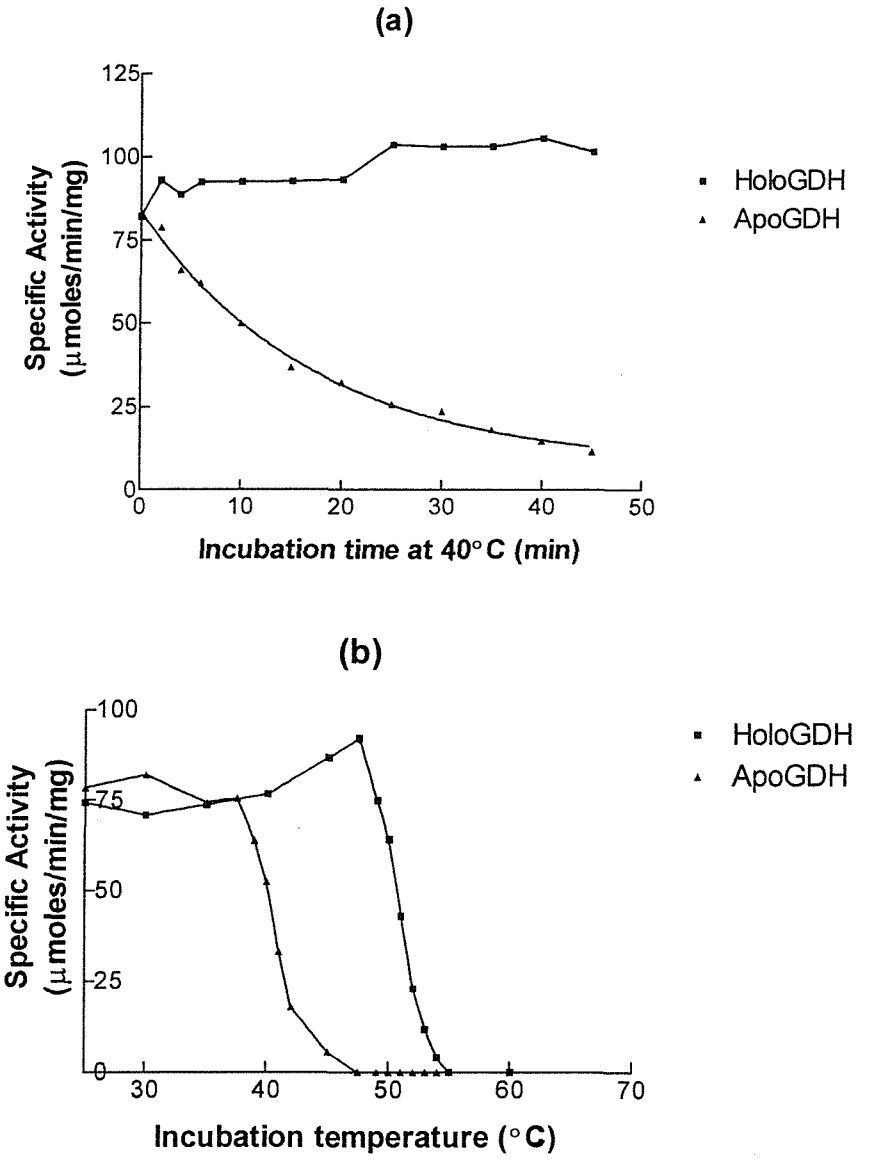

Figure 3.31 The thermal stability of WT-GDH

a) Apo and holoGDH were incubated at 40°C for various periods of time. Then apoGDH was reconstituted under standard conditions with Mg^{2+} and PQQ before activity was measured.

b) Apo and holoGDH were incubated at various temperatures for 10 minutes. Then the enzyme was placed on ice for 5 minutes. ApoGDH was reconstituted under standard conditions with Mg^{2+} and PQQ before activity was measured.

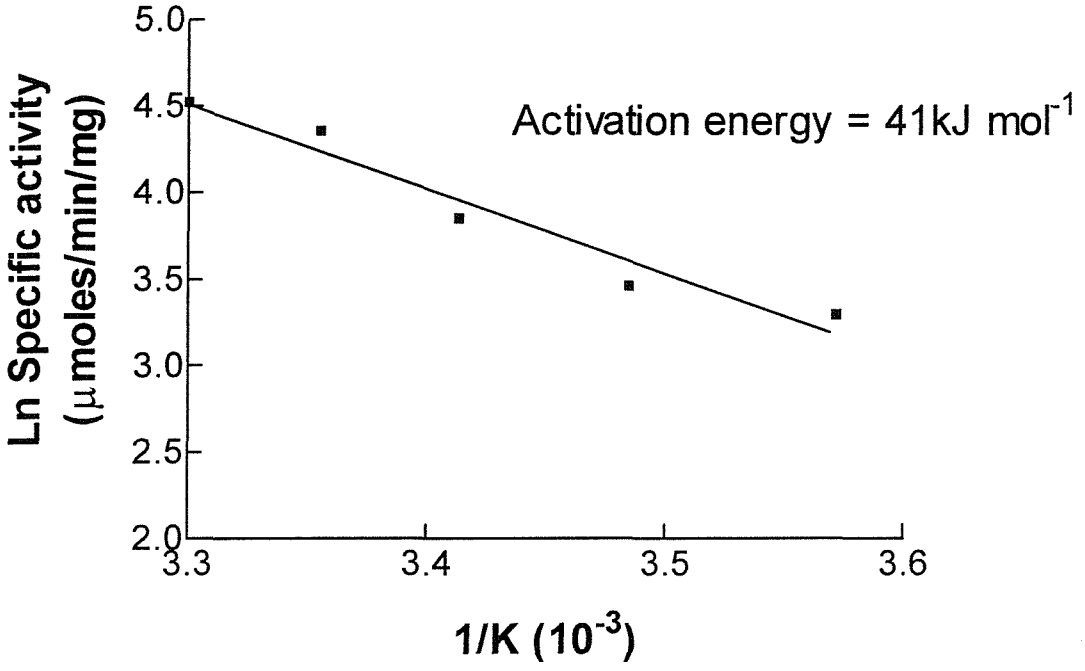

Figure 3.32 Activation energy of Mg^{2+} reconstituted GDH with D-glucose

WT-GDH was reconstituted under standard conditions with 25μM PQQ and 5mM Mg^{2+}. Then activity was measured with the standard assay (40mM D-glucose) at various temperatures (5-40°C). The formula relating activation energy (ΔG*) is $v=A.\exp(-\Delta G^*/RT)$ where A is the Arrhenius constant and R is the gas constant. The ΔG* values were calculated from the slope of the curve.

is much higher than the affinity for Sr^{2+} or Ba^{2+}, giving the illusion that Ca^{2+} acts as competitive inhibitor.

Chapter 4
Site-directed mutagenesis of the proposed metal- binding site

Introduction

MDH has two amino acid residues that bind to the Ca^{2+} ion, Glu-177 and Asn-261 (Figure 4.1a). These residues provide three bonds to the metal ion. The modelled structure of GDH, based on the alignment of the sequence of GDH to MDH shows that these residues are replaced by Asp-354 and Thr-424 (providing three bonds to Ca^{2+}) in GDH and a further bond is provided by Asn-355 (Figure 4.1b). In MDH and GDH the metal is co-ordinated to PQQ at the carbonyl group at C-5 (O-5), the pyridine nitrogen (N-6) and the carboxylate group at position 7. This co-ordination of Ca^{2+} to PQQ has also been shown in solution using ^{1}H and ^{13}C NMR (Itoh *et al.*,1998) and in the X-ray crystal structures of sGDH (Oubrie *et al.*, 1999) and EDH (Keitel *et al.*, 2000). The Ca^{2+} in MDH has hexacoordination and in GDH it has heptacoordination (Figure 4.1). Based on this model for GDH, these metal binding residues were mutated by the Stratagene Quickchange method and the effect on the proteins' characteristics investigated. Three active site mutants were made: D354N, N355D and the double mutant D354N/N355D. A fourth mutant (T424N) was kindly provided by Professor Sode (Yoshida and Sode, 1996). These mutations investigated metal ion specificity when there were six, seven or eight possible protein ligands.

4.1 Site-directed mutagenesis

Two methods were used in the attempt to make D354N, N355D and D354N/N355D mutant GDHs: the Kunkel method and the Stratagene Quickchange method. Even though the two methods are completely different, they both have the same basic principles. In site-directed mutagenesis a primer containing a mutation is annealed to a wild-type DNA template and then a complementary strand is synthesised. The template is then destroyed and mutant DNA is transformed into a host strain of bacteria so that it can be expressed. DNA sequencing is then used to confirm the mutation.

4.2 Primer design

For both methods of mutagenesis, primers had to be designed to introduce the specific mutation. Normally only one or two bases are changed so the percentage mismatch is not too great. The fewer number of bases changed, the higher chance that mutagenesis will succeed. A

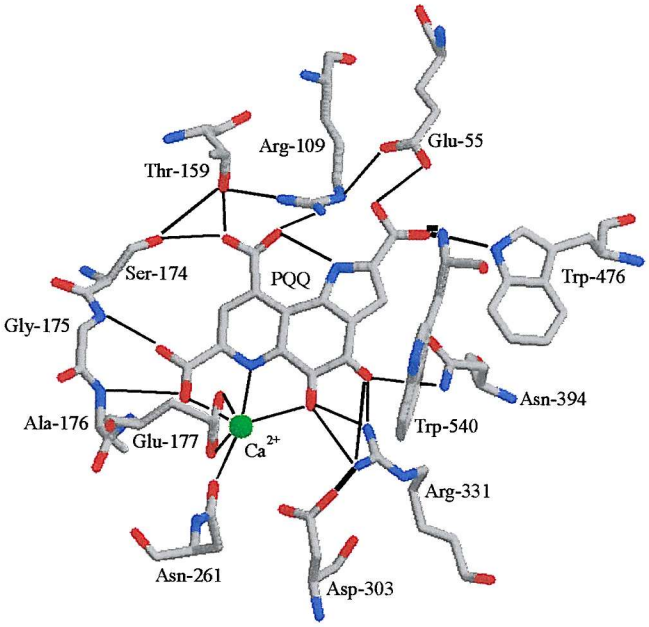

Figure 4.1a The equatorial interactions of PQQ in the active site of methanol dehydrogenase (Ghosh *et al.*, 1995)

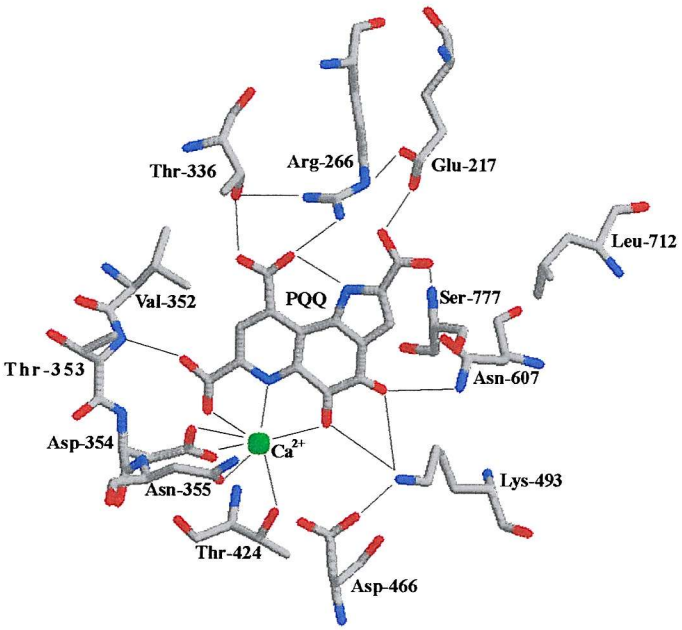

Figure 4.1b The equatorial interactions of PQQ in the active site of the model glucose dehydrogenase (Cozier and Anthony, 1995)

program called DNA * was used to make sure designed primers did not have any secondary structure that would affect binding of the primers to the DNA template. The following considerations were made for the design of the DNA primers used in the Stratagene quickchange method:

1) Both primers must contain the same mutation and anneal to the same sequence on opposite strands of the plasmid.
2) The primer should be 25-45 bases in length with a melting temperature (T_m) of 78°C or greater. The following formula was used to estimate the T_m of the primers:

$$T_m = 81.5 + 0.41(\%GC) - 675/N - \%mismatch$$

Where N is the primer length in base pairs.

3) Primers should have a minimum GC content of 40% and should terminate on one or more C or G bases.
4) The desired mutation should be located in the middle of the primer.
5) Primers do not need to be 5' phosphorylated but purified by fast polynucleotide liquid chromatography (FPLC).

Similar considerations applied in designing primers for the Kunkel method but only one primer was required and it had to be 5' phosphorylated. Primers used in this work are shown in Figures 4.2 and 4.3.

4.3 The Kunkel method

This method of site-directed mutagenesis was developed by Kunkel *et al.*(1987) and the method was previously described in Section 2.6. The DNA to be mutated was cloned into the vector M13 bacteriophage which was used because its DNA can be isolated in a single stranded form or a double stranded form. After mutagenesis the gene has to be cloned back into an appropriate plasmid.

Dr G. Cozier had previously cloned a fragment of the *gcd* gene (which codes for glucose dehydrogenase) from *E. coli* into M13 bacteriophage (Cozier *et al.*, 1999). Dr N. Goosen supplied a pBR322-based plasmid that contained a 3kb fragment from *E. coli* cloned into the *Bam*HI site: the plasmid was called pGP478. The *E. coli* fragment contained the 2.6kb *gcd* gene. The whole gene was not cloned from the plasmid into M13 because this would cause difficulties in site-directed mutagenesis. Firstly, the whole *gcd* gene was cloned into a new plasmid called

1) 5' TCA GTC ACC GAT AAC TTC TCA ACC 3'
Ser Val Thr Asp Asn Phe Ser Thr

2) 5' TGA GAA GTT **ATT** GGT GAC TGA 3'

3) 5' GGT TGA GAA **GTC** ATC GGT GAC 3'

Figure 4.2 DNA primers used in the Kunkel method for the production of D354N and N355D DNA

1) Wild-type sequence around 354 and 355
2) Sequence of the D354N primer (reversed complement)
3) Sequence of the N355D primer (reversed complement)

1) 5' GGT TCA GTC ACC GAT AAC TTC TCA ACC CGC GAA ACG 3'
Gly Ser Val Thr Asp Asn Phe Ser Thr Arg Glu Thr

2) 5' CGT TTC GCG GGT TGA GAA GTT ATC GGT GAC TGA ACC 3'

3) 5' GGT TCA GTC ACC GAT **GAC** TTC TCA ACC CGC GAA ACG 3'
Gly Ser Val Thr Asp Asp Phe Ser Thr Arg glu Thr

4) 5' CGT TTC GCG GGT TGA GAA **GTC** ATC GGT GAC TGA ACC 3'

5) 5' GGT TCA GTC ACC **AAT** AAC TTC TCA ACC CGC GAA ACG 3'
Gly Ser Val Thr Asn Asn Phe Ser Thr Arg glu Thr

6) 5' CGT TTC GCG GGT TGA GAA GTT **ATT** GGT GAC TGA ACC 3'

7) 5' GGT TCA GTC ACC AAT GAC TTC TCA ACC CGC GAA ACG 3'
Gly Ser Val Thr Asn Asp Phe Ser Thr Arg glu Thr

8) 5' CGT TTC GCG GGT TGA GAA GTC ATT GGT GAC TGA ACC 3'

Figure 4.3 Primers used in the Stratagene Quickchange method for the production of D3554N, N355D and D354N/N355D DNA

1) wild-type sequence
2) wild-type sequence
3) Sequence for N355D primer (1)
4) Sequence for N355D primer (2)
5) Sequence for D354N primer (1)
6) Sequence for D354N primer (2)
7) Sequence for D354N/N355D primer (1)
8) Sequence for D354N/N355D primer (2)

Bluescript KS^+ (pBR322 is known to have problems with restriction enzymes). pGP478 was cut with *Sal*I and *Eco*RI; these restriction enzymes cut at either side of the inserted *E. coli* sequence. Bluescript KS^+ was also cut with the same restriction enzymes and the *E. coli* fragment was ligated into the plasmid. This plasmid was designed pGEC1. Then pGEC1 was cut with *Sal*I and *Xma*I to give three fragments of 2.9Kb, 2.1Kb and 1.6Kb. The 2.1Kb fragment was purified and cloned into M13mp18 by cutting with the same enzymes. This produced M13pGEC1 which was used to infect CJ236 cells. M13 single stranded DNA was isolated using a Promega M13 DNA purification kit and the purity of ssDNA was determined on an agarose gel (Figure 4.4).

M13 bacteriophage containing a fragment of the *gcd* gene was grown in *E. coli* strain CJ236, which had a mutation in the in the *dut* and *ung* genes. The *dut*⁻ mutation lacked dUTPase and this caused the cells to have higher dUTP levels. The *ung*⁻ mutant lacked the N-glycosylase that is responsible for the removal of incorporated uracils in DNA. M13 grown in this host had randomly incorporated uracils instead of thymines in its DNA structure. This produced an M13 uracil-containing template. A DNA primer containing the required mutation was made that contained at least one base mismatch. The primer was annealed to the M13 uracil-containing template invitro and a new strand was synthesised. The resulting heteroduplex was transformed into *E. coli* strain MV1190 that contained active dUPTase and N-glycosylase. This allowed only the mutant strand to be replicated in this strain. Resulting plaques were isolated and phage stocks prepared. Infecting MV1190 with this bacteriophage allowed the single stranded and double stranded form of DNA to be isolated. ssDNA was used for DNA sequencing to confirm the mutation.

Despite many attempts, the Kunkel method was unsuccessful and no mutants were made. This was perhaps because the primers were not long enough to prevent binding to other regions of the DNA template that had a similar sequence (Figure 4.2). The quality of the uracil-containing template could be another possible reason for failure. M13 bacteriophage plaques were observed after transforming *E. coli* MV1190 with the DNA produced from the mutagenesis reactions. However, isolation and sequencing of the DNA from these plaques showed that they all contained wild-type sequence around the region of interest.

4.4 The Stratagene Quickchange method

The problems encountered with the Kunkel method led me to pursue an alternate method of site-directed mutagenesis. The Stratagene Quickchange method (Section 2.6) of site directed mutagenesis was chosen because the mutagenic reactions could be completed on the plasmid containing the *gcd* gene and did not require the use of M13 bacteriophage as a vector. The

Figure 4.4 Confirmation of the isolation of M13pGEC1 (ssDNA) M13pGEC1 (ssDNA) was isolated from *E.coli* Strain CJ236 using a Promega M13 DNA purification kit. 10µl of M13PGEC1 ssDNA was mixed with 3µl of loading buffer and DNA separated on a 0.6% agarose gel. Standard M13pGEC1 (ssDNA) that had been used in previous experiments was used as a control.

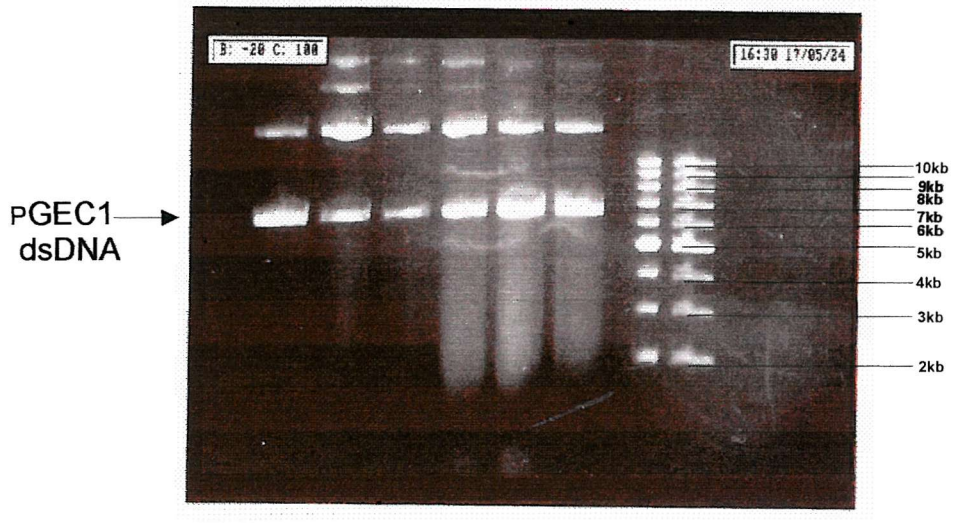

Figure 4.5 Confirmation of the isolation of pGEC1 dsDNA pGEC1 dsDNA was isolated using a Promega SV wizard miniprep DNA purification system. 10µ of isolated dsDNA was mixed with 3µl of loading buffer and separated on a 0.6% agarose gel. A 1-10kb DNA ladder was used to identify pGEC1 dsDNA because the plasmids size was 6.6kb.

pGEC1 template was grown in *E. coli* strain PP2418 and isolated using a Promega SV miniprep DNA purification system. The isolated DNA was checked on a 0.6% agarose gel with a known sample containing pGEC1 or a DNA ladder (Figure 4.5). Two DNA primers containing the required mutation were synthesised, each complementary to opposite strands of the DNA template. They were then added to the double stranded DNA template (Figure 4.6). Mutated plasmids containing staggered nicks were generated using *Pfu* Turbo DNA polymerase and a thermal temperature cycler. Following temperature cycling, the sample was treated with *Dpn*1 endonuclease that targets methylated DNA. This restriction enzyme was specific for methylated and hemimethylated DNA so it digested the parental DNA. This selected the synthesised mutant DNA which was then transformed into a host *E. coli* cell JM109. The low number of PCR cycles and the high fidelity of the *Pfu* Turbo DNA polymerase contributed to higher mutation efficiency and decreased potential for random mutations. As found with the Kunkel method, problems were encountered with shorter DNA primers (Figure 4.2). These short primers had sequences similar to other regions of the *gcd* gene, some being over 50% identical. Therefore the length of the primers was increased from 21 bases to 36 bases to reduce the chance of the primer binding to other regions (Figure 4.3). After the PCR and *Dpn*1 restriction steps the DNA of the samples was separated on a DNA gel; this confirmed that DNA had been produced (Figures 4.7-4.9). All three GDH mutants (D354N, N355D and double mutant D354N/N355D) were successfully made and shown by manual and automated DNA sequencing (Figures 4.10, 4.11 and 4.12). The DNA sequence of the *gcd* gene is shown in Figure 4.13.

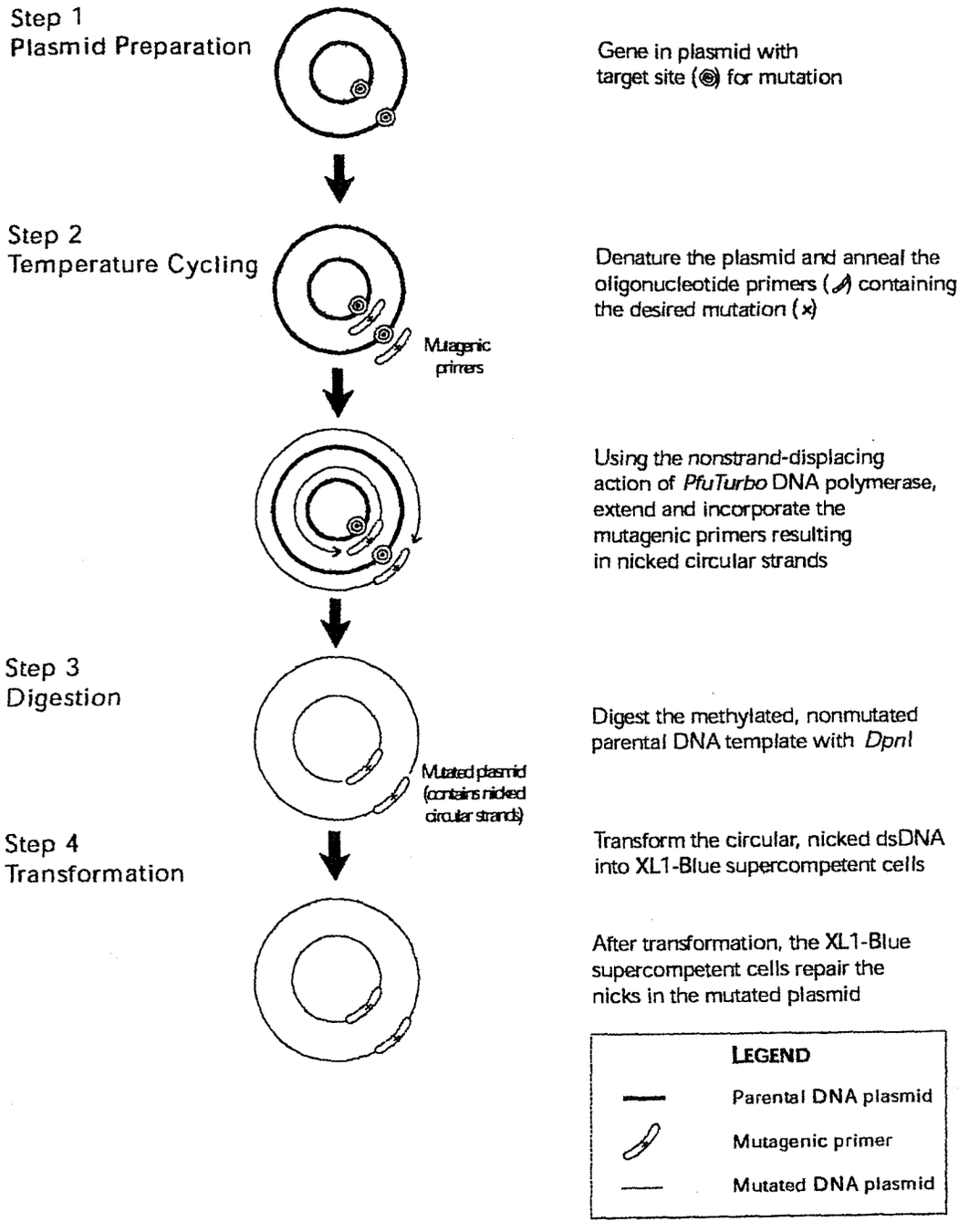

Figure 4.6 Stratagene Quickchange method of mutagenesis

This method allows mutagenesis to be done directly on the plasmid that contains the gene of interest (taken from the Stratagene Quickchange manual).

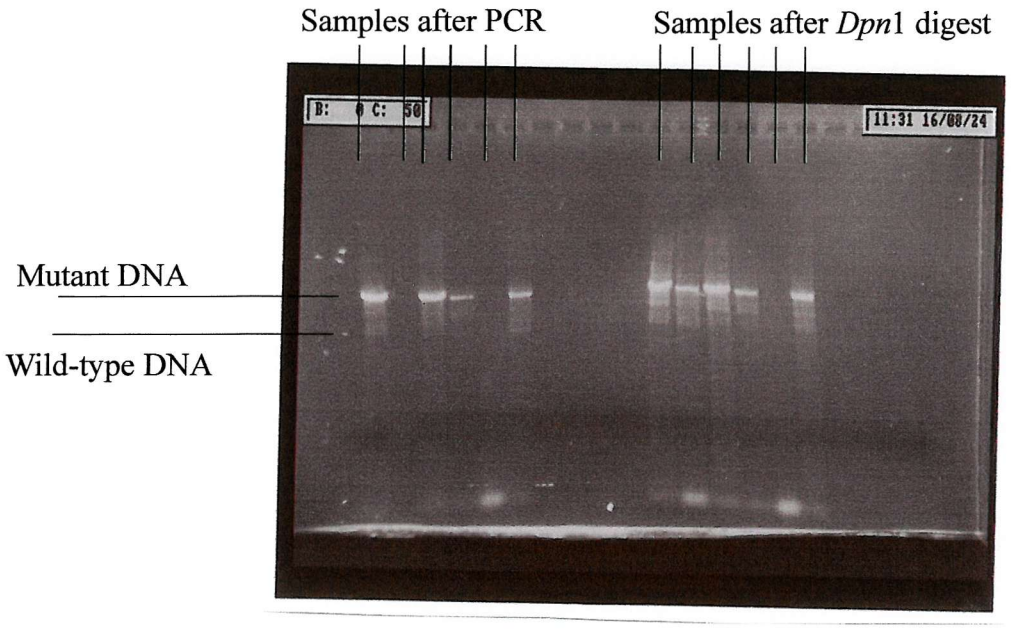

Figure 4.7 Confirmation of the production of D354N dsDNA

After various stages of the Stratagene Quickchange mutagenesis method, DNA samples were separated on a 0.6% agarose gel. Mutant DNA and wild-type DNA were present after the PCR step but only mutant DNA was present after *Dpn*1 digestion.

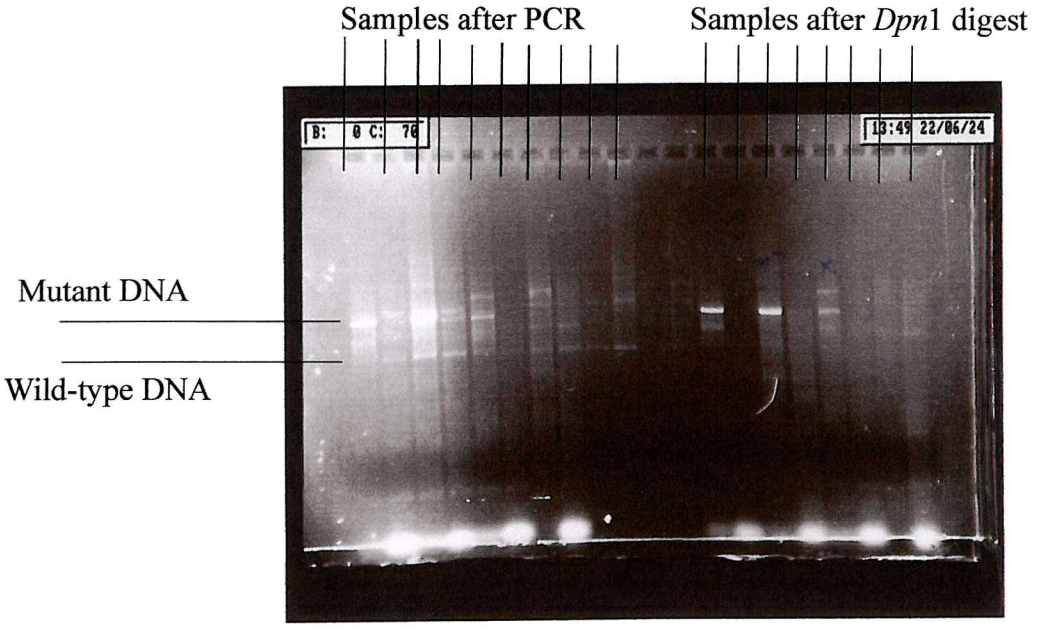

Figure 4.8 Confirmation of the production of N355D dsDNA

After various stages of the Stratagene Quickchange mutagenesis method, DNA samples were separated on a 0.6% agarose gel. Mutant DNA and wild-type DNA were present after the PCR step but only mutant DNA was present after *Dpn*1 digestion.

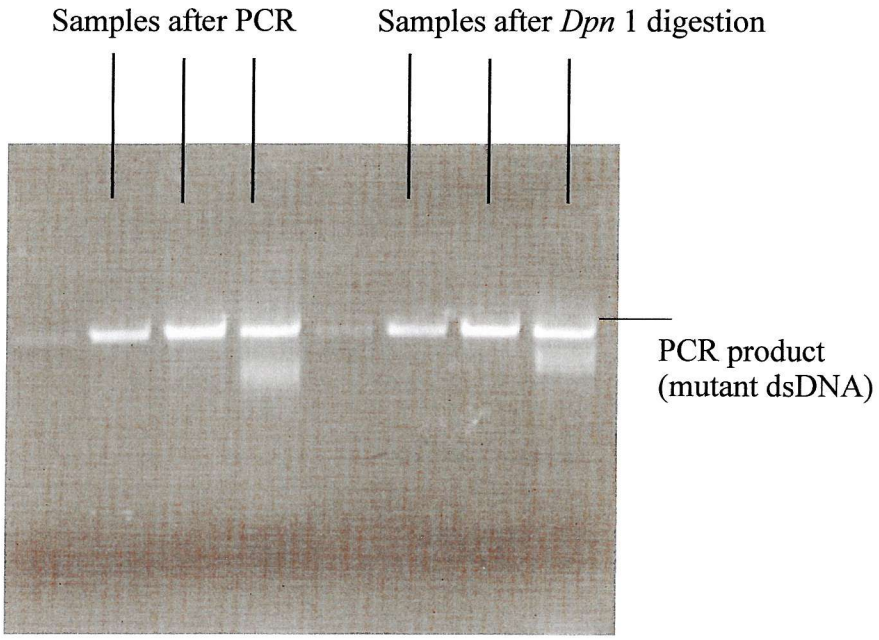

Figure 4.9a Confirmation of the production of D354N/N355D dsDNA

After various stages of the Stratagene Quickchange mutagenesis method, DNA samples were separated on a 0.6% agrose gel.

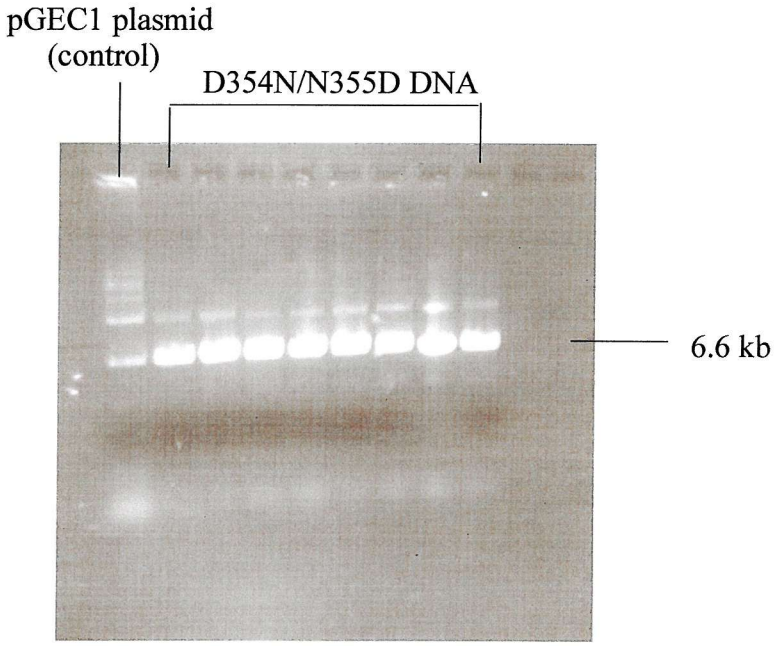

Figure 4.9b Confirmation of the isolation of D354N/N355D dsDNA

D354N/N355D dsDNA was purified using a promega SV wizard miniprep DNA purification system. Isolated DNA was separated on a 0.6% agrose gel and mutant DNA was the correct size (6.6kb)

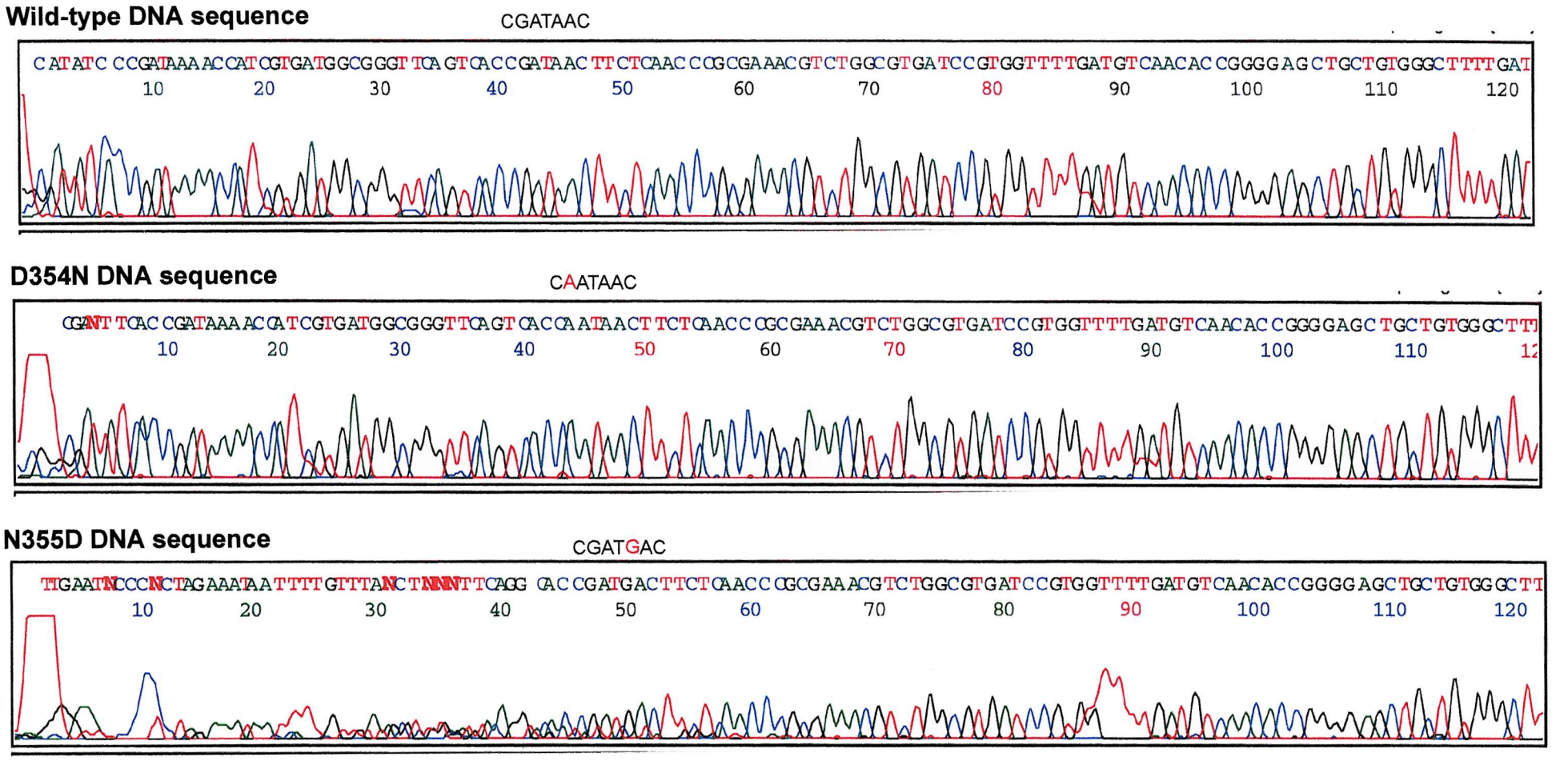

Figure 4.10 Confirmation of mutant DNA by automated DNA sequencing

Wild-type, D354N and N355D DNA sequences from automated DNA sequencing are shown. This sequencing proved that the Stratagene Quickchange method of mutagenesis had produced mutant DNA. Sequencing by Oswel (Southampton, UK).

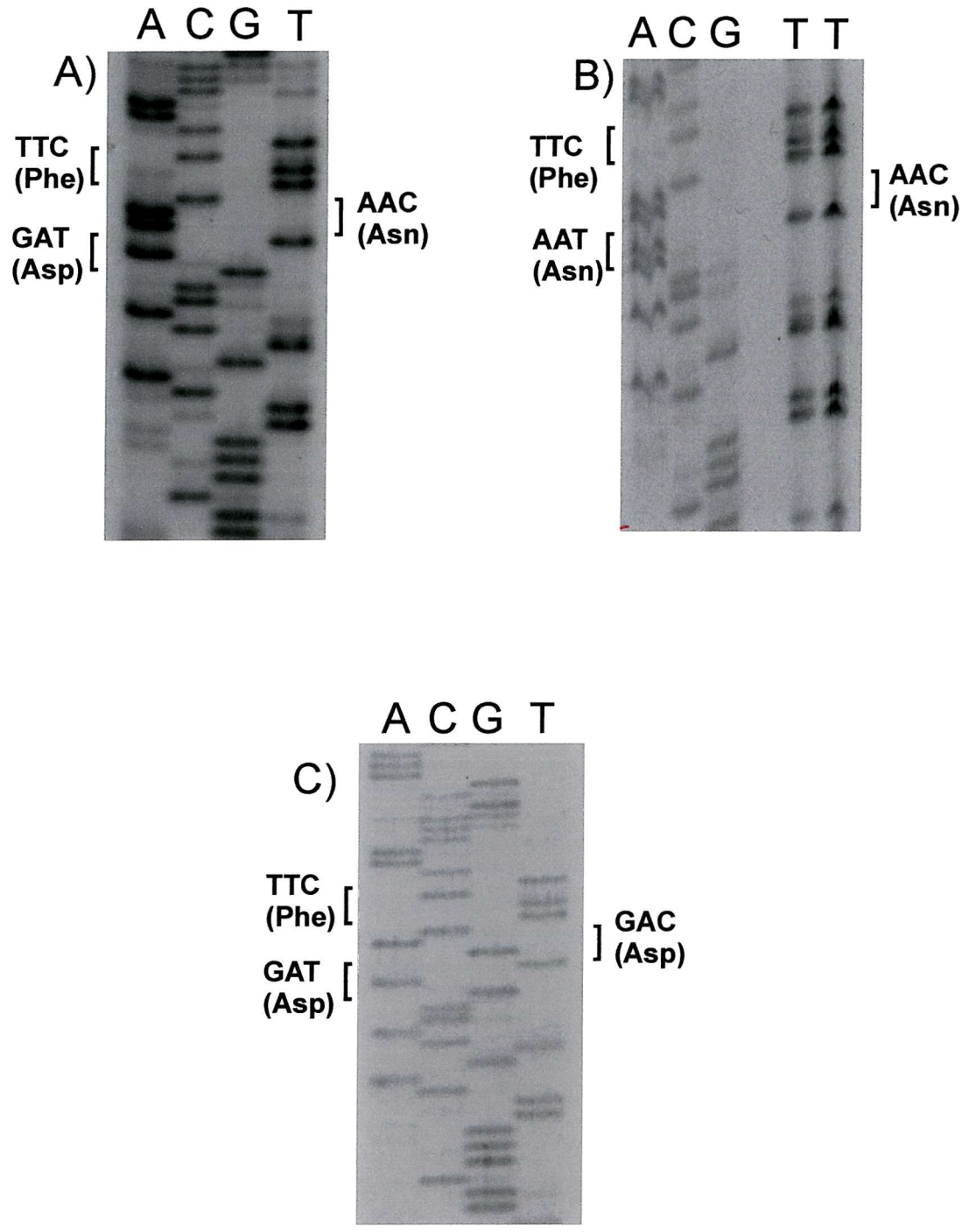

Figure 4.11 Confirmation of mutant DNA by manual sequencing

A) Wild-type sequence around Asp354 and Asn355.

B) The DNA sequence of D354N mutation.

C) The DNA sequence of N355D mutation.

D354N/N355D DNA sequence

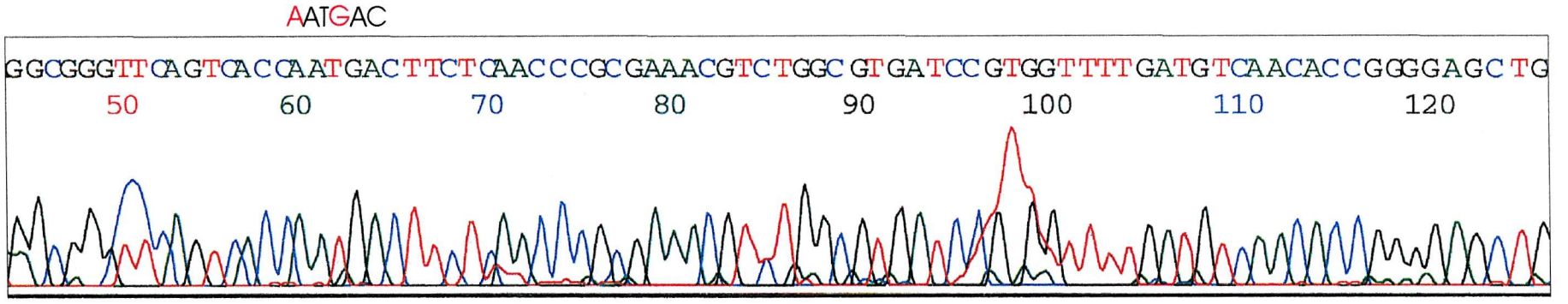

Wild-type DNA sequence

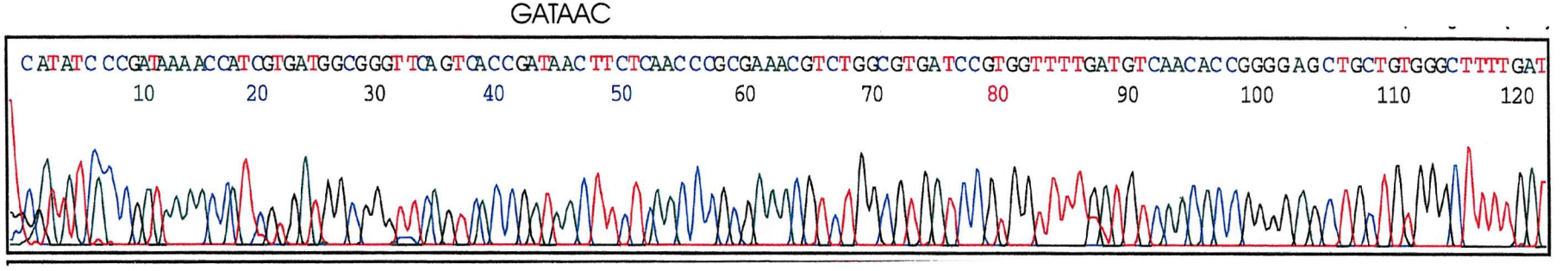

Figure 4.12 Confirmation of D354N/N355D DNA by automated DNA sequencing

Wild-type and D354N/N355D DNA sequences proved PCR mutagenesis had produced mutant DNA. Sequencing done by Oswel (Southampton, UK).

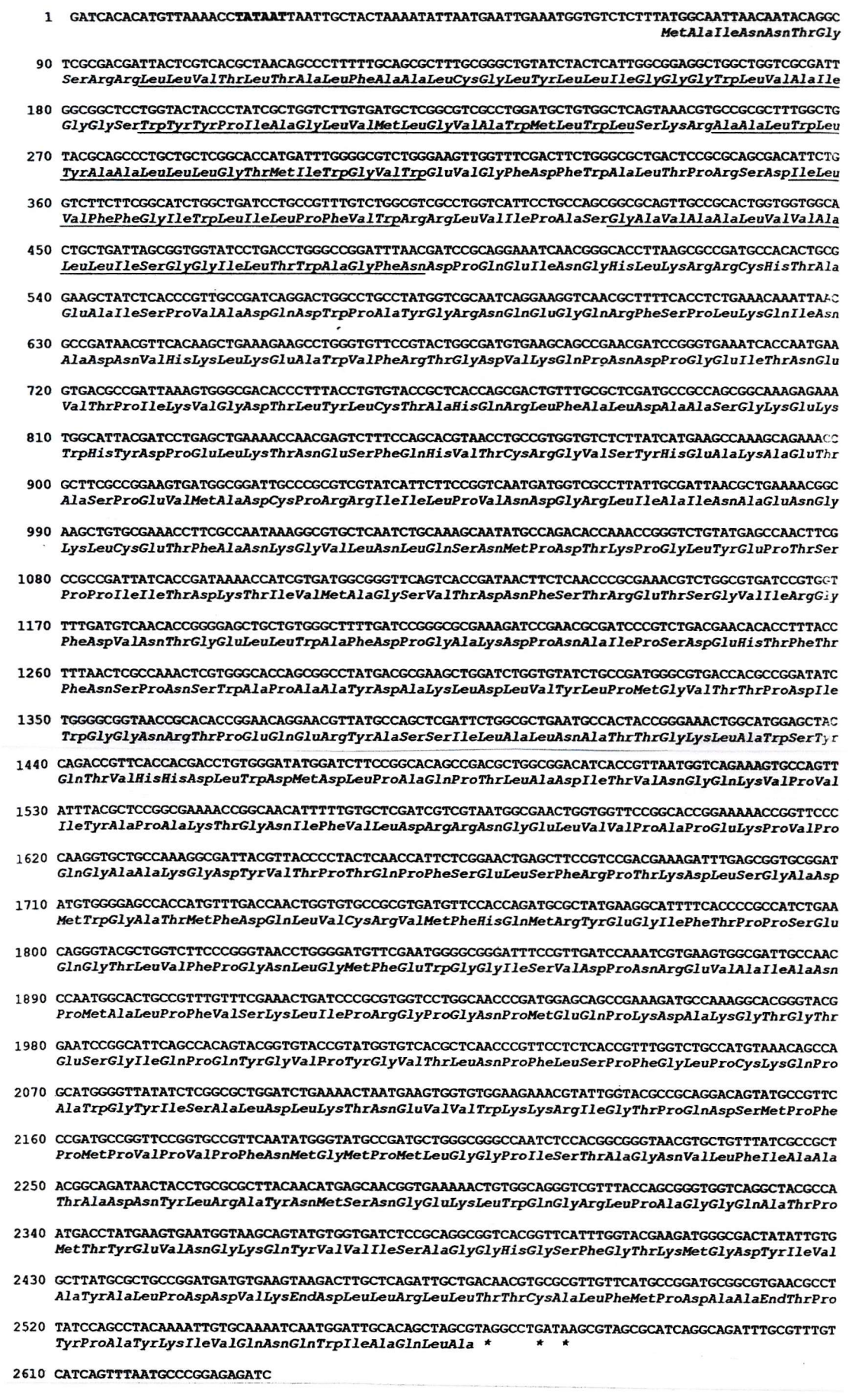

Figure 4.13 - DNA sequence for the *gcd* gene (Cleton-Jansen *et al.*, 1990)

4.5 Characterisation of N355D-GDH

N355D-GDH was purified in Pipes buffer (pH adjusted with NaOH) under conditions previously described (Section 2.4). Preliminary results showed that Ca^{2+} was required for reconstitution instead of Mg^{2+}. The rate of reconstitution with Ca^{2+} was very rapid, becoming 80% active within two minutes and fully reconstituted within 10 minutes. The standard reconstitution mixture was 5mM $CaCl_2$, 25μM PQQ, 50mM Pipes buffer pH 6.5 and GDH. Purified N355D-GDH had 25% of the activity of WT-GDH (Table 4.1). SDS-PAGE showed that it was about 80% pure and the same size as WT-GDH (as expected) (Figure 4.14). The relatively lower activity of solubilised N355D-GDH was not because of sensitivity to Triton X-100 (Figure 4.15AP).

4.5.1 The effect of divalent metals and PQQ on the reconstitution of N355D-GDH

In the absence of metal ions during reconstitution, N355D-GDH activity was very low (0.5μmoles/min/mg) and it could not be removed by 100mM EDTA/EGTA treatment followed by gel filtration. N355D-GDH could not be reconstituted with 5mM Mg^{2+} suggesting that the mutation has affected the metal binding site. Unlike WT-GDH, Ca^{2+}, Sr^{2+} and Ba^{2+} supported reconstitution (Figure 4.16). As with WT-GDH no reconstitution occurred with Fe^{2+}, Ni^{2+}, Cu^{2+} and Mn^{2+} and these metals inactivated the enzyme; subsequent addition of Ca^{2+} could not restore activity.

The affinity of apoN355D-GDH for Ca^{2+}, Sr^{2+} and Ba^{2+} was determined (Table 4.2). The K_d values were between 1.2mM and 3.8mM and the affinity for Ca^{2+} was slightly lower than for Sr^{2+} and Ba^{2+} (the K_d for Mg^{2+} of WT-GDH was 1.5mM; Figure 3.22). The highest A_{max} was obtained with Ca^{2+} and the lowest A_{max} was seen with Sr^{2+}, indicating that the size of the metal ion is not the only characteristic relevant to reconstitution. The lack of activity with Mg^{2+} may be because it is too small. WT-GDH is expected to have 7 bonds to the metal ion but this mutant could make 8 bonds. Mg^{2+} may not be able to fit into the metal ion binding site even though Mg^{2+} can be coordinated to eight ligands in some complexes (Section 1.8).

The K_d values for Ca^{2+} binding (Figure 4.17AP) were not significantly different between pH5.5 and 8.0 (2.3mM - 3.7mM) as shown for Mg^{2+} binding to WT-GDH. This suggests that this mutation has only altered the specificity for metal binding and has not changed the reconstitution process.

The results in Table 4.3 show that the highest affinity for PQQ was measured with Ca^{2+} (K_d, 0.41μM). The affinity with Sr^{2+} and Ba^{2+} were slightly lower (K_d, 1.48μM and 0.48μM respectively). The K_d for PQQ binding to WT-GDH in the presence of Mg^{2+} was 0.28μm.

Table 4.1 Purification of N355D-GDH with Pipes buffer

N355D-GDH was purified by the method described in Section 2.4. The yields and levels of purification were similar to those with WT-GDH. Samples were reconstituted under standard conditions with 25μM PQQ and 5mM Ca^{2+} (instead of the 5mM Mg^{2+} used with WT-GDH). The assay system for N355D-GDH contained 1.5M D-glucose. The specific activity of purified WT-GDH was 84μmoles/min/mg.

Sample	Volume (ml)	Total protein (mg)	Specific activity (μmoles/min/mg)	Yield (%)	Purification (fold)
Crude extract	48	718	1.5	100	1
Membranes	25	204	5.1	96.7	3.4
Soluble GDH	24	91	9.3	79.3	6.2
DEAE-GDH	26	25	20.8	48.6	13.9

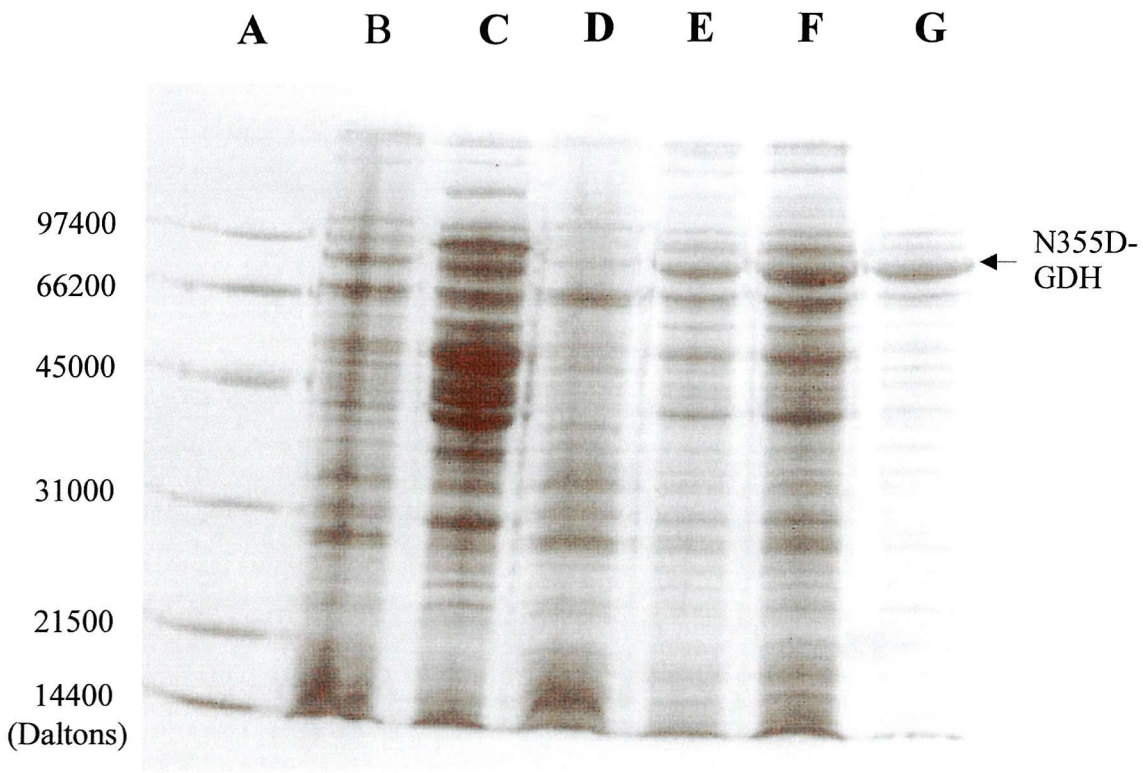

Figure 4.14 SDS-PAGE showing the purity of N355D-GDH

A) Standard proteins
B) Membrane fraction (dil x5)
C) Supernatant from membrane isolation (dil x5)
D) Pellet remaining after solubilisation of GDH (dil x5)
E) Soluble N355D-GDH (dil x5)
F) Soluble N355D-GDH (undiluted)
G) DEAE-sepharose purified N355D-GDH (undiluted)

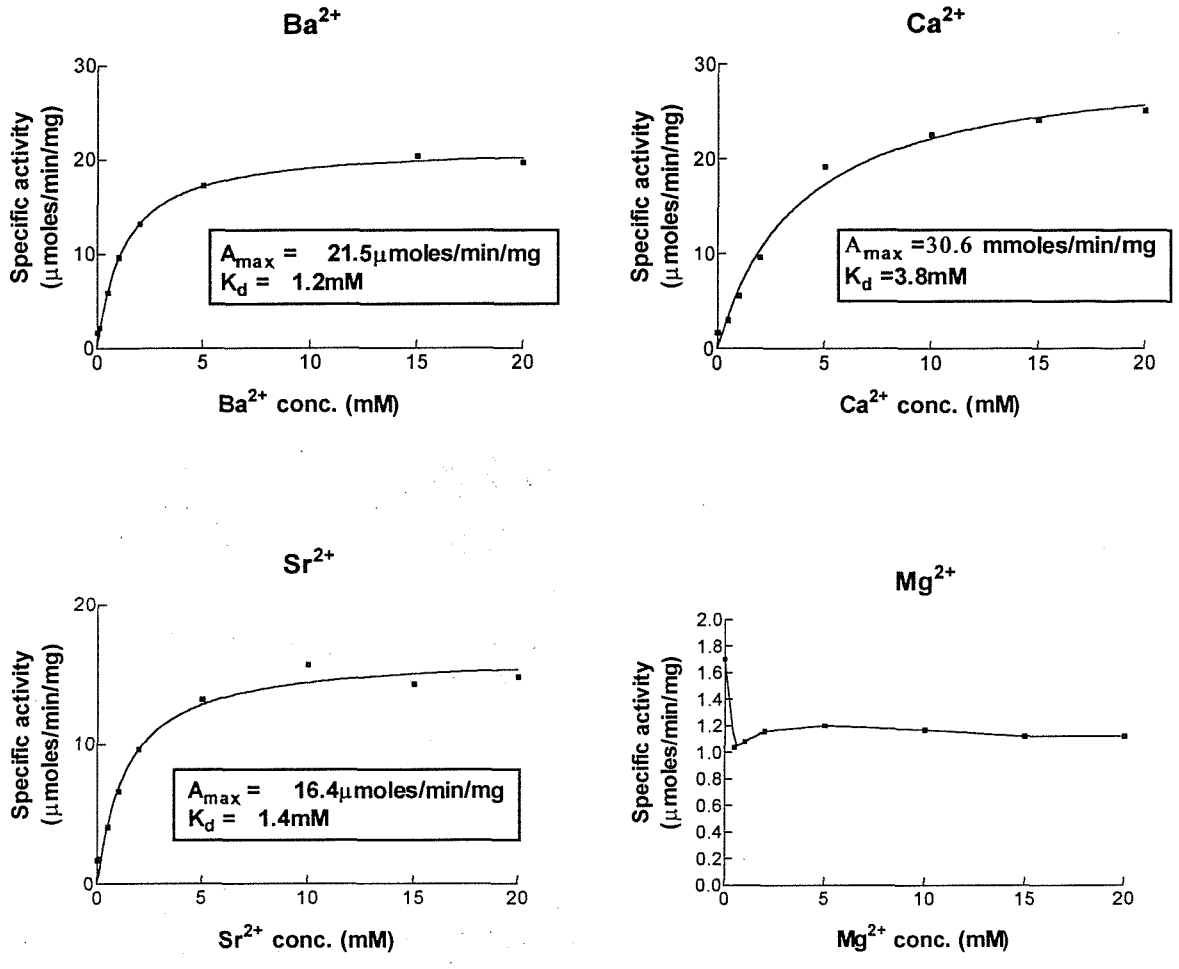

Figure 4.16 Reconstitution of N355D-GDH with Ca^{2+}, Sr^{2+} and Ba^{2+}

N355D-GDH was reconstitued under standard conditions with 25μM PQQ and various concentrations of metal ions (Mg^{2+}, Ca^{2+}, Sr^{2+} and Ba^{2+}). The lines of best fit were calculated by the equation $A=A_{max}[M^{2+}]/(K_d + [M^{2+}])$ where A is GDH activity and M^{2+} represents metal ion. Clearly there was no reconstitution with Mg^{2+}.

Table 4.2 Activity of N355D-GDH after reconstitution with various metal ions

This Table is based on the data from Figure 4.16. N355D-GDH purified in Pipes buffer was reconstituted under standard conditions with 25μM PQQ and various metal ion concentrations. The activity after reconstitution in the absence of metal was 0.5μmoles/min/mg. The k_d for Mg^{2+} in WT-GDH was 1.5mM.

Metal	K_d (mM)	A_{max} (μmoles/min/mg)	Ionic Radius (nm)
Mg^{2+}	No Activity	No Activity	0.065nm
Ca^{2+}	3.8	30.6	0.099nm
Sr^{2+}	1.4	16.4	0.113
Ba^{2+}	1.2	21.5	0.135

Table 4.3 – The affinity of N355D-GDH for PQQ

N355D-GDH purified in Pipes buffer was reconstituted under standard conditions with metal ions and various concentrations of PQQ. 5mM Ca^{2+}, Sr^{2+} and Ba^{2+} were used to reconstitute the enzyme.

Metal ion added in reconstitution	K_d for PQQ (μM)	A_{max} (μmoles/min/mg)
Ca^{2+}	0.41	20.6
Sr^{2+}	1.48	15.7
Ba^{2+}	0.48	19.1
Mg^{2+} (WT-GDH)	0.28	101

Mutating Asn-355 to aspartic acid has thus slightly decreased the affinity for the prosthetic group indicating that either the conformation of the active site has resulted in the movement of binding groups away from PQQ or the replacement of Mg^{2+} at the active site by Ca^{2+}, Sr^{2+} or Ba^{2+} is responsible for this effect.

As shown with WT-GDH, the affinity of N355D-GDH for PQQ decreased at pH values above 7.5 (Figure 4.18AP); K_d values at pH 7.5 and 8.0 were 0.43μM and 2.4μM respectively.

Gel filtration was used to confirm that Ca^{2+} and PQQ binding to apoN355D-GDH was reversible. Similar to WT-GDH, gel filtration removed nearly all the activity from reconstituted N355D-GDH (Table 4.4AP). Full activity being restored after reconstitution with PQQ plus Ca^{2+}.

The mutation of asparagine to aspartic acid did not make the enzyme tolerant towards EDTA (Figure 4.19AP). Treatment with 6-7mM EDTA led to complete loss of activity.

4.5.2 The effect of Mg^{2+} on Ca^{2+} -reconstituted N355D-GDH

Figure 4.20 shows that incubation with Mg^{2+} of holoGDH reconstituted with Ca^{2+} led to loss of activity; 24mM Mg^{2+} caused 50% loss of activity. Figure 4.21 shows that as the concentration of Mg^{2+} increased, the K_d for Ca^{2+} increased and the A_{max} decreased (Table 4.5); this suggests that Mg^{2+} acts as a mixed (non-competitive) inhibitor, binding in the presence or absence of Ca^{2+}. There must be two metal ion binding sites for this to occur. The curve in the absence of Mg^{2+} shows that there is a second (inhibitory) site for Ca^{2+} that causes inhibition with bound Ca^{2+} (K_I, 124mM). Using data taken from the Lineweaver-Burk plot in Figure 4.21 the K_i and K_{ii} values for Mg^{2+} binding were calculated to be 11.4mM and 39.6mM respectively. Mg^{2+} can bind to free GDH and Ca^{2+}-GDH.

4.5.3 The thermal stability of N355D-GDH

ApoN355D-GDH was more tolerant to heat than the apoWT-GDH. Heating at 40°C for 40 minutes destroyed WT-GDH but N355D-GDH was unaffected (Figure 4.22a). HoloN355D-GDH lost 50% within 10 minutes at 55°C (Figure 4.22b) whereas WT-GDH was denatured at this temperature.

These results show that, as WT-GDH, the apo form is not as tolerant to heat as holoGDH; the binding of PQQ may make the structure more rigid. The increase in thermal stability of apoN355D-GDH may occur due to a changed conformation of the active site that affects overall stability. The binding of Ca^{2+} to the enzyme instead of Mg^{2+} cannot be responsible for this increase in tolerance because Ca^{2+} and PQQ were absent from the apoenzyme.

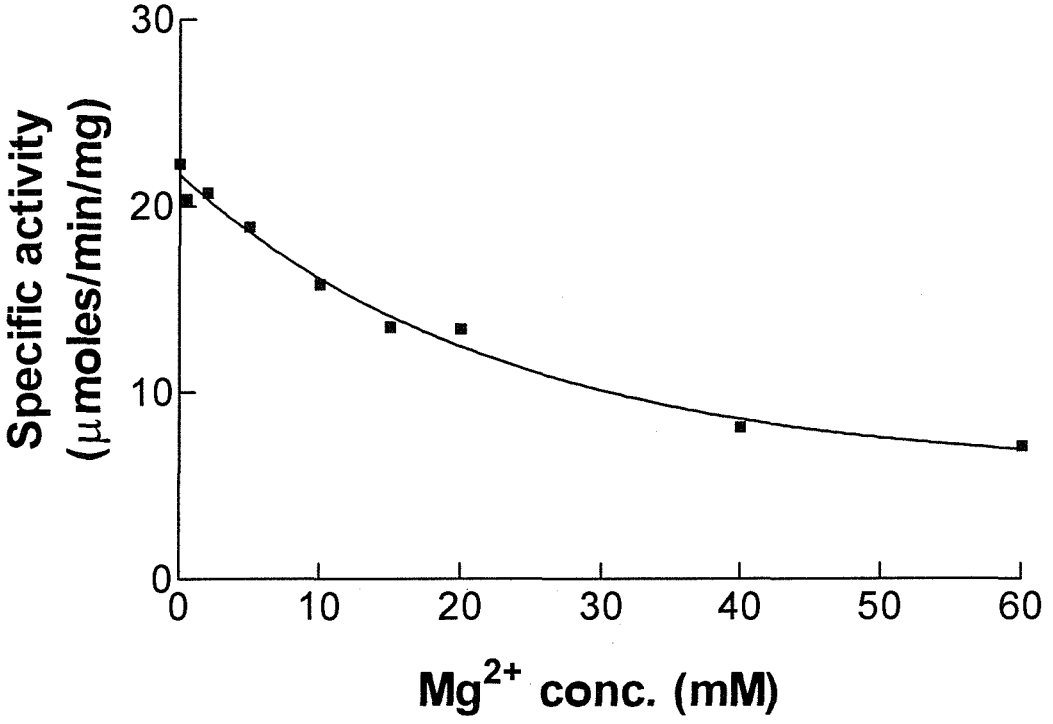

Figure 4.20 The inhibition of Ca^{2+}-reconstituted N355D-GDH by Mg^{2+}

N355D-GDH was reconstituted under standard conditions with 5mM Ca^{2+} and 25μM PQQ. Then it was incubated at 25°C for a further 20 minutes in the presence of Mg^{2+} before activity was measured.

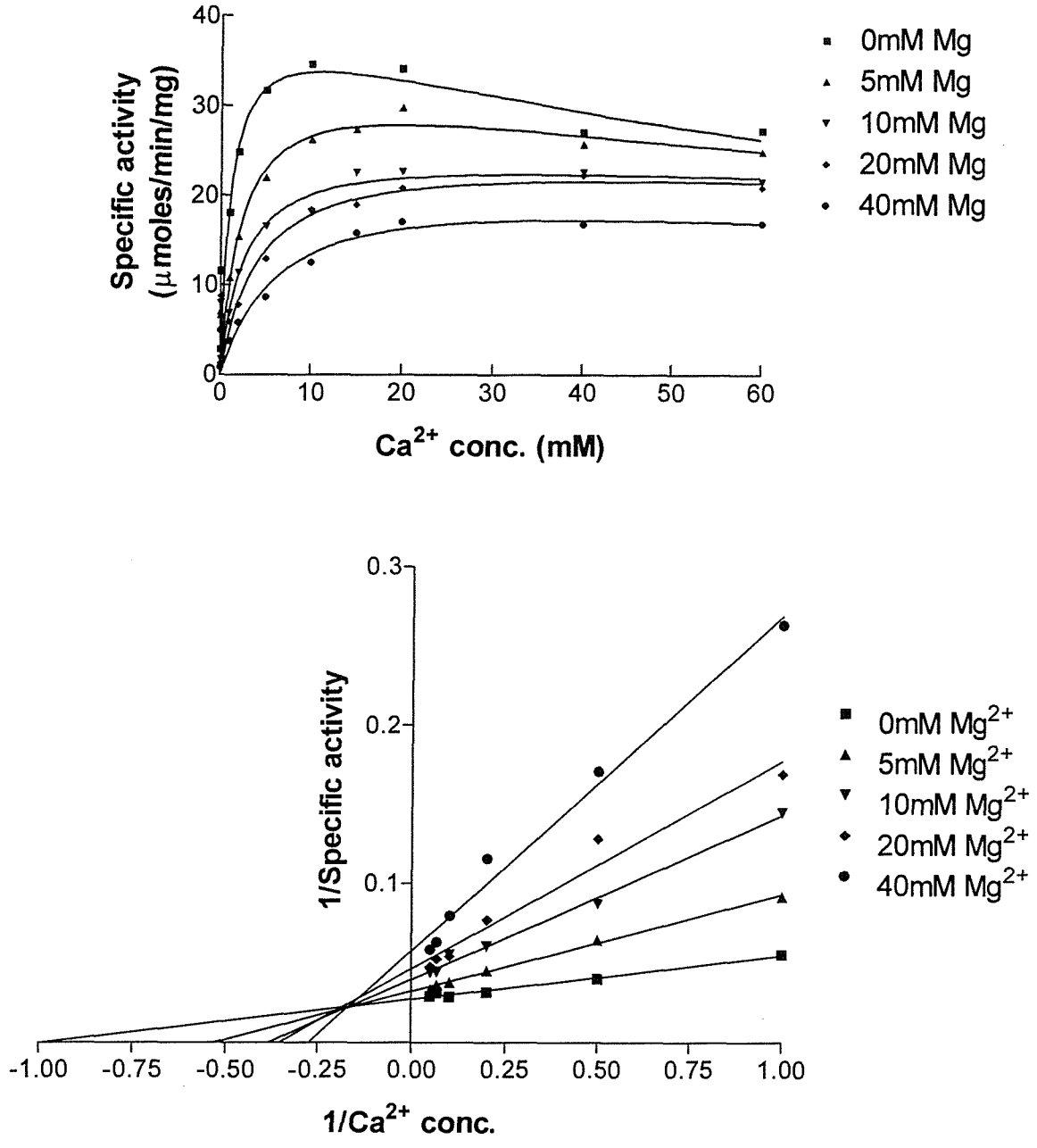

Figure 4.21 The effect of Ca^{2+} on N355D-GDH previously incubated with PQQ and Mg^{2+}

N355D-GDH was incubated for 20 minutes at 25°C with 25μM PQQ and various concentrations of Mg^{2+}. This was followed by incubation at 25°C for a further 20 minutes in the presence of Ca^{2+} (0-60mM) before assaying for activity. The lines of best fit were calculated by the equation $A=A_{max}[Ca^{2+}]/(K_d + [Ca^{2+}]\{1 + [Ca^{2+}]/Ki\})$ where A is GDH activity. Then a Lineweaver-Burk plot was made based on this data.

Table 4.5 A_{max} and K_d values for Ca^{2+} in the presence of Mg^{2+}

N355D-GDH and 25μM PQQ were incubated for 20 minutes at 25°C with various concentrations of Mg^{2+} (0-40mM). Then various concentrations of Ca^{2+} (1-60mM) were added and the mixture incubated for a further 20 minutes before activity was assayed. This table is based on the data from Figure 4.21.

	0mM Mg^{2+}	5mM Mg^{2+}	10mM Mg^{2+}	20mM Mg^{2+}	40mM Mg^{2+}
K_d (mM)	1.0	2.3	2.6	4.2	7.0
K_I (mM)	123.6	175.5	457.2	434.0	215.9
A_{max} (μmoles/min/mg)	39.2	34.2	25.7	25.7	23.4

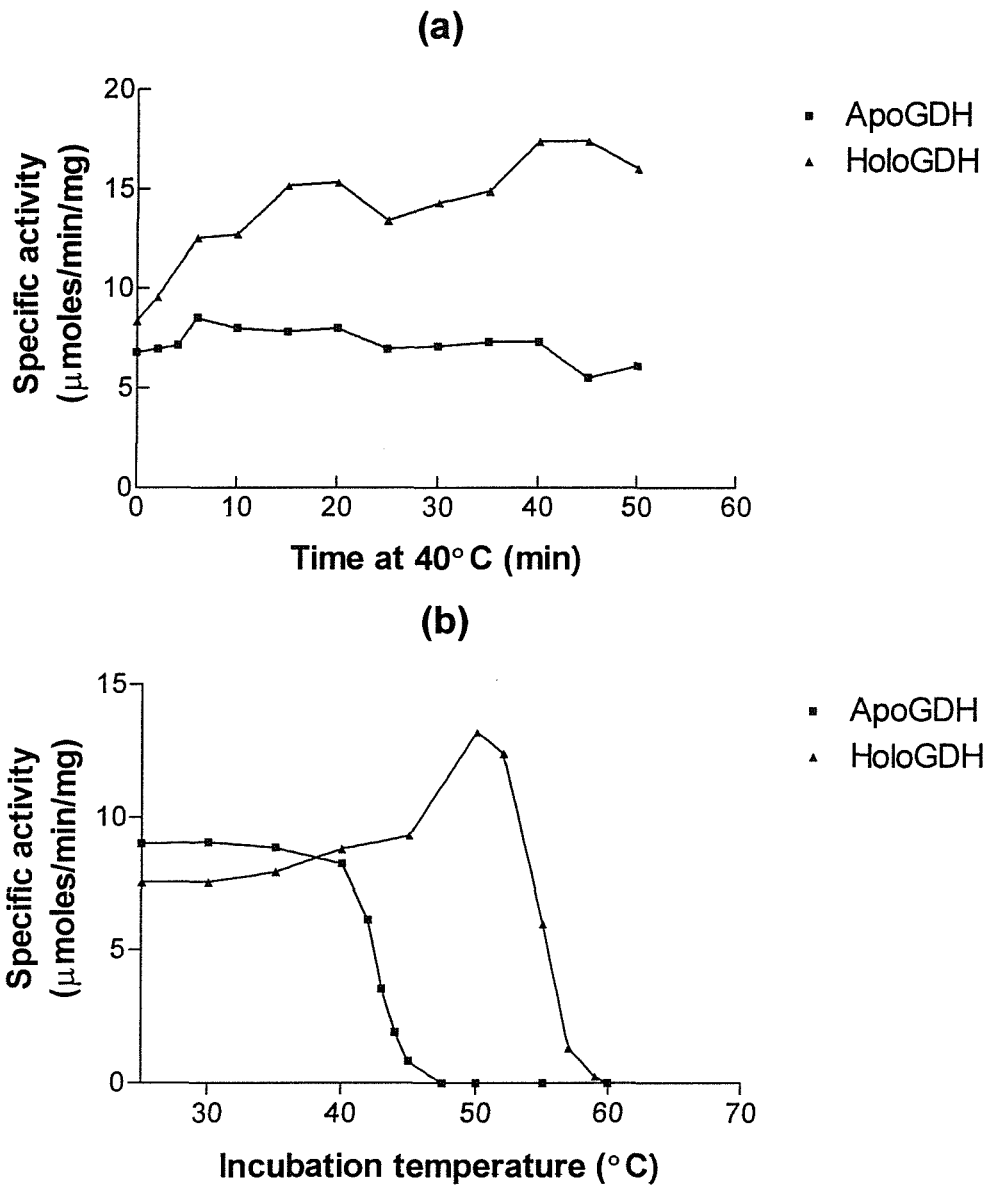

Figure 4.22 The thermal stability of N355D-GDH

a) Apo and holoGDH were incubated at 40°C for various periods of time. Then the enzyme was placed on ice for 5 minutes and apoGDH reconstituted under standard conditions with Ca^{2+} and PQQ before activity was measured.

b) Apo and holoGDH were incubated at various temperatures for 10 minutes. Then the enzyme was placed on ice for 5 minutes. ApoGDH was reconstituted under standard conditions with Ca^{2+} and PQQ before activity was measured.

Figure 3.31 shows results for the same experiment with WT-GDH.

4.5.4 The activation energy of N355D-GDH

The activation energy for WT-GDH was 41kJ/mol and the values for N355D-GDH reconstituted with Sr^{2+} and Ba^{2+} were similar (44kJ/mol and 46 kJ/mol respectively) (Figures 4.23 and 4.24). By contrast, the activation energy with Ca^{2+}-GDH was much higher (68kJ/mol). These results are discussed fully in Chapter 6.

4.5.5 The substrate specificity of N355D-GDH

Table 4.6 shows that N355D-GDH oxidised the same substrates as WT-GDH but the affinity for substrates decreased by 5 to 100 fold and the V_{max} was only 4-40% of WT-GDH values. The metal ion used for reconstitution affected the affinity for substrates; the K_m for D-glucose with Ca^{2+}-, Sr^{2+}- and Ba^{2+}-reconstituted enzyme were 949mM, 15.4mM and 15.3mM respectively. N355D-GDH reconstituted with Sr^{2+} and Ba^{2+} had a greater affinity for all substrates than Ca^{2+} reconstituted enzyme, suggesting that the oxidation of substrates is more effective with larger metal ions bound to the active site. Therefore, the substrate specificity of reconstituted Sr^{2+} and Ba^{2+}-N355D-GDH will be described in detail (structure of sugars shown in Figure 1.10). The catalytic efficiency of Ca^{2+}-, Sr^{2+}- and Ba^{2+}-reconstituted N355D-GDH was 0.11%, 3.4% and 4.1% compared with that for WT-GDH.

L-glucose did not inhibit D-glucose oxidation indicating that (as with WT-GDH) the L form was unable to bind. As suggested by Cozier *et al.* (1999), the C6 hydroxymethyl groups of hexose sugars must not be below the plane of the ring if they are to be oxidized.

As with WT-GDH (Section 3.1.3), no hydroxyl group was absolutely essential for substrate binding. With WT-GDH, D-glucose and 2-deoxy-D-glucose were the best substrates but N355D-GDH had the highest affinity for D-glucose followed by D-mannose; the affinity of N355D-GDH for 2-deoxy-D-glucose was 49-140 fold lower with Sr^{2+} and Ba^{2+} than that of WT-GDH but the V_{max} with 2-deoxy-D-glucose was more than 5 fold higher than the V_{max} values with D-mannose. The lower affinity for 2-deoxy-D-glucose may suggest that the C2 hydroxyl group is important in binding but this is not the case because D-mannose was oxidized and this has the C2 hydroxyl group in a different orientation that in D-glucose. The K_m values with Sr^{2+} and Ba^{2+}-GDH for D-mannose were similar to WT-GDH.

The C3 hydroxyl group may have some importance in substrate binding because the K_m values for 3-O-methyl-D-glucose and D-ribose were high. With Ba^{2+}-GDH the K_m values for 3-O-methyl-D-glucose and D-ribose were 138-140 fold higher than the value for D-glucose. The methyl group at the C3 position in 3-O-methyl-D-glucose may interfere with substrate binding

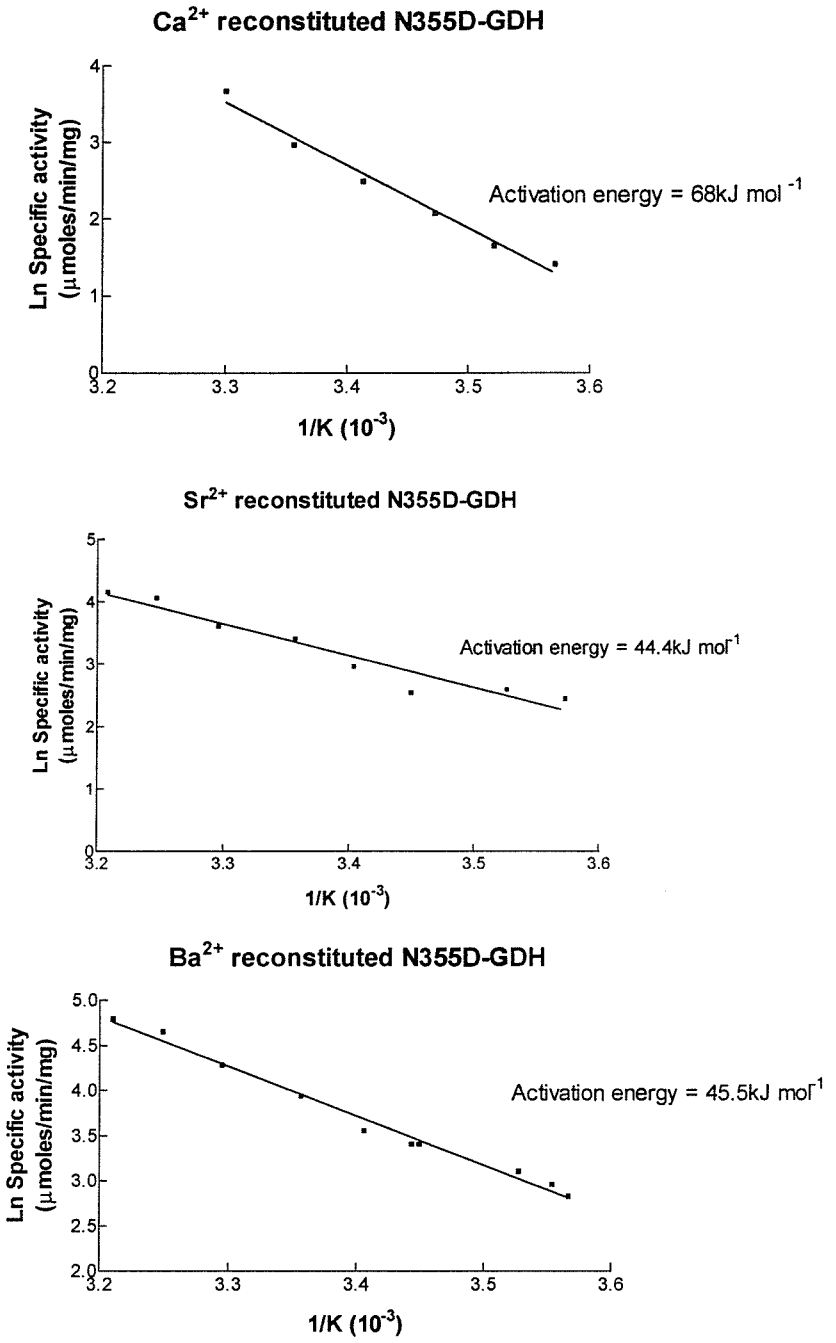

Figure 4.23 Activation energy of N355D-GDH reconstituted with Ca^{2+}, Sr^{2+} and Ba^{2+}

N355D-GDH was reconstituted under standard conditions with 25μM PQQ and 5mM metal ions (Ca^{2+}, Sr^{2+} or Ba^{2+}). Then activity was measured with the standard assay (1.5M D-glucose) at various temperatures (5-40°C).The formula relating activation energy (ΔG*) is v=A.exp(-ΔG*/RT) where A is the Arrhenius constant and R is the gas constant. The ΔG* values were calculated from the slopes of the curves. Figure 3.32 shows results of the same experiment with WT-GDH.

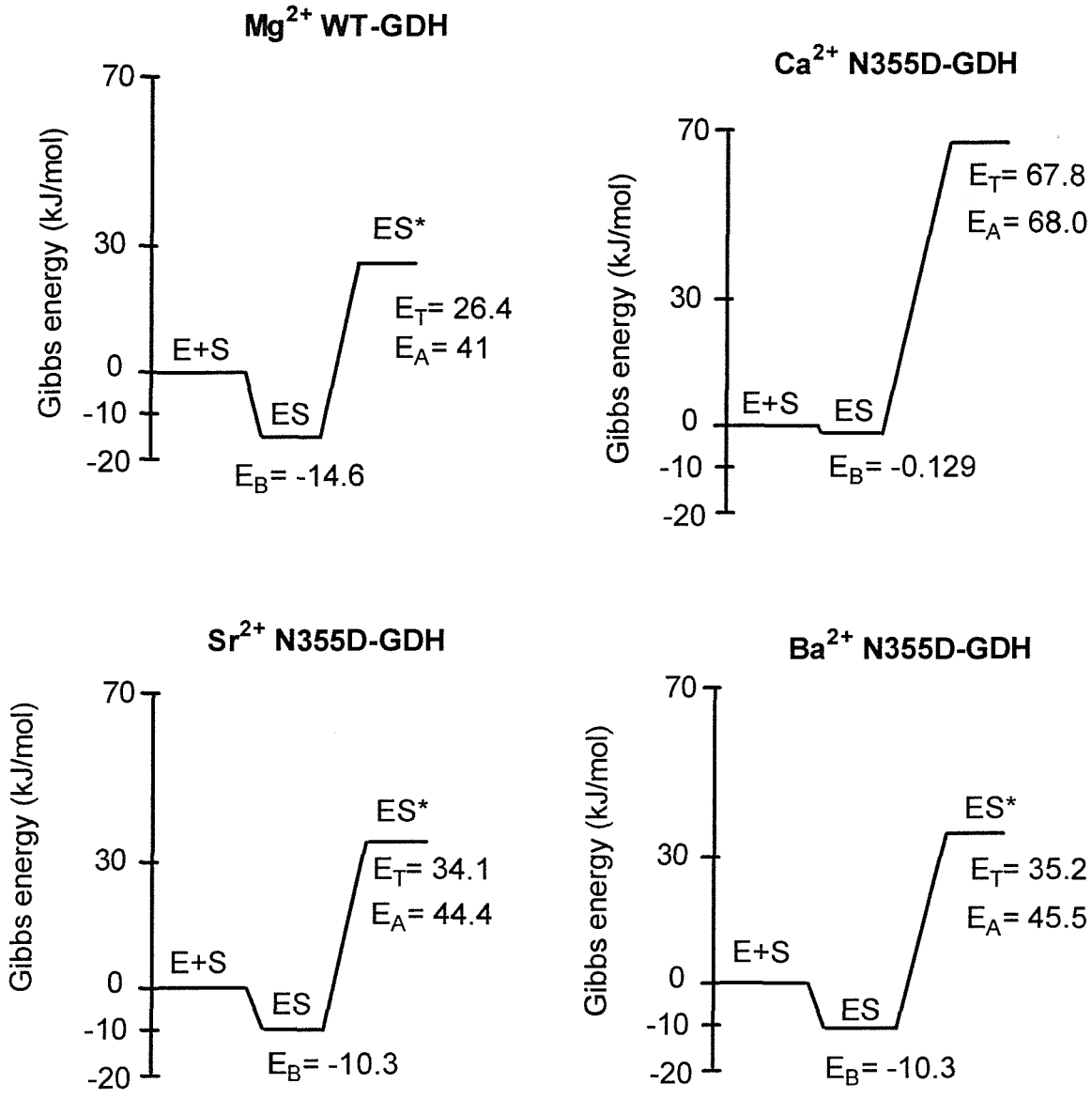

Figure 4.24 Schematic Gibbs free energy changes for the formation of the transition complex during the oxidation of D-glucose by N355D-GDH

The values for Gibbs free energy changes are in kJ/mol. E represents enzyme, S represents substrate, ES represents the enzyme-substrate complex and ES* is the transition state. E_A, E_B and E_T represent activation energy, binding energy and a measure of the energy of the transition complex respectively. E_A was calculated in Figure 4.23 and E_B was calculated by the equation $E_B = -RT \ln K_m$ where R is a gas constant and T is temperature.

Table 4.6 Substrate specificity of N355D-GDH

N355D-GDH was reconstituted under standard conditions with 5mM metal ions (Ca^{2+}, Sr^{2+} or Ba^{2+}) and 25μM PQQ. Activity was measured with the standard dye-linked assay containing various concentrations of substrate. The data from which these have been calculated have not been presented; their "quality" was similar to that seen in the data from WT-GDH. L-glucose, D-arabinose and D-maltose were not oxidised.

Substrate	Ca^{2+}			Sr^{2+}			Ba^{2+}			Mg^{2+} WT-GDH		
	K_m	V_{max}	Catalytic efficiency (V_{max}/K_m)	K_m	V_{max}	Catalytic efficiency (V_{max}/K_m)	K_m	V_{max}	Catalytic efficiency (V_{max}/K_m)	K_m	V_{max}	Catalytic efficiency (V_{max}/K_m)
D-glucose	949	44.0	0.05	15.4	21.7	1.4	15.3	25.9	1.7	2.8	116	41.4
2-deoxy-D-glucose	803	45.3	0.06	170	25.1	0.15	489	40.3	0.08	3.5	137	39.1
D-mannose	>3M	10.5	0.004	106	5.2	0.05	135	5.7	0.04	116	137	1.2
3-O-methyl-glucose	>3M	nd	nd	2126	15.4	0.007	2105	15.6	0.007	79	77	0.97
D-xylose	>3M	nd	nd	219	15.1	0.07	80	2.0	0.025	17	61	3.6
D-ribose	>3M	nd	nd	1033	3.2	0.003	2137	6.2	0.003	166	41	0.25
L-arabinose	>3M	nd	nd	139	10.9	0.08	197	8.9	0.04	31	122	3.9
D-galactose	1650	2.1	nd	1368	13.5	0.01	2270	19.5	0.008	17.5	48	2.7

Units for V_{max} values are μmoles/min/mg

Units for K_m values are mM (unless otherwise stated)

nd represents values that were not determined

and in D-ribose the C3 hydroxyl group is in a different orientation and may reduce substrate binding.

The magnitude of difference between the K_m values for L-arabinose and D-glucose were the same with WT-GDH and N355D-GDH, suggesting that the C4 hydroxyl group is not essential for substrate binding. However, the K_m value for D-galactose was much higher than the value for D-glucose in mutant GDH, indicating that substrate binding to N355D-GDH is less efficient when the C4 hydroxyl group is above the plane of the ring.

The C6 hydroxymethyl group is not essential for binding because both D-glucose and D-xylose were oxidized. The only difference between these substrates is that D-xylose has no hydroxymethyl group at C5 (it only a five carbon compound). The affinity of WT-GDH for D-xylose is only 6 fold higher than for D-glucose; with Ba^{2+} and Sr^{2+}-GDH the affinity was 5-14 fold higher than that for D-glucose.

4.5.6 Summary of N355D-GDH characterisation

N355D-GDH was purified using the standard protocol with Pipes buffer. The major difference between N355D-GDH and WT-GDH was that Ca^{2+} reconstituted the mutant enzyme (K_d, 3.8mM), not Mg^{2+}. The affinity of N355D-GDH for PQQ (K_d, 0.41μM) was slightly lower than the affinity with WT-GDH, indicating that only the metal specificity had changed and not the reconstitution process. N355D-GDH was only 25% active compared with WT-GDH, but this is contributed by the low affinity for D-glucose (K_m, 949mM). The V_{max} values of Ca^{2+}-, Sr^{2+}- and Ba^{2+}-reconstituted N355D-GDH with D-glucose were 38%, 19% and 22% compared with that of WT-GDH. Inhibition studies showed that Mg^{2+} acted as a mixed (non-competitive) inhibitor. The K_i and K_{ii} values for Mg^{2+} binding were 11.4mM and 39.6mM respectively. Like WT-GDH, N355D-GDH had two metal binding sites; one at the active site and a second that binds metal ions to inhibit the enzyme.

4.6 Characterisation of D354N-GDH

D354N-GDH was purified in Pipes buffer (pH adjusted with NaOH) under conditions previously described in Section 2.4 (Table 4.7). Preliminary experiments showed that, in contrast with WT-GDH (but like N355D-GDH), Ca^{2+} supported reconstitution; activity with Mg^{2+} was lower. The standard reconstitution mixture for D354N-GDH was 5mM $CaCl_2$, 25μM PQQ and 50mM Pipes buffer pH 6.5. As with WT-GDH, reconstitution was too fast to measure accurately (the enzyme became 80% active within the first 2 minutes and was fully active within 10 minutes). The purified enzyme had 9% of the activity of WT-GDH and SDS-PAGE showed that it was 80% pure (Figure 4.25). The relatively low activity of solubilised D354N-GDH was not because of sensitivity to Triton X-100 because 0.5% did not inhibit the enzyme. Higher concentrations of Triton X-100 inhibited D354N-GDH to a greater extent than the inhibition observed with N355D-GDH (Figures 4.15AP and 4.26AP). The low affinity for D-glucose contributed to the low activity of the enzyme (Section 4.6.4).

4.6.1 The effect of divalent metals and PQQ on the reconstitution of D354N-GDH

D354N-GDH was 67% active after reconstitution in the absence of metal ions (addition of 5mM Ca^{2+} giving 100% activity). EDTA or EGTA treatment followed by gel filtration could not remove the metal ions that caused this activity (this activity could be removed from WT-GDH by treatment with 100mM EDTA Section 3.7). In an attempt to obtain metal-free enzyme, the membrane fraction was suspended in 10mM Pipes buffer pH 7.0 containing 100mM EDTA and incubated on ice for one hour. After the removal of EDTA and thorough washing, the GDH remained active after reconstitution in the absence of added metal ions. Addition of 5mM Ca^{2+}, Sr^{2+} and Ba^{2+} in the reconstitution process produced an enzyme that was 100%, 93% and 87% active respectively. Low concentrations (1mM) of Mg^{2+} reconstituted D354N-GDH but activity with 5mM was only 53% and this is lower than activity in the absence of added metal ions. Fe^{2+}, Mn^{2+}, Ni^{2+} and Co^{2+} did not support reconstitution.

When D354N-GDH, previously treated with 100mM EDTA, was incubated with low concentrations of Mg^{2+}, Ca^{2+}, Sr^{2+} and Ba^{2+} (Figure 4.27) higher activity was measured than with no added metal ions but in all cases higher concentrations led to a decrease in activity. 0.5-5mM Ca^{2+} reconstituted D354N-GDH but concentrations higher than 5mM inhibited reconstitution.

As shown with N355D-GDH (Section 4.5.1), the metal ion used in reconstitution had no significant effect on the affinity for PQQ; the K_d values with Ca^{2+}, Sr^{2+} and Ba^{2+} reconstituted D354N-GDH were 4.2μM, 3.2μM and 2.9μM respectively (Figure 4.28). The affinity was 10-15 fold greater than the affinity measured with Mg^{2+}-reconstituted WT-GDH (K_d, 0.28μM). As with

Table 4.7 Purification of D354N-GDH

D354N-GDH was purified by the method described in Section 2.4. The yield and levels of purification were similar to those with WT-GDH. Samples were reconstituted under standard conditions with 25μM PQQ and 5mM Ca^{2+} (instead of 5mM Mg^{2+} used with WT-GDH). Enzyme was assayed with 1.5M D-glucose. The specific activity of purified WT-GDH was 84μmoles/min/mg.

Sample	Volume (ml)	Total protein (mg)	Specific activity (μmoles/min/mg)	Yield (%)	Purification (fold)
Crude extract	37	910	0.67	100	1
Membranes	24.5	272	2.38	100	3.6
Soluble GDH	22.5	74	3.8	46	5.7
DEAE-GDH	21	19.5	7.4	24	11.0

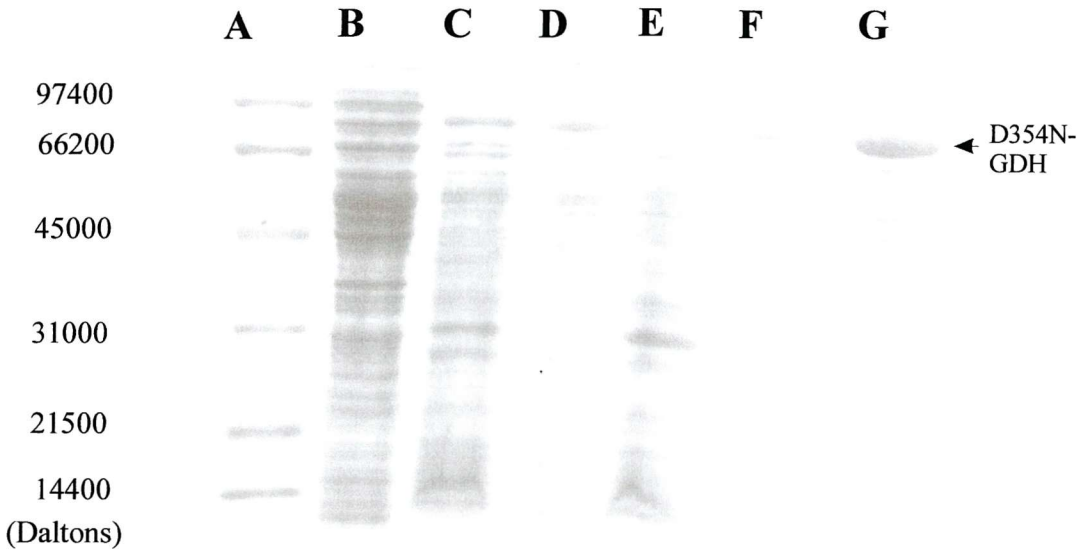

Figure 4.25 SDS-PAGE showing the purity of D354N-GDH

A) Protein standards

B) Crude extract (dil x5)

C) Membrane fraction (dil x5)

D) Soluble D354N-GDH (dil x5)

E) Pellet remaining after solubilisation of GDH (dil x5)

F) DEAE-sepharose purified D354N-GDH (diluted x5)

G) DEAE-sepharose purified D354N-GDH (undiluted)

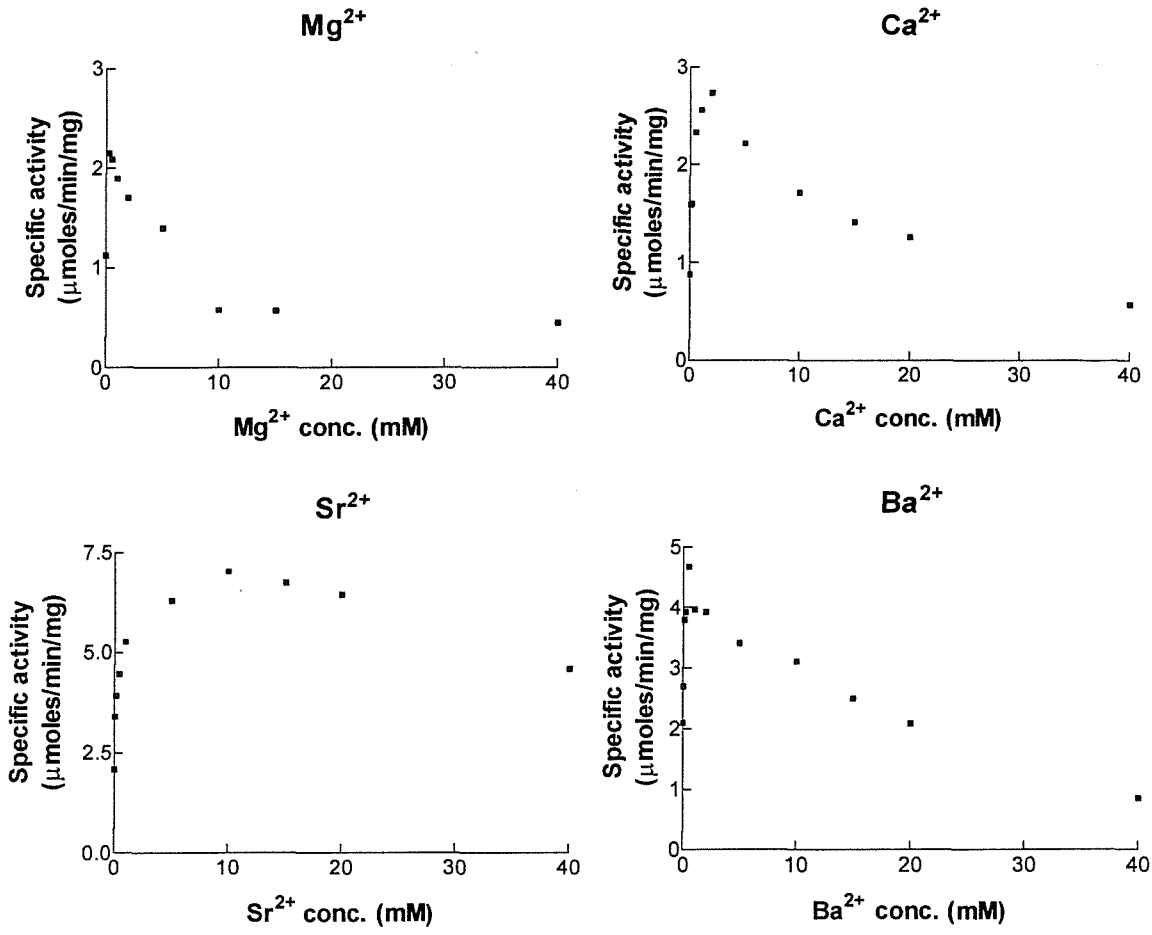

Figure 4.27 Activity of D354N-GDH after reconstitution of apoGDH with Mg^{2+}, Ca^{2+}, Sr^{2+} and Ba^{2+}

D354N-GDH purified in Pipes buffer was reconstituted under standard conditions with 25μM PQQ and various concentrations of metal ions (Mg^{2+}, Ca^{2+}, Sr^{2+} or Ba^{2+}). The enzyme had previously been incubated with 100mM EDTA that was removed by gel filtration. Activity was measured in the presence of 1.5M D-glucose with the standard assay.

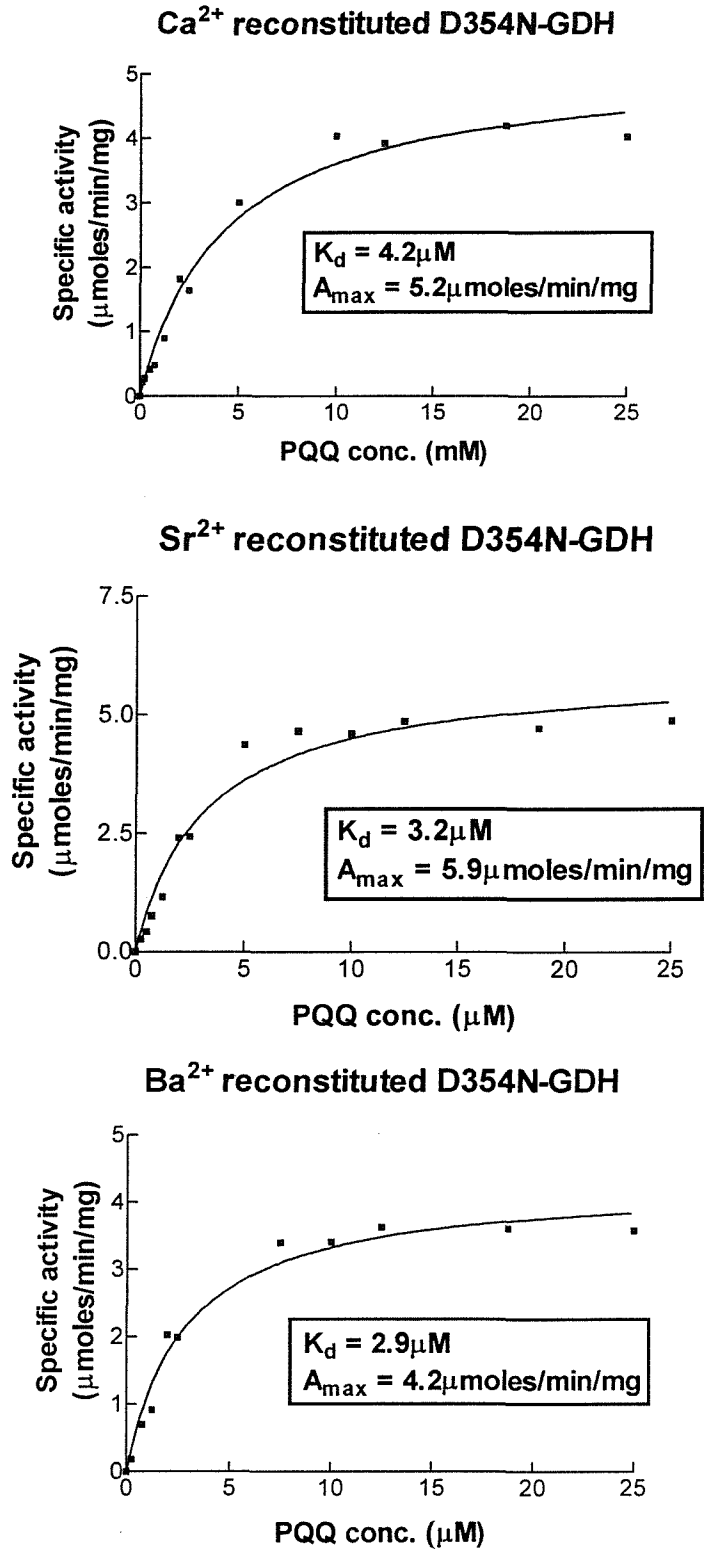

Figure 4.28 Affinity for PQQ with Ca^{2+}, Sr^{2+} and Ba^{2+} D354N-GDH

D354N-GDH was reconstituted under standard conditions with PQQ and 5mM metal ions (Ca^{2+}, Sr^{2+} or Ba^{2+}). Lines of best fit calculated by the equation $A=A_{max}[PQQ]/(K_d + [PQQ])$ where A is GDH activity.

WT-GDH, the affinity of D354N-GDH for PQQ was lower at pH values above 7.5 (Figure 4.29AP).

Gel filtration was used to confirm that metal binding and PQQ binding was reversible (Table 4.8AP). This removed 65% of the activity from reconstituted D354D-GDH suggesting that not all the metal ions were removed. Subsequent reconstitution with PQQ restored activity to 64% but reconstitution with only Ca^{2+} had little effect. Reconstitution with Ca^{2+} and PQQ restored activity to 71% indicating that PQQ binding is reversible but Ca^{2+} binding is not fully reversible.

The tolerance of D354N-GDH to EDTA and EGTA was similar to that observed with WT-GDH; low concentrations (0.5 – 4mM) of EDTA activated Ca^{2+}-reconstituted GDH and higher concentration inhibited it (Figure 4.30AP).

Unlike WT-GDH, Mg^{2+} could not support reconstitution of D354N-GDH and it inhibited Ca^{2+}-reconstituted GDH (Figure 4.31).

4.6.2 The thermal stability of D354N-GDH

Figure 4.32AP shows that the thermal stability of D354N-GDH was almost exactly the same as WT-GDH; incubating mutant and WT-GDH at 40°C for various time periods denatured 50% of the apoenzyme at 13.3 and 14.3 minutes respectively. HoloD354N-GDH was not denatured at this temperature showing that Ca^{2+} and PQQ could make the structure more stable. Incubating the enzymes at various temperatures showed that apoD354N-GDH was 50% denatured at 40.5°C and holo D354N-GDH at 49°C; the values for WT-GDH were 40.8°C and 51°C respectively.

4.6.3 The activation energy of D354N-GDH

The activation energies for the oxidation of D-glucose by Ca^{2+}, Sr^{2+} and Ba^{2+}-reconstituted D354N-GDH were similar to those measured with Mg^{2+} reconstituted WT-GDH (41kJ/mol) (Figures 3.32, 4.33 and 4.34). The value with Sr^{2+}-GDH was slightly lower (37kJ/mol) and with Ba^{2+}-GDH it was slightly higher (48kJ/mol). The value with Ca^{2+}-GDH was identical to the WT-GDH value (41kJ/mol). These results are fully discussed in Chapter 6.

4.6.4 The substrate specificity of D354N-GDH

The K_m values for all substrates were too high to measure. The response to glucose concentration being linear up to 1.5M showed that this mutation has affected glucose binding at the active site (Figure 4.35). The highest activity was with D-glucose and the substrate

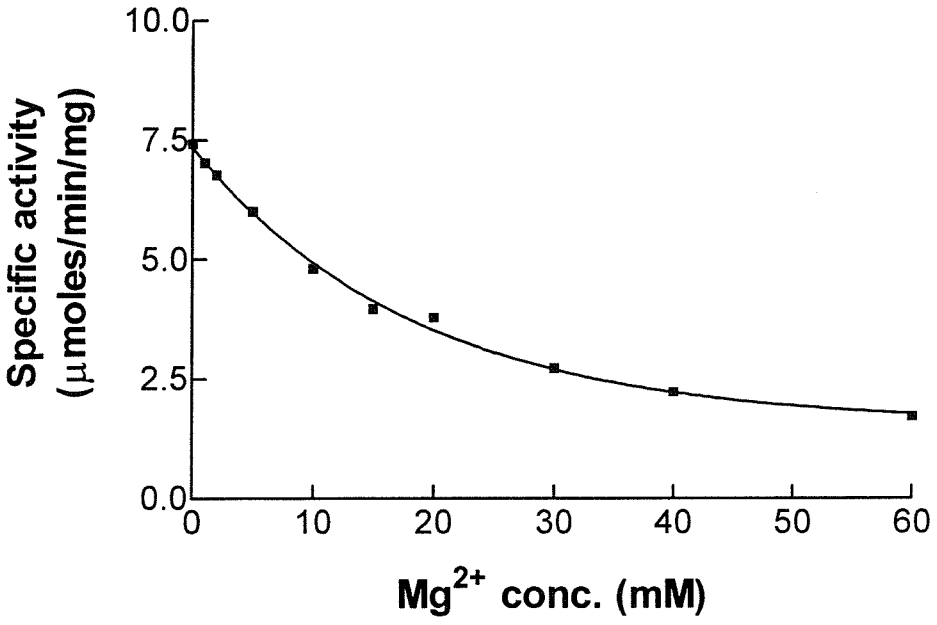

Figure 4.31 Inhibition of Ca^{2+}-reconstituted D354N-GDH by Mg^{2+}

D354N-GDH was reconstituted under standard conditions with 25μM PQQ and 5mM Ca^{2+}. Then various concentrations of Mg^{2+} (1-60mM) were added and incubated at 25°C for a further 20 minutes before activity was measured.

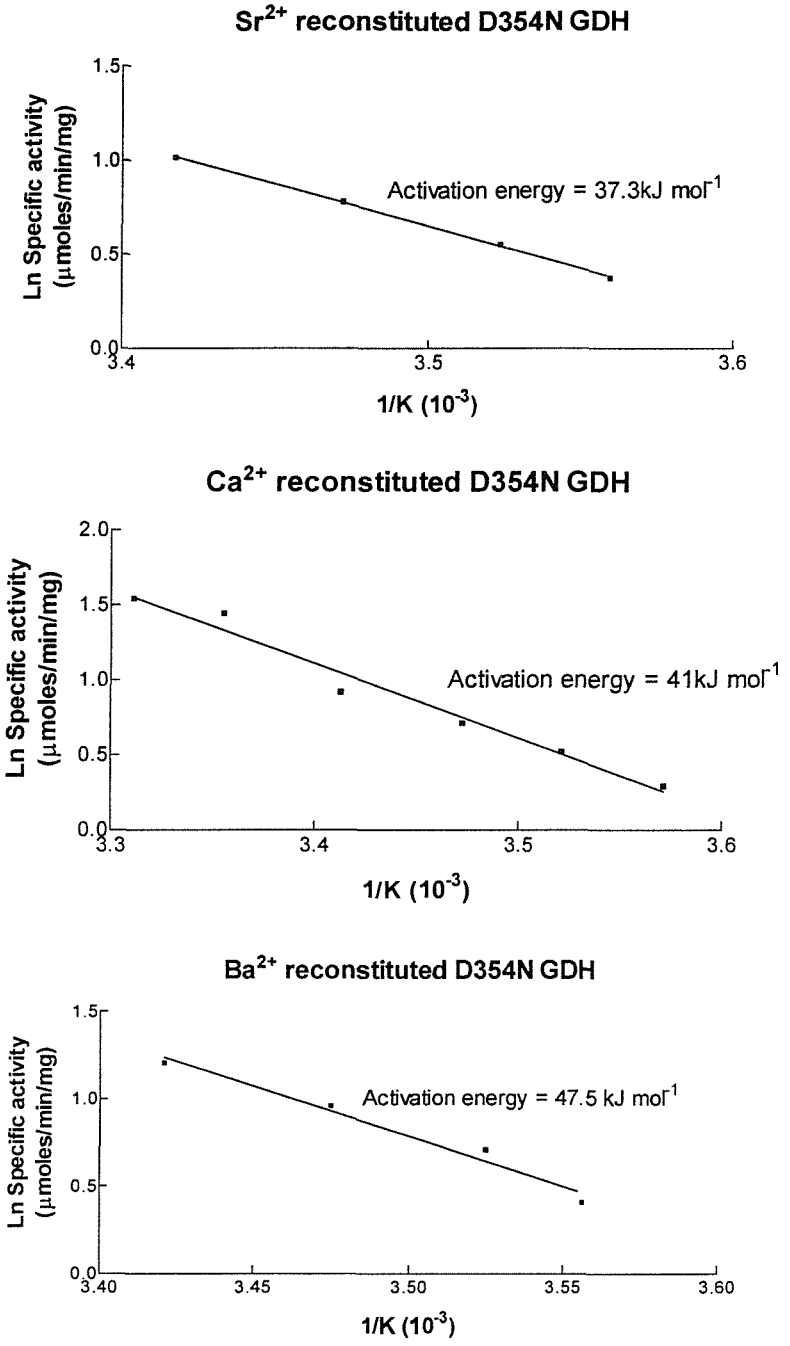

Figure 4.33 Activation energy of D354N-GDH reconstituted with Ca^{2+}, Sr^{2+} and Ba^{2+}

D354N-GDH was reconstituted under standard conditions with 25µM PQQ and 5mM metal ions (Ca^{2+}, Sr^{2+} and Ba^{2+}). Then activity was measured with the standard assay (1.5M D-glucose) at various temperatures (5-40°C). The formula relating activation energy (ΔG^*) is $v=A.\exp(-\Delta G^*/RT)$ where A is the Arrhenius constant and R is the gas constant. The ΔG^* values were calculated from the slopes of the curves. Results for the experiment with WT-GDH is shown in Figure 3.32.

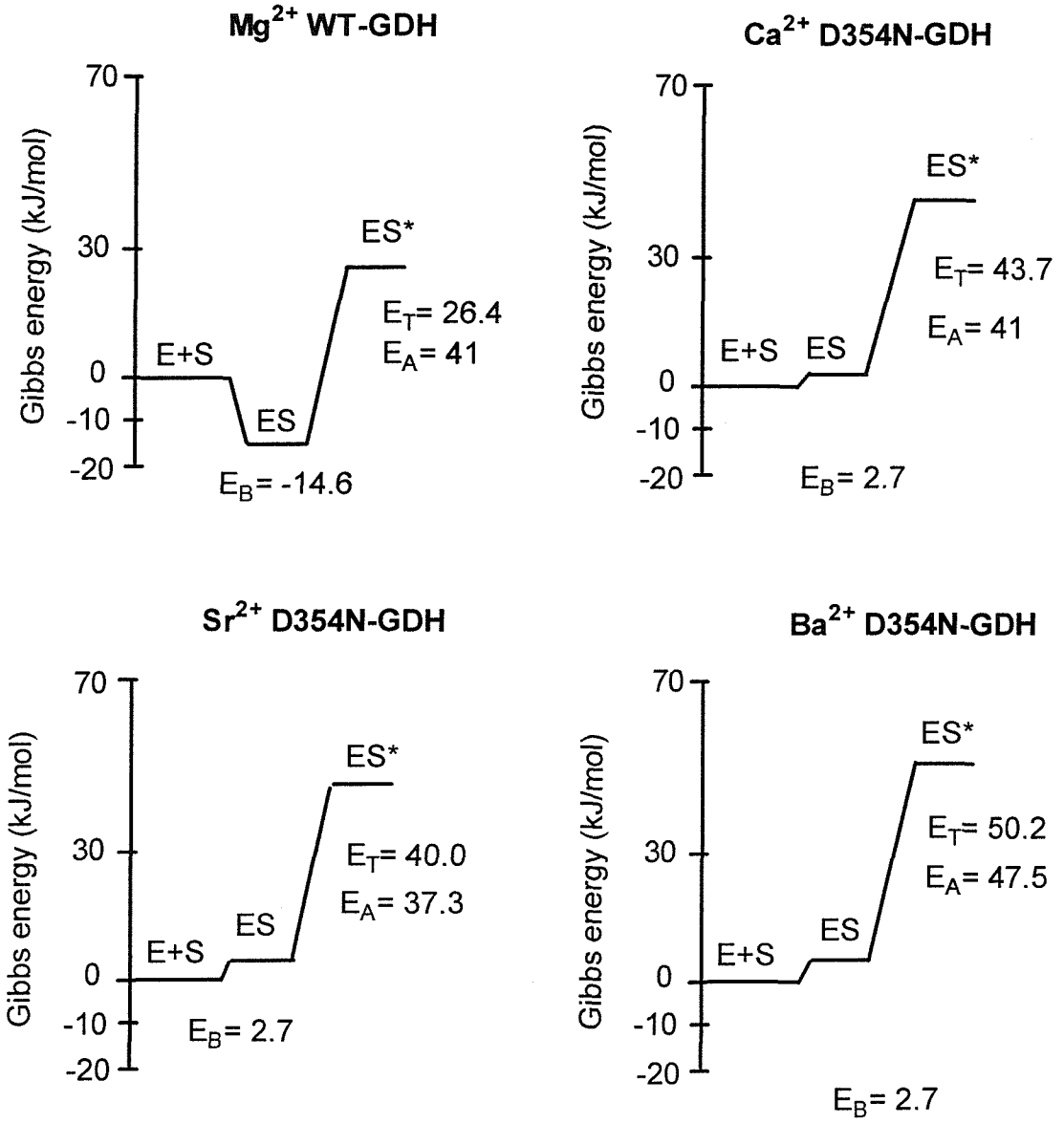

Figure 4.34 Schematic Gibbs free energy changes for the formation of the transition complex during the oxidation of D-glucose by D354N-GDH

The values for Gibbs free energy changes are in kJ/mol. E represents enzyme, S represents substrate, ES represents the enzyme-substrate complex and ES* is the transition state. E_A, E_B and E_T represent activation energy, binding energy and a measure of the energy of the transition complex respectively. E_A was calculated in Figure 4.33 and E_B was calculated by the equation $E_B = -RT \ln K_m$ where R is a gas constant and T is temperature. The K_m value used for D-glcuose was 3M because an accurate value could not be determined for the enzyme.

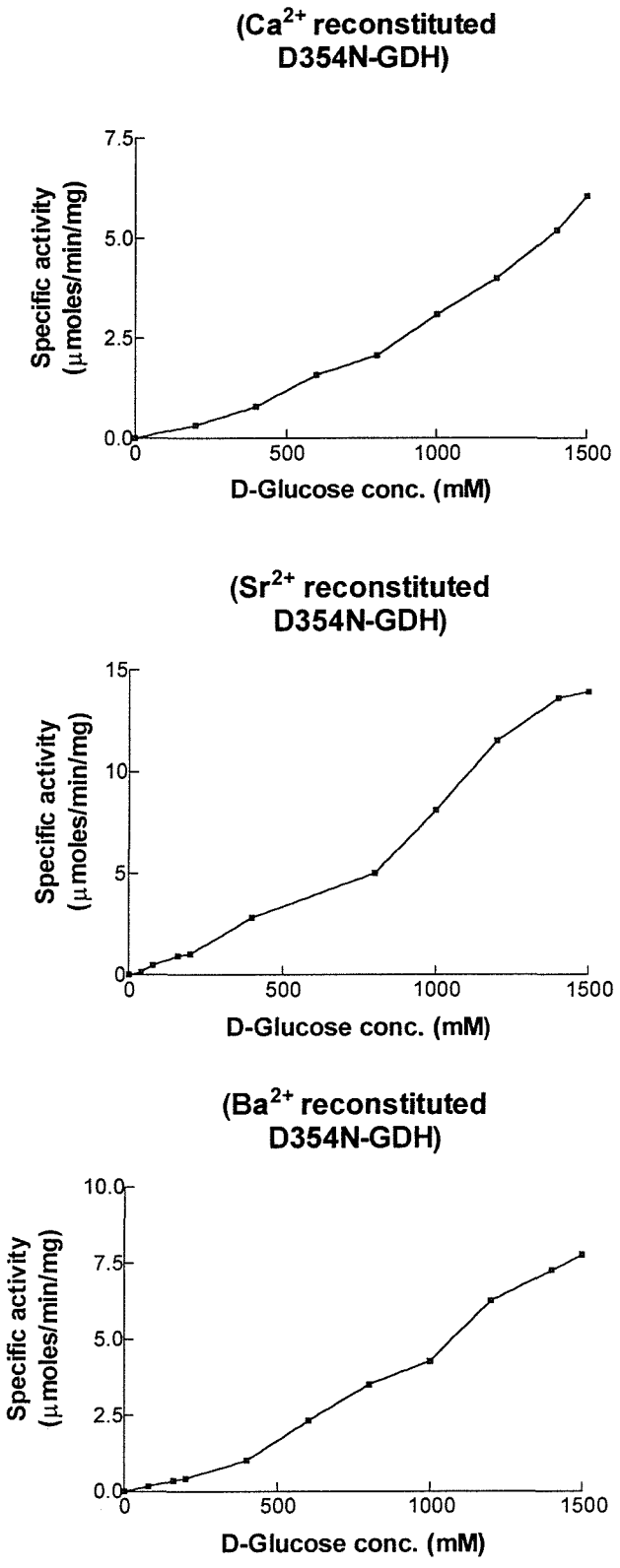

Figure 4.35 Activity of D354N-GDH with D-glucose

D354N-GDH was reconstituted under standard conditions with 25μM PQQ and 5mM metal ions (Ca^{2+}, Sr^{2+} or Ba^{2+}). Then activity was measured with the standard dye-linked assay containing various concentrations of D-glucose.

specificity of the enzyme had changed (Table 4.9). D-galactose and 3-O-methyl D-glucose were not oxidised even though they are by WT-GDH. The methyl group at the C3 position may cause steric hindrance and prevent substrate binding. The only difference between D-glucose and D-galactose is the position of the C4 hydroxy group but this cannot be critical for substrate binding because L-arabinose was oxidized in which the C4 hydroxyl group has the same orientation as in D-galactose. Also, D-mannose and D-ribose were oxidised by Ca^{2+}-reconstituted D354N-GDH but not by Ba^{2+} and Sr^{2+}-reconstituted enzyme suggesting that larger metal ions may prevent binding.

4.6.5 Summary of D354N-GDH characterisation

D354N-GDH was purified in Pipes buffer, the yield and purification levels being similar to WT-GDH. Similar to the N355D-GDH, Ca^{2+} was required to reconstitute D354N-GDH. This enzyme was 9% active compared with Mg^{2+}-reconstituted WT-GDH; the low affinity for D-glucose (K_m, >3M) contributes to this low activity. Sr^{2+} and Ba^{2+} also supported reconstitution, but the affinities of metal binding could not be determined because it was 67% active after reconstitution in the absence of added metal ions. EDTA or EGTA treatment did not give an enzyme that required the addition of metal ions for activity. The activation energies of Ca^{2+}, Sr^{2+} and Ba^{2+}-reconstituted D354N-GDH suggest that the enzyme's mechanism has not been altered by the mutation.

Table 4.9 The substrate specificity of D354N-GDH

D354N-GDH was reconstituted under standard conditions with 5mM metal ions (Ca^{2+}, Sr^{2+} or Ba^{2+}) and 25μM PQQ. Activity was measured with the standard dye-linked assay containing 1.5M of various substrates. The relative activity compared with D-glucose is shown.

	Relative activity compared with D-glucose (%)			
Substrate	Ca^{2+}-GDH	Sr^{2+}-GDH	Ba^{2+}-GDH	WT-GDH*
D-glucose	100	100	100	100
2-deoxy-D-glucose	91	34	24	118
D-xylose	44	30	28	53
L-arabinose	44	32	21	106
D-mannose	4	0	0	118
D-ribose	11	0	0	35
D-galactose	0	0	0	41
L-glucose	0	0	0	0
D-arabinose	0	0	0	0
3-O-methly-glucose	0	0	0	66
D-maltose	0	0	0	0

* The values for WT-GDH are % of the V_{max} with D-glucose

4.7 Characterisation of D354N/N355D-GDH

D354N/N355D-GDH was constructed and characterised to determine if the number of ligands available to the metal ion affects the specificity of metal ions used in the reconstitution process. In the GDHs with a single mutation the number of possible coordinations to the metal ion were different (6 ligands in D354N-GDH and 8 in N355D-GDH). In this double mutant the number of ligands were the same as with WT-GDH (7 in total) but the position of residues 354 and 355 had been reversed, changing the orientation of the side chains in the active site. It was purified in Pipes buffer (pH adjusted with NaOH) under the protocol described in Section 2.4. As with D354N-GDH and N355D-GDH, Ca^{2+} was required for reconstitution instead of Mg^{2+} and the rate of reconstitution was unaffected; it was more than 80% within 2 minutes and 100% active within 10 minutes. Table 4.10 shows that purified D354N/N355D-GDH was about 10 % active compared with WT-GDH. SDS-PAGE confirmed that D354N/N355D-GDH was about 90% pure (Figure 4.36).

4.7.1 The effect of divalent metals and PQQ on the reconstitution of D354N/N355D-GDH

Again, there was a problem of studying the role of metal ions in the reconstitution process because the enzyme was 48% active after reconstituting in the absence of added metal ions (Figure 4.37). Mg^{2+} did not support reconstitution and accurate K_d values for Ca^{2+}, Sr^{2+} and Ba^{2+} could not be calculated because of the high activity without added metal ion (Figure 4.38). As with D354N-GDH, EDTA treatment could not remove the metal ions that caused this activity. 100mM EDTA only decreased activity from 48% to 30% in the absence of metal ions. EGTA was not successful and didn't decrease the activity at all.

The affinity of D354N/N355D-GDH for PQQ was three to four-fold lower than that with WT-GDH (Figure 4.39AP). The K_d values were 0.74μM, 1.01μM and 0.94μM for D354N/N355D-GDH reconstituted with Ca^{2+}, Sr^{2+} and Ba^{2+} respectively. The affinity for PQQ binding (as also shown with WT-GDH and other mutants) decreased at pH values above 7.5 (Figure 4.40AP).

Gel filtration confirmed that Ca^{2+} and PQQ binding to D354N/N355D-GDH was reversible (Table 4.11AP). The double mutation may have increased the enzyme's tolerance to chelating reagents such as EDTA (Figure 4.41AP) because more was required to abolish activity (30-40mM); WT-GDH only required 8mM. However, as observed with WT-GDH, D354N-GDH and N355D-GDH, low concentrations (0.5-5.0mM) inexplicably activated the reconstituted enzyme.

Table 4.10 Purification of D354N/N355D-GDH

D354N/N355D-GDH was purified by the method described in Section 2.4. The yield and levels of purification were similar to those of WT-GDH. Samples were reconstituted under standard conditions with 25μM PQQ and 5mM Ca^{2+} (instead of the 5mM Mg^{2+} used with WT-GDH). Activity measured in the presence of 1.5M D-glucose. The specific activity of purified WT-GDH was 84μmoles/min/mg.

Sample	Volume (ml)	Total protein (mg)	Specific activity (μmoles/min/mg)	Yield (%)	Purification (fold)
Crude extract	51	992	0.82	100	1
Membranes	26	321	2.85	100	3.5
Soluble GDH	24	115	4.22	60	5.1
DEAE-GDH	30.5	29.8	8.13	27	9.9

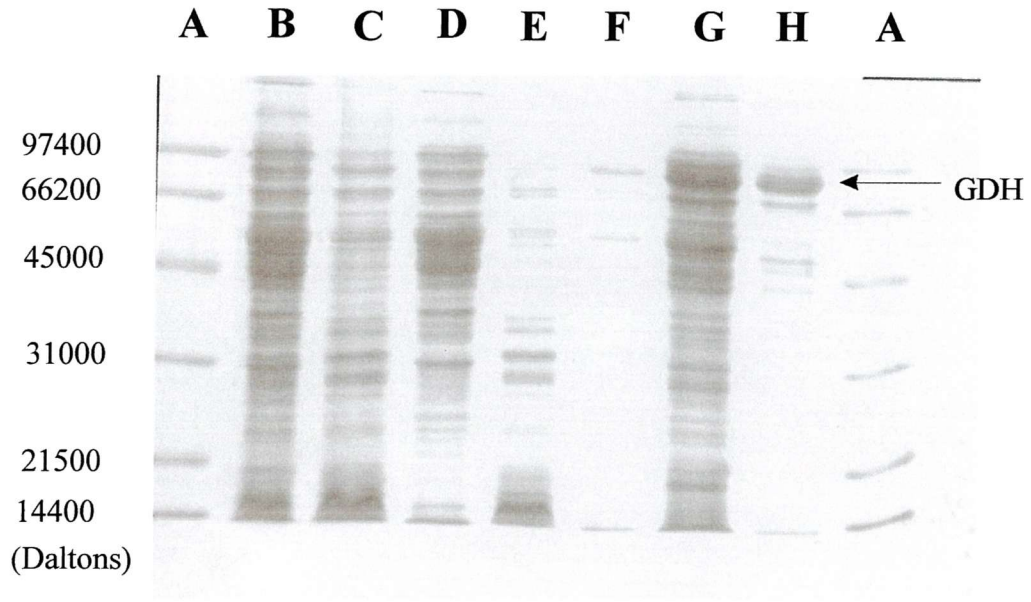

Figure 4.36 SDS-PAGE showing the purity of D354N/N355D-GDH

A) Protein standards

B) Crude extract (dil x6)

C) Membrane fraction (dil x6)

D) Supernatant from membrane isolation (dil x6)

E) Pellet remaining after solubilisation of GDH (dil x6)

F) Soluble D354N/N355D-GDH (dil x6)

G) Soluble D354N/N355D-GDH (undiluted)

H) DEAE-sepharose purified D354N/N355D-GDH (undiluted)

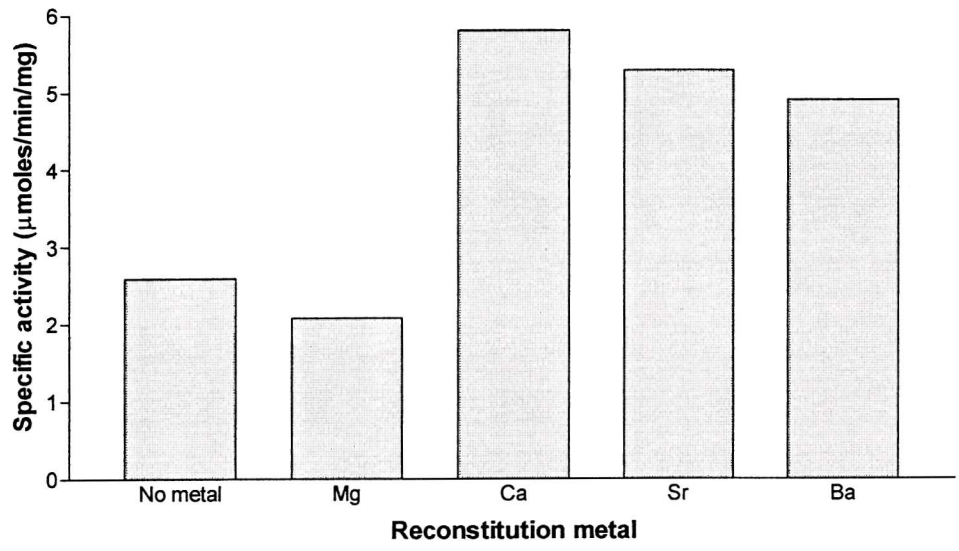

Figure 4.37 Reconstitution of D354N/N355D-GDH with Mg^{2+}, Ca^{2+}, Sr^{2+} and Ba^{2+}

D354N/N355D-GDH was reconstituted under standard conditions with 5mM metal ion (Ca^{2+}, Sr^{2+} or Ba^{2+}) and 25μM PQQ. Activity was measured in the presence of 1.5M D-glucose.

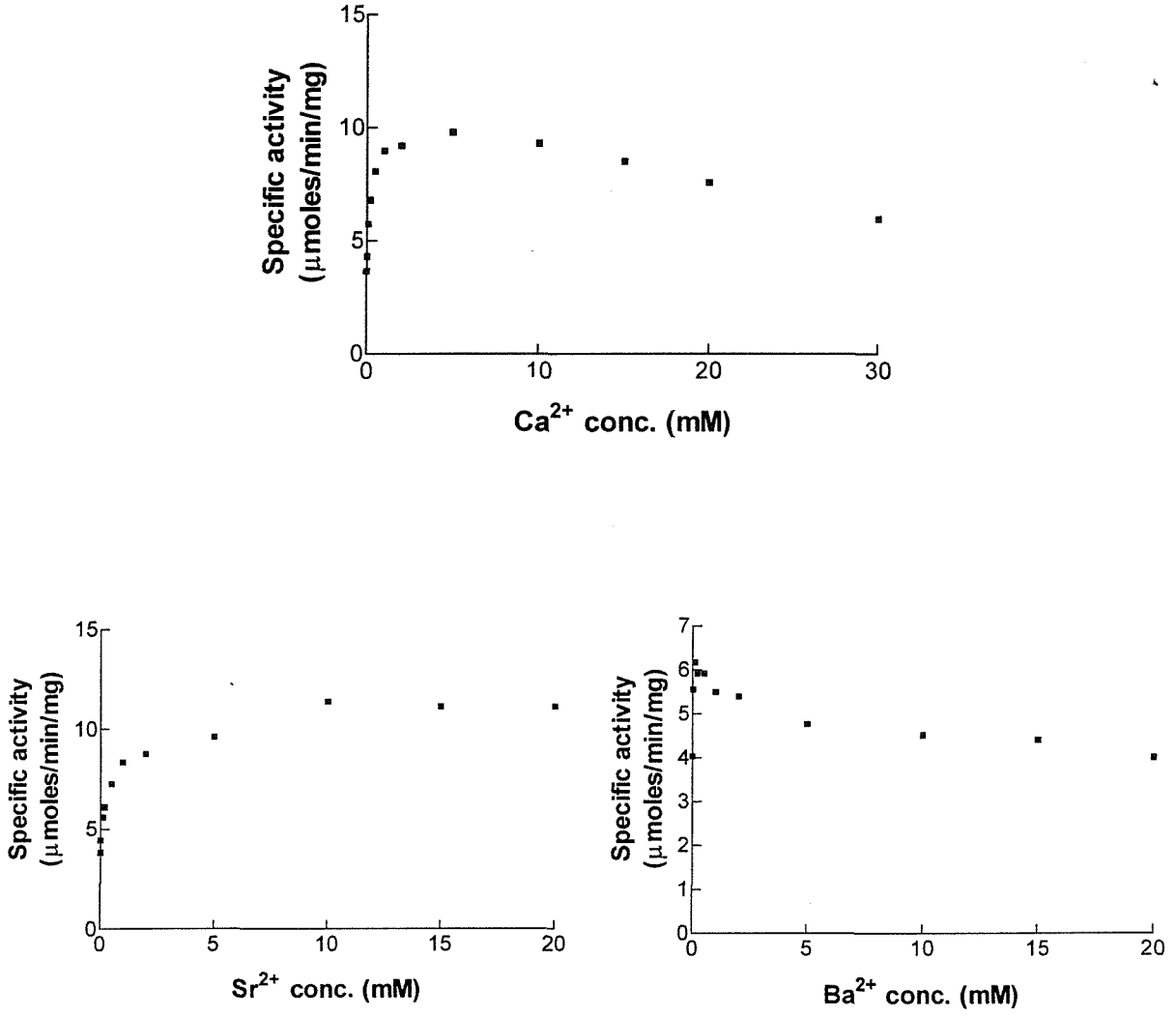

Figure 4.38 Reconstitution of D354N/N355D-GDH with various concentrations of Ca^{2+}, Sr^{2+} and Ba^{2+}

D354N/N355D-GDH purifird in Pipes buffer was incubated with 100mM EDTA at 25°C for 15 minutes. Then EDTA was removed by gel filtration and the enzyme reconstituted under standard conditions with 25μM PQQ and metal ions (Ca^{2+}, Sr^{2+} and Ba^{2+}). Activity measured in the presence of 1.5M D-glucose.

4.7.2 The effect of Mg^{2+} on D354N/N355D-GDH reconstituted with Ca^{2+}

Figure 4.42 shows that incubation with Mg^{2+} of holoGDH reconstituted with Ca^{2+} led to loss of activity, 20mM Mg^{2+} giving 50% loss of activity. Further kinetic studies could not be completed because a sample that did not require metal ions for activity could not be obtained. It was therefore impossible to determine whether Mg^{2+} is a competitive inhibitor or mixed (non-competitive inhibitor).

4.7.3 The thermal stability of D354N/N355D-GDH

The thermal stability of D354N/N355D-GDH was similar to that of WT-GDH (Figure 4.43AP). ApoD354N/N355D-GDH was denatured at 40°C with a half-life of 15 minutes (14.3minutes for WT-GDH) but holoD354N/N355D-GDH was stable at this temperature. Incubating the enzyme at various temperatures showed that 50% denaturation occurred at 41°C and 48.6°C for apo and holoD354N/N355D-GDH (40.8°C and 51°C for apo and holoWT-GDH).

4.7.4 The activation energy of D354N/N355D-GDH

The activation energy for the oxidation of D-glucose with D354N/N355D-GDH reconstituted with Ca^{2+}, Sr^{2+} and Ba^{2+} is shown in Figures 4.44 and 4.45. The activation energy with Ba^{2+} reconstituted enzyme was the same as for Ba^{2+}-D354N-GDH (47kJ mol^{-1}); this was slightly higher than the WT-GDH value (41kJ mol^{-1}). The activation energy with Ca^{2+} reconstituted enzyme was the same as WT-GDH but the value with Sr^{2+} was significantly lower (26kJ mol^{-1}). These results are fully described in Chapter 6.

4.7.5 The substrate specificity of D354N/N355D-GDH

The double mutation caused a large decrease in affinity for all substrates, thus preventing the determination of kinetic constants (Table 4.12). This was similar to D354N-GDH (Section 4.6.4). Only K_m and V_{max} values for 2-deoxy-D-glucose and L-arabinose were determined using D354N/N355D-GDH reconstituted with Sr^{2+} and Ba^{2+}. This indicated that they have a higher affinity for substrates than enzyme reconstituted with Ca^{2+}. The affinity of D354N/N355D-GDH reconstituted with Sr^{2+} or Ba^{2+} for 2-deoxy-D-glucose was more than 314-457 times higher than that measured with WT-GDH (K_m, 3.5mM). As with D354N-GDH, D-mannose was not oxidised. These results suggest that the conformation of the binding site had changed due to the mutations in D354N/N355D-GDH. The affinity of D354N/N355D-GDH for substrates is more like D354N-GDH than N355D-GDH. Asp-354 may be more important for substrate binding that Asn-355.

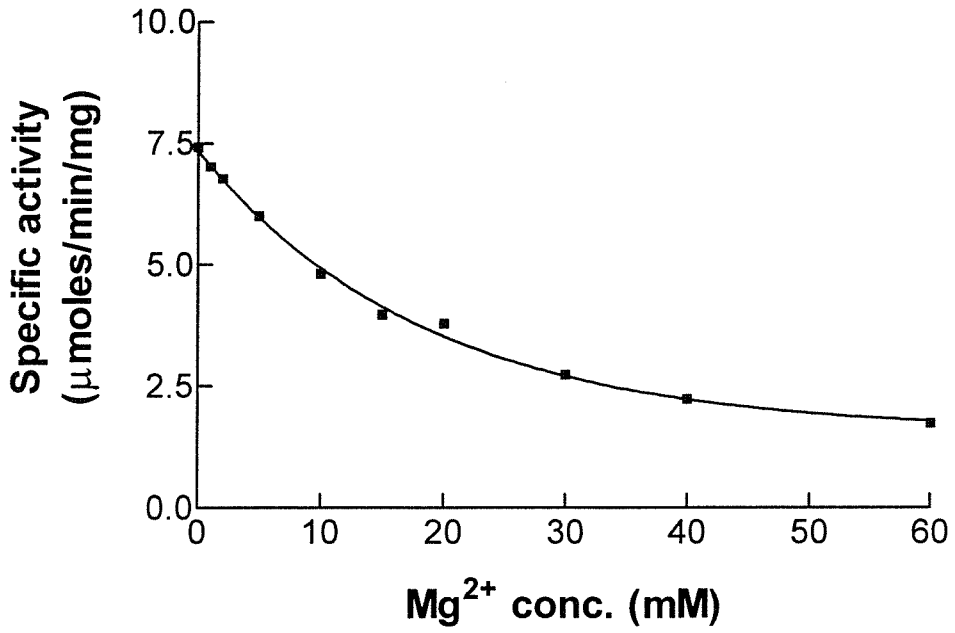

Figure 4.42 The inhibition of Ca^{2+}-reconstituted D354N/N355D-GDH by Mg^{2+}

D354N/N355D-GDH was reconstituted under standard conditions with 5mM Ca^{2+} and 25μM PQQ. Then various concentrations of Mg^{2+} (1-60mM) were added and incubated at 25°C for a further 20 minutes before activity was measured.

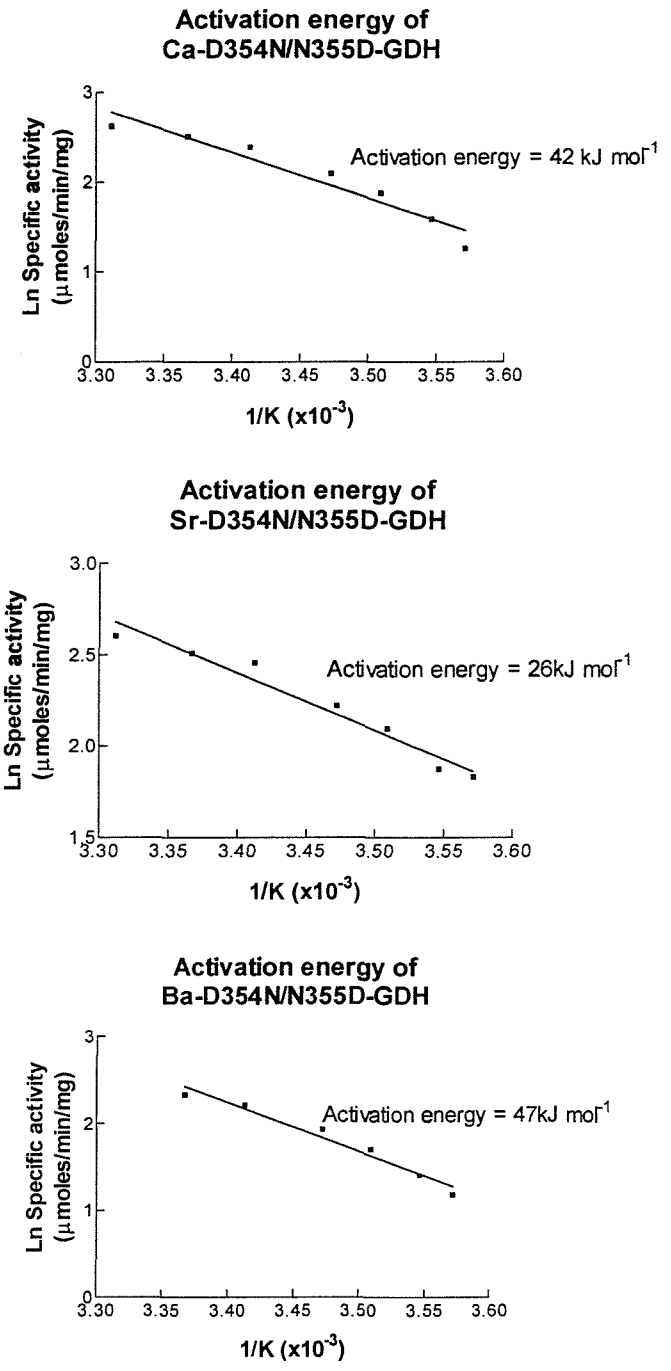

Figure 4.44 Activation energy of D354N/N355D-GDH reconstituted with Ca^{2+}, Sr^{2+} and Ba^{2+}

D354N/N355D-GDH was reconstituted under standard conditions with 25μM PQQ and 5mM metal ions (Ca^{2+}, Sr^{2+} or Ba^{2+}). Then activity was measured with the standard assay (1.5M D-glucose) at various temperatures (5-40°C). The formula relating activation energy (ΔG*) is v=A.exp(-ΔG*/RT) where A is the Arrhenius constant and R is the gas constant. The ΔG* values were calculated from the slopes of the curves. Results with WT-GDH are shown in Figure 3.32.

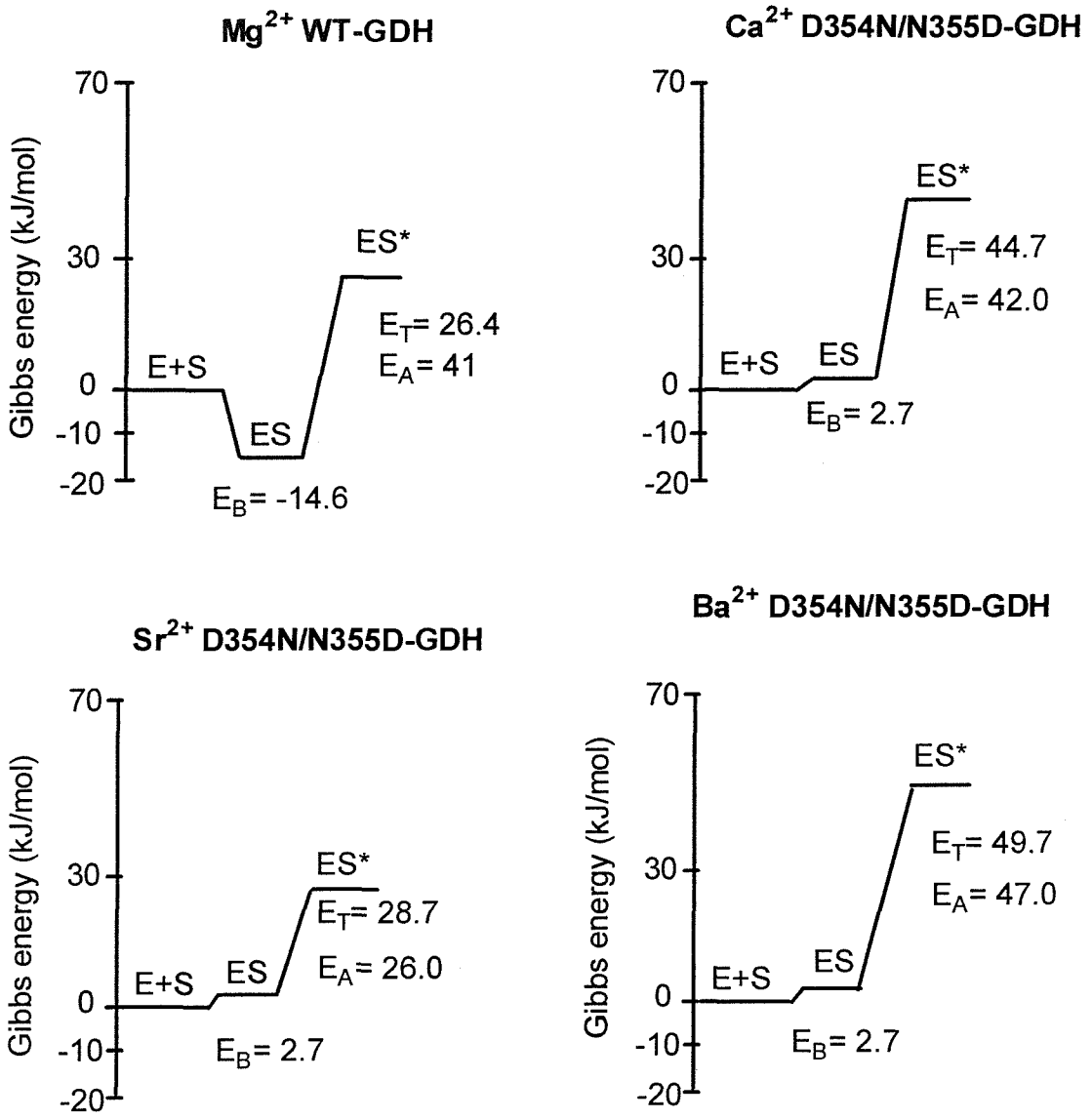

Figure 4.45 Schematic Gibbs free energy changes for the formation of the transition complex during the oxidation of D-glucose by D354N/N355D-GDH

The values for Gibbs free energy changes are in kJ/mol. E represents enzyme, S represents substrate, ES represents the enzyme-substrate complex and ES* is the transition state. E_A, E_B and E_T represent activation energy, binding energy and a measure of the energy of the transition complex respectively. E_A was calculated in Figure 4.44 and E_B was calculated by the equation $E_B = -RT \ln K_m$ where R is a gas constant and T is temperature. The K_m value for D-glucose was 3M because accurate values could not be determined.

Table 4.12 The substrate specificity of D354N/N355D-GDH

D354N/N355D-GDH was reconstituted with 5mM metal ions (Ca^{2+}, Sr^{2+} or Ba^{2+}) and 25μM PQQ. Activity was measured with the standard dye-linked assay containing various concentrations of substrates. Compounds that were not oxidised are indicated by (X). V_{max} values with some sugars were not determined accurately (nd). The activity with all substrates was compared with the activity of Ca^{2+}-reconstituted enzyme with 1.5M D-glucose (%). As with WT-GDH and other mutants the following sugars were not oxidised; L-glucose, D-arabinose and D-maltose.

Substrate	Reconstitution metal	K_m (M)	V_{max} (μmoles/min/mg)	Activity with 1.5M substrate (μmoles/min/mg)	K_m values for WT-GDH (mM)	V_{max} values for WT-GDH (μmoles/min/mg)
D-glucose	Ca^{2+}	>3	nd	8.25 (100%)	2.8	116
	Sr^{2+}	>3	nd	7.42 (90%)	NA	NA
	Ba^{2+}	>3	nd	4.85 (59%)	NA	NA
2-Deoxy-D-glucose	Ca^{2+}	>3	nd	5.03 (61%)	3.5	137
	Sr^{2+}	1.1	8.7	4.95 (60%)	NA	NA
	Ba^{2+}	1.6	14.1	6.56 (80%	NA	NA
D-mannose	Ca^{2+}	X	X	X	116	137
	Sr^{2+}	X	X	X	NA	NA
	Ba^{2+}	X	X	X	NA	NA
L-arabinose	Ca^{2+}	>3	nd	2.44 (30%)	31.2	122
	Sr^{2+}	1.8	7.8	3.49 (42%)	NA	NA
	Ba^{2+}	0.99	3.2	2.04 (25%)	NA	NA
D-xylose	Ca^{2+}	>3	nd	1.91 (23%)	17	61
	Sr^{2+}	>3	nd	5.84 (71%)	NA	NA
	Ba^{2+}	2.1	nd	2.02 (24%)	NA	NA
D-galactose	Ca^{2+}	>3	nd	0.26 (3%)	17.5	48
	Sr^{2+}	>3	nd	0.60 (7%)	NA	NA
	Ba^{2+}	>3	nd	0.34 (4%)	NA	NA

4.7.6 Summary of D354N/N355D-GDH characterisation

D354N/N355D-GDH was purified in Pipes buffer, the yield and purification levels being similar to WT-GDH. As with N355D-GDH and D354N-GDH, Ca^{2+} was required for reconstitution. This enzyme had 10% of the activity of Mg^{2+}-reconstituted WT-GDH, but to a large extent this could be due to the enzyme having such a low affinity for D-glucose (K_m, >3M). Sr^{2+} and Ba^{2+} also supported reconstitution, but the affinities of metal binding to D354N/N355D-GDH could not be determined because it was 48% active in the absence of added metal ions. EDTA treatment did not give an enzyme that required the addition of metal ions for activity (activity in the absence of metal ions only decreased from 48% to 30%). The activation energies of Ca^{2+} and Ba^{2+}-reconstituted D354N-GDH suggest that the enzyme's mechanism has not been altered by the mutation. However, the activation energy with Sr^{2+} reconstituted D354N/N355D-GDH had decreased by nearly half compared with that of WT-GDH.

4.8 Characterisation of T424N-GDH

The T424N mutation was provided by Professor Sode (Sode and Yoshida, 1996). Plasmid pGEcIT424N that codes for the mutant GDH was transformed into *E. coli* strain PP2418. The mutant was then purified and characterised. Based on the model for GDH, Thr-424 is expected to make one bond with the active site metal ion (Figure 4.1b).

T424N-GDH was purified in Pipes buffer (pH adjusted with NaOH) under conditions previously described in Section 2.4 (Table 4.13). Preliminary work showed that Mg^{2+} and Ca^{2+} both supported reconstitution but activity was higher with Ca^{2+}. The rate of reconstitution (with Ca^{2+} or Mg^{2+}) was similar to WT-GDH and other mutant GDHs previously described in this Chapter. The standard reconstitution mixture for T424N-GDH was 50mM Pipes pH 6.5, 25μM PQQ and 5mM $CaCl_2$. Table 4.13 shows that purified T424N-GDH had 20% of the activity of WT-GDH. The relatively low activity of solubilised T424N-GDH was not caused by the sensitivity to Triton X-100 because 0.5% of this detergent did not inhibit the enzyme. The low activity is probably due to the low affinity of Ca^{2+}-reconstituted T424N-GDH for D-glucose (K_m greater than 3M; see Section 4.8.5). SDS-PAGE confirmed that purified T424N-GDH was the correct size (Figure 4.46).

4.8.1 The effect of divalent metals and PQQ on the reconstitution of T424N-GDH

T424N-GDH was 28% active after reconstitution in the absence of metal ions. Treatment with 100mM EGTA reduced this from 28% to 3.5% but 100mM EDTA had no affect. This was unlike WT-GDH, in which EDTA was better than EGTA. T424N-GDH could be reconstituted with Mg^{2+}, Ca^{2+}, Sr^{2+}, Ba^{2+} but as with WT-GDH, Ni^{2+}, Fe^{2+}, Mn^{2+} and Co^{2+} inactivated the enzyme.

The K_d values for Mg^{2+}, Ca^{2+}, Sr^{2+} and Ba^{2+} were 0.36mM, 0.85mM, 0.37mM and 0.09mM respectively (Figure 4.47 and Table 4.14). The highest A_{max} was obtained after reconstitution with Ca^{2+} (11.7μmoles/min/mg) and the lowest with Mg^{2+} (1.7μmoles/min/mg). This mutation affected the metal specificity because WT-GDH can only be reconstituted with Mg^{2+} (K_d, 1.5mM) whereas T424N-GDH could be reconstituted with and Ca^{2+}, Sr^{2+} and Ba^{2+}. These metals inhibited reconstitution of WT-GDH. As with N355D-GDH, the K_d values for Ca^{2+} binding were not affected between pH 5.5 and 8.0. This was also true for Mg^{2+} binding to WT-GDH.

The K_d for PQQ with Ca^{2+}, Sr^{2+} and Ba^{2+} were 1.2μM, 0.82μM and 0.86μM respectively (Figure 4.48); the metal used in reconstitution only had a slight affect on the affinity of T424N-GDH for PQQ. These values are three to four-fold higher than that of WT-GDH (K_d, 0.28μM).

Table 4.13 Purification of T424N-GDH

T424N-GDH was purified by the method described in Section 2.4. The levels of purification were similar to those of WT-GDH. Samples were reconstituted under standard conditions with 25μM PQQ and 5mM Ca^{2+} (instead of 5mM Mg^{2+} used to reconstitute WT-GDH). 1.5M D-glucose used in the enzyme assay. The specific activity of purified WT-GDH was 84μmoles/min/mg.

Sample	Volume (ml)	Total protein (mg)	Specific activity (μmoles/min/mg)	Yield (%)	Purification (fold)
Crude extract	49	1120	0.58	100	1
Membranes	25	242	2.2	82	3.7
Soluble GDH	23	81.4	6.5	81	11.2
DEAE-GDH	29	29.5	16.7	75	28.7

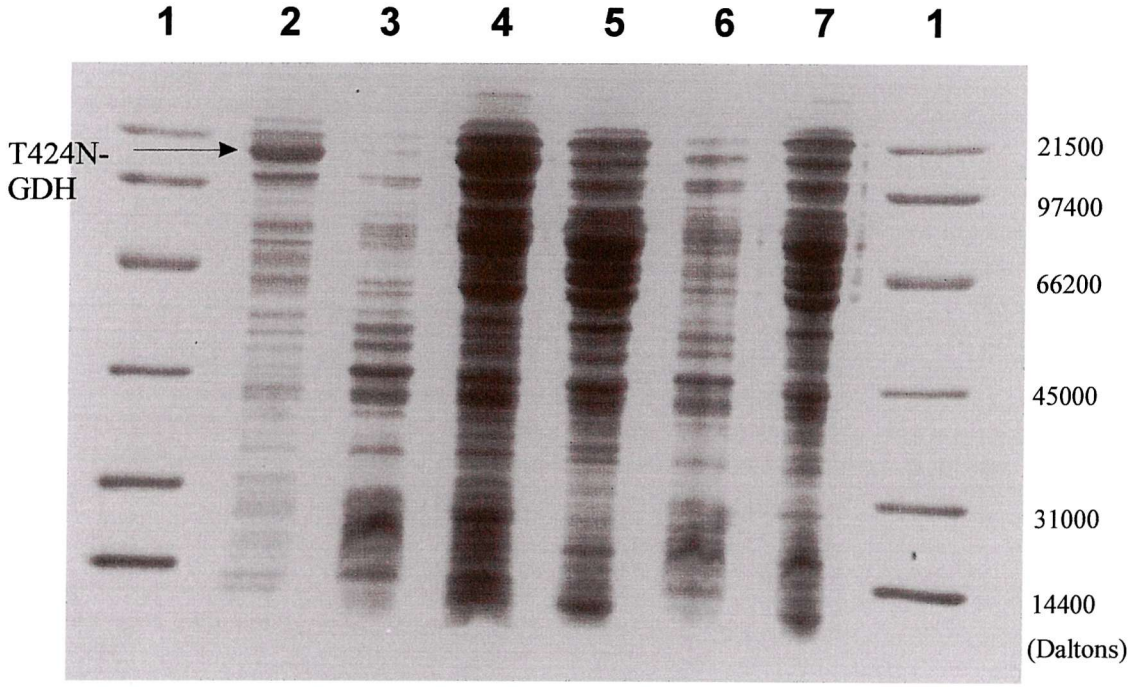

Figure 4.46 SDS-PAGE showing the purity of T424N-GDH

1) Standard proteins

2) DEAE-Sepharose GDH

3) Membrane fraction after GDH solubilization

4) Soluble GDH

5) Membrane fraction

6) Supernatant from membrane isolation step

7) Crude extract (diluted x 20)

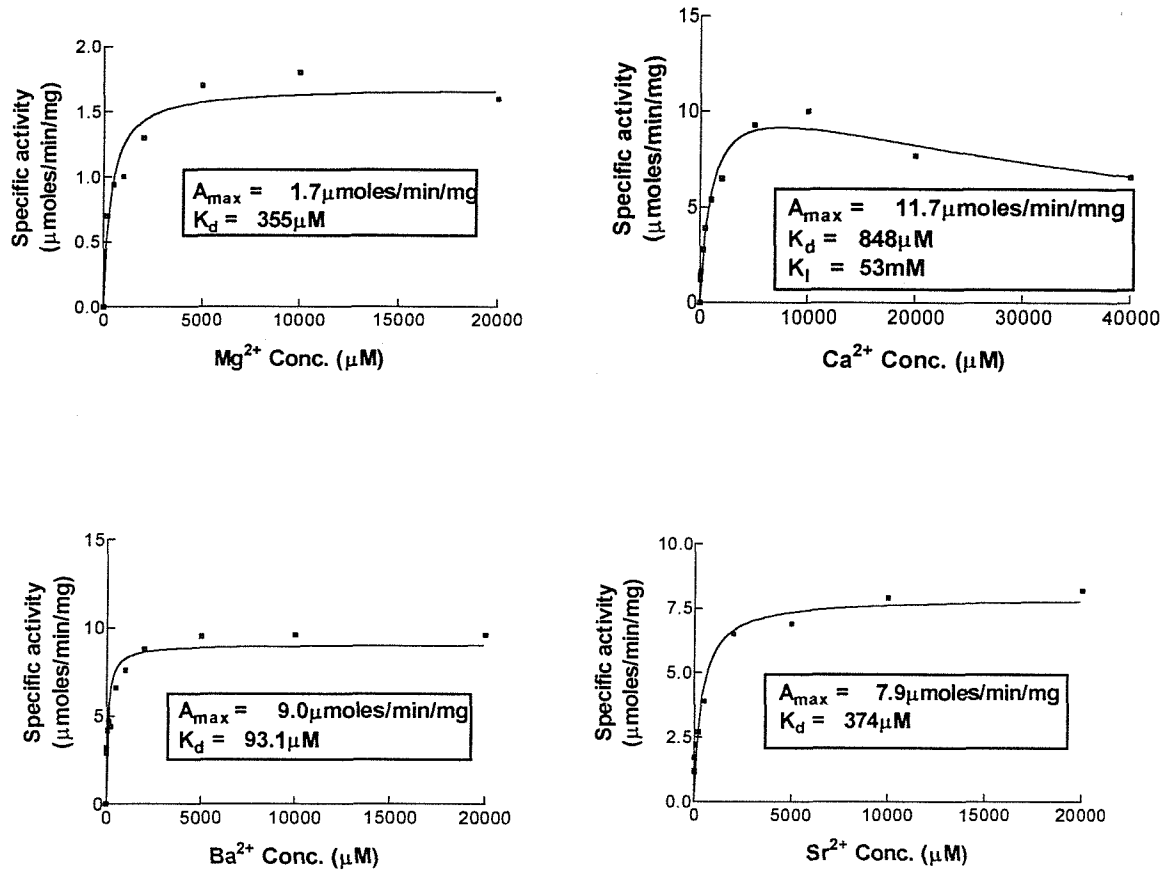

Figure 4.47 Reconstitution of T424N-GDH with Mg^{2+}, Ca^{2+}, Sr^{2+} and Ba^{2+}

T424N-GDH purified in Pipes buffer was incubated with 100mM EGTA for 15 minutes at 25°C. Then EGTA was removed by gel filtration and the enzyme reconstituted under standard conditions with 25μM PQQ and metal ions (Mg^{2+}, Ca^{2+}, Sr^{2+} or Ba^{2+}). The lines of best fit were calculated by the equation $A=A_{max}[M^{2+}]/(K_d + [M^{2+}])$ where A is GDH activity and M^{2+} represents metal ion except for T424N-GDH reconstituted with Ca^{2+} which used the equation $A=A_{max}[Ca^{2+}]/(K_d + [Ca^{2+}]\{1+Ca^{2+}/k_i\})$.

Table 4.14 Metal ion specificity of T424N-GDH

This Table is based on the data from Figure 4.47. T424N-GDH purified in Pipes buffer was reconstituted under standard conditions with 25μM PQQ and various metal ion concentrations.

Metal	Ionic radius (nm)	K_d (μM)	A_{max} (μmoles/min/mg)
Magnesium	0.065	355	1.7
Calcium	0.099	848	11.7
Barium	0.135	93	9.0
Strontium	0.113	374	7.9

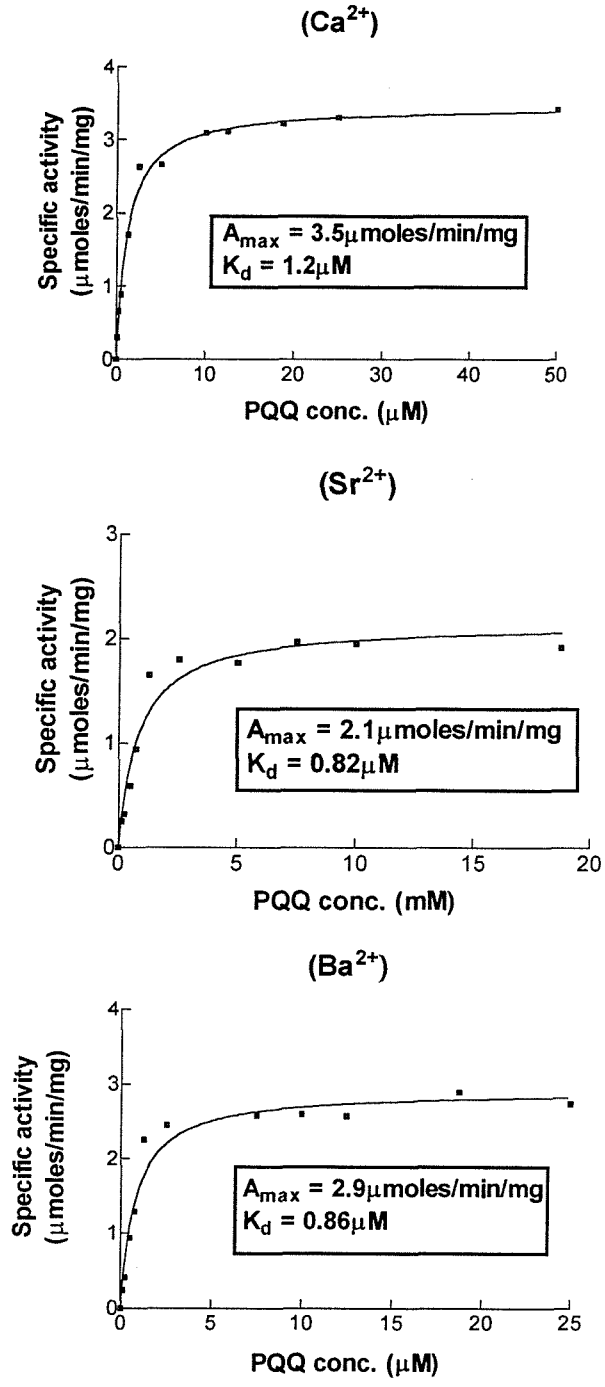

Figure 4.48 K_d for PQQ with T424N-GDH

T424N membrane fractions were reconstituted under standard conditions with 5mM metal ions (Ba^{2+}, Ca^{2+} or Sr^{2+}) and various concentrations of PQQ. The lines of best fit were calculated by the equation $A=A_{max}[PQQ]/(K_d + [PQQ])$ where A is GDH activity.

These results indicate that the mutation has altered the metal binding site but not changed the reconstitution process with respect to PQQ insertion. All the metals may bind to the active site and hold PQQ in its correct conformation.

Figure 4.49AP shows that between pH 5.5 and 8.0 the K_d values for PQQ were between 1.7μM and 3.2μM. This was unlike WT-GDH and the other mutants described in this chapter, which showed a decrease in affinity at pH values above 7.5. The affinity at pH 8.5 was not measured because the T424N-GDH or WT-GDH was not active at this pH.

Gel filtration confirmed that metal and PQQ binding in T424N-GDH was reversible (Table 4.15AP). Addition of EGTA to Ca^{2+}, Sr^{2+} or Ba^{2+} reconstituted T424N-GDH showed that the mutation did not increase the enzymes tolerance to such chelating agents. EGTA (4-6mM) completely inhibited T424N-GDH (Figure 4.50AP). As with WT-GDH and all mutant GDHs described in this Chapter, inhibition was instantaneous and could not be measured over time. EGTA was used instead of EDTA because treatment of T424N-GDH with EGTA gave an enzyme that required the addition of metals to the reconstitution mixture for activity.

4.8.2 The effect of Mg^{2+} on reconstituted T424N-GDH

Addition of Mg^{2+} to GDH previously reconstituted with Ca^{2+}, Ba^{2+} or Sr^{2+} caused a decrease in activity (Figure 4.51). This inhibition may occur because Mg^{2+} replaced Ca^{2+}, Sr^{2+} or Ba^{2+} at the active site. Mg^{2+} does not completely inhibit reconstituted GDH because Mg^{2+} itself can reconstitute apoGDH, but it leads to lower activity compared with Ca^{2+}, Sr^{2+} and Ba^{2+}. Figure 4.51 indicates that Mg^{2+} had a greater effect on Ca^{2+} reconstituted GDH than on Ba^{2+} and Sr^{2+} GDH.

4.8.3 The thermal stability of T424N-GDH

T424N-GDH was slightly less stable than WT-GDH because the mutant apoenzyme was 50% denatured after incubating at 40°C for 10.5 minutes (Figure 4.52a); this required 14.3 minutes for WT-GDH. However, apoWT-GDH and apoT424N-GDH were both 50% denatured after 10 minutes incubation at 41°C indicating the mutation has little effect on the enzyme's stability.

4.8.4 The activation energy for the oxidation of D-glucose by T424N-GDH

The activation energy for WT-GDH was 41kJ/mol and with T424N-GDH the activation energies with Ca^{2+}, Sr^{2+} and Ba^{2+} were 50kJ/mol, 41kJ/mol and 45kJ/mol (Figure 4.53 and 4.54).

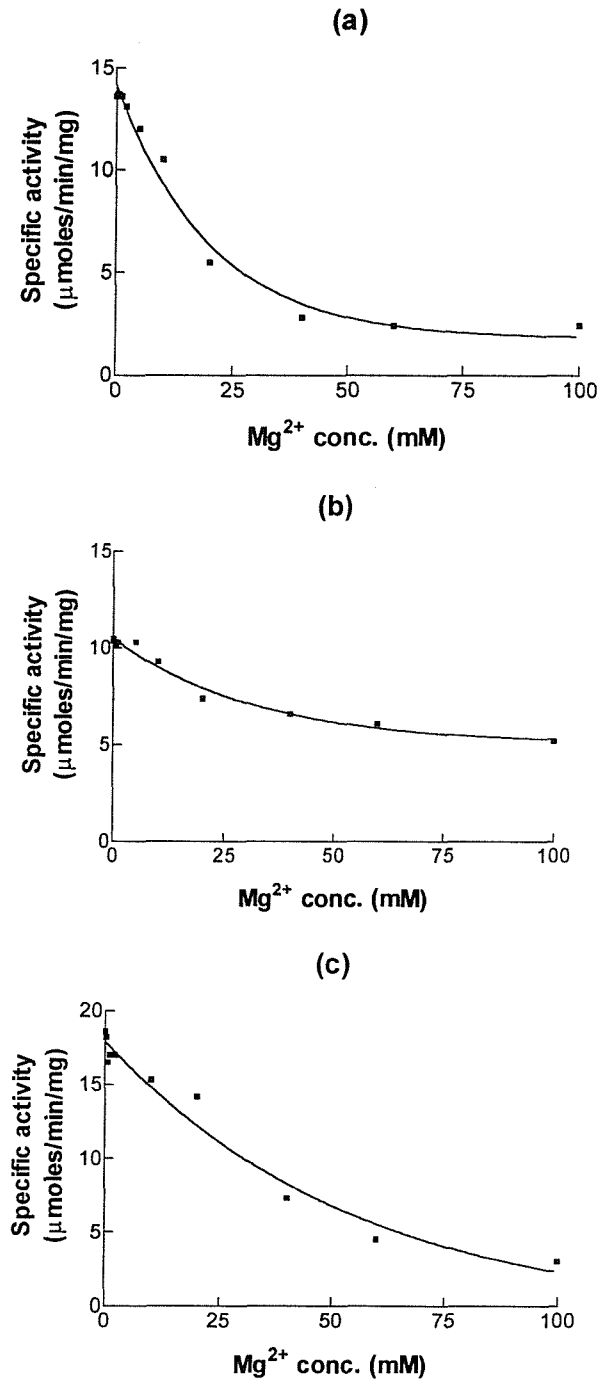

Figure 4.51 The inhibition of Ca^{2+}, Sr^{2+} and Ba^{2+} -reconstituted T424N-GDH by Mg^{2+}

T424N-GDH was reconstituted under standard conditions with 25μM PQQ and 5mM metal ions (Ca^{2+} (a), Sr^{2+} (b) and Ba^{2+} (c)). Then various concentrations of Mg^{2+} were added and incubated at 25°C for a further 20 minutes before activity was measured.

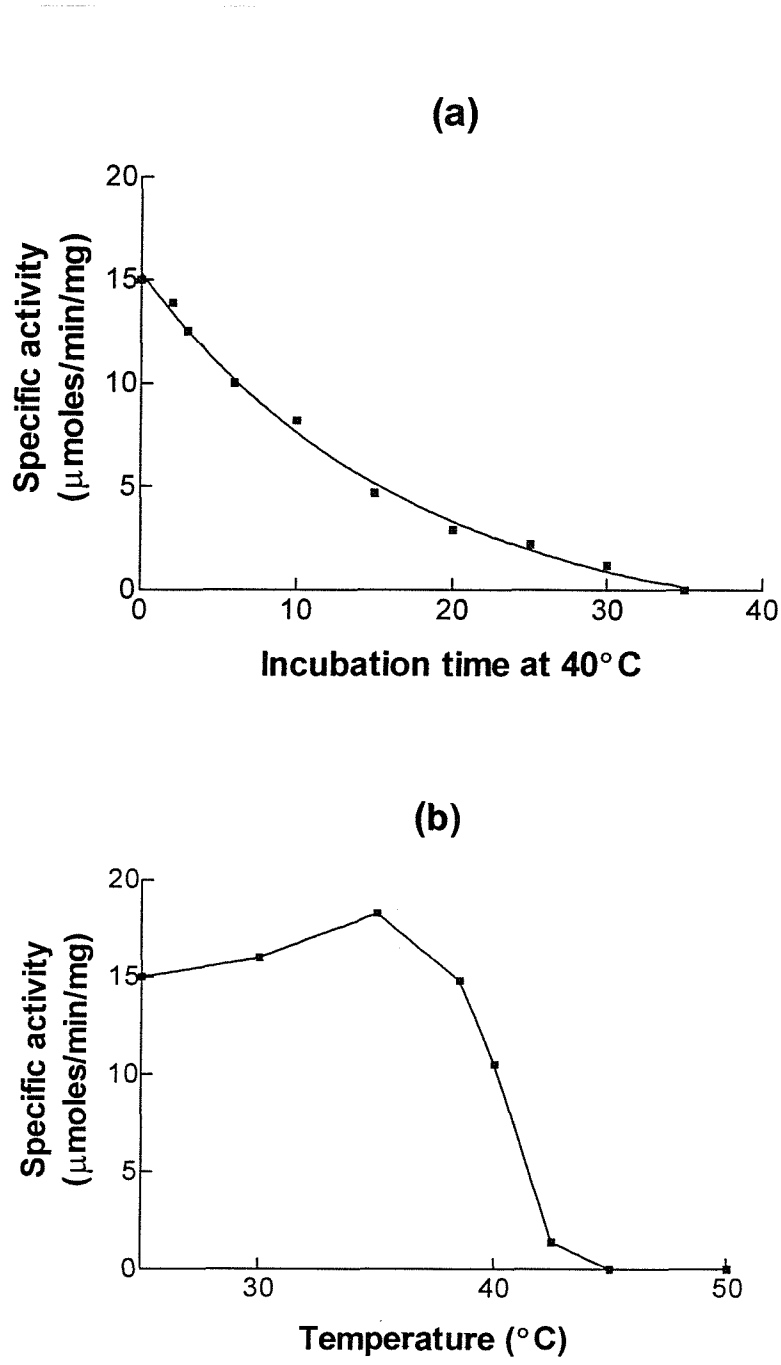

Figure 4.52 Thermal stability of T424N-GDH

(a) ApoGDH was incubated at 40°C for various periods of time. Then the enzyme was placed on ice for 5 minutes before GDH was reconstituted under standard conditions with Ca^{2+} and PQQ before activity was mesured.

(b) ApoGDH was incubated at various temperatures for 10 minutes. Then the enzyme was placed on ice for 5 minutes before GDH was reconstituted under standard conditions with Ca^{2+} and PQQ before activity was measured. Results with WT-GDH are shown in Figure 3.31.

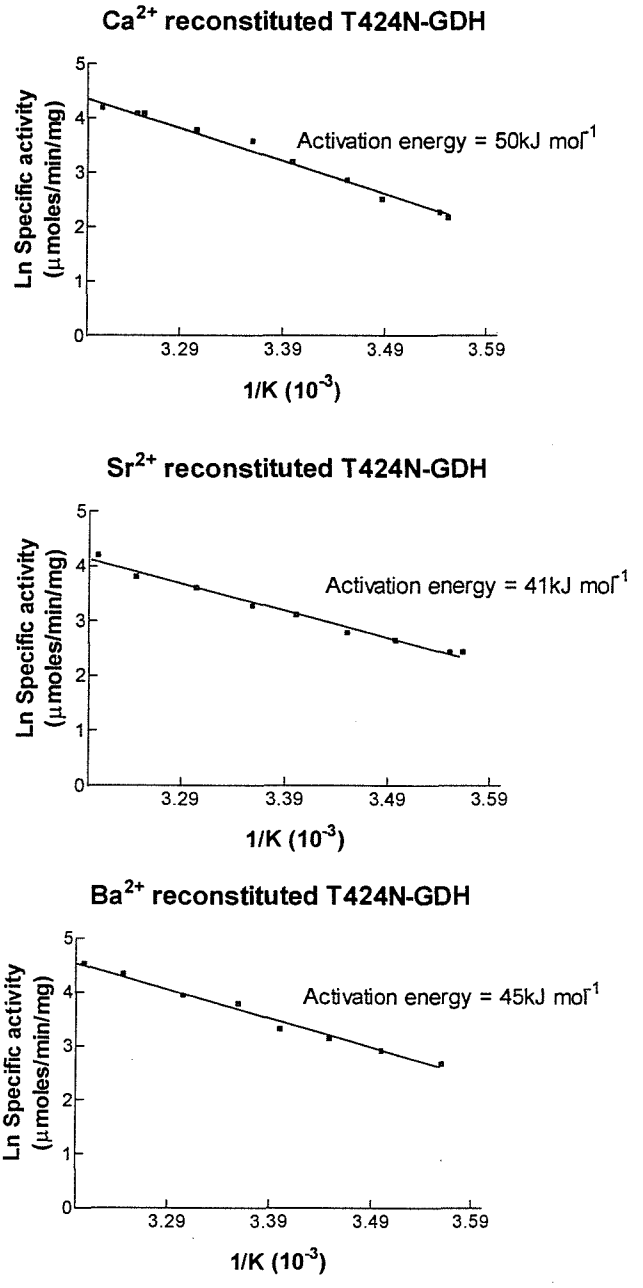

Figure 4.53 Activation energy for the oxidation of D-glucose with T424N-GDH

T424N-GDH was reconstituted under standard conditions with 25μM PQQ and 5mM metal ions (Ca^{2+}, Sr^{2+} and Ba^{2+}). Then activity was measured with the standard assay (1.5M D-glucose) at various temperatures (5-40°C). The formula relating activation energy (ΔG*) is v=A.exp(-ΔG*/RT) where A is the Arrhenius constant and R is the gas constant. The ΔG* values were calculated from the slopes of the curves. Figure 3.32 shows the result from a similar experiment with WT-GDH.

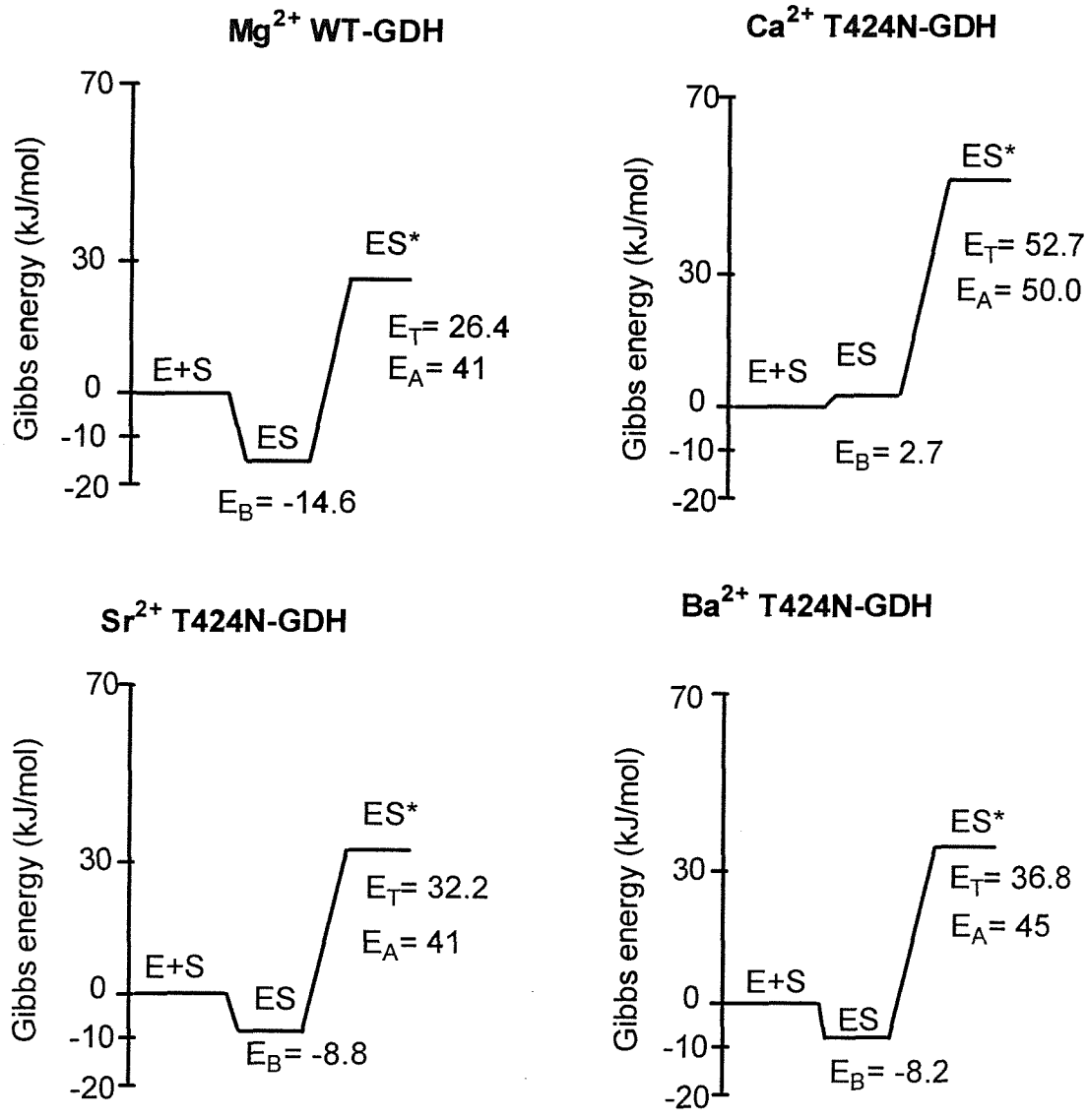

Figure 4.54 Schematic Gibbs free energy changes for the formation of the transition complex during the oxidation of D-glucose by T424N-GDH

The values for Gibbs free energy changes are in kJ/mol. E represents enzyme, S represents substrate, ES represents the enzyme-substrate complex and ES* is the transition state. E_A, E_B and E_T represent activation energy, binding energy and a measure of the energy of the transition complex respectively. E_A was calculated in Figure 4.53 and E_B was calculated by the equation $E_B = -RT \ln K_m$ where R is a gas constant and T is temperature.

The mutation has not had a marked effect on the activation energy. These results are discussed fully in Chapter 6.

4.8.5 The substrate specificity of T424N-GDH

Table 4.16 shows that T424N-GDH oxidised the same substrates as WT-GDH but the affinity had greatly decreased and determined V_{max} values were only 5-25% of WT-GDH values. The metal ion used to reconstitute GDH affected its affinity for substrates; K_m values were lower with Sr^{2+} and Ba^{2+}-reconstituted enzyme than with Ca^{2+}-GDH. Apart from 2-deoxy-D-glucose (K_m, 1.3M; V_{max}, 29μmoles/min/mg), K_m and V_{max} values were not determined accurately for Ca^{2+}-reconstituted T424N-GDH because activity was proportional to substrate concentration and saturation was not approached. Therefore, the substrate specificity of Sr^{2+} and Ba^{2+} reconstituted T424N-GDH will be described. As suggested with N355D-GDH, these results indicated that the oxidation of substrates is more effective with larger metal ions bound to the active site.

As with WT-GDH, T424N-GDH oxidised D-hexoses and D or L-pentoses. The affinity for D-glucose compared with that of WT-GDH had decreased 10-13 fold with Sr^{2+} and Ba^{2+}-reconstituted T424N-GDH.

The affinity for D-galactose was too high to measure with T424N-GDH. However, the C-4 hydroxy group is not essential for binding because L-arabinose was oxidised (the C-4 hydroxy group in this substrate has the same orientation as in D-galactose but not D-glucose). The affinity for L-arabinose compared with WT-GDH values only decreased by 5-8 fold with Sr^{2+} and Ba^{2+}-GDH.

4.8.6 Inhibition of substrate oxidation by L-xylose and D-arabinose

As shown with WT-GDH, D and L-isomers of pentose sugars that are not oxidised are able to bind to T424N-GDH. This was shown by measuring the activity of T424N-GDH with L-arabinose or D-glucose in the presence of D-arabinose or L-xylose. Figure 4.55 and Table 4.17 show that the inhibition of L-arabinose oxidation by D-arabinose was competitive because as the concentration of D-arabinose increased, the K_m for L-arabinose increased and the V_{max} remained constant. The Lineweaver-Burk plot also indicated that D-arabinose was a competitive inhibitor. Figure 4.56 shows that the inhibition of D-glucose oxidation by L-xylose was also competitive; an increase in L-xylose concentration caused the K_m for D-glucose to increase whilst the V_{max} remained constant.

Table 4.16 The substrate specificity of T424N-GDH

T424N-GDH was reconstituted under standard conditions with 5mM Ca^{2+} and 25μM PQQ. Activity was measured with the standard dye-linked assay containing various concentrations of substrates. The K_m and V_{max} values were calculated by the equation $v=V_{max}[S]/(K_d + [S])$. The V_{max} values for some substrates were not determined accurately (nd) whilst other sugars were not oxidised by the enzyme (X).

	Ca^{2+} Reconstituted			Sr^{2+} Reconstituted			Ba^{2+} Reconstituted			WT-GDH		
	K_m	V_{max}	Catalytic efficiency (V_{max}/K_m)	K_m	V_{max}	Catalytic efficiency (V_{max}/K_m)	K_m	V_{max}	Catalytic efficiency (V_{max}/K_m)	K_m	V_{max}	Catalytic efficiency (V_{max}/K_m)
D-glucose	>3M	-	nd	28	12.4	0.44	37	19.6	0.5	2.8	116	41.4
2-deoxy-D-glucose	1342	29	0.02	111	14.1	0.13	321	14	0.04	3.5	137	39.1
3-0-methyl-α-D-glucose	>3M	nd	nd	3M	nd	nd	1059	5.8	0.005	79	77	0.97
D-mannose	>3M	nd	nd	98	3.99	0.04	110	3.4	0.03	116	137	1.2
D-galactose	X	X		>3M	nd	nd	>3M	nd	nd	17.5	48	2.7
L-arabinose	>3M	nd	nd	142	6.3	0.04	259	6.2	0.02	31	122	3.9
D-ribose	>3M	nd	nd	>3M	nd	nd	>3M	nd	nd	166	41	0.25
D-xylose	>3M	nd	nd	521	15.7	0.03	451	15.5	0.03	17	61	3.6
D-glucose	X	X	X	X	X	X	X	X	X	X	X	X
D-arabinose	X	X	X	X	X	X	X	X	X	X	X	X
L-xylose	X	X	X	X	X	X	X	X	X	X	X	X
Maltose	X	X	X	X	X	X	X	X	X	X	X	X

Units for K_m values are mM (unless otherwise stated) and the units for V_{max} values are μmoles/min/mg

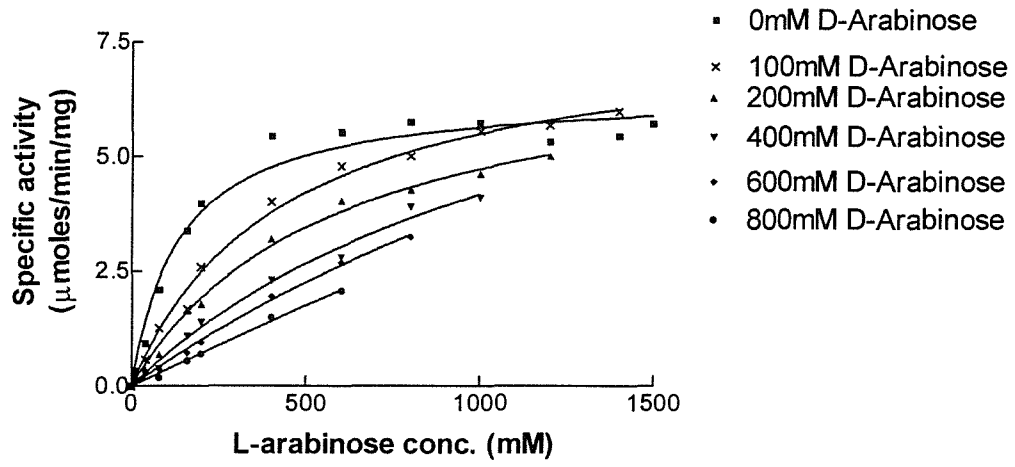

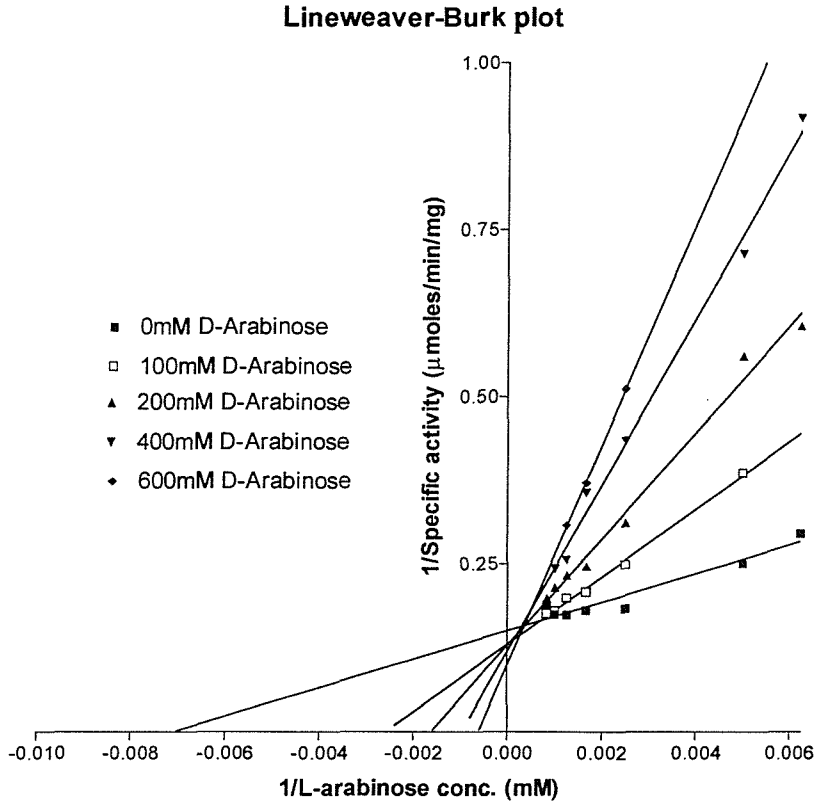

Figure 4.55 Inhibition of L-arabinose oxidation by D-arabinose

T424N-GDH was reconstituted under standard conditions with 25μM PQQ and 5mM Sr^{2+}. Activity was measured with the dye-liked assay in the presence of various concentrations of L-arabinose and D-arabinose.

Table 4.17 K_m values for D-glucose and L-arabinose in the presence of inhibitor

This Table is based on the data from Figures 4.55 and 4.56.

Inhibitor conc. (L-xylose or D-arabinose)	D-glucose		L-arabinose	
	K_m (mM)	V_{max} (μmoles/min/mg)	K_m (mM)	V_{max} (μmoles/min/mg)
0mM	15	12.9	138	6.4
40mM	54	13.6	-	-
100mm	253	14.7	434	7.8
200mM	358	14.3	579	7.4
400mM	621	14.8	1306	9.6
600mM	-	-	2561	13.8
800mM	772	17.2	-	-

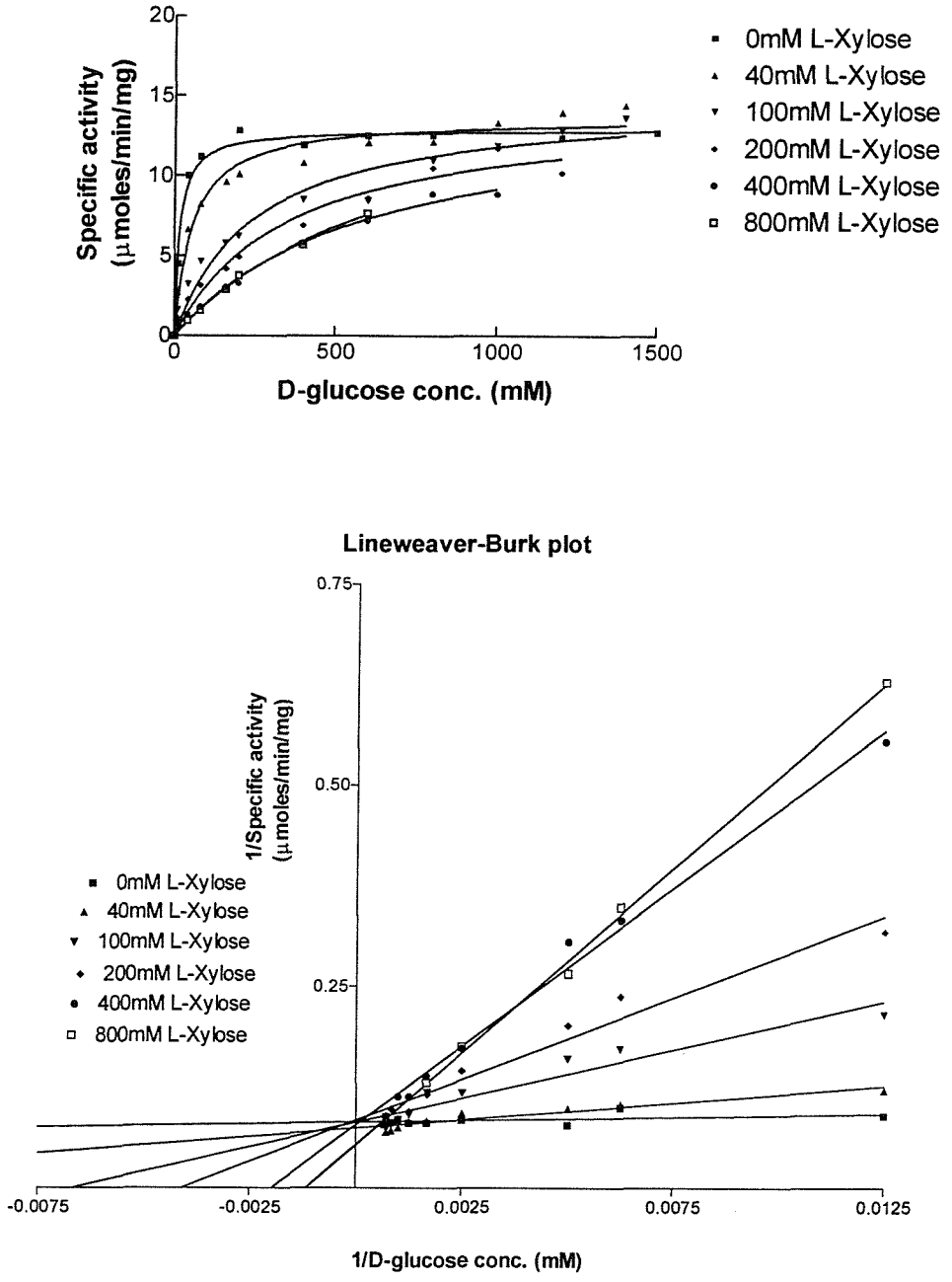

Figure 4.56 Inhibition of D-glucose oxidation by L-xylose

T424N-GDH was reconstituted under standard conditions with 25mM PQQ and 5mM Sr^{2+}. Activity was measured with the dye-liked assay in the presence of various concentrations of D-glucose and L-xylose.

4.8.7 Characterisation of T424N-GDH by Yoshida and Sode

One of the main differences between the work described in this thesis and results published by Yoshida and Sode (1996) is that the latter reported that WT-GDH could be reconstituted with Mg^{2+}, Ca^{2+}, Sr^{2+} and Ba^{2+} (Table 4.18). However, the results in Chapter 3 showed that WT-GDH could only be reconstituted with Mg^{2+} (K_d, 1.5mM) and that Ca^{2+}, Ba^{2+} and Sr^{2+} inhibited reconstitution with Mg^{2+}. These differences cannot be explained. Yoshida and Sode also suggested that substituting Thr-424 by asparagine caused the distance between PQQ and the metal ion binding site to increase; this decreased the stability of Mg^{2+} and Ca^{2+} binding. Table 4.18 shows that activity with Mg^{2+} and Ca^{2+} reconstituted T424N-GDH was lower than WT-GDH activity, but activity with Sr^{2+} and Ba^{2+} had not decreased. The K_d for Mg^{2+}, Ca^{2+}, Sr^{2+} and Ba^{2+} were 0.78mM, 5.64mM, 1.33mM and 1.01mM respectively. These K_d values are different from those reported in Section 4.8.1 (K_d values for Mg^{2+}, Ca^{2+}, Sr^{2+} and Ba^{2+} were 0.36nM, 0.85nM, 0.37nM and 0.09nM respectively).

4.8.8 Summary of T424N-GDH characterisation

T424N-GDH was purified in Pipes buffer, the yield and purification levels being similar to that of WT-GDH. As with D354N-GDH, N355D-GDH and D354N/N355D-GDH, Ca^{2+} could be used to reconstitute T424N-GDH. However, this enzyme was 20% active compared with the activity of Mg^{2+}-reconstituted WT-GDH, but to a large extent this could be due to the enzyme having a low affinity for D-glucose (K_m, >3M). Mg^{2+}, Sr^{2+} and Ba^{2+} also supported reconstitution, but activity with Mg^{2+} was 16% compared with the activity of Ca^{2+}-reconstituted T424N-GDH. The affinities for metal binding to T424N-GDH were determined after treatment with 100mM EGTA; this gave an enzyme that was only 3.5% active in the absence of added metal ions. EDTA treatment did not give an enzyme that required the addition of metal ions for activity. T424N-GDH oxidized the same substrates as WT-GDH, but the affinity of the mutant enzyme for substrates had decreased greatly. T424N-GDH reconstituted with Sr^{2+} or Ba^{2+} had higher affinity for substrates than Ca^{2+}-reconstituted T424N-GDH.

Table 4.18 The affinity of WT-GDH and T424N-GDH for metal ions

Table taken from Yoshida and Sode (1996). These results report that WT-GDH was reconstituted with Ca^{2+}, Sr^{2+} and Ba^{2+}. However, Chapter 3 showed that only Mg^{2+} could reconstitute WT-GDH; Ca^{2+}, Sr^{2+} and Ba^{2+} inhibited reconstitution. The difference between these results cannot be explained.

	WT-GDH		T424N-GDH	
Bivalent metal	K_d (mM)	V_{max} (U/mg protein)	K_d (mM)	V_{max} (U/mg protein
Mg^{2+}	0.32	55.9	0.78	3.54
Ca^{2+}	0.25	28.6	5.64	21.0
Sr^{2+}	0.39	9.56	1.33	9.43
Ba^{2+}	1.20	4.80	1.01	6.05

4.9 Oxygen consumption of membrane fractions containing WT and mutant-GDHs

GDH must transfer electrons from the substrate to ubiquinone that is located in the membrane. Amino acids in the superbarrel domain may have specific roles in the electron transfer from $PQQH_2$ to ubiquinone which is then oxidized by the oxidase cytochrome *bo*. Therefore, the oxygen consumption during glucose oxidation by membrane fractions containing WT and mutant GDHs was measured with an oxygen electrode (Table 4.19). The highest consumption rates were measured with membranes containing WT-GDH. This was expected because membranes containing WT-GDH had the highest activity (measured by the dye-linked assay). The oxygen consumption of all the mutants indicate that Asn-354, Asp-355 and Thr-424 were not directly involved in electron transfer; their oxygen uptake was reduced due to their lower activity measured by the standard dye-linked assay. The ratios between oxygen consumption and activity (measured with the dye-lined assay) compared with WT-GDH values were similar and if a mutant GDH did effect electron transfer then a large difference would be expected.

4.10 The metal ion content of GDHs

The results with WT-GDH and mutant GDHs described in this thesis indicate that the metal ion added during reconstitution binds to the active site. However, another possibility is that Ca^{2+} is already bound and the metal added in the reconstitution has another role such as PQQ insertion. The obvious approach to determine if apoGDH contains a metal ion in the active site of GDH is to measure it directly. The metal ion content of reconstituted GDH was not measured because the excess metal ions (required for reconstitution) could not be removed without also removing metal from the metal binding site (binding is reversible).

The Mg^{2+} and Ca^{2+} contents of purified apoGDHs are shown in Table 4.20. In all the enzymes there was less than one Mg^{2+} ion per molecule of protein; this metal ion may be responsible for the activity of GDH seen after reconstitution in the absence of added metal because WT-GDH, T424N-GDH and D354N/N35D-GDH are 9%, 43% and 50% active in the absence of metal ion, and they contain 0.18, 0.48 and 0.45 Mg^{2+} ions per molecule of enzyme. However, there was more than one Ca^{2+} ion per molecule of protein (ranging from 1.4 Ca^{2+} in D354N-GDH to 20 Ca^{2+} in D354N/N355D-GDH). WT-GDH had 4 Ca^{2+} ions per molecule of protein. This indicates that Ca^{2+} may be bound to the active site of apoGDH.

The Ca^{2+}content but not the Mg^{2+} content of GDH was usually altered by the mutations. N355D-GDH had a similar Ca^{2+} content to WT-GDH thus permitting measurement of the affinity of metals to be calculated. D354N-GDH had a lower content of Ca^{2+} yet the affinity for

Table 4.19 Oxygen consumption of WT-GDH and mutant GDHs

Activities of WT-GDH and mutant GDH (membrane fractions) were measured with the standard dye-linked assay and oxygen consumption with an oxygen electrode. Oxygen uptake over a three minute time period was measured with an assay containing 100µl membrane fraction (containing WT-GDH or mutant GDHs), 10mM Pipes buffer pH 7.0 and 1.5M D-glucose. It was presumed that 3ml of buffer contained 15µl of oxygen.

Enzyme	O_2 electrode activity (µl/hr/mg)	Dye-linked assay activity (µmoles/min/mg)
WT-GDH (Mg^{2+})	1006 (100%)	10.0 (100%)
D354N-GDH (Ca^{2+})	433 (43%)	3.1 (31%)
D354N-GDH (Sr^{2+})	214 (21%)	2.8 (28%)
D354N-GDH (Ba^{2+})	203 (20%)	2.6 (26%)
N355D-GDH (Ca^{2+})	238 (23%)	5.4 (54%)
N355D-GDH (Sr^{2+})	105 (10%)	4.5 (45%)
N355D-GDH (Ba^{2+})	172 (17%)	4.9 (49%)
D354N/N355D-GDH (Ca^{2+})	291 (29%)	4.2 (42%)
D354N/N355D-GDH (Sr^{2+})	227 (23%)	4.0 (40%)
D354N/N355D-GDH (Ba^{2+})	273 (27%)	3.7 (37%)
T424N-GDH (Ca^{2+})	251 (25%)	4.5 (45%)
T424N-GDH (Sr^{2+})	240 (24%)	3.25 (33%)
T424N-GDH (Ba^{2+})	254 (25%)	4.3 (43%)

Table 4.20 The Mg^{2+} and Ca^{2+} content of WT-GDH and mutant GDHs

The metal content of WT-GDH and mutant GDHs (purified in Pipes buffer) were measured by atomic absorption spectrophotometery by Dr. Silke Severnmann. When appropriate, GDH was treated with 100mM EDTA or EGTA and incubated at room temperature for 1 hour. Then the chelating agent was removed by gel filtration. The Mg^{2+} and Ca^{2+} content of the enzymes buffer (10mM Pipes buffer pH 7.0, 0.1% Triton X-100) had been subtracted from these measurements; the average Mg^{2+} and Ca^{2+} content of the buffers were 0.17μM and 5.3μM respectively.

Coordination to metal ion	Sample	GDH conc. (μM)	Mg^{2+}conc. (μM)	Ca^{2+} conc. (μM)	Mg^{2+}:GDH ratio	Ca^{2+} :GDH ratio	Activity without added metal ions (%)
7	WT-GDH	12.8	2.3	51.6	0.18	4.0	9
6	D354N-GDH	9.8	2.0	13.9	0.20	1.4	67
8	N355D-GDH	10.1	2.3	44.1	0.23	4.4	5
7	T424N-GDH	10.3	4.9	125.0	0.48	12.1	43
7	D354N/N355D-GDH	9.5	4.3	192.3	0.45	20.2	50
7	WT-GDH (EDTA)	3.2	3.1	78.0	0.94	24.4	1
6	D354N-GDH (EDTA)	2.0	5.2	64.0	2.60	32.0	67
8	N355D-GDH (EDTA)	1.9	3.0	71.6	1.58	37.7	5
7	T424N-GDH (EGTA)	2.7	1.3	97.6	0.48	36.1	3
7	D354N/N355D-GDH (EDTA)	4.6	1.7	0.0	0.37	0.0	50

metal ions could not be determined because a sample that had no activity in the absence of metal could not be produced. D354N-GDH may have a lower Ca^{2+} content because it could only make 6 bonds to the active site metal and N355D-GDH and WT-GDH can make 8 and 7 bonds respectively. D354N/N355D-GDH had the highest concentration of Ca^{2+} and a sample of this mutant could not be prepared that was not active after reconstitution in the absence of metal ions. T424N-GDH showed a 4-fold increase in the concentration of Ca^{2+} compared to WT-GDH, yet the number of bonds that it can make to the active site metal has remained constant.

Treatment of WT-GDH and mutant GDH with 100mM EDTA or EGTA was expected to reduce the Mg^{2+} and Ca^{2+} content of the samples but Table 4.20 shows the reverse occurred apart from measurements with D354N/N355D-GDH. The ratio of Ca^{2+} per GDH molecule increased between 24:1 and 50:1. These results cannot be explained unless EDTA contained Ca^{2+} contamination.

4.11 Summary and discussion

The major difference between WT-GDH and all mutant GDHs is that WT-GDH requires Mg^{2+} for reconstitution and mutant GDHs prefers Ca^{2+}, Sr^{2+} or Ba^{2+}. Mutating amino acids that have been predicted to bind to the active site metal ion changed the metal ion specificity of GDH; this suggests that the reconstitution metal ion binds to the active site of GDH. These mutations could have also changed the coordination of the metal ion at the active site. D354N-GDH may provide six ligands (one less than WT-GDH) for the metal ion when N355D-GDH provided eight. D354N/N355D-GDH had the same number of metal ligands as WT-GDH but their orientation was changed. This suggests that the number of ligands and their orientation effects metal ion binding. This will be discussed in greater detail in Chapter 6.

Chapter 5

Further site-directed mutagenesis of the *gcd* gene; attempts to isolate the periplasmic superbarrel domain, and disruption of the tryptophan docking motifs

Introduction

The catalytic domain of GDH is expected to occur as a superbarrel domain located in the periplasm (Yamada, 1993; Cozier and Anthony, 1995) (Section 1.5); it has been predicted to consist of eight, four stranded antiparallel β sheets containing PQQ and a metal ion at the centre (Figure 1.16). This domain is anchored to the membrane by five transmembrane regions that are made up from the first 150 amino acids (Figure 1.11). Solving the X-ray crystal structure for holoGDH might indicate that Ca^{2+} or Mg^{2+} is bound to the active site but the formation of GDH crystals is difficult because it is a membrane protein and attempts by the Japanese groups have not succeeded. To simplify this task, the production and purification of the periplasmic domain as a soluble protein was attempted. Also, this Chapter will describe the production and characterisation of W198A-GDH. This mutant was constructed to investigate the role of the tryptophan docking motifs (Section 1.5.1) because replacing Trp-198 with alanine should abolish one of the eight motifs in the protein.

5.1 Purification of the periplasmic domain of GDH (periGDH)

Dr Gyles Cozier had previously amplified the DNA coding for the superbarrel region using PCR and introduced unique restriction sites flanking this region (*Hind*III and *Nco*I). The vector pTrcHisB and the amplified DNA were cut with *Hind*III and *Nco*I and the superbarrel domain ligated into the vector. This resulted in a plasmid called pTrcgcd2. This was then transformed into *E. coli* strain PP2418 producing strain PPSOL2. I have used this strain and the plasmid pTrcgcd2 in the work described below.

PPSOL2 was grown in 2 litres of LB at 37°C and induced with 1mM IPTG because the pTrcHisB vector has an IPTG inducible promoter. The cells were then harvested at late log phase, washed twice with 10mM potassium phosphate buffer and sonicated. The membrane and soluble fractions were separated by high speed centrifugation (1 hour at 40,000rpm). However, no activity was recorded in the membranes or the soluble fractions after reconstitution with 25μM PQQ and 5mM Mg^{2+} or Ca^{2+}. SDS-PAGE showed that a 66kDa protein (the size of the superbarrel domain) was present in the membrane fraction

(Figure 5.1), suggesting that the superbarrel may have been expressed but that it formed insoluble inclusion bodies.

Presuming that the catalytic superbarrel domain of GDH had not folded properly in *E. coli* strain PP2418, plasmid pTrcgcd2 was isolated using a Promega Wizard DNA purification kit and transformed into *E. coli* strain AD494 and the Origami strain (supplied from Novagen). This was done to aid disulphide bond formation. AD494 strains are thioredoxin reductase (*trx B*) deficient mutants that enable disulfide bond formation in the cytoplasm (Derman *et al.*, 1993). Origami strains are K-12 derivatives that lack the genes for thioredoxin reductase (*trx B*) and glutathione reductase (*gor*) and which therefore greatly enhance disulphide bond formation in the cytoplasm (Prinz *et al.*, 1997). AD494 and Origani strains containing pTrcgcd2 were named PPSAL2 and PPSOLO2 respectively.

E. coli strains PPSAL2 and PPSOLO2 were grown and the membrane and soluble fractions isolated. However, no activity was recorded after reconstitution under standard conditions (5mM Mg^{2+} or Ca^{2+}), although SDS-PAGE showed that a 66kDa protein that was absent in the *E. coli* strains lacking the plasmid was present in the crude, membrane and soluble fractions (Figure 5.2). The growth of strain PPSOLO2 in the presence of 25μM PQQ produced a 66kDa protein in the soluble fraction (Figure 5.3) but it did not lead to production of active GDH. This suggested that in this case the addition of the prosthetic group was not able to aid protein folding.

Thus, this method was unsuccessful in the attempt to obtain active soluble GDH. This may be because the membrane domain has a crucial role in the folding or stability of the periplasmic domain of the enzyme.

5.2 Production of the periplasmic superbarrel domain (periGDH) using site-directed mutagenesis

An alternative method of producing "periGDH" could involve cutting the superbarrel domain from the membrane domain using a specific protease. The advantage of this method is that it might allow the catalytic domain to fold properly before it is removed. However, a specific protease site was not present in the region that separates the two domains (around amino acid 150). The site had to be in this area because if it is hidden in the membrane or located in a folded region then the protease would not have access to the site.

Site-directed mutagenesis (Stratagene Quickchange method) was used to insert a Factor Xa protease site between amino acid 145 and 149. Factor Xa protease cleaves after arginine following the sequence Ile-Glu-Gly-Arg. The WT sequence at amino acid 145 is Ile-Asn-Gly-His so only two amino acids had to be mutated (N147E/H149R).

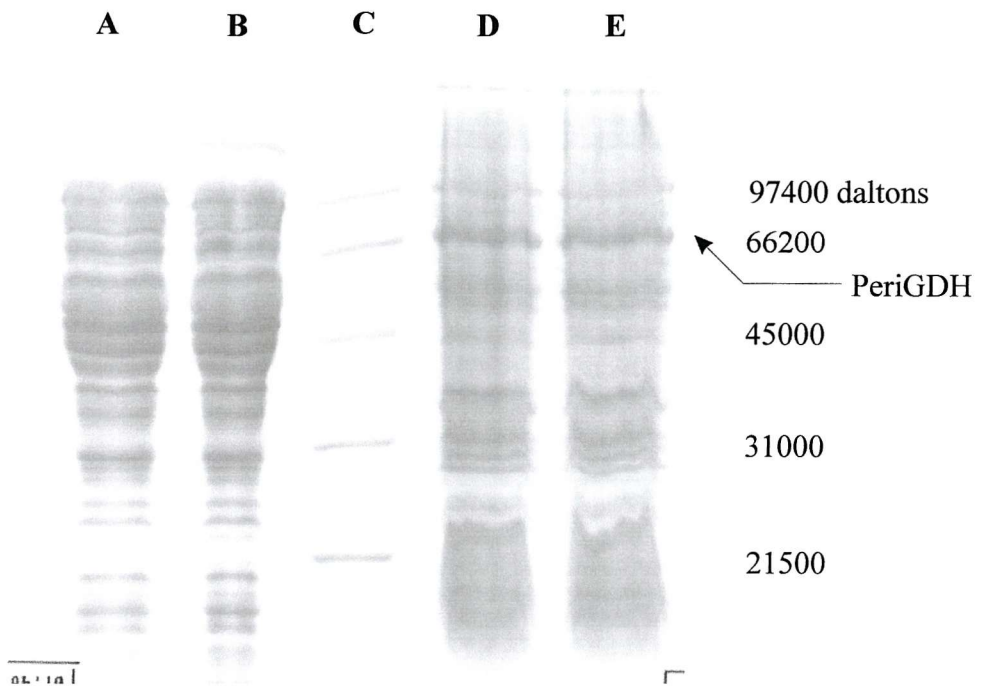

Figure 5.1 SDS-PAGE showing the presence of the periplasmic domain of GDH from strain PPSOL2

A) Soluble fraction

B) Soluble fraction

C) Protein standards

D) Membrane fraction

E) Membrane fraction

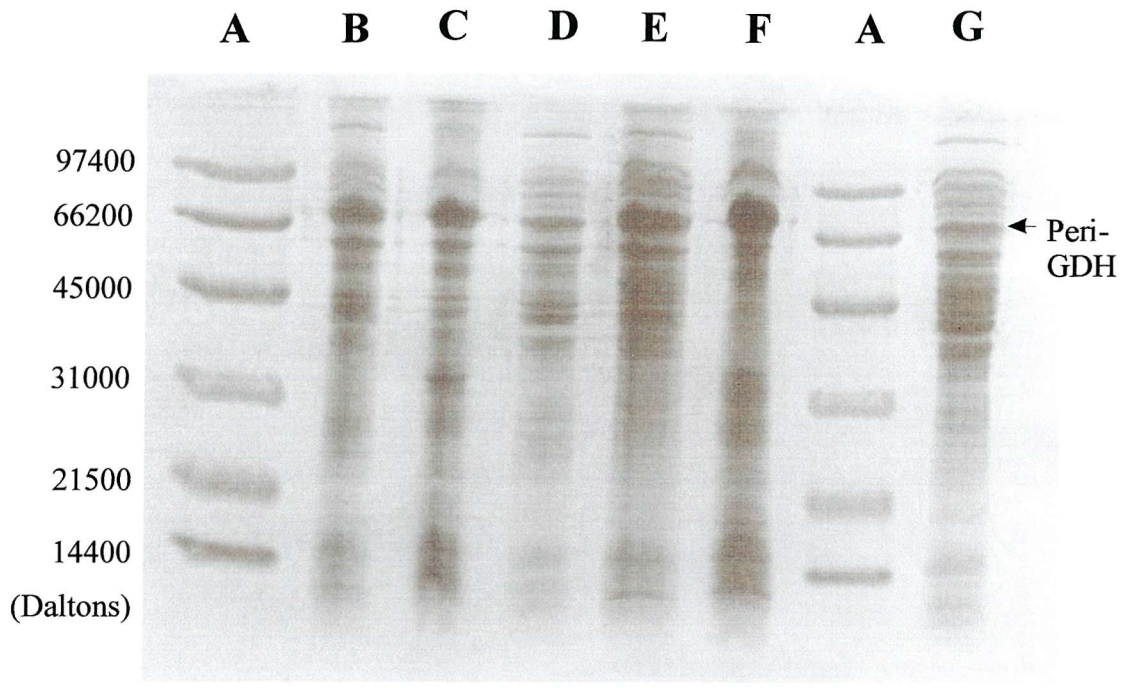

Figure 5.2 SDS-PAGE showing the presence of the periplasmic domain of GDH from strains PPSOLO2 and PPSAL2

A) Protein standards

B) Crude fraction from PPSAL2 (dil x5)

C) Membrane fraction from PPSAL2 (dil x5)

D) Soluble fraction from PPSAL2 (dil x5)

E) Crude fraction from PPSOLO2 (dil x5)

F) Membrane fraction from PPSOLO2 (dil x5)

G) Soluble fraction from PPSOLO2 (dil x5)

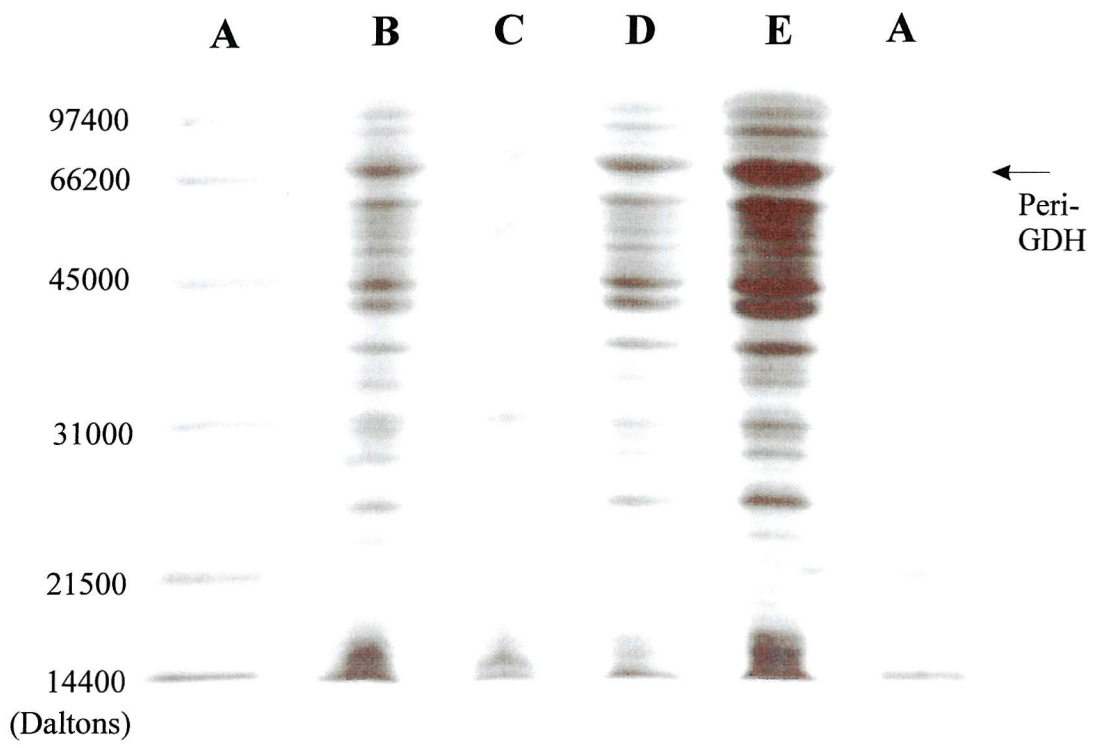

Figure 5.3 SDS-PAGE showing the presence of the periplasmic domain of GDH produced by strain PPSOLO2 in the presence of PQQ

A) Standard proteins

B) Crude fraction (dil x5)

C) Membrane fraction (dil x5)

D) Soluble fraction (dil x2)

E) Soluble fraction (undiluted)

For the mutagenesis reactions the following DNA primers containing these mutations were used:-

```
                    AspProGlnGluIle**Asn**Gly**His**LeuLysArg
WT sequence  5′ CGATCCGCAGGAAATC**AAC**GGG**CAC**CTTAAGCGCCG 3′

                    AspProGlnGluIle**Glu**Gly**Arg**LeuLysArg
Primer 1     5′ CGATCCGCAGGAAATC**GAA**GGG**CGC**CTTAAGCGCCG 3′
Primer 2     5′ CGGCGCTTAAG**GCG**CCC**TTC**GATTTCCTGCGGATCG 3′
```

Mutagenesis was successful using the method described in Section 2.6.5. Figure 5.4 shows that after PCR and *Dpn*I digestion, nicked mutant DNA was present. This DNA was transformed into *E. coli* strain PP2418 and DNA sequencing proved that this DNA contained the double mutation N147E/H149R (Figure 5.5). However, isolation of the membrane fraction showed that N147E/H149R-GDH was not active after reconstitution with 5mM Mg^{2+} or Ca^{2+}. SDS-PAGE showed that less than 25% GDH was present in the membrane fraction compared with WT-GDH, suggesting that this double mutation affected the expression or the stability of the protein (Figure 5.6). Again, these results indicate that apart from its expected role in electron transfer (transferring electrons from GDH to membrane ubiquinone), the membrane region is very important in the overall stability of the protein. It may aid protein folding and/or keep the structure in an active conformation.

5.3 Disruption of a tryptophan docking motif in GDH

The amino acid sequence of GDH contains a repeating 11-residue consensus sequence involved in forming the tryptophan docking motifs (Sections 1.5.1 and 1.5.2). These motifs are found at the CD corners of each beta sheet and form a stabilizing girdle (Cozier and Anthony, 1995). Generally, tryptophan at position 11 is stacked between alanine at position 1 on the same motif and the threonine and glycine peptide bond at position 6 and 7 on the following motif. Mutating Gly-741 in GDH to serine led to the production of an enzyme that was far less stable and active (41%) compared with WT-MDH (Yamada *et al.*, 1998). This glycine was located on W7 and was part of the tryptophan docking motif that held motifs W6 and W7 together.

Trp-198 located on W8 is predicted to form this motif with Ala-790 and the peptide bond between Ser-243 and Gly-244 of W1 (Figure 5.7). This motif may be especially important because it has been predicted to hold together W1 and W8. Trp-198 was mutated to alanine by the Stratagene Quickchange method of mutagenesis to determine if this tryptophan

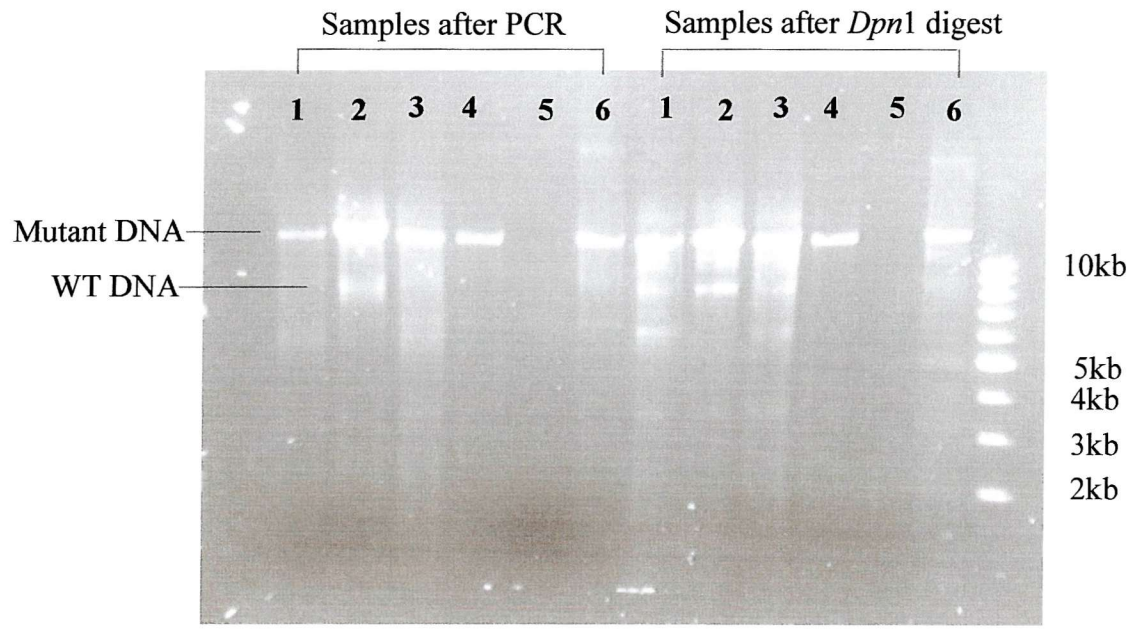

Figure 5.4 Confirmation of the production of N147E/H149R dsDNA

After various stages of the Stratagene Quickchange method DNA samples were separated on a 0.6% agrose gel. Samples 4 and 6 were transformed into *E. coli* strain PP2418 because they did not contain WT DNA after *Dpn*1 digestion.

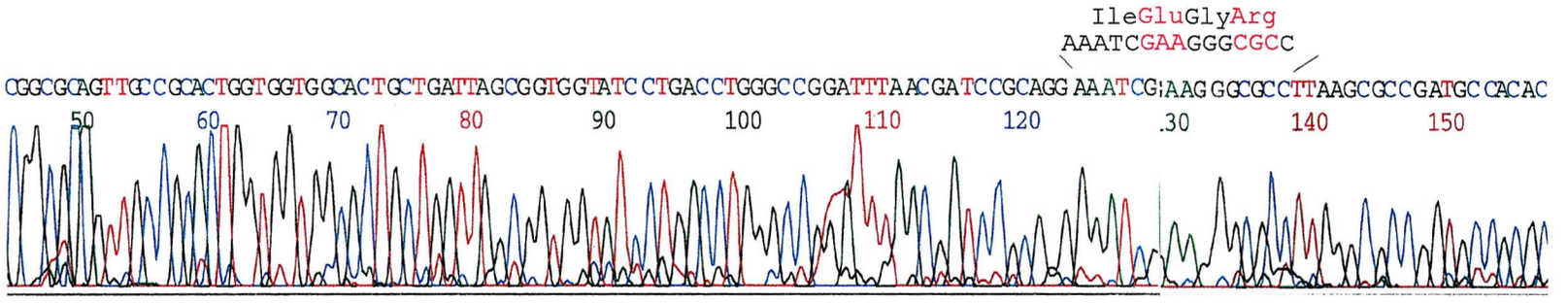

Figure 5.5 Confirmation that the Factor Xa protease site was inserted into the *gcd* gene

Mutant N147E/H149R was shown to be present in purified DNA. Sequencing done by Oswel (Southampton, UK). The mutations (coloured red) show that the Factor Xa protease site was inserted into the protein sequence of GDH.

Figure 5.6 SDS-PAGE showing the presence of N147E/H149R-GDH

A) Crude fraction (dil x6)

B) Supernatant from membrane isolation (dil x6)

C) Membrane fraction (dil x6)

D) Standard proteins

E) Pellet remaining after solubilisation (dil x6)

F) Soluble fraction (dil x6)

G) Soluble fraction (undiluted)

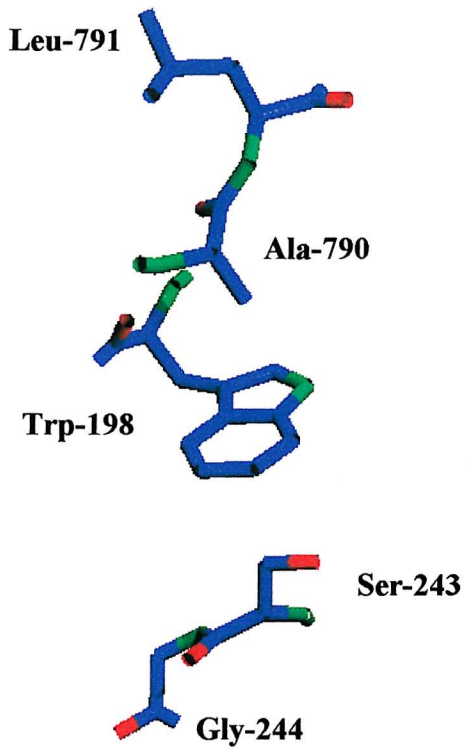

Figure 5.7 A tryptophan-docking motif in GDH

Trp-198 of W8 is stacked in between Ala-790 at position 1 of the same motif and Ser-243 and Gly-244 of W1. Mutating Trp-198 to an alanine prevented the production of GDH.

docking motif was absolutely required for stability. The DNA primers used to make this mutant were:-

```
                    LysLeuLysGluAlaTrpValPheArgThrGly
WT sequence 5′ CAAGCTGAAAGAAGCCTGGGTGTTCCGTACTGGCGA 3′

                    LysLeuLysGluAlaAlaValPheArgThrGly
Primer 1    5′ CAAGCTGAAAGAAGCCGCGGTGTTCCGTACTGGCGA 3′
Primer 2    5′ TCGCCAGTACGGAACACCGCGGCTTCTTTCAGCTTG 3′
```

The mutagenic reactions produced nicked DNA that was then transformed into *E. coli* strain PP2418 and the W198A mutation was confirmed by DNA sequencing (Figure 5.8).

The growth and preparation of W198A-GDH was done under standard conditions but no activity was measured in the crude, membrane or soluble fractions. SDS-PAGE showed that the protein was not expressed, suggesting that this tryptophan docking motif was essential for stability (Figure 5.9). A future program should involve site-directed mutagensis of other, perhaps less critical tryptophan docking motifs, in the hope of producing a protein whose stability and activity can be measured.

5.4 Summary

All attempts to purify the periplasmic domain as a soluble protein (periGDH) failed. The growth of *E. coli* strains PP2418, AD494 and Origami, containing the plasmid pTrcgcd2 (that codes for the soluble periplasmic domain of GDH) did not lead to the production of active periGDH. With all strains mentioned above, a 66kDa protein was expressed that was not present in these strains lacking plasmid pTrcgcd2. This protein was periGDH that was inactive because it had probably formed insoluble inclusion bodies. The removal of the membrane domain had affected protein folding or stability.

Insertion of a protease cleavage site (Factor Xa) in between the membrane and periplasmic domains affected the expression of the protein. The N147E/H149R-GDH was poorly expressed and this confirmed that the membrane domain is essential for the proteins stability.

These results showed that abolishing the tryptophan docking motif that holds W1 and W8 together in GDH prevented the expression of GDH in *E. coli* strain PP2418. Not all tryptophan docking motifs may be as critical as this one because W1 and W8 are made from the N and C-terminal of the protein.

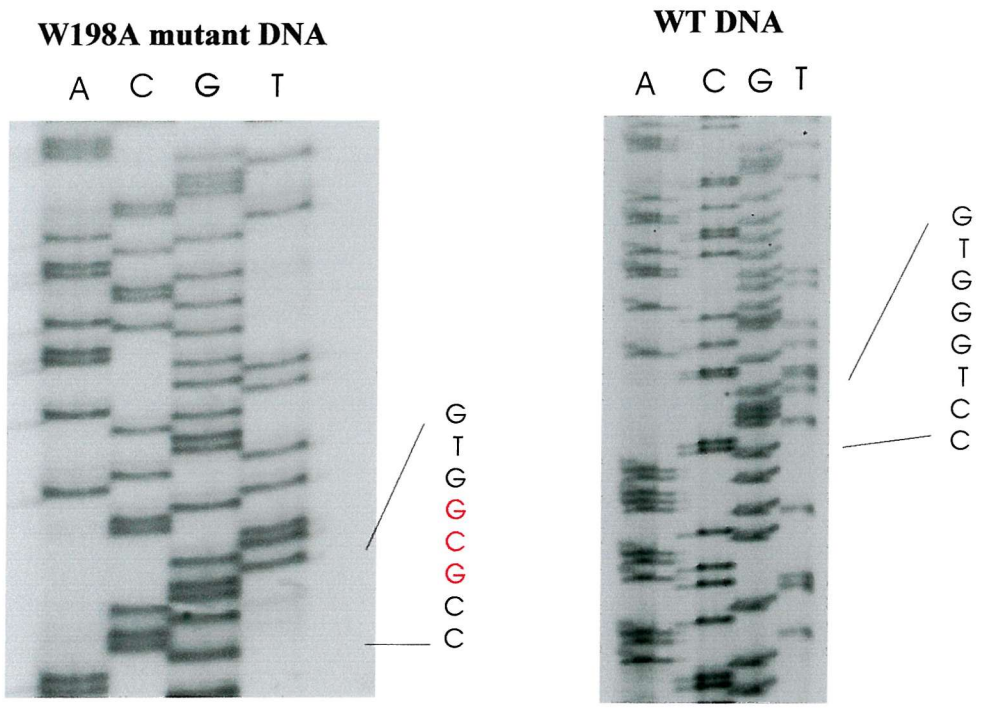

Figure 5.8 Confirmation of W198A DNA by manual sequencing

The DNA sequencing gels show that the codon for Trp-198 (TGG) was mutated to the codon for alanine (GCG) by the Stratagene Quickchange method of mutagenesis.

Figure 5.9 SDS-PAGE showing W198A-GDH was not expressed

A) Protein standards

B) Soluble fraction (dil x2)

C) Membrane fraction (dil x2)

D) Pellet remaining after solubilisation (dil x5)

E) Soluble fraction (dil x5)

F) Membrane fraction (dil x5)

G) Crude extract (dil x5)

Chapter 6
Summary and Discussion

Introduction

The main aim of this thesis was to determine which metal ion is part of the active site of membrane GDH. Other quinoproteins such as MDH and soluble GDH have been shown to contain Ca^{2+}, but Mg^{2+} is required to reconstitute membrane apoGDH from *E. coli*. This has usually been assumed to indicate that GDH has a similar active site to that in all other quinoproteins but that Mg^{2+} replaces Ca^{2+} in the structure of the enzyme. However, Ca^{2+} and Mg^{2+} are not usually exchangeable with each other and so this conclusion seemed unlikely. There remained the possibility that apoGDH contains Ca^{2+} at the active site and that Mg^{2+} was only needed during reconstitution for some other aspect of the process. In my work no single experiment has distinguished whether Mg^{2+} or Ca^{2+} is in the active site so all the evidence will be discussed. This discussion will not have the same "chronology" as the Results Section of the thesis. The first part discusses some of the minor aspects of this work, thus facilitating a clear discussion of main results.

6.1 Attempts to isolate the periplasmic superbarrel domain of GDH

Production of the periplasmic superbarrel domain (periGDH) was attempted so that the X-ray crystal structure of this domain could be determined. This might have shown which is the essential catalytic metal ion in the active site. Also, periGDH could be developed as a biosensor for glucose as the soluble form would be easier to work with than the membrane form. PeriGDH would also be better for further experiments on the mechanism of GDH. However, all attempts to isolate a separate periplasmic catalytic domain were unsuccessful, indicating that the membrane domain is essential for stability or that it has an important role in the folding of the periplasmic domain of the protein.

The expression of pTrcgcd2 (the pTrcHisB plasmid containing the DNA sequence for the catalytic domain) in *E. coli* strains PP2418, AD494 and the Origami strain did not produce an active protein when grown in the presence or absence of PQQ. The protein was expressed but it occurred in insoluble inclusion bodies suggesting that it may not have folded into the correct conformation.

Insertion of a protease site in between the membrane and catalytic domain did not allow the isolation of periGDH because the protein was poorly expressed. The insertion of the Factor Xa protease site abolished activity, again suggesting that the membrane domain is important for overall stability.

During this work, Witarto *et al.* (1999b) showed that the periplasmic domain could be removed from the membrane domain by tryptic digestion. This produced periGDH that was 30% active compared with WT-GDH. Circular dichroism (CD) studies confirmed that consistent with Cozier's model of GDH, the catalytic domain consists largely of β-sheets. It is not obvious what led to their success; many earlier experiments in our laboratory failed to achieve this.

6.2 The importance of the tryptophan docking motif in enzyme stabilisation

Every tryptophan docking motif may be essential for stability because abolishing one of these motifs prevented the production of GDH. Mutating Trp-198 to Ala-198 may have made the protein unstable and caused it to be degraded after expression. Trp-198 is predicted to be located on W8 and to form interactions with Ala-790 on the same W strand and with the peptide bond between Ser-243 and Gly-244 on W1. This motif may be more critical than the other motifs because it holds together W1 and W8 that are formed from the N and C-terminal of the polypeptide chain (Figure 1.16). The only other study of this was by Yamada *et al.* (1998) who showed that mutating Gly-741 (to serine) that forms part of the tryptophan docking motif stabilising motifs W6 and W7 produced a protein that was less active (41%) than WT-GDH. I had hoped to extend this study of the role of tryptophan docking motifs by mutating many of the motifs in periGDH but this proved impossible (see Section 6.1).

6.3 Site-directed mutagenesis of amino acids proposed to be involved in binding the metal ion at the active site

The modelled structure of GDH (Cozier and Anthony, 1995) based on the alignment of the sequence of GDH to MDH predicted that Asp-354, Asn-355 and Thr-424 bind to the metal ion at the active site (Figure 6.1). Asn-354 was predicted to form two bonds with the metal ion, and Asp-355 and Thr-424 one bond each; a further three bonds are expected to be made by the PQQ carboxylate at position 7, the pyridine nitrogen (N-6) and the oxygen at C-5 of PQQ. To confirm the role of these amino acids and to further investigate metal ion binding in GDH, these residues were mutated by site-directed mutagenesis. The Kunkel method and the Stratagene Quickchange method were used but only the Stratagene method was successful. The Kunkel method may have failed due to the poor quality of the uracil-containing template, or the primers were not binding to a sufficiently specific site. The Stratagene Quickchange method was used successfully to make D354N, N355D and D354N/N355D mutations. T424N was kindly supplied by Professor Sode. The remaining part of this discussion will summarise the characterisation of WT-GDH and these mutant GDHs.

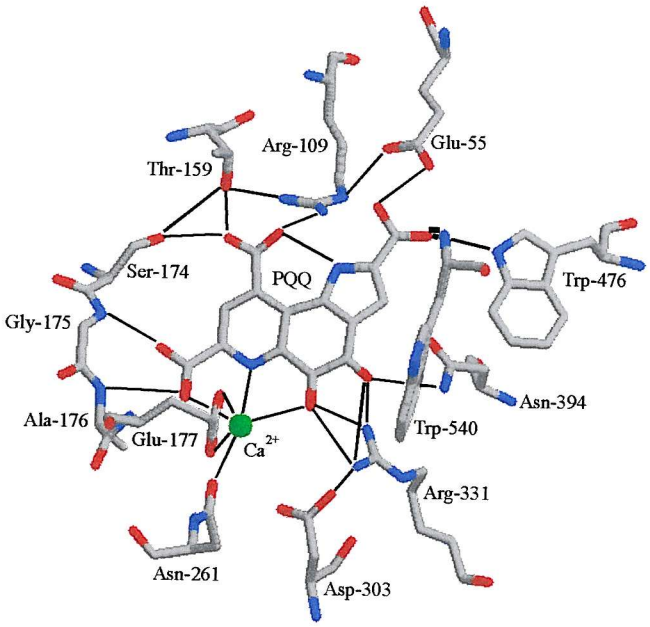

Figure 6.1a The equatorial interactions of PQQ in the active site of methanol dehydrogenase (Ghosh *et al.*, 1995)

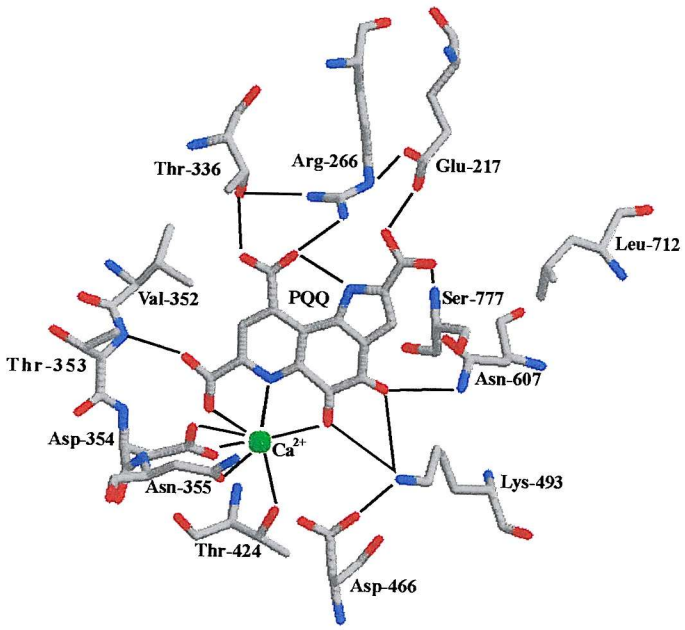

Figure 6.1b The equatorial interactions of PQQ in the active site of the model glucose dehydrogenase (Cozier and Anthony, 1995)

6.4 Purification of WT and mutant GDHs

The protocol used to purify GDH was adapted from the method used by Matsushita *et al.* (1989b) and Yamada *et al.* (1993). 0.5% Triton X-100 was used for solubilisation and as found previously, this caused some inhibition of WT-GDH. Remarkably, all the mutants were less sensitive to the inhibitory effect of Triton X-100. The concentration (0.5%) chosen to solubilise mutant GDHs did not cause any inhibition. WT-GDH and mutant GDHs were successfully purified to more than 80% purity. Reconstitution of WT-GDH and mutant GDHs with metal ions and PQQ was very rapid; they became more than 80% reconstituted within the first two minutes and fully reconstituted within 10 minutes.

A major problem encountered in this work was the production of GDH that had an absolute requirement for metal ions during reconstitution. WT-GDH purified in potassium phosphate buffer had an absolute requirement for Mg^{2+} during reconstitution. However, the effect of Ca^{2+} on reconstitution could not be studied because this metal ion precipitated in this buffer. MOPS buffer could not be used because it led to inactive enzyme, and enzyme purified with Pipes buffer was partially active in the absence of added Mg^{2+}. Pipes buffer made up with NaOH gave an enzyme that was 8% active after reconstitution with PQQ but disodium salt Pipes buffer that required HCl to pH the solution was 41% active. Presumably Na^{2+} had some effect or the starting material contained some Mg^{2+} ions; this was not further investigated. For the purification of WT-GDH and all mutant GDHs, Pipes buffer with least Na^{2+} was used. Purified WT-GDH was treated with 100mM EDTA followed by gel filtration to produce GDH that had an absolute requirement for metal ions for reconstitution (Table 6.1). This treatment was also successful with N355D-GDH and T424N-GDH, although EGTA had to be used with T424N-GDH. However, it was not successful for D354N-GDH and D354N/N355D-GDH in which significant activity was obtained after reconstitution in the absence of added metal ions.

6.5 Characterisation of WT and mutant GDHs

Studies with purified WT-GDH and mutant GDHs showed that some characteristics were common to all GDHs presented in this thesis;

Characteristics common to WT-GDH and all mutant GDHs

1) Reconstitution with metal ions and PQQ is very rapid; 80% reconstituted within the first 2 minutes and 100% reconstituted within 10 minutes.
2) K_d values for binding of metal ions during reconstitution were unaffected by pH.

Table 6.1 Kinetic properties of WT and mutant GDHs

Enzyme	Activity without added metal (%)	Relative activity compared with WT-GDH (%)*	K_d Mg^{2+} (mM)	K_d Ca^{2+} (mM)	K_d Sr^{2+} (mM)	K_d Ba^{2+} (mM)	K_d PQQ (μM)		K_m D-glucose (mM)		V_{max} (μmoles/min/mg)		Mg^{2+}:GDH ratio	Ca^{2+}:GDH ratio	Activation energy (kJ/mol)	
WT-GDH	1	100	1.5	na	na	na	0.28		2.8		116		0.82	3.5	41	
D354N-GDH	67	9	na	nd	nd	nd	Ca	4.2	Ca	>3M	Ca	nd	0.20	1.4	Ca	41
							Sr	3.2	Sr	>3M	Sr	nd			Sr	37.3
							Ba	2.9	Ba	>3M	Ba	nd			Ba	47.5
N355D-GDH	4	25	na	3.8	1.4	1.2	Ca	0.41	Ca	949	Ca	44	0.23	4.4	Ca	68
							Sr	1.48	Sr	15.4	Sr	21.7			Sr	44.4
							Ba	0.48	Ba	15.3	Ba	25.9			Ba	45.5
D354N/N355D-GDH	48	10	na	nd	nd	nd	Ca	0.74	Ca	>3M	Ca	nd	0.45	20.2	Ca	42
							Sr	1.0	Sr	>3M	Sr	nd			Sr	26
							Ba	0.94	Ba	>3M	Ba	nd			Ba	47
T424N-GDH	3	20	0.35	0.85	0.37	0.09	Ca	1.2	Ca	>3M	Ca	nd	0.48	12.1	Ca	50
							Sr	0.82	Sr	28	Sr	12.4			Sr	41
							Ba	0.86	Ba	37	Ba	19.6			Ba	45

nd represents values that were not determined accurately

* Relative activity was calculated by measuring the specific activity of WT-GDH and mutant GDHs by the standard assay (but containing 1.5M D-glucose) after reconstitution in the presence of 5mM Mg^{2+} or Ca^{2+}.

3) Gel filtration showed that PQQ binding is reversible and K_d curves for PQQ binding showed typical reversible kinetics.
4) pH had the same affect on PQQ binding in almost all GDHs; affinity decreased above pH 7.5 (except for T424N-GDH).
5) Metal ion binding was reversible even though D354N-GDH and D354N/N355D-GDH did not have an absolute requirement for metal ions during reconstitution. K_d curves for metal ion binding showed typical reversible kinetics with WT-GDH, N355D-GDH and T424N-GDH.
6) Cu^{2+}, Ni^{2+}, Co^{2+}, Mn^{2+} or Fe^{2+} did not support reconstitution and inactivated the enzyme.
7) Generally, the substrate specificity was not altered but the affinity of mutant GDHs for substrates decreased. The highest affinity was measured with D-glucose or 2-deoxy-D-glucose (Tables 6.1 and 6.2).
8) The thermal stability of all GDHs were similar and holoGDH was more stable than apoGDH (Table 6.3); D354N-GDH was slightly more stable.

The Main differences between WT-GDH and mutant-GDHs

1) Mutant GDHs had lower relative activity than WT-GDH (Table 6.1).
2) Only Mg^{2+} could reconstitute WT-GDH but mutant GDHs preferred Ca^{2+}, Sr^{2+} or Ba^{2+}.
3) Mutant GDHs had a lower affinity for substates than that measured with WT-GDH.
4) The activation energy for the oxidation of D-glucose was markedly different with Sr^{2+}-reconstituted D354N/N355D-GDH and Ca^{2+}-reconstituted N355D-GDH (Table 6.2).
5) The affinity of D354N-GDH for PQQ was much lower than that measured with WT-GDH and all other mutant GDHs.

All mutant GDHs had lower activity (at 1.5M D-glucose) than measured with WT-GDH. The results in Table 6.1 show that the mutant GDHs were 9-25% active compared with WT-GDH. The most important "message" perhaps is that the greatest change in the mutant GDHs is in their binding energies.

The activation energy of Mg^{2+}-reconstituted WT-GDH was 41kJ/mol; the activation energies of mutant GDHs were not markedly different apart from Ca^{2+}-reconstituted N355D-GDH (68kJ/mol) and Sr^{2+}-reconstituted D354N/N355D-GDH (26kJ/mol) (Table 6.2, Figures 4.23-4.24 for N355D-GDH, Figures 4.33-4.34 for D354N-GDH, Figures 4.44-4.45 for D354N/N355D-GDH and Figures 4.53-4.54 for T424N-GDH).

Table 6.2 The activation and binding energies of WT and mutant GDHs required for the oxidation of D-glucose

Enzyme	Metal ion	E_A	E_B	E_T	ΔE_A	ΔE_B	ΔE_T	K_m D-glucose (mM)	V_{max} (μmoles/min/mg)	Catalytic efficiency (V_{max}/K_m)
WT-GDH	Mg^{2+}	41	-14.6	26.4	N/A	N/A	N/A	2.8	116	41.4
D354N-GDH	Ca^{2+}	41	>2.7#	43.7	0	+17.3	+17.3	>3M	nd	0.007*
	Sr^{2+}	37.3	>2.7#	40.0	-3.5	+17.3	+13.6	>3M	nd	0.007*
	Ba^{2+}	47.5	>2.7#	50.2	+6.5	+17.3	+23.8	>3M	nd	0.007*
N355D-GDH	Ca^{2+}	68	-0.12	67.8	+27	+14.48	+41.4	949	44	0.046
	Sr^{2+}	44.4	-10.3	34.1	+3.4	+4.3	+7.7	15.4	21.7	1.41
	Ba^{2+}	45.5	-10.3	35.2	+4.5	+4.3	+8.8	15.3	25.9	1.69
D354N/N355D-GDH	Ca^{2+}	42	>2.7#	44.7	+1	+17.3	+18.3	>3M	nd	0.008*
	Sr^{2+}	26	>2.7#	28.7	-15	+17.3	+2.3	>3M	nd	0.008*
	Ba^{2+}	47	>2.7#	49.7	+6	+17.3	+23.3	>3M	nd	0.008*
T424N-GDH	Ca^{2+}	50	>2.7#	52.7	+9	+17.3	+26.3	>3M	nd	0.016*
	Sr^{2+}	41	-8.8	32.2	0	+5.8	+5.8	28	12.4	0.44
	Ba^{2+}	45	-8.2	36.8	+4	+6.4	+10.4	37	19.6	0.52

All energy values are in kJ/mol. EA, EB and ET represents activation energy, binding energy and a measure of the energy of the transition complex respectively. ΔE_A, ΔE_B and ΔE_T are the differences in these energies occurring when WT-GDH is changed to mutant GDHs.

nd represents values that could not determined and represents estimated catalytic efficiencies. Measuring activity with various concentrations of D-glucose showed that the curve remained linear up to 1.5M D-glucose. If it is assumed that K_m equals 1.5M, then V_{max} is twice the activity measured with 1.5M. The catalytic efficiency can therefore be estimated, but it must be emphasised that these values are only a rough guide.

binding energies might be greater than 2.7kJ/mol because to calculate this energy the K_m for D-glucose was used (3M). The Km for D-glucose is clearly greater than 3M.

Table 6.3 The thermal stability of WT and mutant GDHs

	Temperature causing 50% inactivation after incubation for 10 minutes		Time at which 50% inactivation occurs (incubating at 40°C)	
	Apo	Holo	Apo	Holo
WT-GDH	40.8	51	14.3	Not denatured
D354N-GDH	40.5	49	13.3	Not denatured
N355D-GDH	43.2	55	Not denatured	Not denatured
D354N/N355D-GDH	41.0	48.6	15.0	Not denatured
T424N-GDH	41.0	Not determined	10.5	Not denatured

Table 6.4 The K_i and K_{ii} values for the inhibition of the reconstitution of WT-GDH by metal ions

	Ca^{2+}	Sr^{2+}	Ba^{2+}
K_i	3.41mM	3.47mM	0.45mM
K_{ii}	N/A	11.96mM	3.53mM

The K_d for Mg^{2+} was 1.5mM and the K_I with Mg^{2+} was 190mM

Table 6.5 The K_i and K_{ii} values for the inhibition of the reconstitution of N355D-GDH by Mg^{2+}

	Mg^{2+}
K_i	11.4mM
K_{ii}	39.6mM

The K_d for Ca^{2+} was 1.0mM and the K_I with Ca^{2+} was 123.6mM

Analysing the differences of the activation energies and binding energies between WT-GDH and mutant GDHs (Table 6.2) allowed three possible outcomes:

1) *The change in activation energy is smaller than the change in binding energy* – in this case the change in activation energy is caused by the decrease in the stability of both the transition state complex and the enzyme-substrate complex (this occurred in D303-MDH).
2) *The change in activation energy is equal to the change in binding energy* – in this case the change in activation energy is due to the decrease in the stability of the enzyme-substrate complex with little or no effect on the transition state complex. A change in the conformation of the active site affects substrate binding (this occurred in Ba^{2+}-MDH).
3) *The change in activation energy is greater than the change in binding energy* – in this case a change in activation energy is caused by a decrease in stability of the transition state complex and it may also involve some change in binding energy (no example of this occurs in MDH).

Table 6.2 summarises the results determined with WT-GDH and mutant GDHs. With D354N-GDH reconstituted with Ca^{2+}, Sr^{2+} and Ba^{2+} outcome number 1 was observed, indicating a decrease in the stability of both the transition state-complex and the enzyme-substrate complex.

With N355D-GDH the activation energy depended on the metal ion used in reconstitution process. With Ca^{2+}-reconstituted N355D-GDH the change in activation energy was greater than the change in binding energy indicating that there was a decrease in the stability of the transition state-complex as well as a large change in binding energy (outcome number 3). By contrast, Sr^{2+} and Ba^{2+}-reconstituted N355D-GDH did not have this great change in binding energy; the change in the activation energies was equal to the change in binding energies, indicating a decrease in the stability of the enzyme-substrate complex (outcome number 2).

With the double mutant D354N/N355D-GDH the activation energy again depended on the metal ion used in reconstitution process. With Ca^{2+} and Ba^{2+}-reconstituted enzymes there was a decrease in both the stability of the transition state complex and the enzyme-substrate complex (outcome number 1). The large and unusual decrease in the activation energy that is observed with Sr^{2+}-reconstituted D354N/N355D-GDH is due to a decrease in the stability of the enzyme-substrate complex because the change in activation energy equals the change in binding energy (outcome number 2). However, the change in binding energy could be greater than recorded because an accurate K_m value for D-glucose could not be

measured. If this is the case then a decrease in the stability of the transition state complex would also contribute to the change in activation energy.

The metal used to reconstitute T424N-GDH also affected the activation energy. With Ca^{2+}-reconstituted T424N-GDH there was no change in the activation energy but a large change in the binding energy suggested a decrease in stability of both the transition state complex and the enzyme-substrate complex (outcome number 1). With Sr^{2+}-reconstituted T424N-GDH the change in activation energy was caused by a decrease in the stability of both the transition state complex and the enzyme-substrate complex (outcome number 1) but the change in activation energy with Ba^{2+}-reconstituted T424N-GDH was caused by a decrease in the stability of the enzyme-substrate complex; the change in activation energy was equal to the change in binding energy (outcome number 2).

In all mutant GDHs, changes in binding energies and in the energies of the transition state complex are all likely to be due to relatively large changes in the conformation of the active site, as indicated by the change in substrate affinity and the nature of the metal ion in the active site. In the absence of an X-ray structure little more can be said about this.

There are two possible roles for the added Mg^{2+} during reconstitution of WT-GDH and each will be described in turn, together with the relevant evidence.

1) *The active site model* - Mg^{2+} binds to the active site, holding PQQ in the correct configuration and playing a catalytic role in the reconstituted enzyme (like Ca^{2+} in MDH).

Mutation of the three amino acids that were predicted to bind to the metal ion at the active site changed the specificity for metal ions in the reconstitution process, thus supporting the active site model (Table 6.1). Mg^{2+} was required to reconstitute WT-GDH but mutant GDHs could usually only be reconstituted with Ca^{2+}, Sr^{2+} or Ba^{2+} (Ca^{2+} giving the highest activity). This provides good confirmation that, as predicted in Cozier's model structure, Asp-354, Asn-355 and Thr-424 are involved in binding the metal ion and that the metal ions added in the reconstitution process are incorporated at the active site. The K_d values for Ca^{2+}, Sr^{2+} and Ba^{2+} with N355D-GDH were 1.2-3.8mM and for T424N-GDH they were 0.09mM-0.85mM. T424N-GDH could also be reconstituted with Mg^{2+} (K_d, 0.36mM).

Ca^{2+}, Sr^{2+} and Ba^{2+} did not support reconstitution of WT-GDH but were shown to compete for the same site as Mg^{2+}. Ca^{2+} was a competitive inhibitor whilst Sr^{2+} and Ba^{2+} acted as mixed (non-competitive) inhibitors (Figure 6.2). The K_i values with Ca^{2+}, Sr^{2+} and Ba^{2+} were 3.41mM, 3.47mM and 0.45mM respectively. The K_{ii} values for Sr^{2+} and Ba^{2+} were

Calcium is a competitive inhibitor

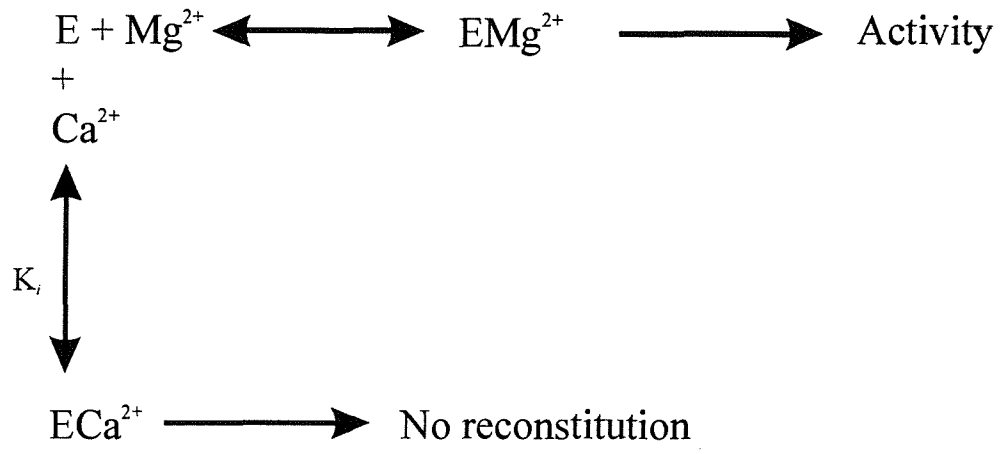

Barium and strontium are mixed (non-competitive) inhibitors

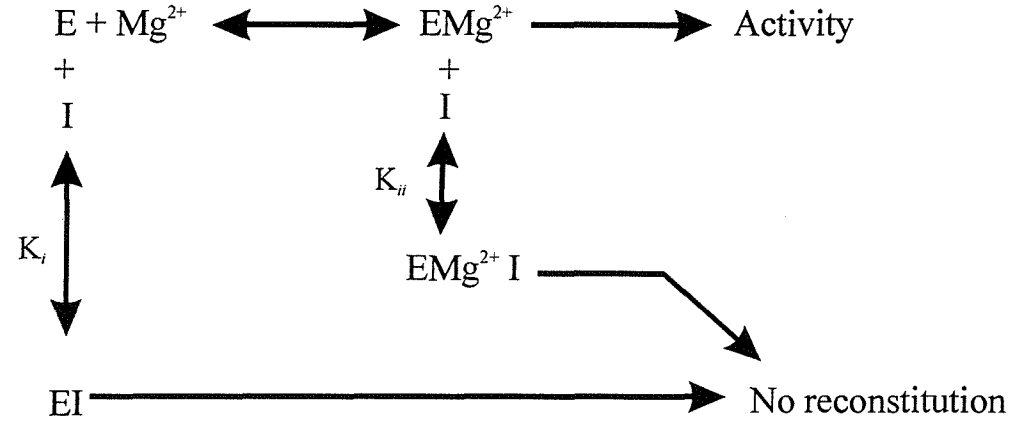

Figure 6.2 Inhibition of reconstitution of WT- GDH by Ca^{2+}, Sr^{2+} and Ba^{2+}

Ca^{2+} binds to GDH when Mg^{2+} is not bound, but Ba^{2+} and Sr^{2+} (represented by I) are able to bind when Mg^{2+} is already bound. Binding of inhibitor to the active site is measured as K_i and binding to a secondary site is measured as K_{ii}.

11.96mM and 3.53mM respectively (Table 6.4). These results support the active site model and suggest that there are two metal ion binding sites in GDH, one at the active site and a second independent inhibitory site; all metals bind at the active site and they all bind to the second (inhibitory) site except for Ca^{2+}. It is possible, however, that Ca^{2+} is able to bind at the second site but with a very low affinity. The highest concentration of Ca^{2+} used was 60mM; if the affinity for Ca^{2+} is similar to that for Mg^{2+} (K_I, 190mM) then the inhibition would possibly not have been observed in the kinetic studies.

Results of inhibition studies with all mutant GDHs showed that Mg^{2+} inhibited reconstitution with Ca^{2+}. The obvious explanation is that Ca^{2+} is incorporated at the active site during reconstitution and that Mg^{2+} competes with Ca^{2+} and can also be incorporated, producing an inactive enzyme. Work with N355D-GDH confirmed that there is a second, inhibitory site for metal ions because Mg^{2+} acted as a mixed inhibitor during reconstitution with Ca^{2+}. The k_i and k_{ii} values for Mg^{2+} were 11.4mM and 39.6mM respectively (Table 6.5).

2) *The PQQ insertion model* - Mg^{2+} could have a direct role in PQQ insertion but does not bind to the active site (a metal ion such as Ca^{2+} is already present at the active site). It may form a complex with PQQ that enables the prosthetic group to bind to the active site or it may bind to a second site than causes a conformational change that allows PQQ to bind to apoGDH.

Evidence that appears at first sight to support the active site model is that purified GDH contained 3-9 molecules of Ca^{2+} in every molecule of GDH plus 0.38-0.82 molecules of Mg^{2+} (Table 3.2 in Section 3.5, Table 3.6 in Section 3.7 and Table 6.1). However, Mg^{2+} is able to reconstitute active enzyme from EDTA-treated GDH (that contained only 0.19 molecules of Ca^{2+} per molecule of apoGDH) suggesting that Mg^{2+} is able to become incorporated at the active site during reconstitution. In the PQQ insertion model, the metal ion must bind in the absence of PQQ to form a stable metal-containing apoenzyme. This is perhaps unlikely as eventually half the bonds to this active site metal ion are provided by PQQ, which is not present until the reconstitution process.

The above results favour the active site model; that is Mg^{2+} binds to the active site, holding PQQ in the correct configuration and playing a catalytic role in the reconstituted enzyme. It was not possible to determine whether PQQ is able to bind at the active site in the absence of metal ion. Figures 6.3–6.7 shows the structures of each mutant GDH, modelled using the program Swissprot, and Table 6.6 lists the lengths of the coordination bonds to the metal ion. Only the position of the mutated residue has been changed in the models, but

Table 6.6 Metal ion ligands at the active site of GDH

These values are based on the predicted structure using the Cozier model of GDH, modified for each mutant GDH. Only the mutated amino acid(s) has been changed using the program Swissprot that placed the mutant residue in a position with the lowest steric hindrance from other residues.

	Distance between ligand and metal ion		
	Residue-354	Residue-355	Residue-424
WT-GDH	Asp-354 2.50 Å and 2.70 Å	Asn-355 3.27Å	Thr-424 4.05Å
D354N-GDH	Asn-354 4.93Å	Asn-355 3.27Å	Thr-424 4.05Å
N355D-GDH	Asp-354 2.50Å and 2.70Å	Asp-355 3.31Å and 3.99Å	Thr-424 4.05Å
D354N/N355D-GDH	Asn-354 4.93Å	Asp-355 3.21Å and 4.04Å	Thr-424 4.05Å
T424N-GDH	Asp-354 2.50Å and 2.70Å	Asn-355 3.27Å	Asn-424 2.67Å

Although clearly untrue, the PQQ-metal ion bonds are assumed to be unchanged in all mutant GDHs. The distances between the carbonyl group (C5), the N-6 nitrogen and the carboxylate group at position 7 of PQQ and the metal ion are 2.77Å, 2.45Å and 2.52Å respectively.

Table 6.7 Metal-ligand distances measured in crystal structures of small molecules

Cation	Minimum metal-oxygen distances (Å) in metal carboxylates
Mg^{2+}	1.95
Ca^{2+}	2.23
Ba^{2+}	2.61

These values are similar in protein structures; the average Ca^{2+} to oxygen bond is 2.2-2.5Å. Table taken from Carrell *et al.* (1988).

obviously the local conformation around the mutated amino acid(s) is also likely to have changed and the "actual" bond lengths would reflect this change. In the models, the green sphere represents Ca^{2+} and the size of Mg^{2+} and Ba^{2+} are also shown. In the Cozier model of GDH, Thr-424 is reported as having a coordination to Ca^{2+}; however the usual bond lengths for these divalent metal ions and oxygen ligands are 1.95-2.61Å (Table 6.7) and the distance of 4.05Å suggests that Thr-424 is not involved in coordination to the metal ion at the active site. The distance between the metal ion and the three ligated atoms of PQQ have been unchanged from that predicted in WT-GDH. The number of protein ligands to Ca^{2+} changed for each mutant and generally the distance between metal ion and the mutated residue increased. The exception was in T424N-GDH in which a bond can now be formed between Asn-424 and the Ca^{2+} (bond length of 2.67Å), which may explain the higher affinity for metals in T424N-GDH (Table 6.1). D354N-GDH, N355D-GDH and D345N/N355D-GDH may have become able to bind to Ca^{2+}, Sr^{2+} and Ba^{2+} in such a way to produce an active enzyme, because the space at the active site has increased to accommodate these larger metal ions.

Prediction of which metal ion binds at the active site of GDH could not be done by analysing the protein's sequence or the modelled structure because of the large diversity of Ca^{2+} and Mg^{2+} binding sites in proteins, with large variations in bond lengths. Also, this task is complicated by the fact that water molecules act as metal ligands in a number of proteins. However, Ca^{2+} binding sites are usually larger than Mg^{2+} binding sites, they often involve more ligands and rarely involve nitrogen ligands. The only sites that have been predicted in the past are proteins containing a helix-loop-helix motif that is common in a number of Ca^{2+} binding proteins but is absent in GDH and other quinoproteins.

The binding of Mg^{2+} in GDH, and Ca^{2+} in MDH suggests that these metal ions have similar roles in their respective enzymes because these enzymes are expected to have a similar mechanism (Section 1.5.4). Both metal ions can act as a Lewis acid but Mg^{2+} is a stronger Lewis acid than Ca^{2+} because it is smaller and more electronegative. The inactivity of WT-GDH containing Ca^{2+} is presumably caused by a conformational change caused by Ca^{2+} binding to the active site. An example supporting this argument is Troponin C in which Mg^{2+} can bind to the calcium binding sites but cannot induce skeletal muscle contraction because Mg^{2+} binding stabilises an inactive conformation. Ca^{2+} and Mg^{2+} can play catalytic roles in reaction mechanisms as shown by phospholipase A_2 and enolase. In phospholipase A_2, Ca^{2+} catalyses the hydrolysis of phospholipids. A histidine-aspartic acid catalytic diad activates a water molecule at the active site for nucleophilic attack on the ester bond of the phospholipid, while Ca^{2+} stabilises the oxyanion transition state; Mg^{2+} is unable to replace Ca^{2+} in this function. By contrast, Mg^{2+} is essential for enolase which catalyses the

dehydration of 2-phosphoglycerate forming phosphoenolpyruvate (in glycolysis). A water molecule that is hydrogen bonded to the carboxyl groups of Glu-198 and Glu-211 acts as a base to abstract a proton from 2-phosphoglyerate. This is followed by the elimination of an $^{-}$OH ion which is coordinated to Mg^{2+}. Mg^{2+} makes this $^{-}$OH ion a better leaving group, and Ca^{2+} is unable to replace Mg^{2+} in this function.

All mutant GDHs had lower affinities for their substrates, the K_m values sometimes being too high to calculate (>3M). Also, the metal ion used in reconstitution affected the affinity for substrates, affinity being higher with Sr^{2+} and Ba^{2+} than with Ca^{2+}. This suggests that the reason that mutant enzymes reconstituted with Mg^{2+} were not active is due to their inability to bind substrates. Binding of Ca^{2+}, Sr^{2+} and Ba^{2+} to the active site of mutant GDHs may stabilise a conformation that allows substrates to bind and it is possible that Mg^{2+} is unable to stabilise an active site conformation suitable for substrate binding. This obviously indicates that some change in the conformation of the substrate binding site has occurred in the mutant GDHs but X-ray structures would be required to fully understand this.

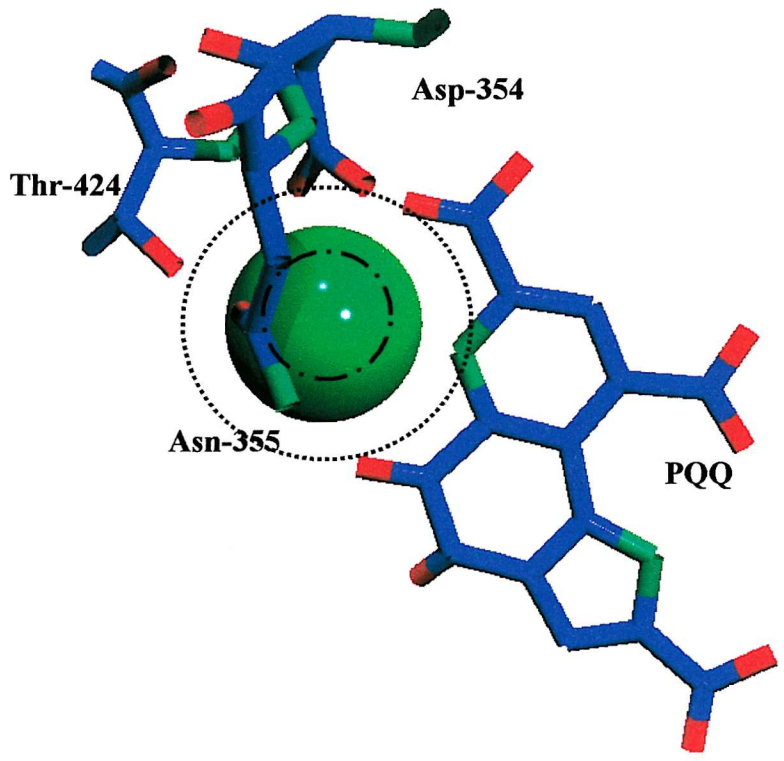

Figure 6.3 Metal binding at the active site of WT-GDH

This model is based on the original MDH structure and so it shows Ca^{2+} (green sphere) bonded to seven ligands contributed from PQQ, Asp-354, Asn-355 and Thr-424. The distance between the two oxygen atoms of Asp-354, the oxygen of Asn-355 and the oxygen of Thr-424 and Ca^{2+} are 2.5Å, 2.70Å, 3.27Å and 4.05Å respectively. Thr-424 may not be able to form a bond with the metal ion because the bond length is 4.05Å, which is too long for a standard M^{2+}-bond. The dotted line represents the size of Ba^{2+} and the broken line represents the size of Mg^{2+}.

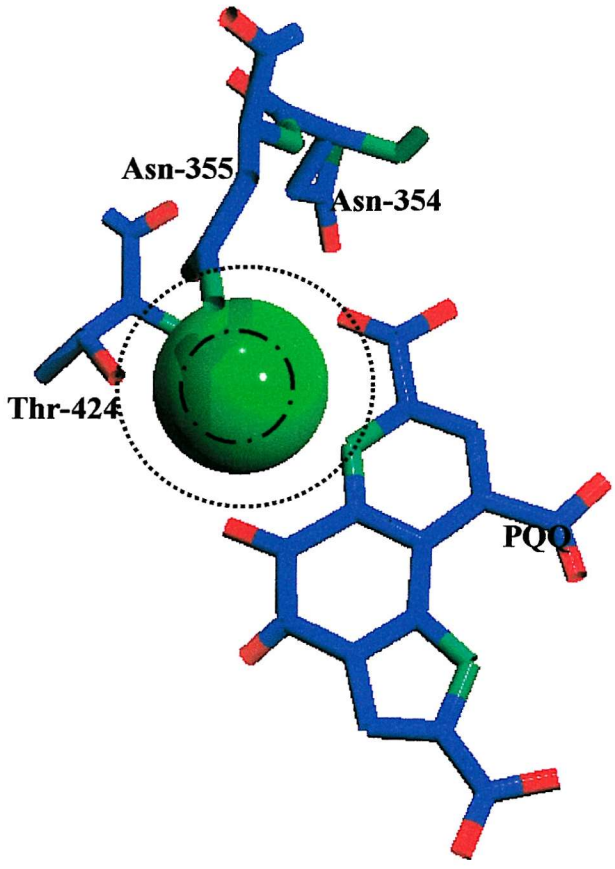

Figure 6.4 Metal binding at the active site of D354N-GDH

The green sphere represents Ca^{2+} (model based on the MDH structure) The inner broken line represents Mg^{2+} and the outer dotted line represents Ba^{2+}.The oxygen atom of Asn-354 is not facing in the direction of the distant Ca^{2+} (4.93Å). This suggests that D354N-GDH has a larger metal binding site than WT-GDH and the number of metal ligands has decreased.

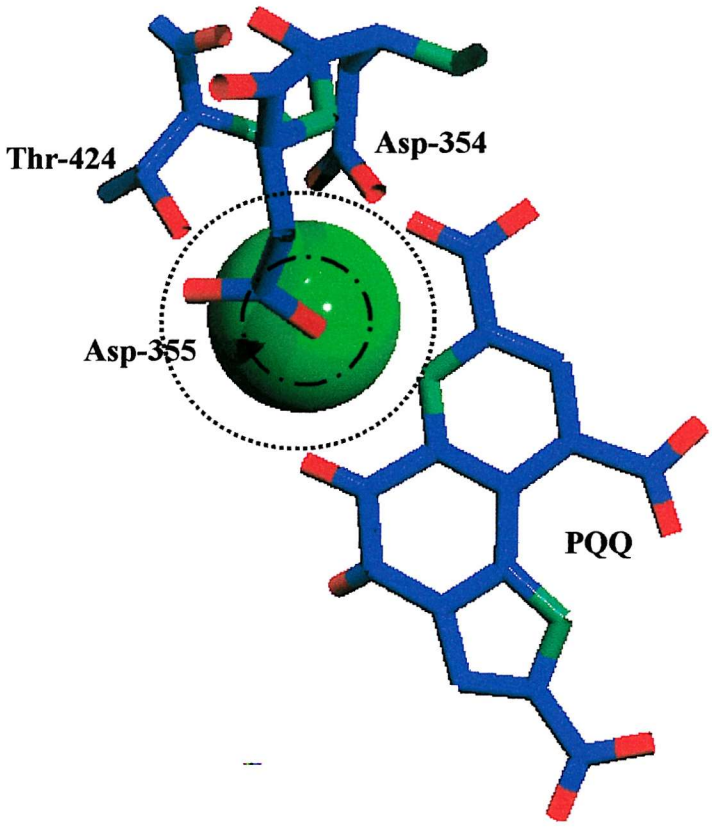

Figure 6.5 Metal binding at the active site of N355D-GDH

The green sphere represents Ca^{2+} (model based on the MDH structure). The inner broken line represents Mg^{2+} and the outer dotted line represents Ba^{2+}. Modeling the position of Asp-355 in N355D-GDH using Swissprot showed that an extra ligand was available to the Ca^{2+}. The distance between the two oxygen atoms of Asp-355 and Ca^{2+} are 3.31Å and 3.99Å. The size of the metal binding site has slightly increased.

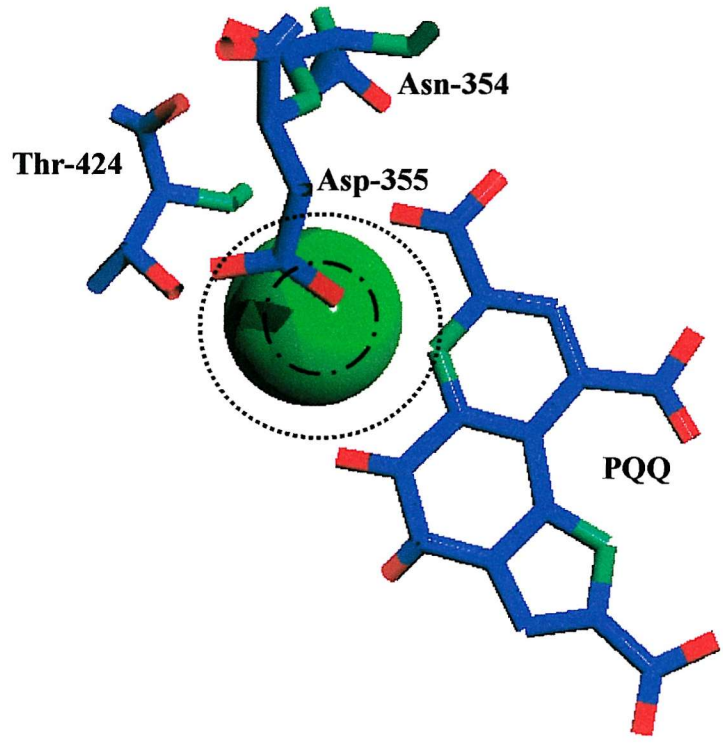

Figure 6.6 Metal binding at the active site of D354N/N355D-GDH

The green sphere represents Ca^{2+} (model is based on the MDH structure). The inner broken circle represents Mg^{2+} and the outer dotted line represents Ba^{2+}. The metal binding site has increased in size. The orientation of Asp-355 may allow it to provide two bonds to the metal ion but these bond lengths are greater than standard values (3.21Å and 4.04Å).

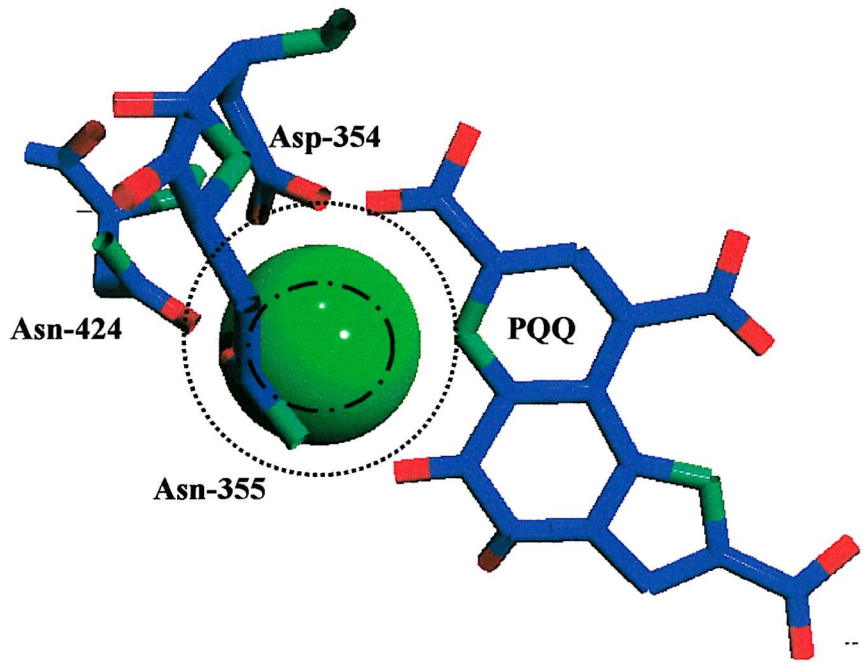

Figure 6.7 Metal binding at the active site of T424N-GDH

The green sphere represents Ca^{2+} (model based on the MDH structure). The inner broken circle represents Mg^{2+} and the outer dotted line represents Ba^{2+}. Modeling the position of Asn-424 in T424N-GDH using Swissprot showed that the size of the metal binding site decreased. The distance between Ca^{2+} and the oxygen ligand of Asn-424 is only 2.67Å (distance between oxygen ligand of Thr-434 and Ca^{2+} is 4.05Å in WT-GDH) suggesting Asn is coordinated to the metal ion. The broken line represents Ba^{2+} at the active site.

References

Adachi, O., Matsushita, K., Shinagawa, E. and Ameyama, M. (1990) Calcium in quinoprotein methanol dehydrogenase can be replaced by strontium. *Agric. Biol. Chem.* **54**, 2833-2837.

Afolabi, P.R., Mohammed, F., Amaratunga, K., Majekodunmi, O., Dales, S. L., Gill, R., Thompson, D., Cooper, J.B., Wood, S. P., Goodwin, P.M. and Anthony, C. (2001) Site-directed mutagenesis and X-ray crystallography of the PQQ-containing quinoprotein methanol dehydrogenase and its electron acceptor, cytochrome c_L. *Biochem.* **40**, 9799-9809

Ameyama, M., Shinagawa, E., Matsushita, K. and Adachi, O. (1981) D-glucose dehydrogenase of *Gluconobacter suboxydans* : solubilization, purification and characterization. *Agric. Biol. Chem.* **45**, 851-861.

Ameyama, M., Nonobe, M., Hayashi, M.,Shinagawa, E., Matsushita, K. and Adachi, O. (1985) Mode of binding of pyrroloquinoline quinone to apo-glucose dehydrogenase. *Agric. Biol. Chem.* **49**, 1227-1231.

Ameyama, M., Nonobe, M., Shinagawa, E., Matsushita, K., Takimoto, K. and Adachi, O. (1986) Purification and characterisation of the quinoprotein D-glucose dehydrogenase apoenzyme from *E. coli*. *Agric. Biol. Chem.* **50**, 49-57.

Anthony, C. (1986) The bacterial oxidation of methane and methanol. *Adv. Microbiol Physiol.* **27**, 113-210.

Anthony, C. (1988) Quinoprotein and energy transduction. In: *Bacterial energy transduction, Academic Press, London* p293-316

Anthony, C. (1992) The c-type cytochromes of methylotrophic bacteria. *Biochem. Biophys. Acta.* **1099**, 1-15

Anthony, C. (1996) Quinoprotein-catalysed reactions. *Biochem. J.* **320**, 697-711

Anthony, C. and Zatman, L.J. (1967) The microbial oxidation of methanol: The prosthetic group of alcohol dehydrogenase of *Pseudomonas* sp. M27; a new oxidoreductase prosthetic group. *Biochem. J.* **104**, 960 – 969.

Anthony, C., Ghosh, M. and Blake, C.C.F. (1994) The structure and function of methanol dehydrogenase and related quinoproteins containing pyrrolo-quinoline quinone. *Biochem. J.* **304**, 665 – 674.

Anthony, C. and Ghosh, M. (1998) The structure and function of the PQQ-containing quinoprotein dehydrogenases. *Progress in Biophysics and Molecular Biology* **69**, 1-21.

Avezoux, A., Goodwin, G. and Anthony C. (1995) The role of the novel disulfide ring in the active site of the quinoprotein dehydrogenase from *Methylobacterium extorquens*. *Biochem. J.* **307**, 735-741.

Bishop, A., Gallop, P.M., and Karnovsky, M.L. (1998) Pyrroloquinoline: a novel vitamin? *Nutrition Reviews*. **56**, 287-292.

Buurman, E.T., Boiardi, J.L., Texeira de Mattos, M.J and Neijssel, O.M. (1990) The role of magnesium and calcium ions in the glucose dehydrogenase activity of *Klebsiella pneumoniae* NCTC 418. *Arch. Microbiol.* **153**, 502-505.

Buurman, E.T., Tenvoorde, G.J. and Demattos, M.J.T. (1994). The physiological function of periplasmic glucose oxidation in phosphate-limited chemostat cultures of *Klebsiella pneumoniae* NCTC418. *Microbiology*. **63**, 71-76.

Bradford, M. (1976) A rapid and sensitive method for the quantitation of microgram quantities of protein utilizing the principle of protein-dye binding. *Analyt. Biochem.* **72**, 248-254.

Brown, I.D. (1988) What factors determine cation coordination numbers? Acta Crystallogr., Sect. B **44**, 545-553.

Chan, H.T.C. and Anthony, C. (1992) Characterization of a red form of methanol dehydrogenase from the marine methylotroph *Methylophaga marina*. *FEMS Microbiol. Lett.* **97**, 293-298.

Cleton-Jansen, A., Goosen, N., Odle, G. and van de Pult, P. (1998). Nucleotide sequence of the gene coding for quinoprotein glucose dehydrogenase from *Acinetobacter calcoaceticus*. *Nucleic Acids Res.* **16**, 6228.

Cleton-Jansen, A., Goosen, N., Fayet, O. and van de Pult, P. (1990). Cloning, mapping, and sequencing of the gene encoding *Escherichia coli* quinoprotein glucose dehydrogenase. *J. Bacteriol.* **172**, 6308-6315.

Cleton-Jansen, A., Dekker, S., van de Puttr, P., and Goosen, N. (1991). A single aminoacid substitution changes the substrate specificity of quinoprotein glucose dehydrogenase in *Gluconobacter oxydans*. *Mol. Genet.* **229**, 206-212

Cohen, S.N., Chang, A.C.Y. and Hsu, L. (1972). Nonchromosomal antibiotic resistance in bacteria: Genetic transformation of *Escherichia coli* by R-factor DNA. *Proc. Natl. Acad. Sci.* **69**, 2110.

Cozier, G.E. and Anthony, C. (1995) Structure of the quinoprotein glucose dehydrogenase of *Escherichia coli* modelled on that of methanol dehydrogenase from *Methylobacterium extorquens*. *Biochem. J.* **312**, 679-685.

Cozier, G.E., Giles, I.G. and Anthony, C. (1995). The structure of the quinoprotein alcohol dehydrogenase of *Acetobacter aceti* modelled on that of methanol dehydrogenase from *Methylobacterium extorquens*. *Biochem. J.* **307**, 375-379.

Cozier, G.E., Salleh, R., Anthony, C. (1999) Characterisation of the membrane quinoprotein glucose dehydrogenase from *E. coli* and characterisation of a site directed mutant in which His262 has changed to tyrosine. *Biochem. J.* **340**, 639-647.

De Jong, G.A.H., Geerlof, A., Stoorvogel, J., Jongejan, J.A., DeVries, S. and Duine, J.A. (1995) Quinohaemoprotein ethanol dehydrogenase from *Comamonas testosteroni-*

purification, characterization and reconstitution of the apoenzyme with pyrroloquinoline quinone analogues. *Eur. J. Biochem.* **230**, 899-905.

Dekker, R.H., Duine, J. A., Frank, J., Verwiel, P.E. J. and Westerling, J. (1982) Covalent addition of water, enzyme substrates and activators to pyrroloquinoline quinone, the coenzyme of quinoproteins. *Eur. J. Biochem.* **125**, 69-73.

Derman, A.I., Prinz, W.A., Belin, D. and Beckwith, J. (1993) Mutations that allow disulfide bond formation in the cytoplasm of *Escherichia coli. Science,* **262**, 1744-1744

Dewanti, A.R. and Duine, J.A. (1998) Reconstitution of membrane-integrated quinoprotein glucose dehydrogenase apoenzyme with PQQ and the holoenzyme's mechanism of action. *Biochem.* **37**, 6810-6818.

Dewanti, A.R. and Duine, J.A. (2000) Ca^{2+}-assisted direct hydride transfer, and rate-determining tautomerization of C5-reduced PQQ to $PQQH_2$, in the oxidation of β-D-glucose by soluble quinoprotein glucose dehyrogenase. *Biochemistry* **39**, 9384-9392.

Dijkstra, M., Frank, J., Duine, J. A. and Duine, J. M. (1989) Studies on electron-transfer from methanol dehydrogenase to cytochrome c_L, both purified from *Hyphomicrobium X. Biochem. J.* **257**, 87-94.

Dokter, P., Frank, J. and Duine, J. A. (1986) Purification and characterization of quinoprotein glucose dehydrogenase from *Acinetobacter calcoaceticus* L. M. B 7e41. *Biochem.J.* **239**, 163-167.

Duine J. A. (1991) Quinoproteins : enzymes containing the quinonoid cofactor pyrroloquinoline quinone, topaquinone or tryptophan-tryptophan quinone. *Eur J. Biochem.* **200**, 271-284.

Duine, J.A., Frank, J. and van Zeeland, J.K. (1979) Glucose dehydrogenase from *Acinetobacter calcoaceticus. FEBS Lett.* **108**, 443-446.

Duine, J. A., Frank, J. and Werwiel, P.E.J. (1980) Structure and activity of the prosthetic group of methanol dehydrogenase. *Eur. J. Biochem.* **108**, 187-192.

Duine, J. A., Frank, J. and Jongejan, J.A. (1983) Detection and determination of pyrroloquinoline quinone, the coenzyme of quinoproteins. *Anal. Biochem.* **133**, 239-243.

Duine, J. A., Frank, J. and Jongejan, J.A. (1987) Enzymology of quinoproteins. *Adv. Enzymol.* **59**, 169-212.

Elias, M.D., Tanaka, M., Izu, H., Matsushita, K., Adachi, O. and Yamada, M. (2000) Function of amino acid residues in the active site of *Escherichia coli* pyrroloquinoline quinone-containing quinoprotein glucose dehydrogenase. *J. Biol. Chem.* **275**, 7321-7326.

Entner, N. and Doudoroff, M. (1952) Glucose and gluconic acid oxidation of *Pseudomonas saccharophila. J. Biol. Chem.* **196**, 853-892.

Esienberg, R.C. and Dobrogosz, W.J. (1967) Gluconate metabolism *in E. coli. J. Bacteriol.* **93**, 941-949.

Felder, M., Gupta, A., Verma, K., Kumar, A., Qazi, G.N. and Cullum, J. (2000). The pyrroloquinoline quinone synthesis genes of *Gluconobacter oxydans. FEMS Microbiol. Lett.* **193**, 231-236.

Fliege, R., Tong, S.X., Shibata, A., Nickerson, K. W. and Conway, T. (1992) The Entner-Doudoroff pathway in *Escherichia coli* is induced for oxidative glucose metabolism via pyrroloquinoline quinine-dependent glucose dehydrogenase. *Appl. Environ. Microbiol.* **58**, 3826-3829.

Frank, J., Dijkstra, M., Duine, J.A. and Balny, C. (1988) Kinetic and special spectral studies on the redox forms of methanol dehydrogenase from *Hyphomicrobium X. Eur. J. Biochem.***174**, 331-338.

Frank, J., Dijkstra, M., Balny, C. Verwiel, P.E.J. and Duine, J.A. (1989) Methanol dehydrogenase: mechanism of action. In: *PQQ and quinoproteins* (eds Jongejan, J.A. and Duine, J.A.) pp13-22. Kluwer Academic Publishers, Dordrecht.

Friedrich, T., Strohdeicher, H., Hofhaus, G., Preis, D., Sahm, H. and Weiss, H. (1990) The same motif for ubiquinone reduction in mitochondria or chloroplasts NADH dehydrogenase and bacterial glucose dehydrogenase. *FEBS Lett.* **265**, 37-40.

Geiger, O. and Gorisch, H. (1989) Reversible thermal inactivation of the quinoprotein glucose dehydrogenase from *Acinetobacter calcoaceticus.* Biochem J. **261**, 415-421.

Ghosh, M., Anthony, C., Harlos, K., Goodwin, M.G. and Blake, C.C.F. (1995) The refined structure of the quinoprotein methanol dehydrogenase from *Methylobacterium extorquens* at 1.94Å. *Structure* **3**, 177-187.

Goodwin, M.G. and Anthony, C. (1996) Characterisation of a novel methanol dehydrogenase containing barium instead of calcium. *Biochem. J.* **318**, 673-679.

Goodwin, M.G., Avezoux, A., Dales, S.C. and Anthony, C. (1996) Reconstitution of the quinoprotein MDH from inactive Ca^{2+}-free enzyme with Ca^{2+}, Sr^{2+} or Ba^{2+}. *Biochem J.* **319**, 839-842.

Goodwin, P. M. and Anthony, C. (1998) The biochemistry, physiology and genetics of PQQ and PQQ containing enzymes. *Advances in Microbial Physiology* **40**, 1-80.

Goosen, N., Horsman, H.P.A., Huinen, R.G.M. and van de Putte, P. (1989) *Acinetobacter calcoaceticus* genes involved in biosynthesis of the coenzyme pyrrolo-quinoline quinone : nucleotide sequence and expression in *Escherichia coli* K-12. *J. Bacteriol,* **171**, 447-455.

Groen, B.W., van Kleef, M.A.G. and Duine, J.A. (1986) Quinohaemprotein alcohol dehydrogenase apoenzyme from *Pseudomonas testosteroni. Biochem. J.* **234**, 611-615.

Harris, T. K. and Davidson, V. L (1994) Replacement of enzyme-bound calcium with Strontium alters the kinetic properties of methanol dehydrogenase. *Biochem. J.* **300**, 175-182.

Hauge, J. G. (1964) Glucose dehydrogenase from *Bacterium anitratum* : an enzyme with a novel prosthetic group. *J. Biol. Chem.* **239**, 3630-3639.

Hommes, R.W.J., Postma, P.W., Neijssel, O.M., Tempest, D.W, Dokter, P. and Duine, J.A. (1984) Evidence of a quinoprotein glucose dehydrogenase apoenzyme in several strains of *Escherichia coli. FEMS Microbiol. Lett.* 24, 329-333

Hommes, R.W.J., van Hell, B., Postma, P.W., Neijssel, O.M., and Tempset, D.W. (1985) The functional significance of glucose dehydrogenase in *Klebsiella aerogenes. Arch. Microbiol.* **143**, 163-168.

Houck, D.R., Hanners, J.L. and Unkefer, C.J. (1988) Biosynthesis of pyrroloquinoline quinone. Identification of biosynthetic precursors using ^{13}C labeling and NMR-spectroscopy. *J. Am. Chem. Soc.* **110**, 6920-6921.

Houck, D.R., Hanners, J.L., Unkefer, C.J., van Kleef, M.A.G and Duine, J.A. (1989) PQQ biosynthetic studies in *Methylobacterium AM1* and *Hyphomicrobium* X using specific ^{13}C labeling and NMR. *Ant. Van. Leeuw.* **56**, 93-101.

Imanaga, Y. (1989) Investigation on the active site of glucose dehydrogenase from *Pseudomonas fluorescens*. In: *PQQ and Quinoproteins* (J.X. Jongejan and J.A. Duine, eds), pp. 87-96. Kluwer Academic Publishers, Dordrecht.

Itoh, S., Ogino, M., Fukui, Y., Murao, H., Komatsu, M., OshiroY., Inoue T., Kai, Y. and Kasai, N. (1993) C4 and C5 adducts of cofactor PQQ (pyrroloquinoline quinone). Model studies directed towards the action of quinoprotein methanol dehydrogenase. *J. Am. Chem. Soc.* **115**, 9960-9967.

Itoh, S., Kawakami, H. and Fukuzumi, S. (1998). Model studies on calcium-containing quinoprotein alcohol dehydrogenases. Catalytic role of Ca^{2+} for the oxidation of alcohols by coenzyme PQQ. *Biochemistry* **37**, 6562-6571.

Itoh, S., Kawakami, H. and Fukuzumi, S. (2000) Development of the active site model for calcium-containing quinoprotein alcohol dehydrogenases. *Journal of Molecular CatalysisB; Enzymatic* **8**, 85-94.

Janes, S.M., Mu, D., Wemmer, D., Smith, A.J., Kaur, S., Maltby, D., Buringame, A.L. and Klinman. J.P. (1990) A new redox cofactor in eukaryotic enzymes; 6-hydroxydopa at the active site of bovine serum amine oxidase. *Science* **248**, 981-987.

Keitel, T., Diehl, A., Knaute, T., Stezowski, J.J, Hohne, W. and Gorisch, H. (2000) X-ray structure of the quinoprotein ethanol dehydrogenase from *Pseudomonas aeruginosa*: basis of substrate specificity. *J. Mol Biol.* **297**, 961-974.

Kojima, K., Watertown, A.B. and Sode, K. (2000) The production of soluble pyrroloquinoline quinone glucose dehydrogenase by *Klebsiella pneumoniae*, the alternative host of PQQ enzymes. *Biotechnol. Lett.* **22**, 1343-1347.

Konrad, E.B. and Lehman, I.R. (1970) Novel mutants of *Escherichia coli* that accumulate very small DNA replicative intermediates. *Pro. Natl. Acad. Sci.* **72**, 2150.

Kundig, W., Ghosh, S and Roseman, S. (1964) Proc. Natl. Acad. Sci. USA **52**, 1097-1074.

Kunkel, T.A. (1985) Rapid and efficient site-directed mutagenesis without phenotyoic selection. *Proc. Natl. Acad. Sci.* USA **82**, 488-492.

Laemmli, U.K. (1970) Cleavage of structural proteins during the assembly of the head of bacteriophage T4. *Nature* **227**, 680-685.

Mandel, E.B. and Higa, A. (1970) Calcium-dependent bacteriophage DNA infection. *J. Mol. Biol.* **53**, 159.

Matsushita, K., Nonobe, M., Shinagawa, E., Adachi, O. and Ameyama, M. (1987) Reconstitution of pyrroloquinoline quinone – dependent D-glucose oxidase respiratory chain of *E. coli* with cytochrome o oxidase. *Journal of Bacteriology*, p205-209

Matsushita, K., Nonobe, M., Shinagawa, E., Adachi, O. and Ameyama, M. (1989a). Quinoprotein D-glucose of the *Acinetobacter calcoaceticus* respiratory chain : membrane bound and soluble forms are different molecular species. *Biochem.* **28**, 6276-6280.

Matsushita, K., Shinagawa, E., Adachi, O. and Ameyama, M. (1989b) Reactivity with ubiquinone of quinoprotein D-glucose dehydrogenase from Gluconobacter suboxydans. *J. Biochem.* **105**, 633-637.

Matsushita, K. and Adachi, O. (1993) Bacterial quinoproteins glucose dehydrogenase and alcohol dehydrogenase. In: *Principles and applications of quinoproteins (Edit. Davidson V.L.)* p47-63, Marcel Dekker Inc. New York.

Matsushita, K., Toyama, H. and Adachi, O. (1994) Respiratory chains and bioenergetics of acetic acid bacteria. *Adv. Microbiol. Physiol.* **36**. 247-301.

Matsushita, K., Toyama, H., Adachi, O., Dewanti, A. and Duine, J.A. (1995) Soluble and membrane-bound quinoprotein D-glucose dehydrogenase of *Acinetobacter calcoaceticus*: the binding process of PQQ to the apoenzymes. *Biosci. Biotechnol. Biochem.* **59**, 1548-1555.

Matsushita, K., Yakushi, T., Toyama, H. and Adachi, O. (1996) Function of multiple heme c moieties in intramolecular electron transport and ubiquinone reduction in the quinohemoprotein alcohol dehydrogenase cytochrome c complex of *Gluconobacter suboxydans. J. Biol. Chem.* **271**, 4850-4857.

McIntire, W.S., Wemmer, D.E., Chistoserdov, A and Lidstrom, M.E. (1991) A new cofactor in a prokaryotic enzyme- tryptophan tryptophylquinone as the redox prosthetic group in methylamine dehydrogenase. *Science* **252**, 817-824.

Meadow, N., Fox, D. and Roseman, S. (1990) The bacterial phosphoenolpyuvate: glucose phosphotransferase system. *Ann, Rev. Biochem.* **59**, 497-542.

Meulenberg, J.J.M., Sellink, E., Loenen, W.A.M., Riegman, N.H., van Kleef, M. and Postma, P.W. (1990) Cloning of *Klebsilla pneumoniae* pqq genes and PQQ biosynthesis in *Escherichia coli. FEMS Microbiol. Lett.* **71**, 337-344.

Meulenberg, J.J.M., Sellink, E., Riegman, N.H. and Postma, P.W. (1992) Nucleotide sequencing and structure of the *Klebsiella pneumoniae* pqq operon. *Mol. Gen. Genet.* **232**, 284-294.

Miyoshi, H., Niitome, Y., Matsushita, K., Yamada, M. and Iwanura, H. (1999) Topographical characterization of the ubiquinone reduction site of glucose dehydrogenase in *E. coli* using depth-dependent fluorescent inhihitors. *Biochimica et Biophysica Acta* **1412**, 29-36.

Morris, C.J., Biville, F., Turlin, E., Lee, E., Ellermann, K., Fan, W.H., Ramamoorthi, R., Springer, A.C. and Lidstrom, M.E. (1994) Isolation, phenotypic characterization and complementation analysis of mutants of *Methylobacterium extorquens AM1* unable to synthesize pyrroloquinoline quinone and sequences of *pqqB*, *pqqG* and *pqqC*. *Bacteriol.* **176**, 1746-1755.

Mutzel, A. and Gorisch, H. (1991) Quinoprotein ethanol dehydrogenase: preparation of the apo-form and reconstitution with PQQ and Ca^{2+} or Sr^{2+} ions. *Agric. Biol. Chem.* **55**, 1721-1726.

Naito, Y.K., Kino, T. and Suzuki, O. (1993) Effects of pyrroloquinoline quinone (PQQ) and PQQ-oxazole on DNA synthesis of cultured human fibroblasts. *Life Science* **52**, 1909-1915.

Neijssel, O.M., Tempest, D.W., Postma, P.W., Duine, J.A. and Frank, J. (1983) Glucose metabolism by K^+-limited *Klebsiella aerogenes*: evidence for the involvement of a quinoprotein glucose dehydrogenase. *FEMS Microbiol. Lett.* **20**, 35-39.

Olsthoorn, A.J.J. and Duine, J.A. (1996) Production, characterization and reconstitution of recombinant quinoprotein glucose dehydrogenase (soluble type; EC 1.1.99.17) apoenzyme of *Acinetobacter calcoaceticus*. *Arch Biochem. Biophys.* **336**, 42-48.

Oubrie, A., Rozeboom, H.J., Kalk, K.H., Duine, J.A and Dijkstra, B.W. (1999a) The 1.7Å crystal structure of the apo form of the soluble quinoprotein glucose dehydrogenase from *Acinetobacter calcoaceticus* reveals a novel internal conserved sequence repeat. *J. Mol. Biol.* **289**, 319-333.

Oubrie, A., Rozeboom, H.J., Kalk, K.H., Olsthoorn, A.J.J., Duine, J.A and Dijkstra, B.W. (1999b) Structure and mechanism of soluble quinoprotein glucose dehyrogenase. *The EMBO Journal* **18**, 5187-5194.

Oubrie, A., Rozeboom, H.J. and Dijkstra, B.W. (1999c). Active-site structure of the soluble quinoprotein glucose dehydrogenase complexed with methylhydrazine : a covalent cofactor-inhibitor complex. *PNAS*, **96**, 11787-11791.

Peekhaus, N. and Conway, T. (1998) What's for dinner? : Entner-Doudoroff metabolism in *Escherichia coli*. *Journal of Bacteriology* **180**, 3494-3502.

Pope, B. and Kent, H.M. (1996) High-efficiency 5 minutes transformation of *Escherichia coli*. *Nucl. Acids Res.* **24**, 536-537.

Prinz, W.A., Aslund, F., Holmgren, A. and Beckwith, J. (1997) *J. Biol. Chem.* **272**, 1566-15667

Redinbaugh, M.G. and Turley, R.B. (1986) Adaptation of the bicinchoninic acid protein assay for use with microliter plates and sucrose gradient fractions. *Anal. Biochem.* **153**, 267-271.

Richardson, I.W. and Anthony C. (1992) Characterisation of mutant forms of the quinoprotein MDH lacking an essential Ca^{2+} ion. *Biochem J.* **287**, 709-715.

Robillard, G. and Bros. J. (1999) Structure and function studies on the bacterial carbohydrate transporter, enzyme II of the phosphoenolpyruvate-dependent phototransferase system. *Biochemica et Biophysica Acta reviews on biomembranes* **1422**, 72-104.

Romano, A.H. and Conway, T. (1996) Evolution of carbohydrate metabolic pathway. *Res. Microbiol.* **147**, 448-455.

Sakamoto, K., Miyoshi, H., Matshita, K., Nakagawa, M., Ikeda, J., Ohshima, M., Adachi, O., Akagi,T. and Iwamura, H. (1996). Comparison of the structural features of ubiquinone reductase sites between glucose dehydrogenase in *E.coli* and bovine heart mitochondrial complex I. *Eur. J. Biochem.* **237,** 128-135.

Salisbury, S.A., Forrest, H.S., Cruse, W.B.T. and Kennard, O. (1979). *Nature* **280**, 842-844.

Sanger, F., Nicklen, S. and Coulson, R. (1977) DNA sequencing with chain terminating inhibitors. *Proc. Natl. Acad. Sci. USA*. **74**, 5463-5467.

Schrover, J.M.J., Frank, J., van Wielink, J.E. and Duine J.A. (1993) Quaternary structure of quinoprotein ethanol dehydrogenase from *Pseudomonas aeruginosa* and its reoxidation with a novel cytochrome c from this organism. *Biochem. J.* **290**, 123-127.

Shinagawa, E., Matsushita, K., Nonobe, M., Adachi, O., Ameyama, M., Ohshiro, Y., Itoh, S. and Kitamura, Y. (1986) The 9-carboxyl group of pyrroloquinoline quinone, a novel prosthetic group, is essential in the formation of holoenzyme of D-glucose dehydrogenase. *Biochem. Biophys. Res. Commun.* **139**, 1279-1284.

Shinagawa, E., Matsushita, Adachi, O. and Ameyama, M. (1989) Formation of the apo-form of quinoprotein alcohol dehydrogenase from *Gluconobacter suboxydans. Agric. Biol. Chem.* **53**, 1823-1828.

Smith, P.K., Krohn, R.I., Hermanson, G.T., Mallia, A.K., Gartner F.H., Provenzano, M.D., Fujimoto, E.K., Goeke, N.M., Olson, B.J. and Klenk, D.C. (1985) Measurement of protein using bicinchonic acid. *Anal. Biochem.* **150**, 76-85.

Sode, K. and Sano, H. (1994) Glu742 substitution to Lys enhances the EDTA tolerance of *Escherichia coli* PQQ glucose dehydrogenase. *Biotechnol. Lett.* **16**, 455-460.

Sode, K., Yoshida, H., Matsumura, k., Ito, S. and Sano, H. (1995a) Elucidation of the region responsible for EDTA tolerance in PQQ glucose dehydrogenase by constructing *Escherichia coli* and *Acinetobacter calcoaceticus* chimeric enzymes. *Biochemical and Biophysical research communications* **211**, 268-273.

Sode, K., Watanbe, K. Ito, S., Matsumura, K. and Kikuchi, T. (1995b) Thermostable chimeric PQQ glucose dehydrogenase. (1995) *FEBS Letters* **365**, 325-327.

Sode, K., Shimakita, T., Ohuchi, S. and Yamazaki, T. (1996) Stabilization of pyrroloquinone quinone glucose dehydrogenase by cross-linking chemical modification. *Biotechnol. Lett*, **18**, 997-1002.

Sode, K. and Kojima, K. (1997) Improved substrate specificity and dynamic range for glucose measurement of *Escherichia coli* PQQ glucose dehydrogenase by site directed mutagenesis. *Biotechnol. Lett.* **19**, 1073-1077.

Sode, K. and Yasutake, N. (1997) Preparation of lyophilized pyrroloquinoline quinone glucose dehydrogenase using trehalose as an additive. *Biotechnology Techniques* 11, 577-580.

Sode, K. and Yoshida, H. (1997) Construction and characterization of a chimeric *Escherichia coli* PQQ glucose dehydrogenase (PQQGDH) with increased EDTA tolerance. *Denki Kagaku.* **65**, 444-451.

Sode, K., Ootera, T., Shirehane, M., Witarto,A.B., Igarashi, S. and Yoshida, H. (2000) Increasing the thermal stability of the water-soluble pyrroloquinoline quinone glucose

dehydrogenase by single amino acid replacement. *Enzyme and Microbial Technology* **26**, 491-496.

Steinberg, F.M., Gershwin,E. and Rucker, R.B. (1994). Dietary pyrroloquinoline quinone: growth and immune response in BALB/c mice. *J. Nutr.* **124**, 744-753.

Stites, T.E., Mitchell, A.E. and Rucker, R.B. (2000) Physiological importance of quinoenzymes and the O-quinone family of cofactors. *J. Nutr.***130**, 719-727.

Stoorvogel, J., Kraayreld, P.E., Vanslvis, C.A, Jongejan. J.A, Devries, S. and Duine, J.A. (1996) Characterisation of the gene encoding quinohaemprotein ethanol dehydrogenase of *Comamonas testosteroni*. *Eur. J. Biochem.* **235**, 690-698.

Stryer. L (1995) *Biochemistry. K.H. Freeman and company, New York.*

Sweeney, N.J.P., Klemm, P., McCormick, B.A., Moller-Nielsen, E., Utley, M., Schembri,M.A., Laux, D.C. and Cohen, P.S. (1996) The *E.coli* K-12 *gnt P* gene allows *E.coli* F-18 to occupy a distinct niche in the streptomycin-treated mouse large intestine. *Infect. Immun.* **64**, 3497-3503.

Takahashi, Y., Igarashi, S., Nakazawa, Y., Tsugawa, W. and Sode, K. (2000) Construction and characterisation of glucose enzyme sensor employing engineered water soluble PQQ glucose dehydrogenase with improved thermal stability. *Electrochemistry* **68**, 907-911.

Unkefer, C.J., Houck, D.R., Britt, B.M., Sosnick, T.R. and Hanners, J.L. (1995) Biogenesis of pyrroloquinoline quinone from ^{3}C-labeled tyrosine. *Met. Enzymol.* **258**, 227-235.

van Kleef, M.A.G. and Duine, J.A. (1988) L-Tyrosine is the precursor of PQQ biosynthesis in *Hyphomicrobium X. FEBS Letts.* **237**, 91-97.

van Schie, B.J., van Dijken, J.P. and Kuenen, J.G. (1984) Non-coordination synthesis of glucose dehydrogenase and its prosthetic group in *Acinetobacter* and *Pseudomonas* species. *FEMS Microbiol. Lett.* **24**, 133-138.

van Schie, B.J., de Mooy, O.H., Linton, J.D., van Dijken, J.P. and Kuenen. J.G. (1987) PQQ-dependent production of gluconic acid by *Acinetobacter agrobacterium* and *Rhizobium* species. *J. Gen. Microbiol.* **133**, 867-875.

Wang, S.X., Mure, M., Medzihradszky, K.F., Burlingame, A.L., Brown, D.E., Dooley, D.M., Smith, A.J., Kagan, H.M. and Klinman, J.P (1996) A crosslinked cofactor in Lysyl oxidase: redox function for amino acid side chains. *Science* **273**, 1078-1084.

Witarto, A.B., Oh-uchi, S., Narita, M. and Sode, K. (1999a) Secondary structure of pyrroloquinoline quinone glucose dehydrogenase. *J. Biochem. Mol. Biol. And Biophys.* **2**, 209-213.

Witarto, A.B., Ohtera, T. and Sode, K. (1999b) Site-directed mutagenesis study on the thermal stability of a chimeric PQQ glucose dehydrogenase and its structural interpretation. *Applied Biochem and Biotechnology* **77-79**, 159-168.

Xia, Z. Dai, W., Zhang, Y., White, S.A., Boyd, G.D. and Mathews, F.S. (1996) Determination of the gene sequence and the three-dimensional structure at 2 angstrom resolution of methanol dehydrogenase from *Methylophilus* W3A1. *J. Mol. Biol.* **259**, 480-501.

Yamada, M., Sumi, K., Adachi, O., and Yamada, Y. (1993) Topological analysis of quinoprotein glucose dehydrogenase in *Escherichia coli* and its ubiquinone binding site. *Journal of Biological Chemistry* **268**, 12812 – 12817.

Yamada, M., Inbe, H., Tanaka, M., Sumi, K., Matsushita, K. and Adachi, O. (1998) Mutant isolation of the *Escherichia coli* quinoprotein glucose dehydrogenase and analysis of crucial residues Asp730 and His775 for its function. *Journal of Biological Chemistry* **273,** 22021-22027

Yamazaki, T., Katsuhiro, K. and Sode K. (2000a) Extended-range glucose sensor employing engineered glucose dehyrogenases. *Anal. Chem.* **72**, 4689-4689.

Yamazaki, T., Yasutake, N. and Sode, K. (2000b). Surface deposition method; a novel protein immobilization proceedure on a sensor surface. *Electrochemistry* **68**, 882-885.

Yoshida, H. and Sode, K. (1996) Thr424 to Asn substitution alters bivalent metal specificity of pyrroloquinoline quinone glucose dehydrogenase. *J. Biochem. Mol. Biol and Biophys*. **1**, 89-93.

Yoshida, H., Kojima, K., Witarto, A.B. and Sode, K. (1999) Enginerring a chimeric pyrroloquinoline quinone glucose dehydrogenase: improvement of EDTA tolerance, thermal stability and substrate specificity. Protein Engineering **12**, 63-70.

Yoshida, H., Iguchi, T. and Sode, K. (2000) Construction of multi-chimeric pyrroloquinoline quinone glucose dehydrogenase with improved enzymatic properties and application in glucose monitoring. *Biotechnol. Lett.* **22**, 1505-1510.

Zheng, Y.J., Xia, Z. Chen, Z. Mathews, F.S. and Bruice, T.C. (2001) Catalytic mechanism of quinoprotein methanol dehydrogenase: a theoretical and X-ray crystallographic investigation. *PNAS* **98**, 432-435.

Appendix

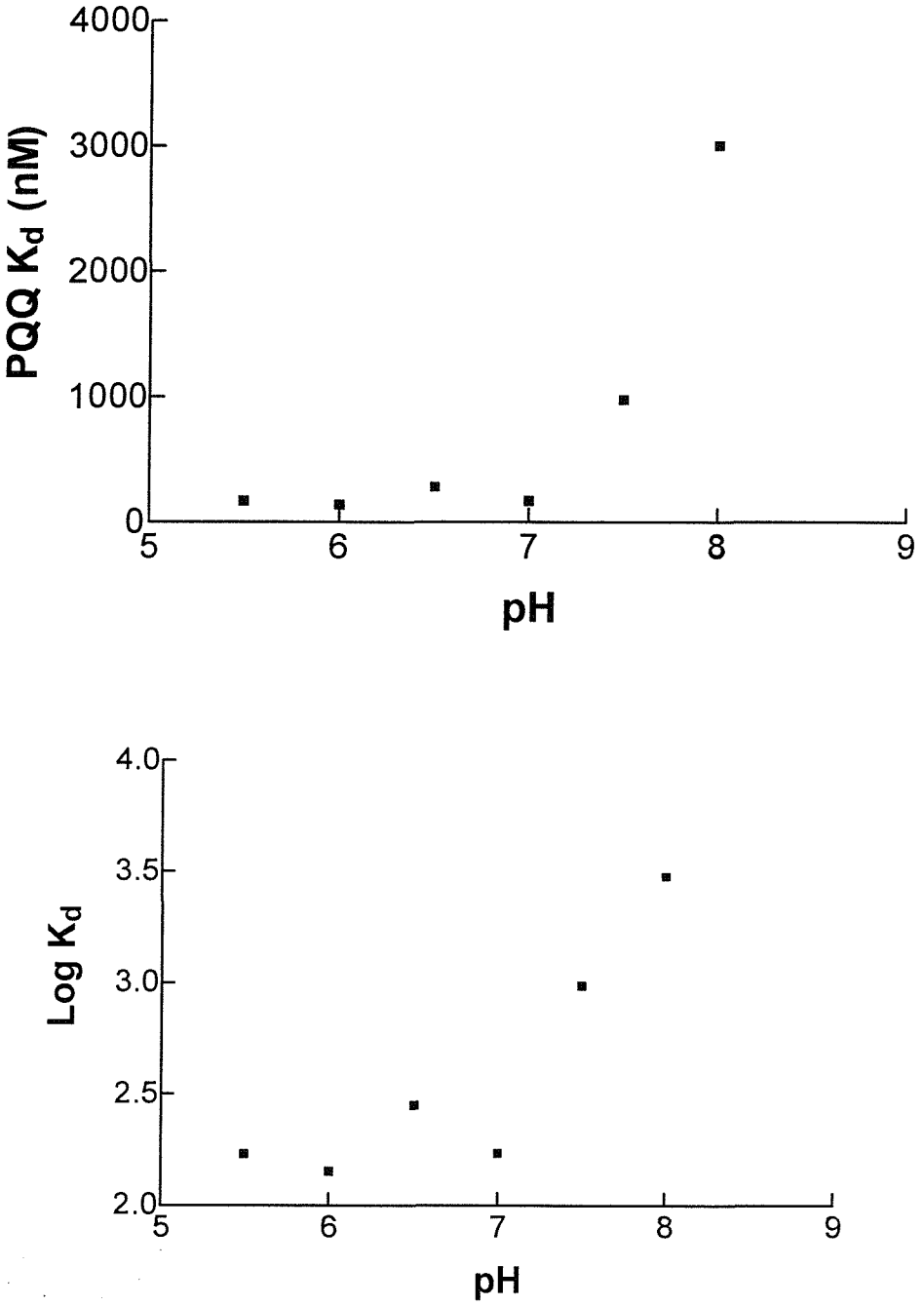

Figure 3.4 The effect of pH on the affinity for PQQ

The K_d and Log K_d for PQQ binding to WT-GDH were plotted against pH of the reconstitution mixture. Data taken from Figure 3.3.

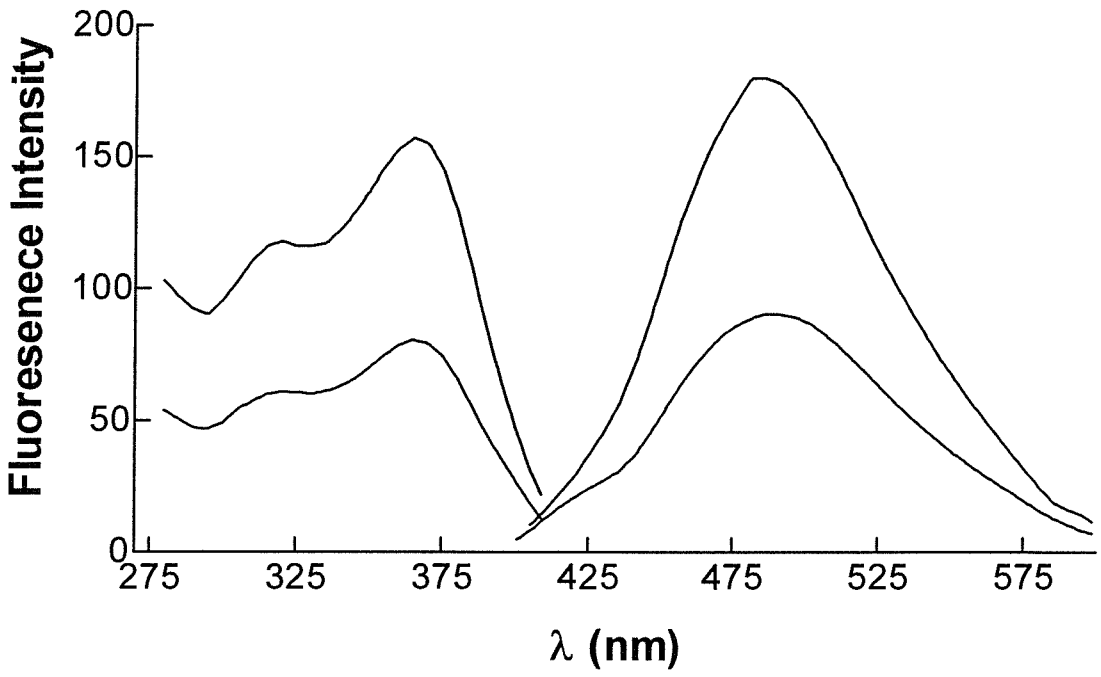

Figure 3.19 The fluoresence spectra of PQQ

The fluorescence spectra of PQQ were measured in 10mM Pipes buffer pH 7.0. Emission spectra were obtained by excitation at 365nM and the excitation spectra by monitoring the emission at 469nM. Spectra measured with 2μM and 4μM PQQ.

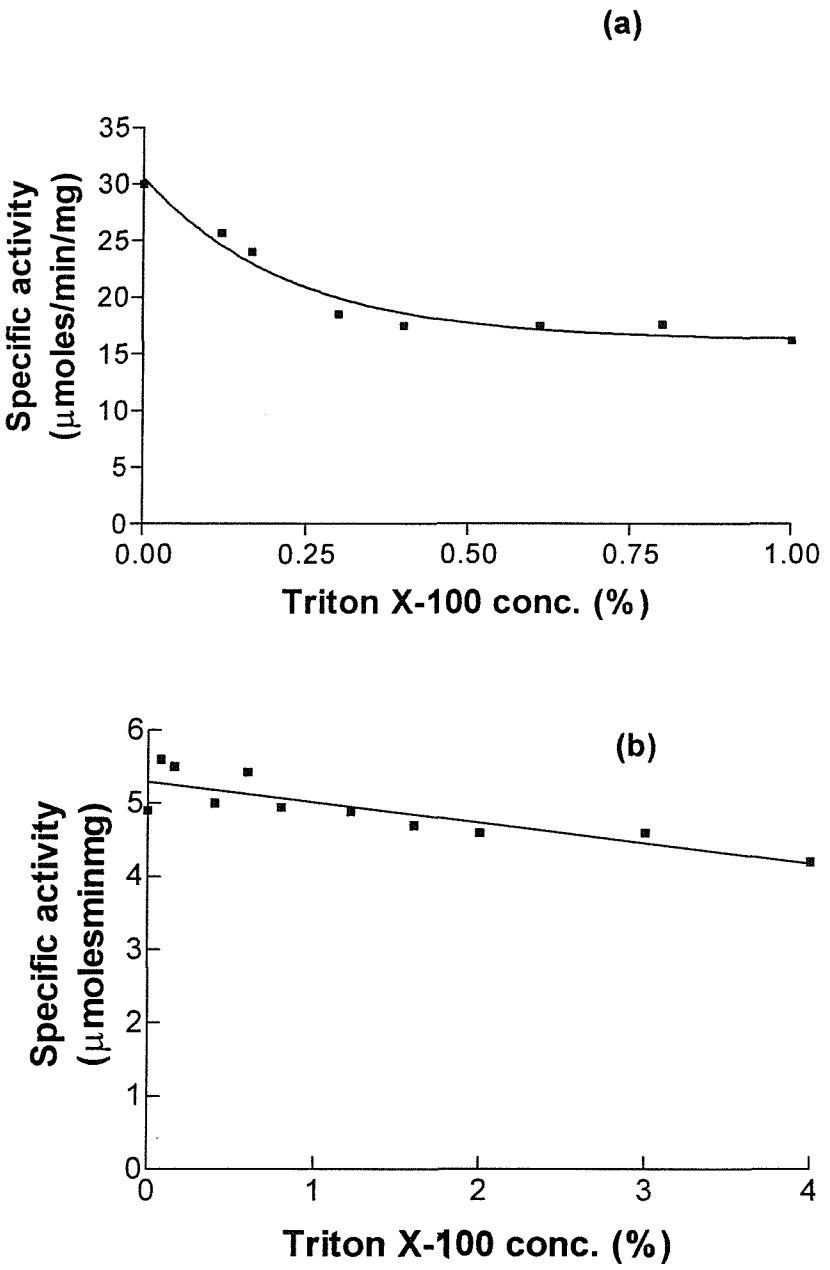

Figure 4.15 The effect of Triton X-100 on activity of membrane fractions containing WT-GDH and N355D-GDH

Membrane fractions containing WT-GDH (a) or N355D-GDH (b) were incubated with various concentrations of Triton X-100 for 30 minutes on ice. Then the samples were reconstituted under standard conditions with 5mM Ca^{2+} (N355D-GDH) or 5mM Mg^{2+} (WT-GDH) and 25μM PQQ and then activity measured.

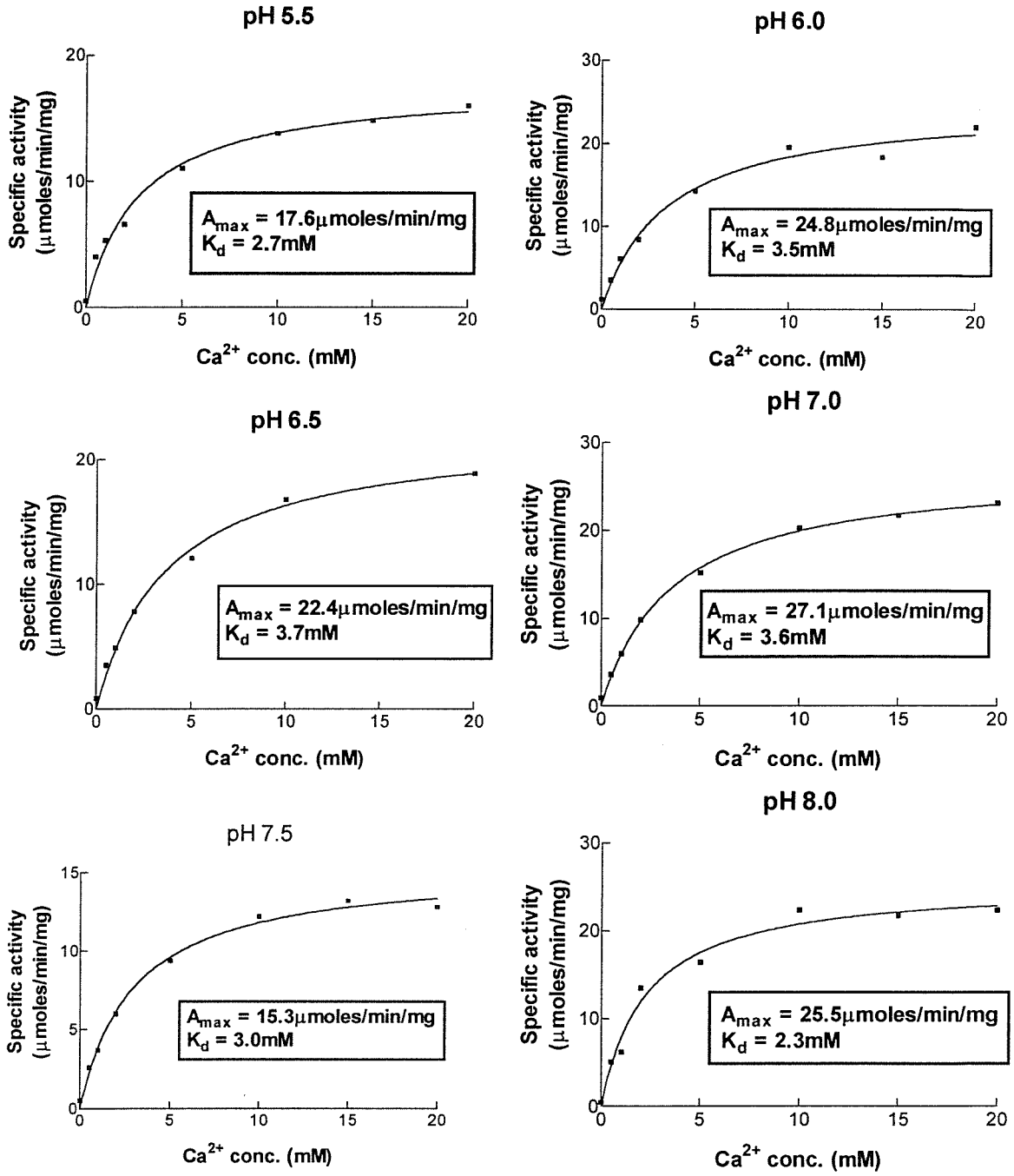

Figure 4.17 The effect of pH on calcium binding to N355D-GDH

The activity of N355D-GDH was measured after 20 minutes reconstitution with 25μM PQQ between pH 5.5 and 8.0. The following buffers (50mM) were used: Bis-tris (pH 5.5), MES (pH 6.0), Pipes buffer (pH 6.5-7.5) and Tris (pH 8.0). Lines of best fit were calculated by the equation $A=A_{max}[Ca^{2+}]/(K_d + [Ca^{2+}])$ where A is GDH activity.

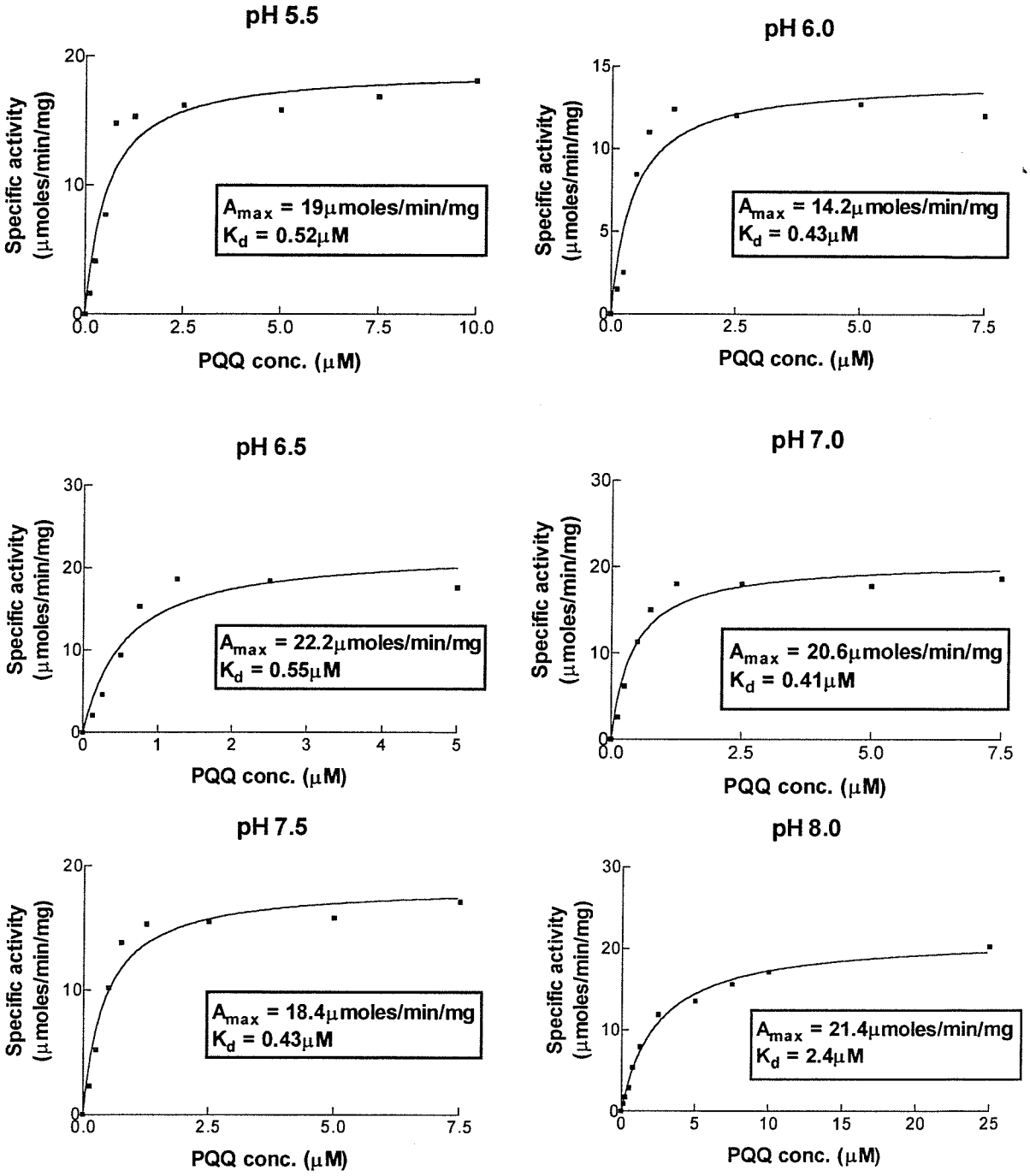

Figure 4.18 The effect of pH on PQQ binding to N355D-GDH

The activity of N355D-GDH was measured after 20 minutes reconstitution with 5mM Ca^{2+} between pH 5.5 and 8.0. The following buffers (50mM) were used: Bis-tris (pH 5.5), MES (pH 6.0), Pipes (pH 6.5-7.5) and Tris (pH 8.0). Lines of best fit were calculated by the equation $A=A_{max}[PQQ]/(K_d + [PQQ])$ where A is GDH activity. Figure 3.3 shows similar results obtained with WT-GDH.

Table 4.4 The removal of Ca^{2+} and PQQ from N355D-GDH by gel filtration

N355D-GDH purified in Pipes buffer was reconstituted with 5mM Ca^{2+} and 25μM PQQ under standard conditions. Gel filtration was then used to determine if Ca^{2+} and PQQ could be removed from the reconstituted enzyme. After gel filtration, GDH was incubated for a further 20 minutes at 25°C with 5mM Ca^{2+}, 25μM PQQ or 5mM Ca^{2+} plus 25μM PQQ. Activity was measured by the standard dye-linked assay at various stages.

Sample	Specific activity (μmoles/min/mg)
GDH before gel filtration	Zero
Reconstituted GDH before gel filtration	25.4
GDH + Ca^{2+} before gel filtration	Zero
GDH + PQQ before gel filtration	1.4
Reconstituted GDH after gel filtration	1.5
Reconstituted GDH after gel filtration + Ca^{2+}	21.6
Reconstituted GDH after gel filtration + PQQ	3.7
Reconstituted GDH after gel filtration + PQQ + Ca^{2+}	31.7

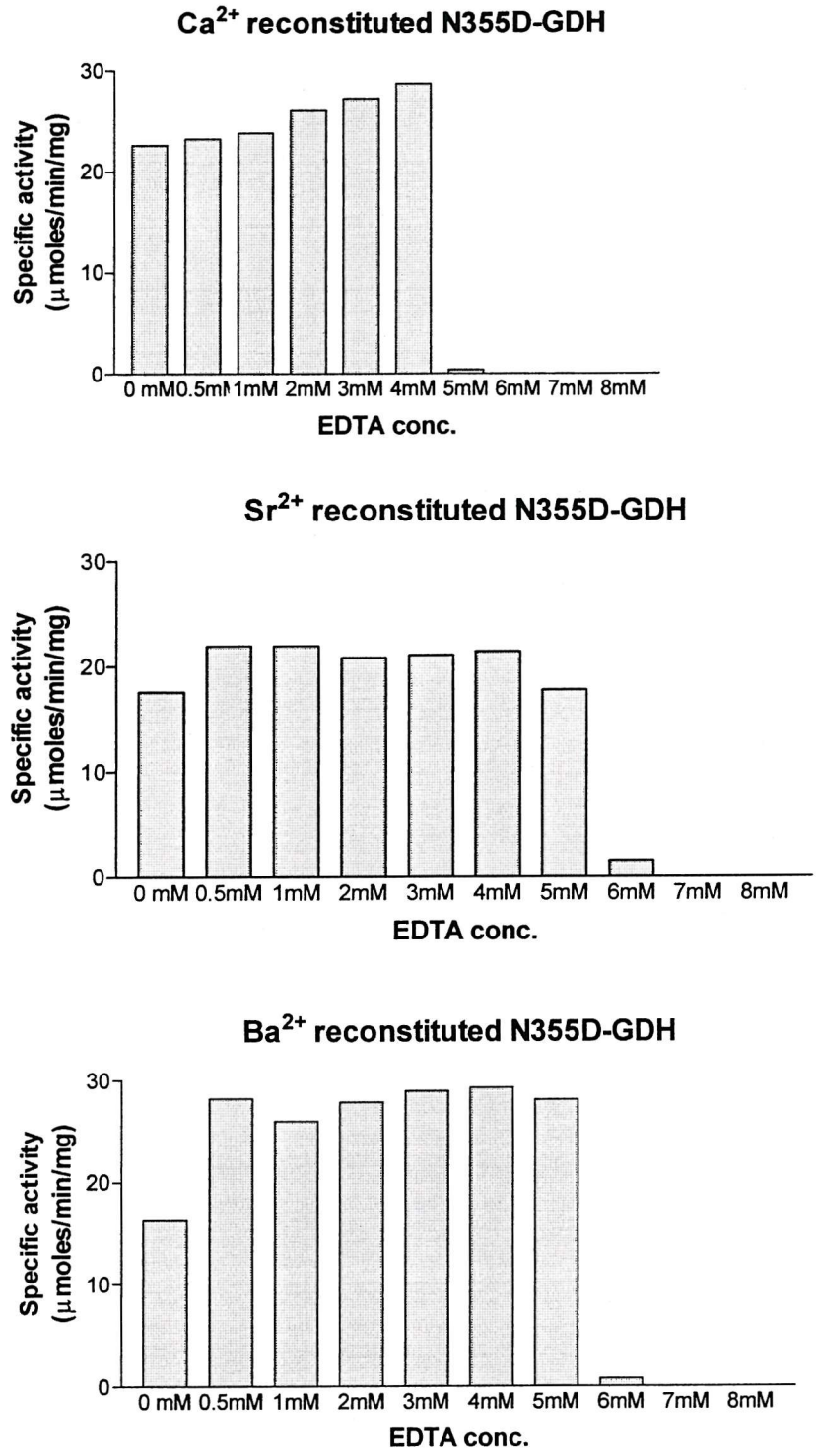

Figure 4.19 The effect of EDTA on N355N-GDH reconstituted with Ca^{2+}, Sr^{2+} and Ba^{2+}

N355D-GDH was reconstituted under standard conditions with 25μM PQQ and 5mM metal ions (Ca^{2+}, Sr^{2+} or Ba^{2+}). Then various concentrations of EDTA were added and the mixture incubated at 25°C for 15 minutes before activity was measured. Figure 3.8 shows similar results obtained with WT-GDH.

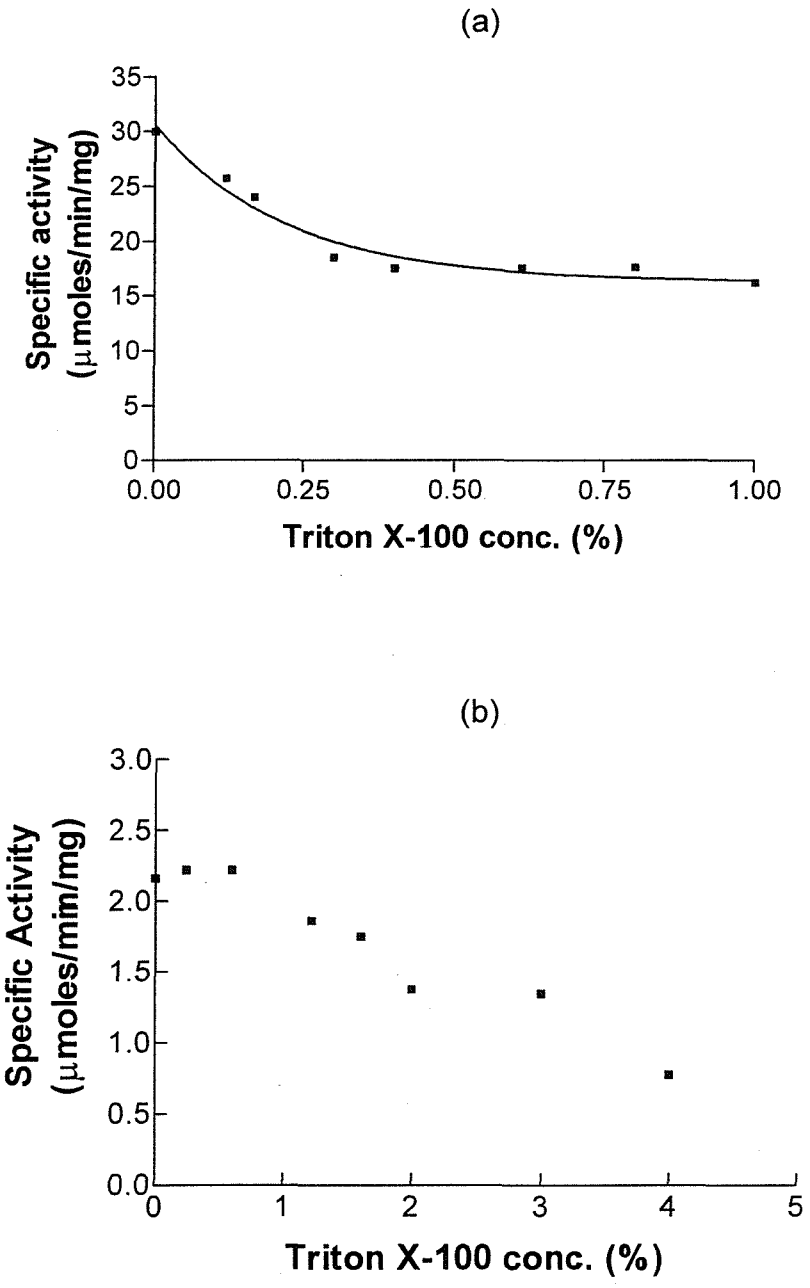

Figure 4.26 The effect of Triton X-100 on membrane fractions containing D354N-GDH

Membrane fractions containing WT-GDH (a) and D354N-GDH (b) were incubated with various concentration of Triton X-100 for 30 mniutes on ice. Then the enzyme was reconstituted under standard conditions with 25μM PQQ and 5mM metal ion. Figure 4.15AP shows results of similar experiments with WT-GDH and N355D-GDH.

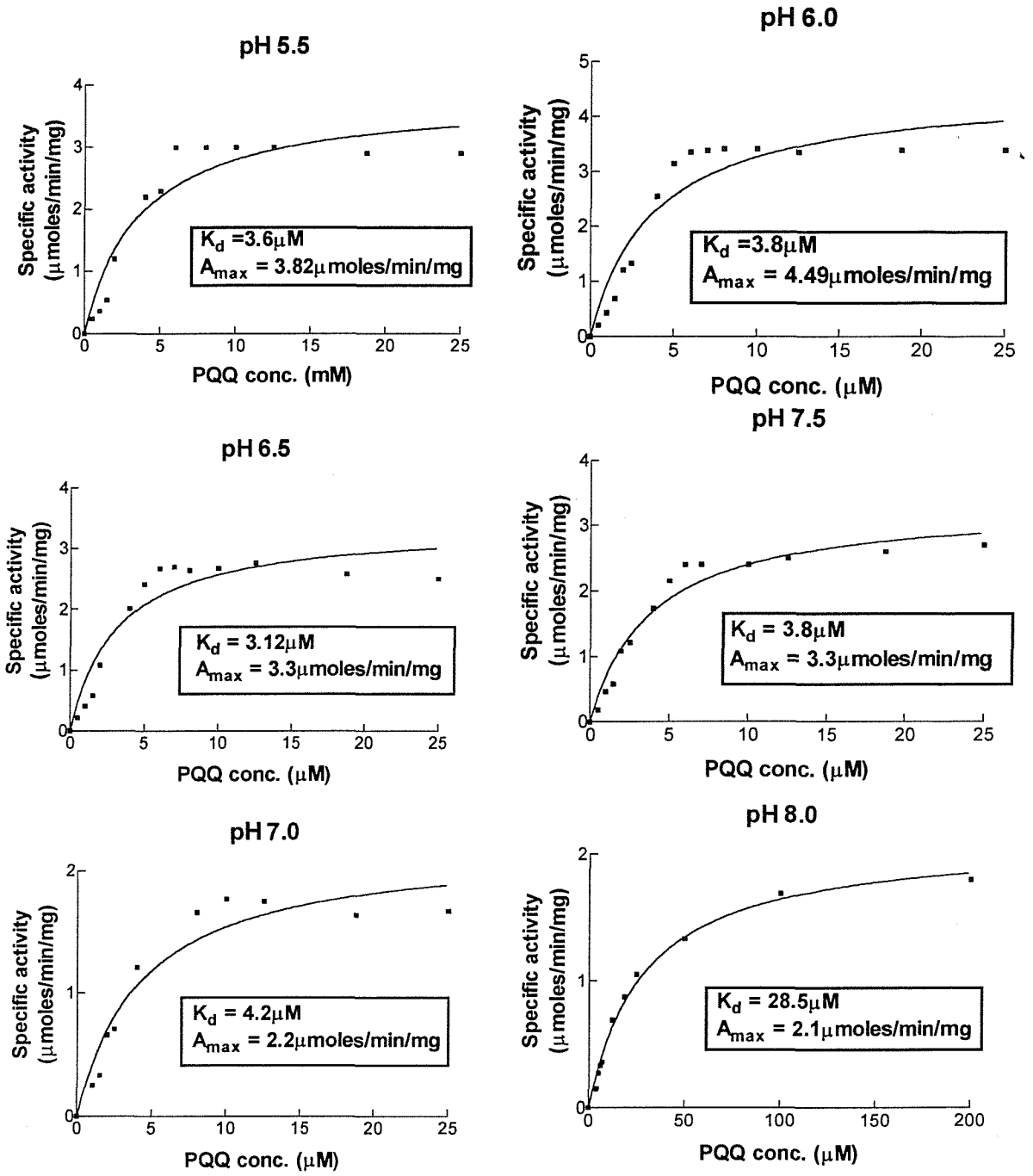

Figure 4.29 Affinity of D354N-GDH for PQQ between pH 5.5 and 8.0

The activity of D354N-GDH was measured after 20 minutes reconstitution with 5mM Ca^{2+} between pH 5.5 and 8.0. The following buffers (50mM) were used: Bis-tris (pH 5.5), MES (pH 6.0), Pipes (pH 6.5-7.5) and Tris (pH 8.0). Lines of best fit were calculated by the equation $A=A_{max}[PQQ]/K_d + [PQQ])$ where A is activity of GDH. Figure 3.3 shows the results for similar experiments with WT-GDH.

Table 4.8 Gel filtration of reconstituted D354N-GDH

D354N-GDH purified in Pipes buffer was reconstituted with 5mM Ca^{2+} and 25μM PQQ under standard conditions. Gel filtration was then used to determine if Ca^{2+} and PQQ could be removed from the reconstituted enzyme. After gel filtration, GDH was incubated for a further 20 minutes at 25°C with 5mM Ca^{2+}, 25μM PQQ or 5mM Ca^{2+} plus 25μM PQQ. Activity was measured by the standard dye-linked assay (containing 1.5M D-glucose) at various stages.

Sample	Specific activity (μmoles/min/mg)
GDH before gel filtration	Zero
Reconstituted GDH before gel filtration	4.82
GDH + Ca^{2+} before gel filtration	Zero
GDH + PQQ before gel filtration	1.8
Reconstituted GDH after gel filtration	1.7
Reconstituted GDH after gel filtration + Ca^{2+}	1.9
Reconstituted GDH after gel filtration + PQQ	3.1
Reconstituted GDH after gel filtration + PQQ + Ca^{2+}	3.4

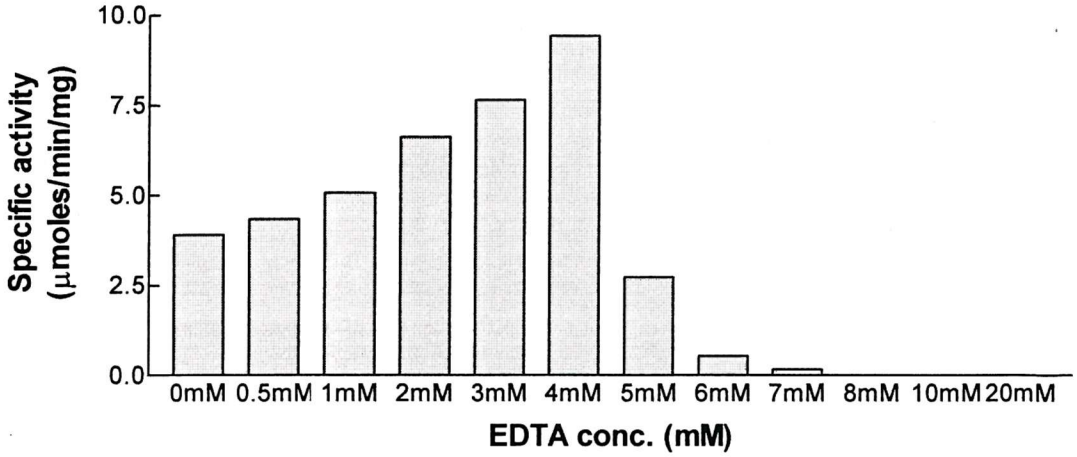

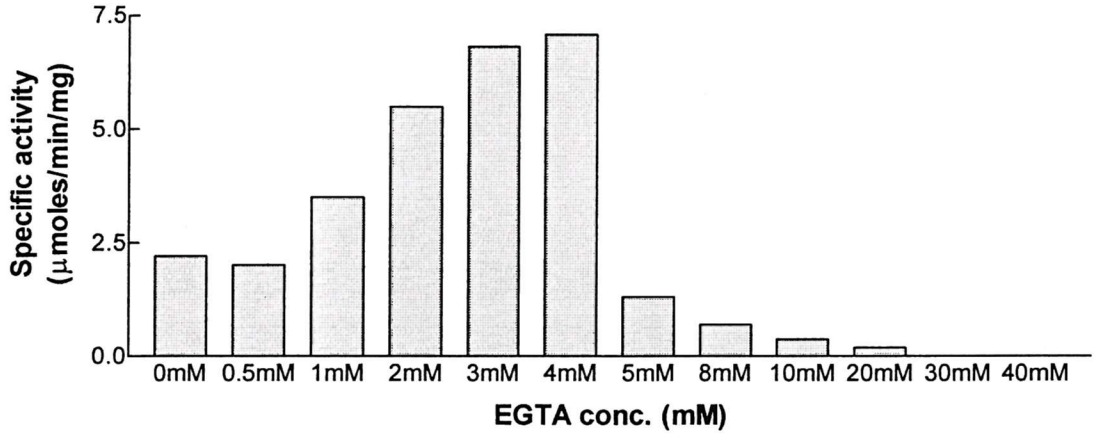

Figure 4.30 The effect of EDTA and EGTA on D354N-GDH reconstituted with Ca^{2+}

D354N-GDH was reconstituted under standard conditions with 25μM PQQ and 5mM Ca^{2+}. Then various concentrations of EDTA or EGTA were added and the mixture incubated at 25°C for 15 minutes before activity was measured. The effect of EDTA on WT-GDH reconstituted with Mg^{2+} is shown in Figure 3.8.

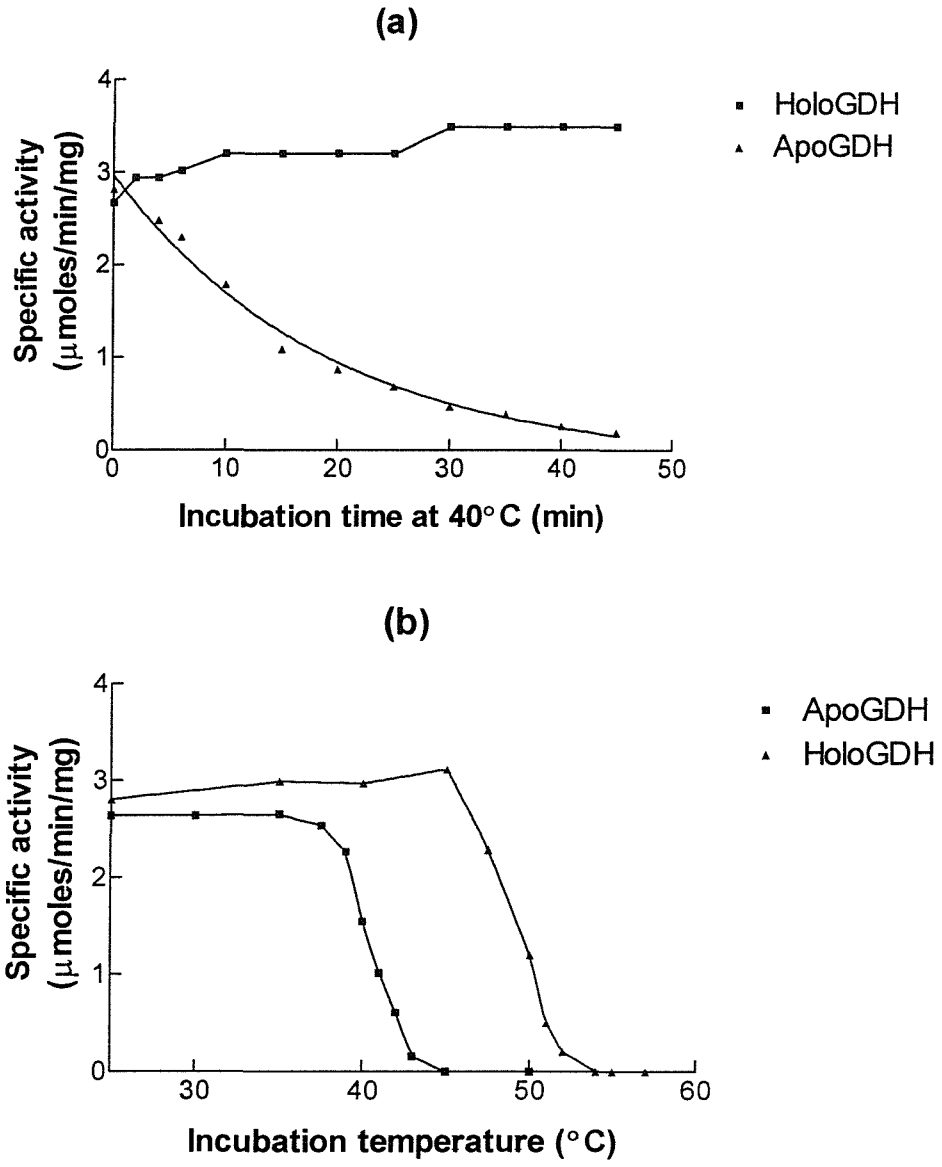

Figure 4.32 Thermal stability of D354N-GDH

a) Apo and holoGDH were incubated at 40°C for various periods of time. Then the enzyme was placed on ice for 5 minutes and apoGDH reconstituted under standard conditions with Ca^{2+} and PQQ before activity was measured.

b) Apo and holoGDH incubated at various temperatures for 10 minutes. Then the enzyme was placed on ice for 5 minutes. ApoGDH was reconstituted under standard conditions with Ca^{2+} and PQQ before activity was measured.

Results for the experiment with WT-GDH is shown in Figure 3.31.

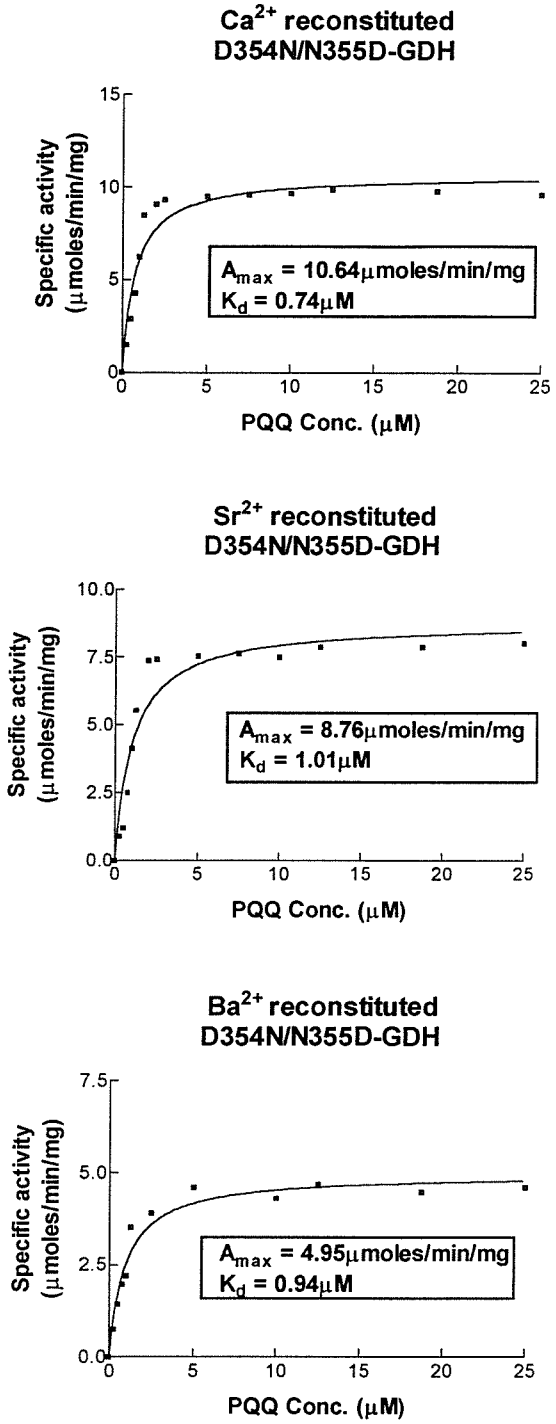

Figure 4.39 The K_d for PQQ with D354N/N355D-GDH

D354N/N355D-GDH was reconstituted under standard conditions with 5mM metal ions (Ca^{2+}, Sr^{2+} and Ba^{2+}). Activity was measured in the presence of 1.5M D-glucose. The lines of best fit were calculated by the equation $A=A_{max}[PQQ]/(K_d + [PQQ])$ where A is enzyme activity after reconstitution.

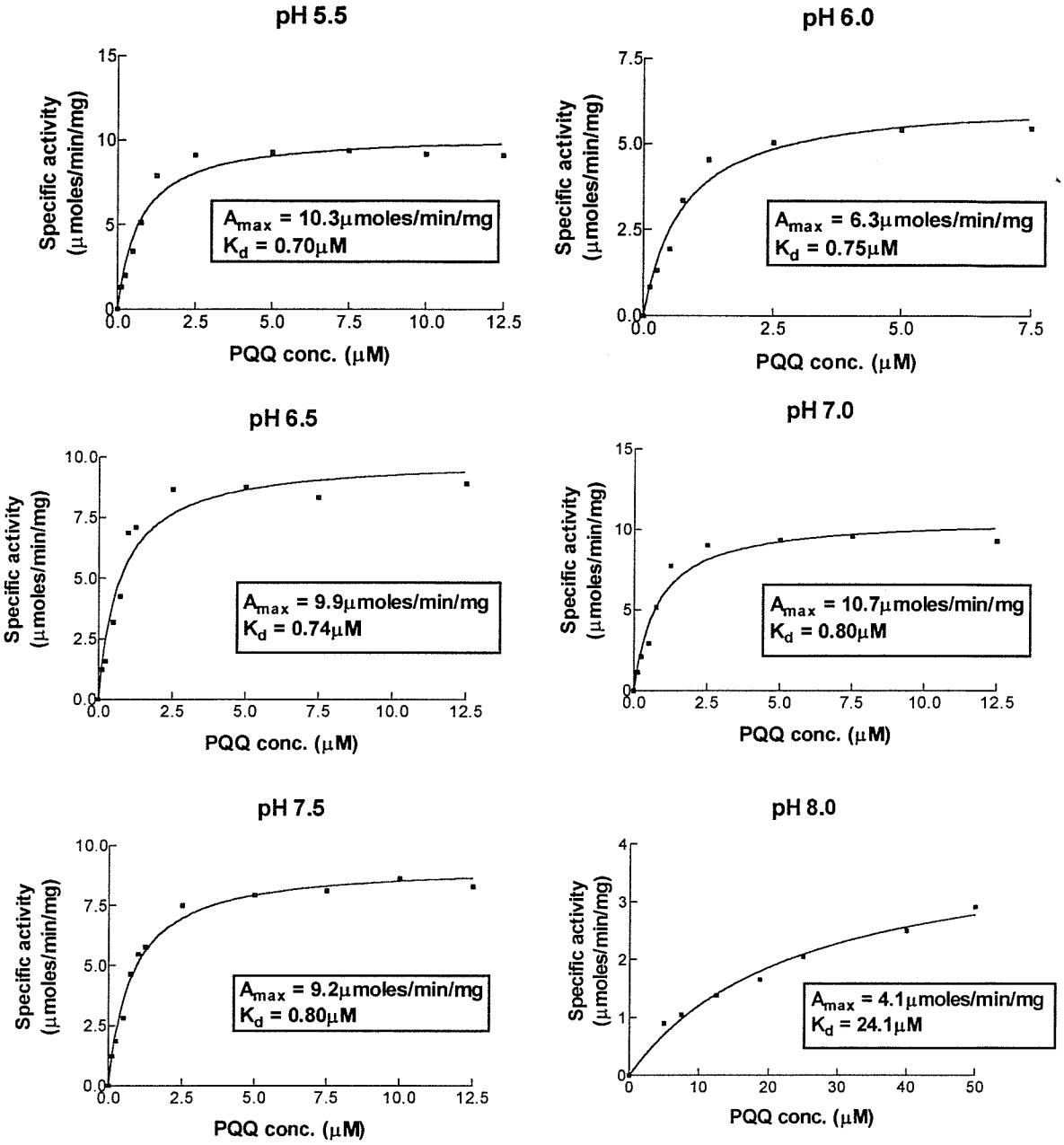

Figure 4.40 The effect of pH on PQQ binding to D354N/N355D-GDH

The activity of D354N/N355D-GDH was measured after 20 minutes reconstitution with 5mM Ca^{2+} between pH 5.5 and 8.0. The following buffers (50mM) were used: Bis-tris (pH5.5), MES (pH6.0), Pipes (pH 6.5-7.5) and Tris (pH 8.0). Lines of best fit were calculated by the equation $A=A_{max}[PQQ]/(K_d + [PQQ])$ where A is activity of GDH. Results with WT-GDH are shown in Figure 3.3)

Figure 4.11 Gel filtration of reconstituted D354N/N355D-GDH

D354N/N355D-GDH was reconstituted with 5mM Ca^{2+} and 25μM PQQ under standard conditions. Gel filtration was then used to determine if Ca^{2+} and PQQ could be removed from the reconstituted enzyme. After gel filtration GDH was reconstituted for a further 20 minutes at 25°C with 5mM Ca^{2+}, 25μM PQQ or 5mM Ca^{2+} plus 25μM PQQ. Activity was measured with the standard dye-linked assay at various stages.

Sample	Specific activity (μmoles/min/mg)
GDH before filtration	Zero
Reconstituted GDH before gel filtration	8.8
GDH + Ca^{2+} before gel filtration	Zero
GDH + PQQ before gel filtration	4.5
Reconstituted GDH after gel filtration	1.6
Reconstituted GDH after gel filtration + Ca^{2+}	5.3
Reconstituted GDH after gel filtration + PQQ	3.6
Reconstituted GDH after gel filtration + PQQ + Ca^{2+}	6.4

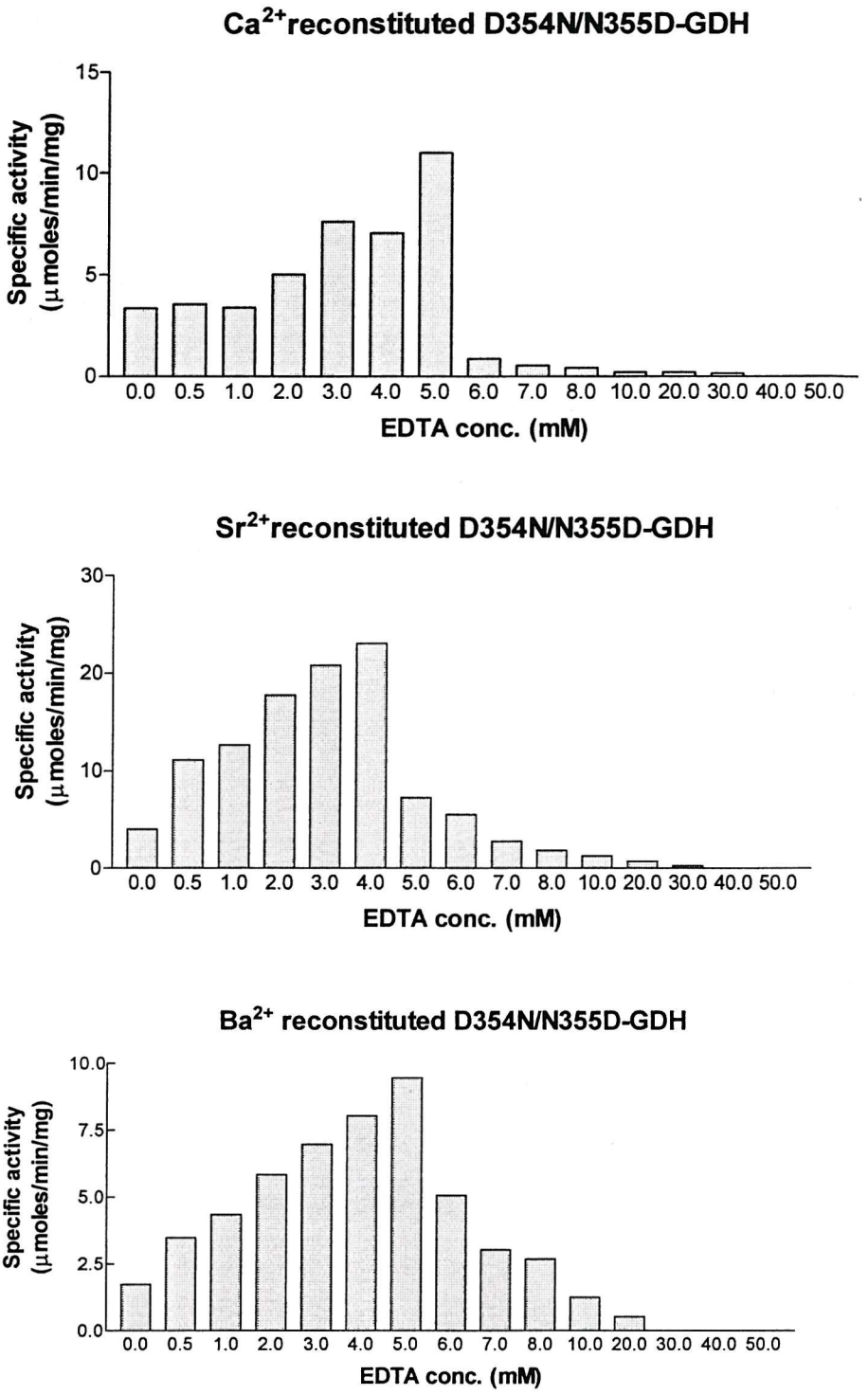

Figure 4.41 The effect of EDTA on D354N/N355D-GDH reconstituted with Ca^{2+}, Sr^{2+} and Ba^{2+}

D354N/N355D-GDH was reconstituted under standard conditions with 25μM PQQ and 5mM metal ions (Ca^{2+}, Sr^{2+} or Ba^{2+}). Then various concentrations of EDTA were added and the mixture incubated at 25°C for 15 minutes before activity was measured. Figure 3.8 shows the effect of EDTA on WT-GDH reconstituted with Mg^{2+}

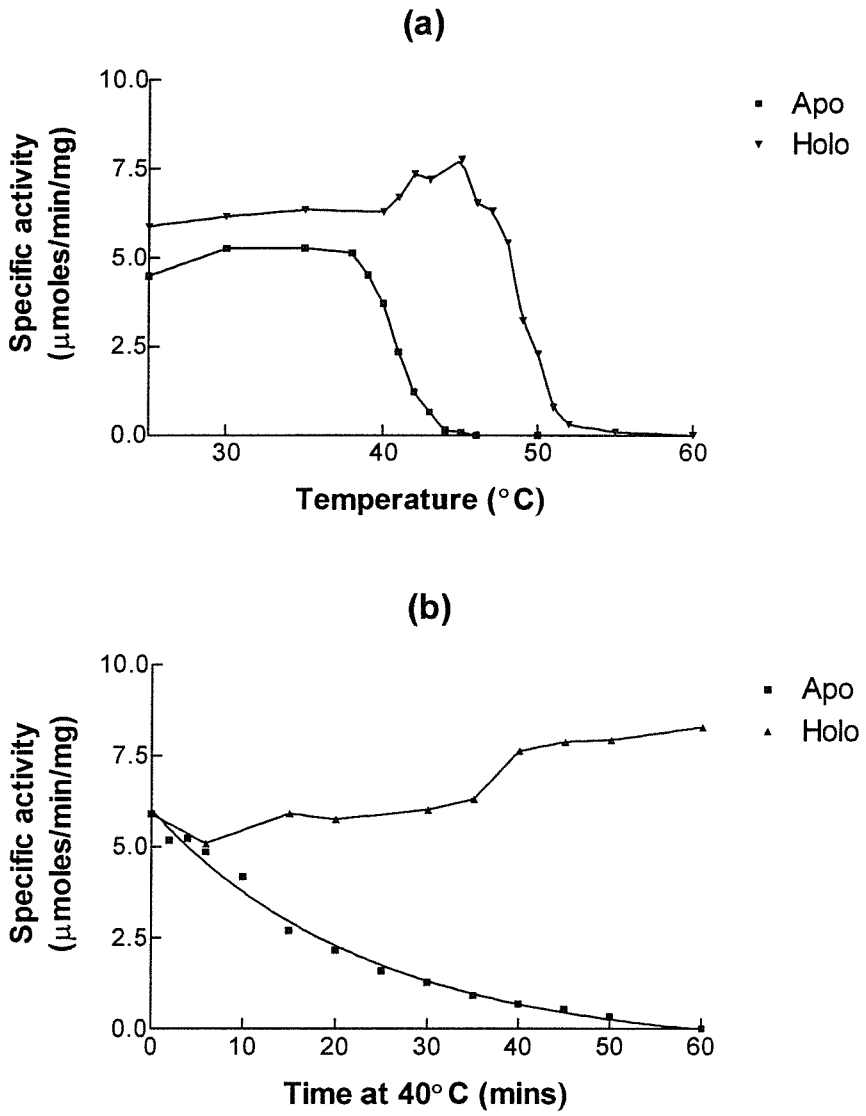

Figure 4.43 The thermal stability of D354N/N355D-GDH

a) Apo and holoGDH were incubated at various temperatures for 10 minutes. Then the enzyme was placed on ice for 5 minutes. ApoGDH was reconstituted under standard conditions with Ca^{2+} and PQQ before activity was measured.

b) Apo and holoGDH incubated at 40°C and samples removed at various periods of times. Then the enzyme was placed on ice for 5 minutes and apoGDH reconstituted under standard conditions with Ca^{2+} and PQQ before activity was measured.

Figure 3.31shows results of a similar experiment with WT-GDH.

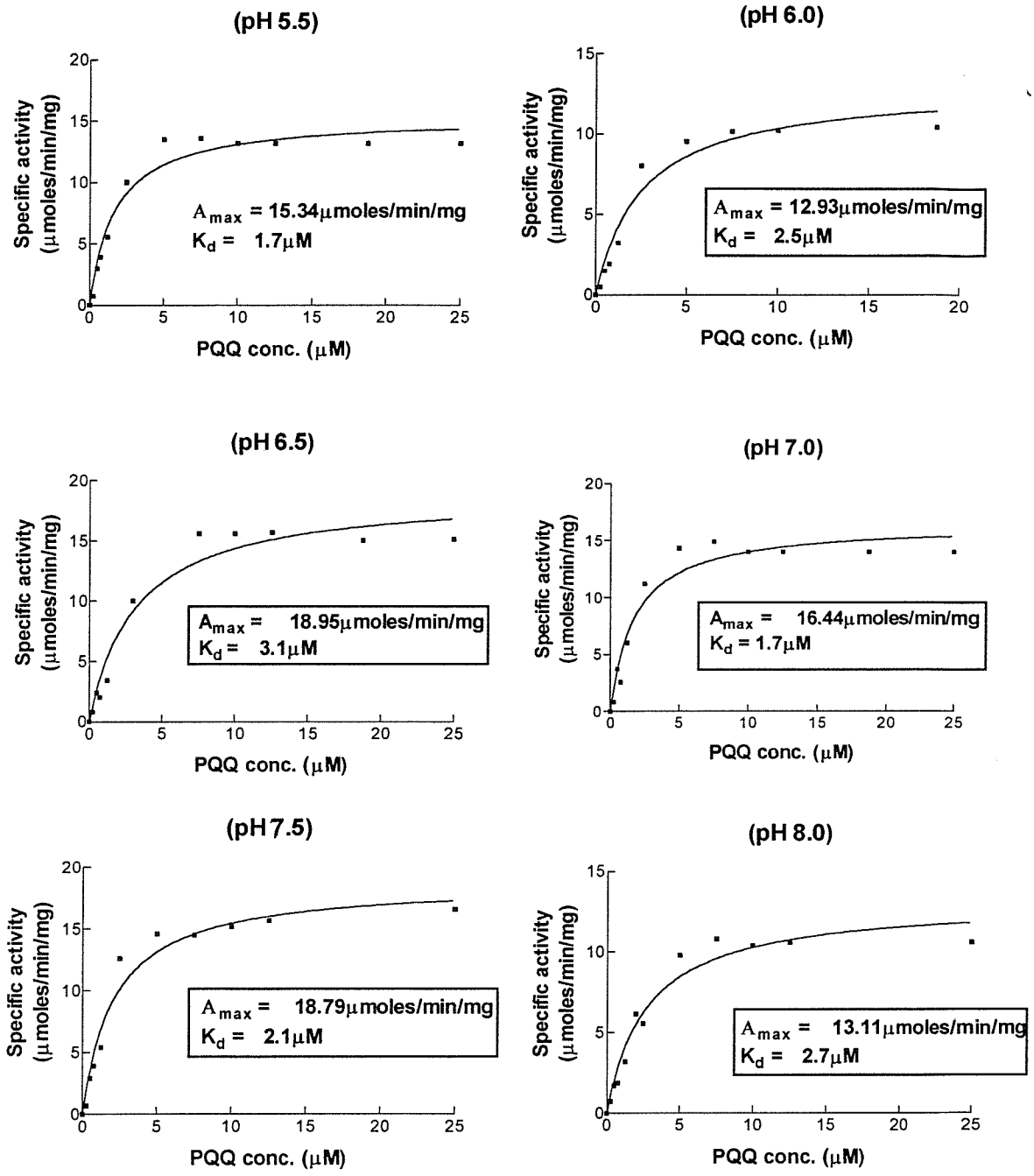

Figure 4.49 The effect of pH on PQQ binding to T424N-GDH

The activity of T424N-GDH was measured after 20 minutes reconstitution with 5mM Ca^{2+} between pH 5.5 and 8.0. The following buffers (50mM) were used: Bris-tris (pH5.5), MES (pH6.0), Pipes (pH6.5-7.5) and Tris (pH 8.0). Lines of best fit were calculated by the equation $A=A_{max}[PQQ]/(K_d + [PQQ])$ where A is GDH activity.

Table 4.15 Gel filtration of Ca^{2+} reconstituted T424N-GDH

T424N-GDH was reconstituted with 5mM Ca^{2+} and 25μM PQQ under standard conditions. Gel filtration was then used to determine if Ca^{2+} and PQQ could be removed from the reconstituted enzyme. After gel filtration GDH was reconstituted for a further 20 minutes at 25°C with 5mM Ca^{2+}, 25μM PQQ or 5mM Ca^{2+} plus 25μM PQQ. Activity was measured by the standard dye-linked assay at various stages.

Sample	Specific activity (μmoles/min/mg)
GDH before gel filtration	Zero
Reconstituted GDH before gel filtration	12.5
GDH + Ca^{2+} before gel filtration	Zero
GDH + PQQ before gel filtration	4.2
Reconstituted GDH after gel filtration	1.0
Reconstituted GDH after gel filtration + Ca^{2+}	2.8
Reconstituted GDH after gel filtration + PQQ	1.5
Reconstituted GDH after gel filtration + PQQ + Ca^{2+}	9.4

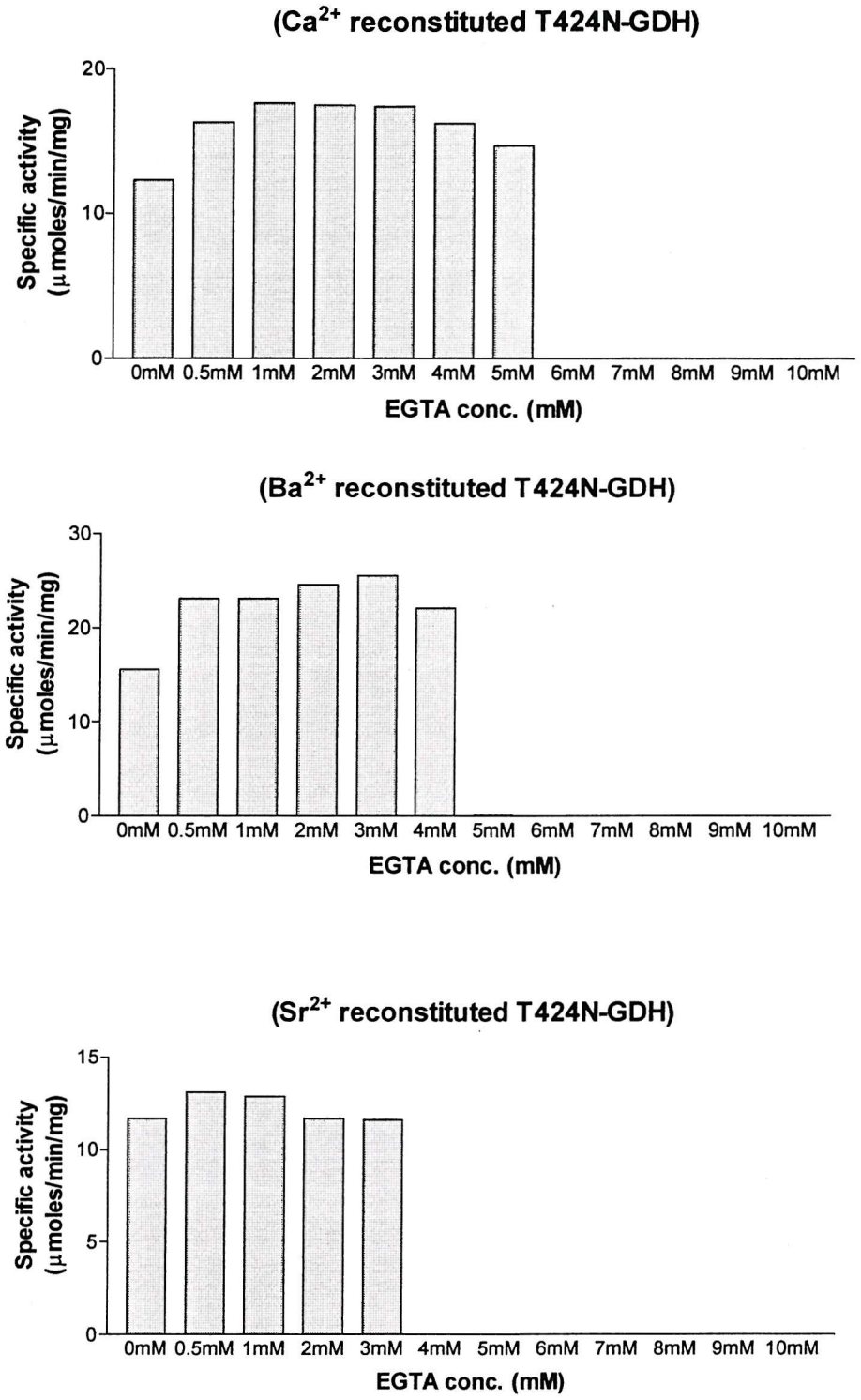

Figure 4.50 The effect of EGTA on T424N-GDH reconstituted with Ca^{2+}, Sr^{2+} and Ba^{2+}

T424N-GDH was reconstituted under standard conditions with 25μM PQQ and 5mM metal ions. Then various concentrations of EDTA were added and incubated at 25°C for 15 minutes.